

Effects of Frame Design and Cab Suspension on the Ride Quality of Heavy Trucks

Paul Stephen Patricio

Thesis submitted to the Faculty of the
Virginia Polytechnic Institute and State University
in partial fulfillment of the requirements for the degree of

Master of Science
in
Mechanical Engineering

Approved:

Mehdi Ahmadian
Chairman

Daniel J. Inman

Donald J. Leo

July 3, 2002
Blacksburg, Virginia

Keywords: Cab Suspension, Heavy Truck, Frame, Test Analysis, Ride

Effects of Frame Design and Cab Suspension on the Ride Quality of Heavy Trucks

by

Paul Stephen Patricio

Mehdi Ahmadian, Chairman

Mechanical Engineering

Frame and cab suspension designs of Class 8 heavy trucks were investigated to see their effects on ride comfort. Four trucks were used in this study, each with a different frame: a factory low frame, a lightweight low frame, a factory high frame, and a lightweight high frame. There were two different frame heights and three thicknesses. Two different rear cab suspensions were also tried out on each truck. Both suspensions used two airsprings and two dampers mounted vertically to control the vertical motion. The first suspension used two horizontally mounted dampers to control the lateral motion, while the second used a panhard rod connected to a torsion spring. In addition, two different sets of airsprings and two sets of vertical shocks were tried with each suspension, giving eight suspension combinations.

The trucks were shaken through the forward drive (second) axle using two 5500 lb hydraulic actuators with displacement control. The steering (first) axle was left in contact with the ground (through the tires) and the rear drive (third) axle was strapped to the truck's frame and acted solely as dead weight. The actuators were given various inputs including single frequency sinusoidal signals, step signals, and decreasing amplitude chirp signals. Both roll and heave modes of the truck were excited.

The ride was measured using three accelerometers located at the B-post inside the truck cab. These accelerometers were oriented in the vertical, fore/aft (longitudinal), and lateral (left/right) directions. Numerous other accelerometers and LVDTs were used to measure frame and cab motion.

This study found that there while the beaming frequency shifted downward with the lighter frames, there was only a small decrease in ride quality. The panhard suspension rod had significantly higher roll motion, but the heave amplitudes were similar to the lateral damper suspension. Switching vertical shocks had a significant effect on heave motion, but none on the cab's roll. Switching the airsprings on the cab suspension in this study had no effect.

Acknowledgements

To start with, I would like to thank my advisor, Dr. Mehdi Ahmadian, for his guidance and especially his patience while pursuing my Masters. I even forgive him for the shifty strategy he employs while playing Seven Stones. I would also like to thank Drs. Dan Inman and Don Leo for taking the time out of their busy schedules to serve on my committee.

Money doesn't buy happiness, but it sure makes it easier to pay the rent. On that note, I would like to thank my sponsors, Volvo Trucks North America, especially Jeff Peddycord and Brian Schneider, who were a pleasure to work with.

I would also like to thank all my lab mates, especially Fernando Goncalves, Jeong-Hoi Koo, Michael Siegler, and Dave Simon, who all helped with my research questions and made life enjoyable both in the lab and out. My friends outside the lab, especially Mike Russell, Bob Maher, and David Ruppert, deserve credit for keeping me out of trouble (or getting me in just the right amount of trouble in some cases...) when I wasn't staring at frequency response spectrums.

Finally, none of this would have been possible without the support of my parents, Greg and Sandra Patricio, and my siblings Andrew, Kenneth, and Fiona.

Contents

ABSTRACT	ii
ACKNOWLEDGEMENTS.....	iii
LIST OF TABLES	vi
LIST OF FIGURES	vii
CHAPTER 1 INTRODUCTION.....	1
CHAPTER 2 BACKGROUND.....	2
2.1 VEHICLE RIDE	2
2.1.1 <i>Definition of ride</i>	2
2.1.2 <i>Factors affecting ride</i>	3
2.1.3 <i>The primary suspension</i>	3
2.2 HEAVY TRUCK FRAMES	5
2.3 CAB SUSPENSIONS.....	8
2.4 LITERATURE REVIEW	13
CHAPTER 3 TEST SETUP.....	15
3.1 TEST VEHICLES	15
3.1.1 <i>Vehicle Descriptions</i>	15
3.1.2 <i>Vehicle Modifications for Shake Rig</i>	16
3.2 DYNAMIC TEST SYSTEM	21
3.2.1 <i>Actuation of Suspension</i>	21
3.2.2 <i>Data Acquisition</i>	21
3.2.3 <i>Instrument Locations</i>	22
CHAPTER 4 RIDE NUMBER METRIC.....	28
4.1 RIDE METRICS.....	28
4.2 SUMMARY OF RESULTS	28
4.3 CALCULATION PROCESS.....	29
4.4 STANDARD LOW RESULTS.....	32
4.5 THIN LOW RESULTS	34
4.6 STANDARD HIGH RESULTS.....	35
4.7 THIN HIGH RESULTS	36
4.8 COMPARISON BETWEEN TRUCKS.....	38
CHAPTER 5 FREQUENCY RESPONSE SPECTRUM.....	41
5.1 CHIRP INPUT SIGNAL.....	41
5.2 SUMMARY OF RESULTS	42
5.3 STANDARD LOW RESULTS.....	43
5.3.1 <i>Vibration Effects of Fuel Level</i>	43
5.3.2 <i>Heave Cab Suspension Study</i>	47
5.3.3 <i>Roll Cab Suspension Study</i>	51

5.4	THIN LOW RESULTS	56
5.4.1	<i>Heave Cab Suspension Study</i>	56
5.4.2	<i>Roll Cab Suspension Study</i>	62
5.5	STANDARD HIGH RESULTS	67
5.5.1	<i>Heave Cab Suspension Study</i>	67
5.5.2	<i>Roll Cab Suspension Study</i>	73
5.6	THIN HIGH RESULTS	78
5.6.1	<i>Heave Cab Suspension Study</i>	78
5.6.2	<i>Roll Cab Suspension Study</i>	84
5.7	COMPARISON BETWEEN TRUCKS	89
5.7.1	<i>Heave Comparison</i>	89
5.7.2	<i>Roll Comparison</i>	93
CHAPTER 6 VIBRATION TRANSMISSIBILITY		97
6.1	TRANSFER FUNCTIONS AND TRANSMISSIBILITIES	97
6.2	CALCULATION PROCESS	98
6.3	STANDARD LOW RESULTS.....	98
6.3.1	<i>Heave Cab Suspension Study</i>	99
6.3.2	<i>Roll Cab Suspension Study</i>	104
6.4	THIN LOW RESULTS	108
6.4.1	<i>Heave Cab Suspension Study</i>	108
6.4.2	<i>Roll Cab Suspension Study</i>	112
6.5	STANDARD HIGH RESULTS	114
6.5.1	<i>Heave Cab Suspension Study</i>	114
6.5.2	<i>Roll Cab Suspension Study</i>	118
6.6	THIN HIGH RESULTS	121
6.6.1	<i>Heave Cab Suspension Study</i>	121
6.6.2	<i>Roll Cab Suspension Study</i>	124
6.7	COMPARISON BETWEEN TRUCKS	127
6.7.1	<i>Heave Comparison</i>	127
6.7.2	<i>Roll Cab Suspension Study</i>	130
CHAPTER 7 BUMP RESPONSE		133
7.1	BUMP INPUT	133
7.2	SUMMARY OF RESULTS	134
7.3	CALCULATION PROCESS	134
7.4	STANDARD LOW RESULTS.....	136
7.5	THIN LOW RESULTS	140
7.6	STANDARD HIGH RESULTS	144
7.7	THIN HIGH RESULTS	148
CHAPTER 8 CONCLUSION AND RECOMMENDATIONS		153
REFERENCES		154
VITA		155

List of Tables

<i>Table 3-1. Important test vehicle parameters</i>	15
<i>Table 4-1. Average ride numbers</i>	29
<i>Table 4-2. Cab suspension abbreviations for plots</i>	32
<i>Table 5-1. Test vehicle summary</i>	42
<i>Table 5-2. Important test vehicle parameters</i>	43
<i>Table 5-3. Important test vehicle parameters</i>	56
<i>Table 5-4. Important test vehicle parameters</i>	67
<i>Table 5-5. Important test vehicle parameters</i>	78
<i>Table 6-1. Important test vehicle parameters</i>	98
<i>Table 6-2. Important test vehicle parameters</i>	108
<i>Table 6-3. Important test vehicle parameters</i>	114
<i>Table 6-4. Important test vehicle parameters</i>	121
<i>Table 6-5. Important test vehicle parameters</i>	127
<i>Table 7-1. Cab suspension abbreviations for plot</i>	136
<i>Table 7-2. Standard Low parametric evaluation (heave)</i>	138
<i>Table 7-3. Standard Low parametric evaluation (roll)</i>	140
<i>Table 7-4. Thin Low parametric evaluation (heave)</i>	142
<i>Table 7-5. Thin Low parametric evaluation (roll)</i>	144
<i>Table 7-6. Standard High parametric evaluation (heave)</i>	146
<i>Table 7-7. Standard High parametric evaluation (roll)</i>	148
<i>Table 7-8. Thin High parametric evaluation (heave)</i>	150
<i>Table 7-9. Thin High parametric evaluation (roll)</i>	152

List of Figures

<i>Figure 2-1. Single-Degree-of-Freedom Base Excitation Model</i>	3
<i>Figure 2-2. Transmissibility as a function of frequency ratio and damping</i>	5
<i>Figure 2-3. Frame Diagram</i>	6
<i>Figure 2-4. Cross-section Geometry of Frame</i>	8
<i>Figure 2-5. Examples of Panhard Rod Cab Suspensions on (a) Mach CH and (b) Freightliner Century Class</i>	9
<i>Figure 2-6. Factory Cab Suspension (Lateral Shocks)</i>	10
<i>Figure 2-7. Factory Cab Suspension (Airspring)</i>	11
<i>Figure 2-8. Prototype Cab Suspension</i>	11
<i>Figure 2-9. Elastomeric Torsion Spring of Prototype Suspension</i>	12
<i>Figure 2-10. Cab Suspension Airsprings</i>	12
<i>Figure 3-1. Important test vehicle parameters</i>	16
<i>Figure 3-2. Original Rear Suspension Plumbing Layout</i>	17
<i>Figure 3-3. Modified Rear Suspension Plumbing Layout</i>	17
<i>Figure 3-4. Rear Drive Axle</i>	18
<i>Figure 3-5. Weight Stack on Test Vehicle</i>	19
<i>Figure 3-6. Dynamic Actuation Setup with Auxiliary Airspring</i>	19
<i>Figure 3-7. Air Dryer with Inlet Bypass Hose</i>	20
<i>Figure 3-8. Inlet to Air Dryer</i>	20
<i>Figure 3-9. MTS 458.20 Hydraulic Controller</i>	21
<i>Figure 3-10. PCB Model U352C65 Accelerometer</i>	22
<i>Figure 3-11. Accelerometer Layout</i>	23
<i>Figure 3-12. LVDT Layout</i>	23
<i>Figure 3-13. Rear Cab Suspension Sensors (LVDTs labeled)</i>	24
<i>Figure 3-14. Sensors at Rear, Bottom of Cab near Cab Suspension: (a) Lateral and Fore/Aft Accelerometers; (b) Vertical Accelerometer</i>	25
<i>Figure 3-15. Other sensors at Back of Cab: (a) Vertical Accelerometer on Frame at Cab Suspension; (b) Lateral Accelerometer at Drip Rail</i>	25
<i>Figure 3-16. Accelerometers Mounted at B-post</i>	25
<i>Figure 3-17. Frame Accelerometers (a) at Front and (b) at Second Axle</i>	26

<i>Figure 3-18. Frame Accelerometers (a) at Rear and (b) at Fifth Wheel Stack</i>	<i>26</i>
<i>Figure 3-19. Frame LVDTs at Back of Cab.....</i>	<i>27</i>
<i>Figure 3-20. Frame LVDTs (a) at Front and (b) at Rear of Driver-Side Frame Rail.....</i>	<i>27</i>
<i>Figure 4-1. ISO weighting charts.....</i>	<i>30</i>
<i>Figure 4-2. Unweighted and weighted B-post fore/aft acceleration response</i>	<i>30</i>
<i>Figure 4-3. Standard Low heave ride numbers.....</i>	<i>32</i>
<i>Figure 4-4. Standard Low roll ride numbers</i>	<i>33</i>
<i>Figure 4-5. Standard Low total ride number change compared to factory configuration</i>	<i>33</i>
<i>Figure 4-6. Thin Low heave ride numbers.....</i>	<i>34</i>
<i>Figure 4-7. Thin Low roll ride numbers</i>	<i>34</i>
<i>Figure 4-8. Thin Low total ride number change compared to factory configuration.....</i>	<i>35</i>
<i>Figure 4-9. Standard High heave ride numbers</i>	<i>35</i>
<i>Figure 4-10. Standard High roll ride numbers.....</i>	<i>36</i>
<i>Figure 4-11. Standard High total ride number change compared to factory configuration</i>	<i>36</i>
<i>Figure 4-12. Thin High heave ride numbers.....</i>	<i>37</i>
<i>Figure 4-13. Thin High roll ride numbers</i>	<i>37</i>
<i>Figure 4-14. Thin High total ride number change compared to factory configuration.....</i>	<i>38</i>
<i>Figure 4-15. Thin Low total ride number change compared to Standard Low with factory configuration.....</i>	<i>39</i>
<i>Figure 4-16. Thin High total ride number change compared to Standard High with factory configuration.....</i>	<i>39</i>
<i>Figure 4-17. Best suspensions total ride numbers</i>	<i>40</i>
<i>Figure 4-18. Change from mean of the best suspension for each truck.....</i>	<i>40</i>
<i>Figure 5-1. Sample chirp input signal</i>	<i>41</i>
<i>Figure 5-2. Standard Low Vertical Acceleration of Frame at Rear Cab Suspension for Various Tank Fluid Levels.....</i>	<i>45</i>
<i>Figure 5-3. Standard Low Vertical Acceleration of Cab at Rear Cab Suspension for Various Tank Fluid Levels.....</i>	<i>45</i>
<i>Figure 5-4. Standard Low Vertical Acceleration of B-post for Various Tank Fluid Levels.....</i>	<i>46</i>
<i>Figure 5-5. Standard Low Fore/Aft Acceleration of B-post for Various Tank Fluid Levels</i>	<i>46</i>

<i>Figure 5-6. Standard Low Vertical Acceleration of Frame at Rear Cab Suspension for Different Cab Suspension</i>	47
<i>Figure 5-7. Standard Low Vertical Acceleration of Frame at Rear Cab Suspension for Different Cab Suspensions</i>	48
<i>Figure 5-8. Standard Low Vertical Acceleration of Cab at Rear Cab Suspension for Different Cab Suspensions</i>	48
<i>Figure 5-9. Standard Low Vertical Acceleration of Cab at Rear Cab Suspension for Different Cab Suspensions</i>	49
<i>Figure 5-10. Standard Low Vertical Acceleration of B-post for Different Cab Suspensions</i>	49
<i>Figure 5-11. Standard Low Vertical Acceleration of B-post for Different Cab Suspensions</i>	50
<i>Figure 5-12. Standard Low Fore/Aft Acceleration of B-post for Different Cab Suspensions</i>	50
<i>Figure 5-13. Standard Low Fore/Aft Acceleration of B-post for Different Cab Suspensions</i>	51
<i>Figure 5-14. Standard Low Vertical Acceleration of Frame at Rear Cab Suspension</i>	52
<i>Figure 5-15. Standard Low Vertical Acceleration of Frame at Rear Cab Suspension</i>	52
<i>Figure 5-16. Standard Low Vertical Acceleration of Cab at Rear Cab Suspension</i>	53
<i>Figure 5-17. Standard Low Vertical Acceleration of Cab at Rear Cab Suspension</i>	53
<i>Figure 5-18. Standard Low Vertical Acceleration of B-post</i>	54
<i>Figure 5-19. Standard Low Vertical Acceleration of B-post</i>	54
<i>Figure 5-20. Standard Low Fore/Aft Acceleration of B-post</i>	55
<i>Figure 5-21. Standard Low Fore/Aft Acceleration of B-post</i>	55
<i>Figure 5-22. Thin Low Vertical Acceleration of Frame at Rear Cab Suspension</i>	57
<i>Figure 5-23. Thin Low Vertical Acceleration of Frame at Rear Cab Suspension (Low Frequencies)</i>	57
<i>Figure 5-24. Thin Low Vertical Acceleration of Cab at Rear Cab Suspension</i>	58
<i>Figure 5-25. Thin Low Vertical Acceleration of Cab at Rear Cab Suspension (Low Frequencies)</i>	58
<i>Figure 5-26. Thin Low Vertical Acceleration of B-post</i>	59
<i>Figure 5-27. Thin Low Vertical Acceleration of B-post (Low Frequencies)</i>	59
<i>Figure 5-28. Thin Low Fore/Aft Acceleration of B-post</i>	60
<i>Figure 5-29. Thin Low Fore/Aft Acceleration of B-post (Low Frequencies)</i>	60
<i>Figure 5-30. Thin Low Lateral Acceleration of B-post</i>	61

<i>Figure 5-31. Thin Low Lateral Acceleration of B-post (Low Frequencies)</i>	61
<i>Figure 5-32. Thin Low Vertical Acceleration of Frame at Rear Cab Suspension</i>	62
<i>Figure 5-33. Thin Low Vertical Acceleration of Frame at Rear Cab Suspension (Low Frequency)</i>	63
<i>Figure 5-34. Thin Low Vertical Acceleration of Cab at Rear Cab Suspension</i>	63
<i>Figure 5-35. Thin Low Vertical Acceleration of Cab at Rear Cab Suspension (Low Frequency)</i>	64
<i>Figure 5-36. Thin Low Vertical Acceleration of B-post</i>	64
<i>Figure 5-37. Thin Low Vertical Acceleration of B-post (Low Frequency)</i>	65
<i>Figure 5-38. Thin Low Fore/Aft Acceleration of B-post</i>	65
<i>Figure 5-39. Thin Low Fore/Aft Acceleration of B-post (Low Frequency)</i>	66
<i>Figure 5-40. Thin Low Lateral Acceleration of B-post</i>	66
<i>Figure 5-41. Thin Low Lateral Acceleration of B-post (Low Frequency)</i>	67
<i>Figure 5-42. Standard High Vertical Acceleration of Frame at Rear Cab Suspension</i>	68
<i>Figure 5-43. Standard High Vertical Acceleration of Frame at Rear Cab Suspension (Low Frequency)</i>	68
<i>Figure 5-44. Standard High Vertical Acceleration of Cab at Rear Cab Suspension</i>	69
<i>Figure 5-45. Standard High Vertical Acceleration of Cab at Rear Cab Suspension (Low Frequency)</i>	69
<i>Figure 5-46. Standard High Vertical Acceleration of B-post</i>	70
<i>Figure 5-47. Standard High Vertical Acceleration of B-post (Low Frequency)</i>	70
<i>Figure 5-48. Standard High Fore/Aft Acceleration of B-post</i>	71
<i>Figure 5-49. Standard High Fore/Aft Acceleration of B-post (Low Frequency)</i>	71
<i>Figure 5-50. Standard High Lateral Acceleration of B-post</i>	72
<i>Figure 5-51. Standard High Lateral Acceleration of B-post (Low Frequency)</i>	72
<i>Figure 5-52. Standard High Vertical Acceleration of Frame at Rear Cab Suspension</i>	73
<i>Figure 5-53. Standard High Vertical Acceleration of Frame at Rear Cab Suspension (Low Frequency)</i>	74
<i>Figure 5-54. Standard High Vertical Acceleration of Cab at Rear Cab Suspension</i>	74
<i>Figure 5-55. Standard High Vertical Acceleration of Cab at Rear Cab Suspension (Low Frequency)</i>	75
<i>Figure 5-56. Standard High Vertical Acceleration of B-post</i>	75

<i>Figure 5-57. Standard High Vertical Acceleration of B-post (Low Frequency)</i>	76
<i>Figure 5-58. Standard High Fore/Aft Acceleration of B-post</i>	76
<i>Figure 5-59. Standard High Fore/Aft Acceleration of B-post (Low Frequency)</i>	77
<i>Figure 5-60. Standard High Lateral Acceleration of B-post</i>	77
<i>Figure 5-61. Standard High Lateral Acceleration of B-post (Low Frequency)</i>	78
<i>Figure 5-62. Thin High Vertical Acceleration of Frame at Rear Cab Suspension</i>	79
<i>Figure 5-63. Thin High Vertical Acceleration of Frame at Rear Cab Suspension (Low Frequency)</i>	79
<i>Figure 5-64. Thin High Vertical Acceleration of Cab at Rear Cab Suspension</i>	80
<i>Figure 5-65. Thin High Vertical Acceleration of Cab at Rear Cab Suspension (Low Frequency)</i>	80
<i>Figure 5-66. Thin High Vertical Acceleration of B-post</i>	81
<i>Figure 5-67. Thin High Vertical Acceleration of B-post (Low Frequency)</i>	81
<i>Figure 5-68. Thin High Fore/Aft Acceleration of B-post</i>	82
<i>Figure 5-69. Thin High Fore/Aft Acceleration of B-post (Low Frequency)</i>	82
<i>Figure 5-70. Thin High Lateral Acceleration of B-post</i>	83
<i>Figure 5-71. Thin High Lateral Acceleration of B-post (Low Frequency)</i>	83
<i>Figure 5-72. Thin High Vertical Acceleration of Frame at Rear Cab Suspension</i>	84
<i>Figure 5-73. Thin High Vertical Acceleration of Frame at Rear Cab Suspension (Low Frequency)</i>	85
<i>Figure 5-74. Thin High Vertical Acceleration of Cab at Rear Cab Suspension</i>	85
<i>Figure 5-75. Thin High Vertical Acceleration of Cab at Rear Cab Suspension (Low Frequency)</i>	86
<i>Figure 5-76. Thin High Vertical Acceleration of B-post</i>	86
<i>Figure 5-77. Thin High Vertical Acceleration of B-post (Low Frequency)</i>	87
<i>Figure 5-78. Thin High Fore/Aft Acceleration of B-post</i>	87
<i>Figure 5-79. Thin High Fore/Aft Acceleration of B-post (Low Frequency)</i>	88
<i>Figure 5-80. Thin High Lateral Acceleration of B-post</i>	88
<i>Figure 5-81. Thin High Lateral Acceleration of B-post (Low Frequency)</i>	89
<i>Figure 5-82. Vertical Displacement of Frame at Back of Cab</i>	90
<i>Figure 5-83. Vertical Displacement of Rear of Frame</i>	91

<i>Figure 5-84. Vertical Acceleration of B-post.....</i>	<i>91</i>
<i>Figure 5-85. Vertical Acceleration of B-post (Low Frequency).....</i>	<i>92</i>
<i>Figure 5-86. Fore/Aft Acceleration of B-post.....</i>	<i>92</i>
<i>Figure 5-87. Fore/Aft Acceleration of B-post (Low Frequency)</i>	<i>93</i>
<i>Figure 5-88. Vertical Displacement of Frame at Back of Cab.....</i>	<i>94</i>
<i>Figure 5-89. Vertical Displacement of Rear of Frame.....</i>	<i>94</i>
<i>Figure 5-90. Vertical Acceleration of B-post.....</i>	<i>95</i>
<i>Figure 5-91. Vertical Acceleration of B-post (Low Frequency).....</i>	<i>95</i>
<i>Figure 5-92. Fore/Aft Acceleration of B-post.....</i>	<i>96</i>
<i>Figure 5-93. Fore/Aft Acceleration of B-post (Low Frequency)</i>	<i>96</i>
<i>Figure 6-1. Actuator Displacement, Driver.....</i>	<i>100</i>
<i>Figure 6-2. Vertical Acceleration of Cab, RCS, Center, vs. Vertical Acceleration of Frame, RCS, Center.....</i>	<i>100</i>
<i>Figure 6-3. Vertical Acceleration of B-post, Driver, vs. Vertical Acceleration of Frame, RCS, Center.....</i>	<i>101</i>
<i>Figure 6-4. Fore/Aft Acceleration of B-post, Driver, vs. Vertical Acceleration of Frame, RCS, Center.....</i>	<i>101</i>
<i>Figure 6-5. Vertical Acceleration of Frame, Second Axle, Driver, vs. Actuator Displacement, Driver</i>	<i>102</i>
<i>Figure 6-6. Vertical Acceleration of Frame, Front, Driver, vs. Vertical Acceleration of Frame, Second Axle, Driver.....</i>	<i>102</i>
<i>Figure 6-7. Vertical Acceleration of Frame, Rear, Driver, vs. Vertical Acceleration of Frame, Second Axle, Driver.....</i>	<i>103</i>
<i>Figure 6-8. Vertical Acceleration of Frame, RCS, Driver, vs. Vertical Acceleration of Frame, Second Axle, Driver.....</i>	<i>103</i>
<i>Figure 6-9. Actuator Displacement, Driver.....</i>	<i>105</i>
<i>Figure 6-10. Vertical Displacement across RCS, Driver, vs. Vertical Displacement of Frame, Back of Cab, Driver</i>	<i>105</i>
<i>Figure 6-11. Vertical Acceleration of B-post, Driver, vs. Vertical Displacement of Frame, Back of Cab, Driver</i>	<i>106</i>

<i>Figure 6-12. Lateral Acceleration of Cab, Drip Rail, Center, vs. Lateral Acceleration of Cab, RCS, Center.....</i>	<i>106</i>
<i>Figure 6-13. Vertical Acceleration of Frame, Second Axle, Driver, vs. Actuator Displacement, Driver.....</i>	<i>107</i>
<i>Figure 6-14. Vertical Acceleration of Frame, Front, Driver, vs. Vertical Acceleration of Frame, Second Axle, Driver.....</i>	<i>107</i>
<i>Figure 6-15. Vertical Acceleration of Cab, RCS, Center, vs. Vertical Acceleration of Frame, RCS, Center.....</i>	<i>109</i>
<i>Figure 6-16. Vertical Acceleration of B-post, Driver, vs. Vertical Acceleration of Frame, RCS, Center.....</i>	<i>109</i>
<i>Figure 6-17. Fore/Aft Acceleration of B-post, Driver, vs. Vertical Acceleration of Frame, RCS, Center.....</i>	<i>110</i>
<i>Figure 6-18. Vertical Acceleration of Frame, Front, Driver, vs. Vertical Acceleration of Frame, Second Axle, Driver.....</i>	<i>110</i>
<i>Figure 6-19. Vertical Acceleration of Frame, Rear, Driver, vs. Vertical Acceleration of Frame, Second Axle, Driver.....</i>	<i>111</i>
<i>Figure 6-20. Vertical Acceleration of Frame, RCS, Driver, vs. Vertical Acceleration of Frame, Second Axle, Driver.....</i>	<i>111</i>
<i>Figure 6-21. Vertical Displacement across RCS, Driver, vs. Vertical Displacement of Frame, Back of Cab, Driver.....</i>	<i>112</i>
<i>Figure 6-22. Lateral Acceleration of B-post, Driver, vs. Vertical Displacement of Frame, Back of Cab, Driver.....</i>	<i>113</i>
<i>Figure 6-23. Vertical Acceleration of B-post, Driver, vs. Vertical Displacement of Frame, Back of Cab, Driver.....</i>	<i>113</i>
<i>Figure 6-24. Lateral Acceleration of Cab, Drip Rail, Center, vs. Lateral Acceleration of Cab, RCS, Center.....</i>	<i>114</i>
<i>Figure 6-25. Vertical Acceleration of Cab, RCS, Center, vs. Vertical Acceleration of Frame, RCS, Center.....</i>	<i>115</i>
<i>Figure 6-26. Vertical Acceleration of B-post, Driver, vs. Vertical Acceleration of Frame, RCS, Center.....</i>	<i>116</i>

<i>Figure 6-27. Fore/Aft Acceleration of B-post, Driver, vs. Vertical Acceleration of Frame, RCS, Center.....</i>	<i>116</i>
<i>Figure 6-28. Vertical Acceleration of Frame, Front, Driver, vs. Vertical Acceleration of Frame, Second Axle, Driver.....</i>	<i>117</i>
<i>Figure 6-29. Vertical Acceleration of Frame, Rear, Driver, vs. Vertical Acceleration of Frame, Second Axle, Driver.....</i>	<i>117</i>
<i>Figure 6-30. Vertical Acceleration of Frame, RCS, Driver, vs. Vertical Acceleration of Frame, Second Axle, Driver.....</i>	<i>118</i>
<i>Figure 6-31. Vertical Displacement across RCS, Driver, vs. Vertical Displacement of Frame, Back of Cab, Driver</i>	<i>119</i>
<i>Figure 6-32. Lateral Acceleration of B-post, Driver, vs. Vertical Displacement of Frame, Back of Cab, Driver.....</i>	<i>119</i>
<i>Figure 6-33. Vertical Acceleration of B-post, Driver, vs. Vertical Displacement of Frame, Back of Cab, Driver</i>	<i>120</i>
<i>Figure 6-34. Lateral Acceleration of Cab, Drip Rail, Center, vs. Lateral Acceleration of Cab, RCS, Center.....</i>	<i>120</i>
<i>Figure 6-35. Vertical Acceleration of Cab, RCS, Center, vs. Vertical Acceleration of Frame, RCS, Center.....</i>	<i>121</i>
<i>Figure 6-36. Vertical Acceleration of B-post, Driver, vs. Vertical Acceleration of Frame, RCS, Center.....</i>	<i>122</i>
<i>Figure 6-37. Fore/Aft Acceleration of B-post, Driver, vs. Vertical Acceleration of Frame, RCS, Center.....</i>	<i>122</i>
<i>Figure 6-38. Vertical Acceleration of Frame, Front, Driver, vs. Vertical Acceleration of Frame, Second Axle, Driver.....</i>	<i>123</i>
<i>Figure 6-39. Vertical Acceleration of Frame, Rear, Driver, vs. Vertical Acceleration of Frame, Second Axle, Driver.....</i>	<i>123</i>
<i>Figure 6-40. Vertical Acceleration of Frame, RCS, Driver, vs. Vertical Acceleration of Frame, Second Axle, Driver.....</i>	<i>124</i>
<i>Figure 6-41. Vertical Displacement across RCS, Driver, vs. Vertical Displacement of Frame, Back of Cab, Driver</i>	<i>125</i>

<i>Figure 6-42. Lateral Acceleration of B-post, Driver, vs. Vertical Displacement of Frame, Back of Cab, Driver.....</i>	<i>125</i>
<i>Figure 6-43. Vertical Acceleration of B-post, Driver, vs. Vertical Displacement of Frame, Back of Cab, Driver</i>	<i>126</i>
<i>Figure 6-44. Lateral Acceleration of Cab, Drip Rail, Center, vs. Lateral Acceleration of Cab, RCS, Center.....</i>	<i>126</i>
<i>Figure 6-45. Vertical Acceleration of Cab, RCS, Center, vs. Vertical Acceleration of Frame, RCS, Center.....</i>	<i>128</i>
<i>Figure 6-46. Vertical Acceleration of B-post, Driver, vs. Vertical Acceleration of Frame, RCS, Center</i>	<i>128</i>
<i>Figure 6-47. Fore/Aft Acceleration of B-post, Driver, vs. Vertical Acceleration of Frame, RCS, Center.....</i>	<i>129</i>
<i>Figure 6-48. Vertical Acceleration of Frame, Rear, Driver, vs. Vertical Acceleration of Frame, Second Axle, Driver.....</i>	<i>129</i>
<i>Figure 6-49. Vertical Acceleration of Frame, RCS, Driver, vs. Vertical Acceleration of Frame, Second Axle, Driver.....</i>	<i>130</i>
<i>Figure 6-50. Vertical Displacement across RCS, Driver, vs. Vertical Displacement of Frame, Back of Cab, Driver</i>	<i>131</i>
<i>Figure 6-51. Vertical Acceleration of B-post, Driver, vs. Vertical Displacement of Frame, Back of Cab, Driver</i>	<i>131</i>
<i>Figure 6-52. Lateral Acceleration of B-post, Driver, vs. Vertical Displacement of Frame, Back of Cab, Driver.....</i>	<i>132</i>
<i>Figure 7-1. Sample bump input displacement at the actuator</i>	<i>133</i>
<i>Figure 7-2. Sample data from accelerometers: (a) acceleration and (b) displacement</i>	<i>135</i>
<i>Figure 7-3. Standard Low peak-to-peak accelerations (heave).....</i>	<i>136</i>
<i>Figure 7-4. Standard Low peak-to-peak displacements (heave).....</i>	<i>137</i>
<i>Figure 7-5. Standard Low damping ratios (heave).....</i>	<i>137</i>
<i>Figure 7-6. Standard Low peak-to-peak accelerations (roll).....</i>	<i>139</i>
<i>Figure 7-7. Standard Low peak-to-peak displacements (roll).....</i>	<i>139</i>
<i>Figure 7-8. Standard Low damping ratios (roll)</i>	<i>140</i>
<i>Figure 7-9. Thin Low peak-to-peak accelerations (heave).....</i>	<i>141</i>

<i>Figure 7-10. Thin Low peak-to-peak displacements (heave)</i>	141
<i>Figure 7-11. Thin Low damping ratios (heave)</i>	142
<i>Figure 7-12. Thin Low peak-to-peak accelerations (roll)</i>	143
<i>Figure 7-13. Thin Low peak-to-peak displacements (roll)</i>	143
<i>Figure 7-14. Thin Low damping ratios (roll)</i>	144
<i>Figure 7-15. Standard High peak-to-peak accelerations (heave)</i>	145
<i>Figure 7-16. Standard High peak-to-peak displacements (heave)</i>	145
<i>Figure 7-17. Standard High damping ratios (heave)</i>	146
<i>Figure 7-18. Standard High peak-to-peak accelerations (roll)</i>	147
<i>Figure 7-19. Standard High peak-to-peak displacements (roll)</i>	147
<i>Figure 7-20. Standard High damping ratios (roll)</i>	148
<i>Figure 7-21. Thin High peak-to-peak accelerations (heave)</i>	149
<i>Figure 7-22. Thin High peak-to-peak displacements (heave)</i>	149
<i>Figure 7-23. Thin High damping ratios (heave)</i>	150
<i>Figure 7-24. Thin High peak-to-peak accelerations (roll)</i>	151
<i>Figure 7-25. Thin High peak-to-peak displacements (roll)</i>	151
<i>Figure 7-26. Thin High damping ratios (roll)</i>	152

Chapter 1 Introduction

The purpose of this study was to assist the manufacturer in investigating the dynamics of its new lightweight truck frames. In particular, the Advanced Vehicle Dynamics Laboratory (AVDL) of Virginia Tech will help the manufacturer ensure that trucks equipped with the new frames will meet the ride quality established by the manufacturer's baseline trucks. This will incorporate examining possible solutions to the ride issues, including studying a prototype cab suspension design, hereafter referred to as "Suspension P," as a possible alternative to the factory suspension, "Suspension F".

The study used the dynamic test rig at AVDL. This setup allows us to control the vertical displacement of a drive axle of the test vehicle through two hydraulic actuators. This gives us the capability to shake the vehicle in a controlled and repeatable manner, allowing us to observe and measure the dynamic response of the trucks at specific frequencies. More details on the testing rig and data acquisition systems appear later in the report.

As mentioned earlier, besides comparisons between trucks, the tests analyzed how the prototype cab suspension performed relative to the current factory cab suspension on each truck. Both the prototype and factory suspensions have three main components. They both have two airsprings for two vertical shocks to control the vertical motion of the cab. To control lateral movement, the factory suspension uses two shocks; the prototype suspension uses a panhard rod with a torsion spring. The lateral stiffnesses of the two suspensions are similar, but the factory suspension has much higher damping inherent in the design.

Background information on some of the topics involved in this study and a literature review are contained in Chapter 2. Chapter 3 of the report contains information on the trucks themselves and the shaker rig. After that, the results follow divided into four chapters. The chirp signal and the frequency response spectrums are discussed in Chapter 4 Chapter 5 contains the ride number analysis, which was also developed from the chirp signal. In Chapter 6 transmissibilities from the pure tone data are examined. Chapter 7 contains information on the bump responses of the trucks. Following the results, the conclusions and recommendations are given in Chapter 8.

Chapter 2 Background

This chapter gives some background information helpful to the understanding of this thesis. Section 2.1 contains background information on vehicle ride. Section 2.2 contains information on heavy truck frames. After that, various heavy truck cab suspensions are discussed in Section 2.3, including the different configurations tested in this study. The literature review is given in Section 2.4.

2.1 Vehicle Ride

The focus of the testing is to evaluate the ride of the four trucks and of the different cab suspensions. This section defines what is meant by ride and discusses some of the factors that affect ride quality.

2.1.1 Definition of ride

Ride is a subjective measure of the comfort of a moving vehicle. The main factor that drivers use to judge the ride quality of their vehicles is the motion that their body goes through. The *perception* of motion, however, is also a factor. Besides what he feels, this perception is influenced by what the driver hears as well [1]. As such, squeaks, rattles, buzzes, and other noises from vibrating components will negatively influence the driver's opinion of the ride quality of the vehicle. Most of the aural cues that affect the driver's opinion are produced by high frequency vibrations (>25 Hz). All of the input signals in this study were below 25 Hz, and the influence of noise was not considered.

Vehicle ride is important in two regards. The most apparent aspect is that a comfortable vehicle leads to a more enjoyable driving experience. When long trips are concerned, ride becomes even more important. A vehicle with poor ride can cause driver fatigue. Fatigue reduces driver alertness and increases reaction times, increasing the likelihood of an accident. Thus, a vehicle with good ride is a safer vehicle. This aspect is even more important for heavy-duty highway trucks such as the ones in this study. Drivers of these trucks spend up to 16 hours per day on the road. Small vibrations that go unnoticed after ten minutes of driving can easily lead to fatigue on these longer trips. In addition, if an accident does occur, it is often deadlier because of the size of these vehicles.

2.1.2 Factors affecting ride

There are several design factors affecting vehicle ride. The most significant factor is the axle (primary) suspension. Wheels, tires, and the suspension are almost completely responsible for the ride of the vehicle in automobile design. When designing heavy trucks, however, other factors also play significant roles. Relative to their smaller mass, cars are much stiffer than trucks. With trucks, their relatively flexible frames create a major source of ride problems. In addition, trucks have many large masses such as exhaust stacks, fuel tanks, and battery boxes that have their own dynamics at different frequencies. Many trucks use a secondary suspension to mount the cab to the frame to better isolate the occupants from the dynamics of the components mounted to the truck frame.

2.1.3 The primary suspension

Road input is transmitted through the tires to the axles of the truck. The primary suspension transmits motion between the axle and the frame. Vehicle suspensions serve two main functions: keeping the tires in contact with the road (handling) and isolating the body from road input (ride comfort). Suspension design involves a compromise between handling and ride comfort. Higher spring rates will cause less body roll and more even load distribution on the wheels in cornering situations, thus producing better handling. Lower spring rates can lead to a more comfortable ride, because they transmit less vibration energy from the axle to the rest of the truck.

The natural frequency of a mass is the frequency that the mass will vibrate at in response to a disturbance. For a suspension, the disturbance could be a bump in the road. The primary suspension natural frequency can be calculated by using a simple model of a suspension that is illustrated in Figure 2-1.

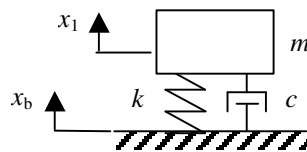


Figure 2-1. Single-Degree-of-Freedom Base Excitation Model

The mass used in this model, m , is the sprung mass supported by the axle. This term does not include the weight of the axle itself and some other suspension components. The suspension stiffness is represented by k . The motion of the vehicle body is given by x_1 and the base motion,

the road input to the tire, is shown as x_b . The undamped natural frequency, ω_n , of this system is given by:

$$\omega_n = \sqrt{\frac{k}{m}} \quad (1)$$

If damping is included in the calculation, the natural frequency decreases slightly (usually less than 10%). The most convenient method to calculate the damped natural frequency, ω_d , is to first calculate the damping ratio, ζ :

$$\zeta = \frac{c}{2\sqrt{km}} \quad (2)$$

The damped natural frequency is then calculated as follows:

$$\omega_d = \omega_n \sqrt{1 - \zeta^2} \quad (3)$$

From equations (1) and (3), observe that the natural frequency increases as the suspension stiffness increases, and decreases as the mass increases.

The suspension natural frequency has two influences on ride quality. A higher frequency will lead to higher accelerations and a harsher feel over bumps. Secondly, the transmissibility between the road input and the body is affected. The transmissibility is simply the ratio of the output over the input. As shown in Figure 2-2, the transmissibility changes depending on the input frequency. Transmissibilities higher than 1 indicate that the input motion is being amplified; in this case, it would mean that the body is moving more than the tire. Similarly, transmissibilities lower than 1 mean that the suspension is isolating the body from the wheel dynamics (attenuating the motion of the body, relative to the motion of the wheel). At the natural frequency, the transmissibility is at its maximum (damping can shift the peak slightly). Depending mostly on damping, the amplification at the natural frequency can be greater than 10. When the input frequency is equal to $1.414 \cdot \omega_n$, the transmissibility is equal to 1. Below this frequency, the transmissibility is greater than 1; above it, the transmissibility is below 1 and decreases as the input frequency increases.

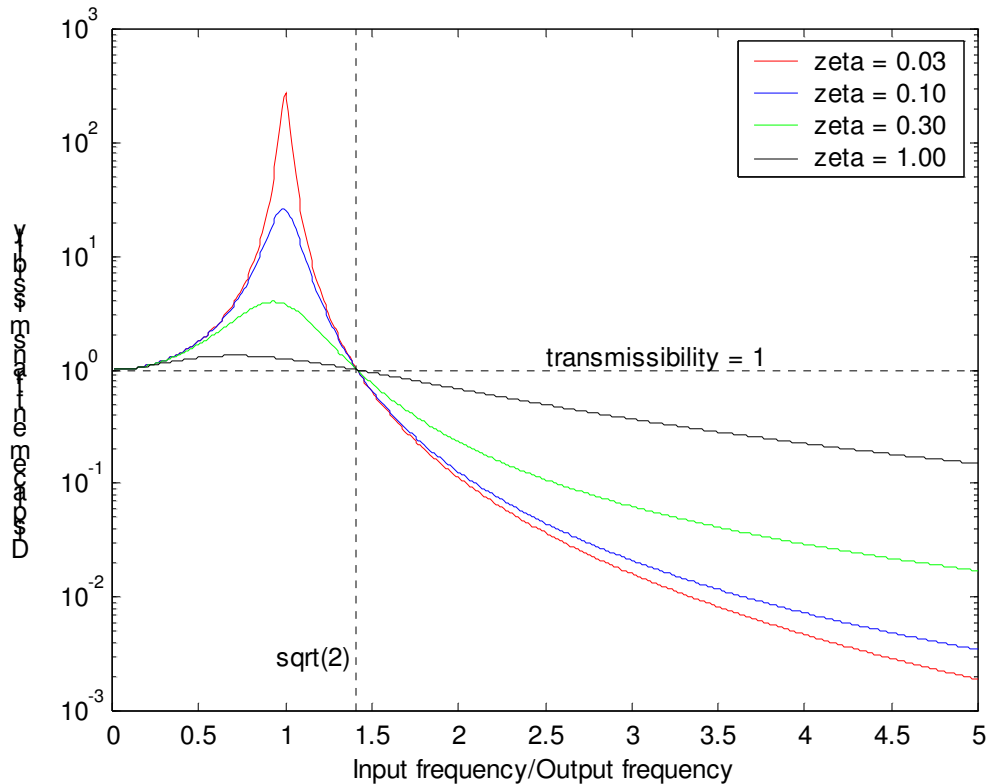


Figure 2-2. Transmissibility as a function of frequency ratio and damping

The frequencies above $1.414 \cdot \omega_n$ are referred to as the isolation range. A low natural frequency leads to a broader isolation range. A natural frequency of 1.0 Hz is considered ideal for highway ride (lower natural frequencies than this produce the floating ride typical of large American luxury cars in the seventies and eighties) [1]. Trucks have suspensions in the 1.5 – 2.0 Hz range [1]. Heavy trucks have high centers-of-gravity, so the stiffer suspension is needed for added stability.

2.2 Heavy Truck Frames

Originally, cars were built using body-on-frame design. As the name implies, the body was built separate from the frame and then the two were joined together near the end of the manufacturing process. Almost all of the structural rigidity comes from the frame. The main advantage of this type of design is ease of manufacturing. Today, most cars and many SUVs are built utilizing a unibody design: the body and frame form a single unit. Unlike body-on-frame designs, the body of a unibody vehicle contributes significantly to structural strength.

Early trucks often started out as cars with heavy-duty parts. Later on, they became more specialized to the larger loads they had to carry. Unlike cars, however, trucks never made the transition to unibody design. This is because unibody designs lack flexibility of function. The same basic truck chassis design must accomplish many different tasks. One chassis might be used with different truck bodies ranging from cement mixers to furniture trucks. The same chassis would also have to accommodate different wheelbases (the distance between the front and rear axles) several feet apart. In addition, while cross-country haulers from the same manufacturer may look similar, they are often significantly different from each other. Manufacturers often use the same chassis with several different cabs. Even trucks with the same cab can have different wheelbases. To accommodate these major differences – not to mention hundred of other options, such as fuel tank size, transmissions, and body aerodynamics – dozens of separate unibody designs would be required. Combined with the low production numbers of heavy trucks, body-on-frame designs are much more cost-efficient.

As mentioned earlier, with a body-on-frame design, the frame is responsible for most of the vehicle’s rigidity. This frame consists of two long frame rails connected to each other with cross members every few feet, as shown in Figure 2-3. In addition, the engine, transmission, and fifth wheel (shown cross-hatched in Figure 2-3) double as structural members. The frames of highway trucks are about 20-30 feet long, 1 foot high, and 3 feet wide.

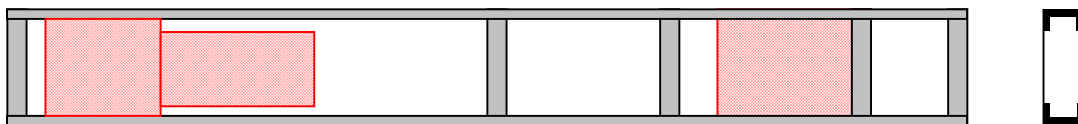


Figure 2-3. Frame Diagram

Just as with the suspension, there are natural frequencies associated with the frame. The frame has several vibration modes, occurring at different frequencies. The most important of these is the bending mode, which is also called “beaming.” The beaming frequency is usually the first mode of vibration, occurring between 6-9 Hz [1]. Truck frames are long compared to their height, so they are relatively flexible along their length. If the end of a diving board is held down and then released, it will oscillate up and down at its bending natural frequency. Truck frames behave in the same way. Recall that when you excite a system at its natural frequency, the motion of the input is greatly amplified. In the same manner, when the truck frame is excited (by the primary suspension) at its beaming frequency, the frame becomes very active. The large

displacements that occur at the beaming resonance are often the major source of ride deterioration, even when compared to the vibrations caused by the resonances of other components.

With suspensions, low natural frequencies are desirable. With structures such as frames, good ride quality is obtained with *high* natural frequencies. Recall that suspensions attenuate input motions at frequencies above 1.414 time the suspension natural frequency. If the frame's modal frequencies are much higher than that, the modes won't get excited because the input vibrations to the frame (in other words, the output vibrations from the suspension) will be low. Additionally, high frequency vibrations are less important because the human body is less sensitive to them.

If we model the frame as a simple beam, then there are six parameters that govern its natural frequency, as given by equation 4 (adapted from Inman [2]):

$$\omega_n = \frac{c_1}{l^2} \sqrt{\frac{EI}{\rho A}} \quad (4)$$

The first two parameters are material properties and geometry determines the next three factors:

- the density, ρ ,
- the modulus of elasticity, E ,
- the cross-section moment of inertia, I ,
- the cross-section area, A , and
- the length of the frame, l .

The method that the beam is supported (whether the end of the beam is fixed, free to move in certain directions, etc.) determines the last variable, c_1 . The truck's frame is supported by the suspension, so the closest support condition would likely be between simply supported and free.

The length of the truck frame is usually fixed by its function. The material used is steel because of its high modulus of elasticity and its low cost. Heavy-truck frame rails are made of steel and have uniform cross-sections through most of their length. This leaves the cross-section shape as the main difference between frame designs. To design a strong cross-section – that is, a cross-section resistant to bending – as much of the mass as possible should be away from the bending axis (this is the reason that a rolled up sheet of paper is much stiffer than a flat sheet). For heavy trucks, C-section beams, as shown in Figure 2-4, are the standard.

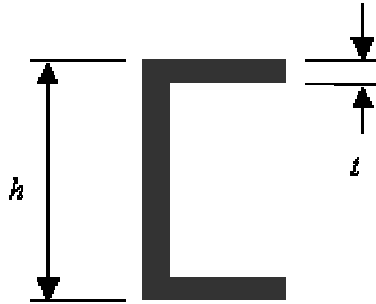


Figure 2-4. Cross-section Geometry of Frame

Much like I-beams used in buildings, C-section beams have much of their mass on their outer edges. Four different trucks were included in this study and each one of them had a different frame cross-section. There were two different heights, h , and each height had two different thicknesses, t . More details on the trucks are contained in Section 2.1 Test Vehicles.

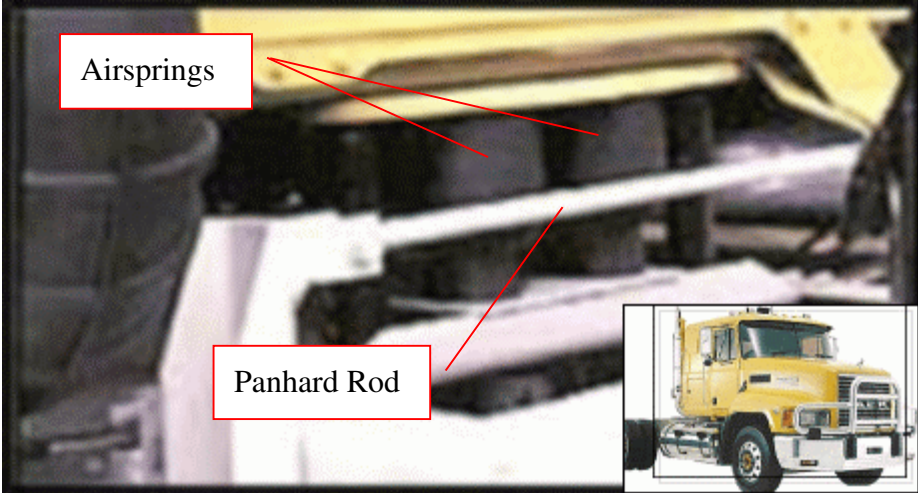
2.3 Cab Suspensions

The ride quality of trucks is much harsher than that of automobiles. As the effects of vibration levels on driver fatigue and performance became better known, cab suspensions were developed to better isolate the driver from road disturbances. The first cab suspensions placed coil springs at all four points of the cab. This greatly reduced the vibration levels of the cab. Studies have shown that rear cab suspensions have a much greater affect on cab vibration levels than front cab suspensions. Eventually, the front cab suspension was removed altogether and replaced with elastomer mounts. As mentioned earlier, the highest vibration levels usually occur during the beaming modes. By using computers to locate the front mounts at nodal points of the frame beaming modes, the decline in ride quality (from removing the front suspension) was minimal.

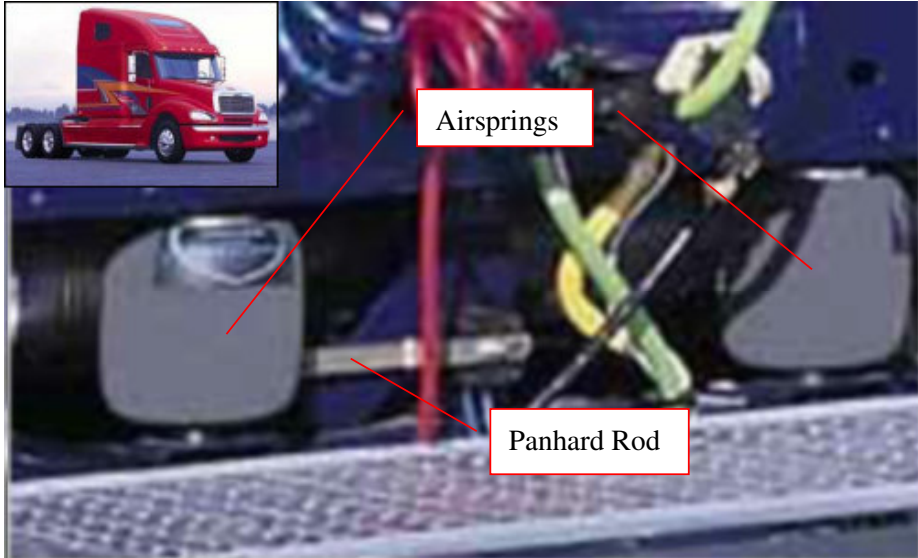
Cab suspension design is similar to the design of the primary suspension. The most important factor is still the natural frequency. A low natural frequency is desired so that the isolation band is large. The natural frequency should be well above the primary suspension's natural frequency. If the natural frequencies of the suspensions were close together, then they would be amplifying the road input at the same frequency range, compounding the problem. Because trucks often have their axle suspension natural frequencies between 1 and 2 Hz, the cab suspension natural frequency is usually designed to be between 2 and 3 Hz.

There are several types of cab suspensions in use today. Most use two springs and two dampers to control the vertical motion of the cab. The springs are usually metal coil springs or

rubber air springs. Using coil springs is simpler and cheaper, but air springs perform better because their ride height and stiffness can be changed to adjust for different cab loading or road surfaces. For controlling the lateral motion, most truck companies use a simple panhard rod, as shown for a Mack CH series and a Freightliner Century Class trucks in Figure 2-5.



(a)



(b)

Figure 2-5. Examples of Panhard Rod Cab Suspensions on (a) Mach CH and (b) Freightliner Century Class

There were two suspensions tested in these experiments from the same manufacturer. The factory suspension currently used on the highway tractors and a new prototype suspension. The current factory suspension uses two air springs and four dampers. The main difference between the factory design and the panhard designs shown earlier is the use of laterally mounted shock absorbers, shown in Figure 2-6, in place of a panhard rod to control lateral loads. These shock

absorbers have stiffness to absorb a lateral impact and damping to dissipate the energy over time. With a panhard rod, lateral impacts would feel much more jolting to the driver because of their large stiffness. The air springs support the weight of the cab along with the front cab mounts and control the vertical motion of the cab. Another distinction of this manufacture's design is that the air springs are placed much farther outboard, as shown in Figure 2-7. This placement allows the air springs to experience larger displacements when the cab rolls. Furthermore, the farther spacing allows a larger moment arm around the cab roll center. These two effects make the air springs much more effective in controlling cab roll than competitive designs. Just inboard of the air springs are two vertically mounted dampers, similar to other cab suspensions. They are mainly used to control the vertical motion and pitch of the cab.

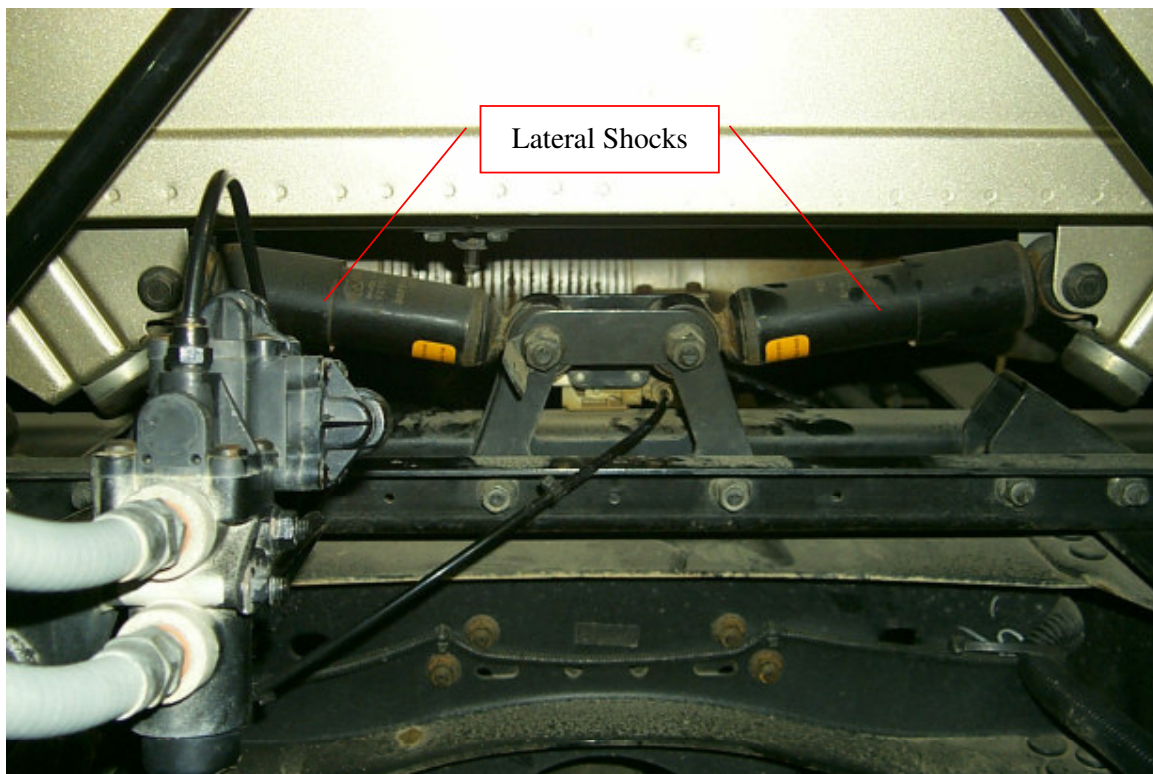


Figure 2-6. Factory Cab Suspension (Lateral Shocks)

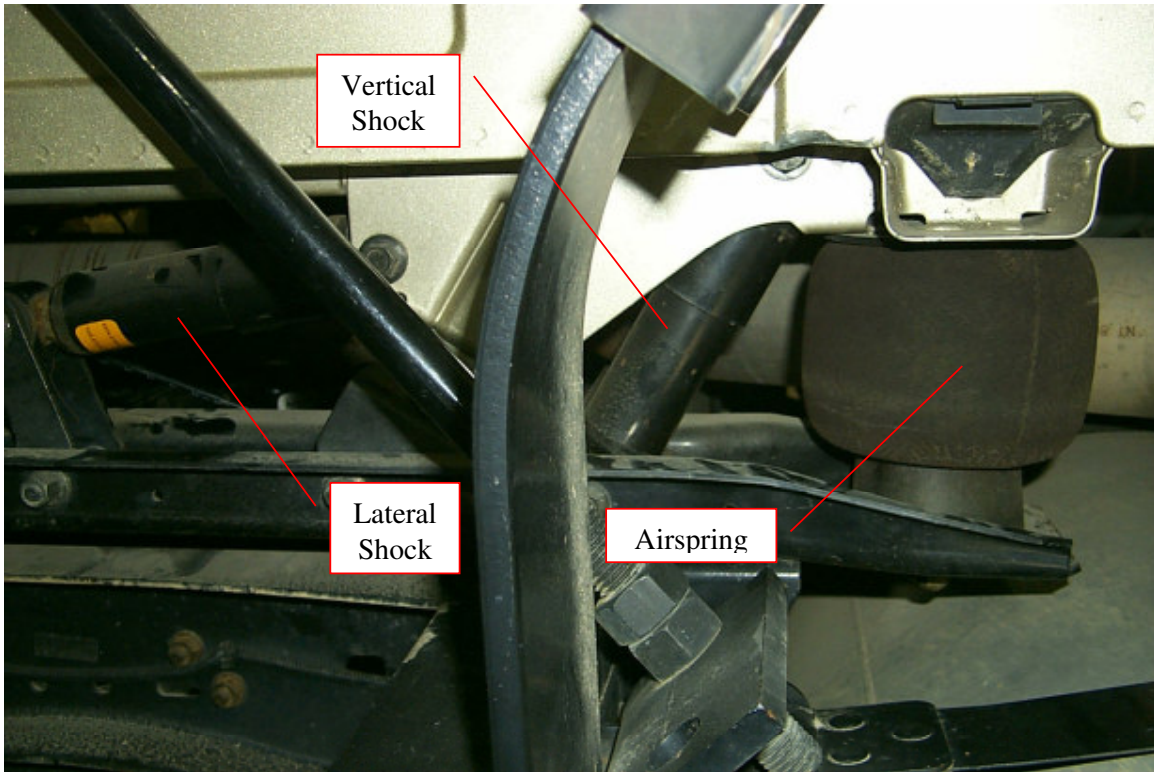


Figure 2-7. Factory Cab Suspension (Airspring)

As can be seen in Figure 2-8, the prototype suspension is quite similar to the factory design. The air springs and vertical shock placement is identical in both suspensions. However, the prototype suspension uses a panhard rod in place of the lateral shocks. Unlike other designs, the panhard rod is connected to an innovative elastomeric torsion spring (Figure 2-9) instead of directly to the frame. This allows much lower stiffness than using a panhard rod alone, thus better isolating the cab from lateral impact loads.

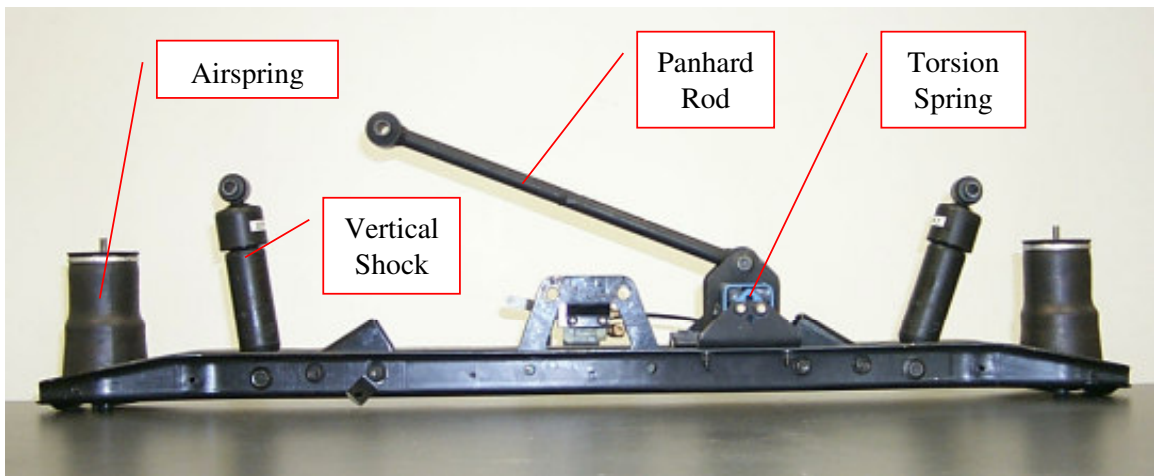


Figure 2-8. Prototype Cab Suspension



Figure 2-9. Elastomeric Torsion Spring of Prototype Suspension

Besides testing the overall suspension layout, different suspension components were also tried. Two different brands of vertical shock absorber were tried. The factory suspension currently uses shock absorbers, which will be referred to as “Shock C”. These are twin-tube dampers and have no stiffness – they only produce force while the shocks are being compressed or extended. The prototype shocks are mono-tube shocks and will be referred to as “Shock M.” Unlike Shock C, these are gas-charged so that they have stiffness as well as damping properties. Also tested were two types of airsprings, shown in Figure 2-10. The L4 airsprings are currently used with the smaller cabs; the L5 airsprings are used with the heavier cabs. The larger base area of the L5 airsprings allows the same load to be supported with less air pressure than the L4 airsprings.



Figure 2-10. Cab Suspension Airsprings

2.4 Literature Review

There are two primary topics covered by this research. The first topic is on frame beaming; the second is on cab suspension design. The majority of the research on these topics was found through the Compendex database.

Before the test phase was started, the effects of reducing the frame thickness were known: the frame would be lighter and more flexible and therefore would likely transmit more motion to the cab. Determining *how much* the ride deteriorated was the goal of this study. To reach this goal, two branches of research were pursued. To start with, a basic background on the phenomenon of frame beaming was necessary. In addition, a proven method of quantifying the ride quality was needed.

There are two papers helpful in gaining an understanding of frame beaming. A. R. Smith had written about the phenomenon of frame beaming as early as 1965 [3]. That paper discusses how the frame material influences the bending stiffness. The effects of load placement on beaming for straight trucks as well as for truck-tractors are also explained. Another much more recent look at beaming was done by Ibrahim, et al. [4]. Using finite element methods (FEM), power spectrums were computed for truck models using both rigid frames and multi-element frames. The results were compared and confirm previous works finding that frame flexibility strongly affects the accelerations of the truck as well as the occupants.

Concerning ride quality, Norsworthy's article in which he correlated subjective driver opinions with various combinations of objective measurements is very helpful. The truck used in the study was a cab-over-engine (COE), but the article is also useful for conventional cabs [5]. The article demonstrates that longitudinal acceleration had a larger effect on driver comfort than vertical acceleration. An article by Sakuma, et al., compares frequency response and power spectrum between simulation results and experimental results [6]. The model was then refined to account for non-linearities and other details; the improved model agreed well with the experimental results. There was also an SAE standard related to measuring whole body vibration [7].

Research on specific cab suspension designs was difficult to locate because of the specialized function and proprietary nature of cab suspensions. Many of the papers were on active and semi-active suspensions such as articles by Nakano, et al. [8], Tong, et al. [9], and

others. Active cab suspensions are not yet offered on any production truck (as of the time of this writing). As trucks designs become more similar, however, a manufacture will likely offer a semi-active suspension to distinguish their vehicle(s).

On the recommendation of Jeff Peddycord, a cab engineer at the manufacturer, I did a patent search on cab suspensions so that I could compare specific designs. There were some interesting ideas. Conway and McKenzie proposed mounting the airsprings at an angle instead of vertically as they are usually mounted [10]. This allows the airsprings to control lateral motion as well as vertical motion. Volvo has a patent on their current suspension [11]. Navistar has a patent on a dual-stage damping design [12]. A low-rate damper is always active in the design and a high-rate damper is engaged only after the displacement exceeds a set threshold value. An anti-sway bar – similar to those on many automobile suspensions – is incorporated in a Freightliner design to control the roll of a COE vehicle [13].

This chapter gave information on vehicle ride and factors that affect vehicle ride, particularly truck frames and cab suspensions. The relevant past works were discussed in the literature review. In the next chapter, the test vehicles and the method of testing will be discussed.

Chapter 3 Test Setup

This chapter provides a detailed description of the tests for the truck frame and truck frame and cab suspension testing that has been in progress. This chapter will describe the details of the test vehicles that were included in this program as well as the dynamic test setup.

3.1 Test Vehicles

The first subsection contains information on the trucks' equipment and condition when they arrived at the test site. Temporary changes had to be made to the trucks to set them up for the shake rig. These changes are contained in Section 3.1.2.

3.1.1 Vehicle Descriptions

There were four trucks tested. All of the vehicles were complete and operational Class 8, 6x4 road tractors such as the one shown below in Figure 3-1. The first truck was a standard production vehicle with a low-frame design. This truck was used to establish baseline measurements and will be referred to as the "Standard Low." The next truck was similar to the first one, except that it had a prototype lightweight frame. To judge its ride quality, the vibration levels of the second truck, the "Thin Low," were compared to the Standard Low. The next two trucks were larger models equipped with high frames. One truck, the "Standard High," had a factory frame and served as a benchmark for the fourth truck, the "Thin High," which had a prototype lightweight frame. The main differences between the vehicles, summarized in Table 3-1, were in the sleeper sizes and wheelbases indicated in Figure 3-1, and in the frame cross section. In Table 3-1, h refers to the frame height and t refers to the frame thickness, as indicated in Figure 2-4.

Table 3-1. Important test vehicle parameters

Name	Model	Sleeper length	Wheelbase	Frame, $h \times t$
Standard Low	VNL 660	61 in. (1550 mm)	215 in. (5460 mm)	266 mm x 8 mm
Thin Low	VNL 660	61 in. (1550 mm)	215 in. (5460 mm)	266 mm x 7 mm
Standard High	VNL 770	77 in. (1960 mm)	229 in. (5810 mm)	300 mm x 7 mm
Thin High	VNL 770	77 in. (1960 mm)	239 in. (6070 mm)	300 mm x 6 mm

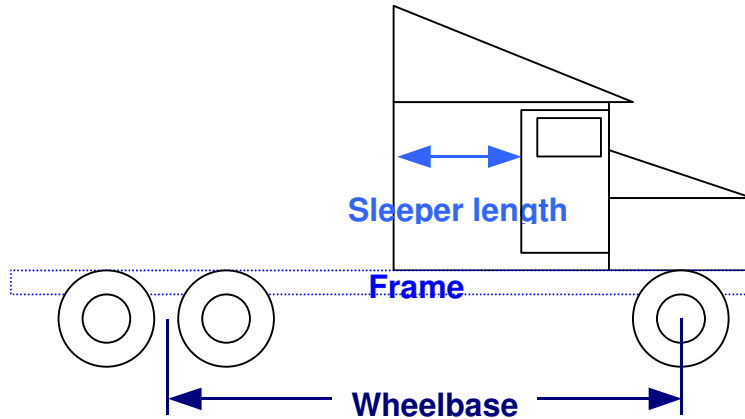


Figure 3-1. Important test vehicle parameters

There were several other differences between the trucks that contributed to the vibration modes of the vehicles. These included the fuel tank size and number, the type of exhaust system, and whether or not the trucks had lower chassis fairings.

In addition, the first truck tested had a special fuel tank arrangement. Only the driver-side tank was supplying fuel to the engine. This tank was removed at our test facility and replaced with an empty 570 L (150 gal) tank (supplied by the manufacturer) that was not reconnected to the fuel system. These modifications were necessary to simulate the effects that various fuel loads had on vehicle vibration and driver comfort. The tanks were filled with various levels of water in place of diesel fuel for testing convenience.

3.1.2 Vehicle Modifications for Shake Rig

Several temporary changes had to be made to each test vehicle before dynamic testing could begin. In order to have greater control over the stiffness of the suspension and the ride height of the vehicle, the load-leveling system and accompanying plumbing had to be modified. With the original bogey suspension, the two driver-side airsprings were linked to each other and the two passenger-side airsprings were linked together as diagrammed in Figure 3-2. The plumbing for the air suspension was rerouted, as diagrammed in Figure 3-3, so that the front drive axle is on an independent air supply. This allowed the ride height of each drive axle to be modified independent of each other. By removing the connection between the truck's air supply and the drive axles, changes to the ride height could be made without affecting other truck components that used compressed air such as the secondary (cab) suspension and the brakes. Dynamic testing was performed only on the front drive axle; the wheels were removed from the rear drive axle and then that axle was strapped to the frame as shown in Figure 3-4.

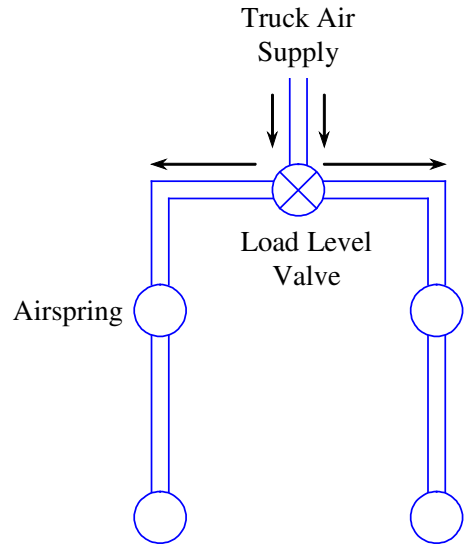


Figure 3-2. Original Rear Suspension Plumbing Layout

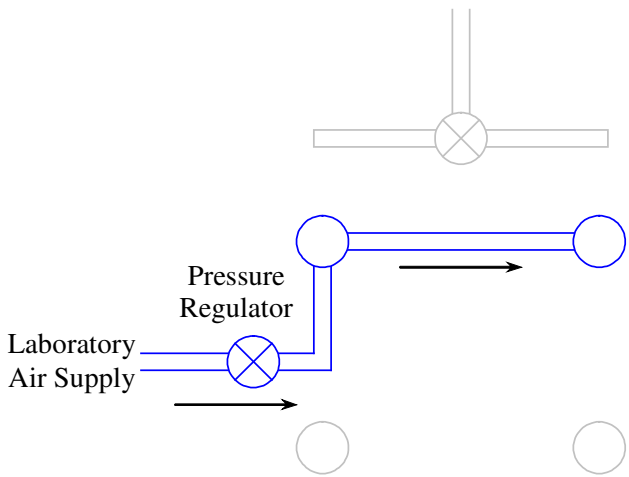


Figure 3-3. Modified Rear Suspension Plumbing Layout

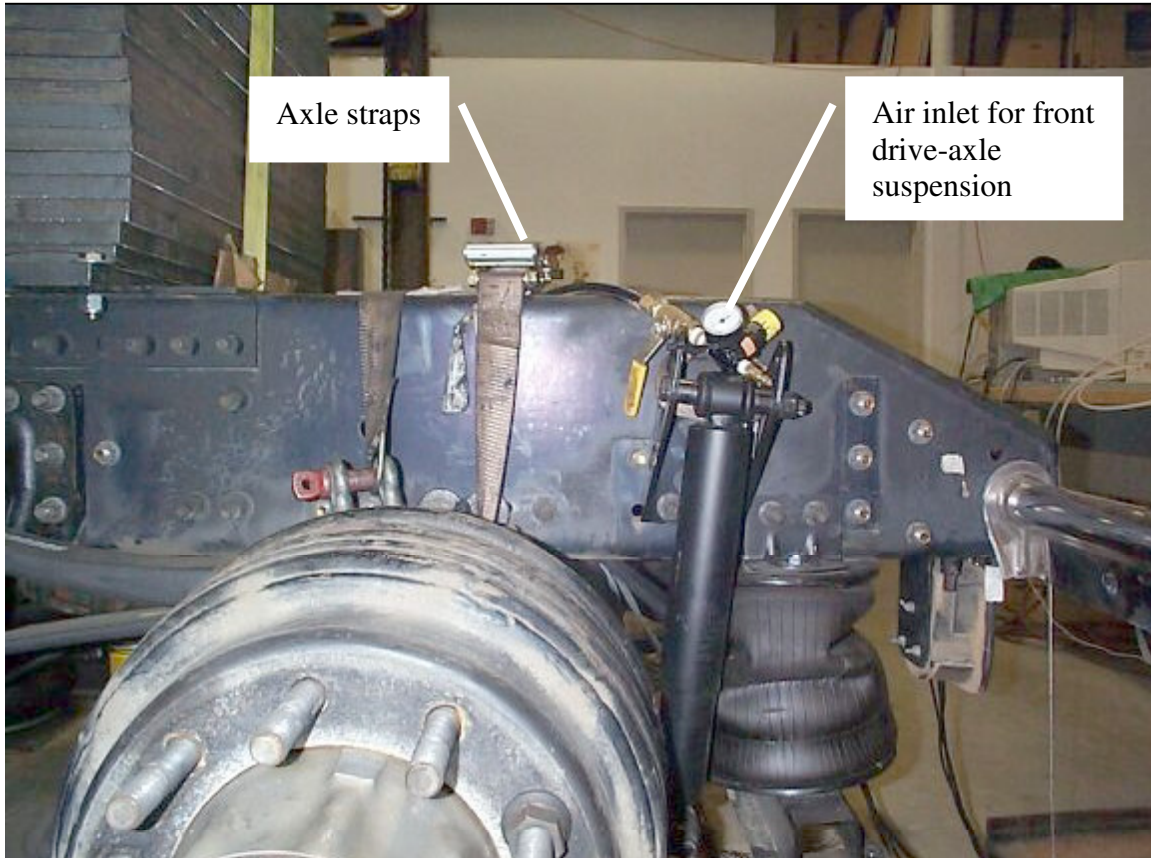


Figure 3-4. Rear Drive Axle

The vehicles arrived at our laboratory equipped with a fifth wheel. Testing requires attachment to the vehicle frame at the location of the fifth wheel, so it had to be removed. In its place, a 1-in. thick steel plate (called the fifth wheel adapter plate) was mounted to the frame so that the truck could accept the weight plates for dynamic testing. To simulate a trailer load, weight was added to the vehicle frame on top of the fifth wheel plate. This additional weight consisted of a stack of 34 metal plates, 350 lb (159 kg) each, that were strapped to the fifth wheel plate. Figure 3-5 shows the weight stack on a test vehicle. With these modifications, the weight on the test axle was approximately 15,000 lb (6800 kg).

In order to support the static axle load, two airsprings (Goodyear Model 1B14-350) were attached to the axle, one at each end. An “L”-shaped metal fixture was bolted between the brake drum on the axle and the modified brake drum; this fixture was attached to the top of the auxiliary airspring, as shown in Figure 3-6. One of the two actuators and its mounting system is also shown in this figure. By regulating the auxiliary airsprings to 70 psi (483 kPa), each actuator supported approximately 3000 lb (1361 kg) at rest and was not overloaded during testing.

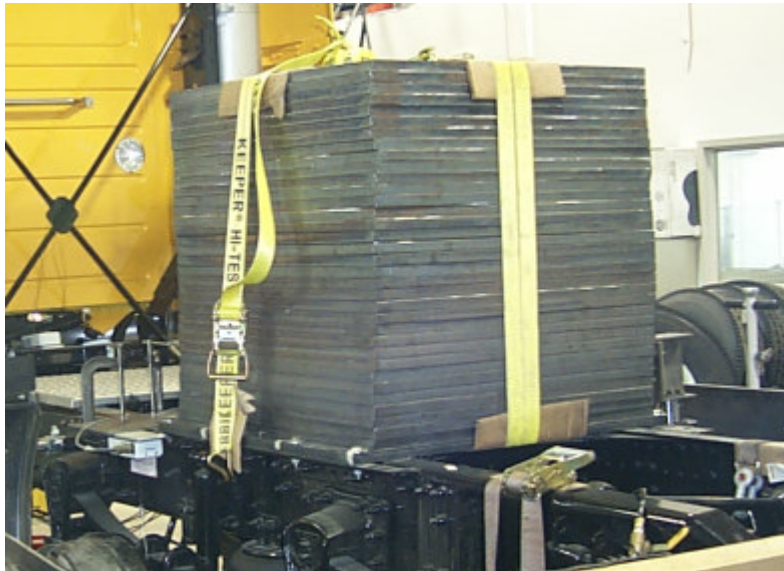


Figure 3-5. Weight Stack on Test Vehicle

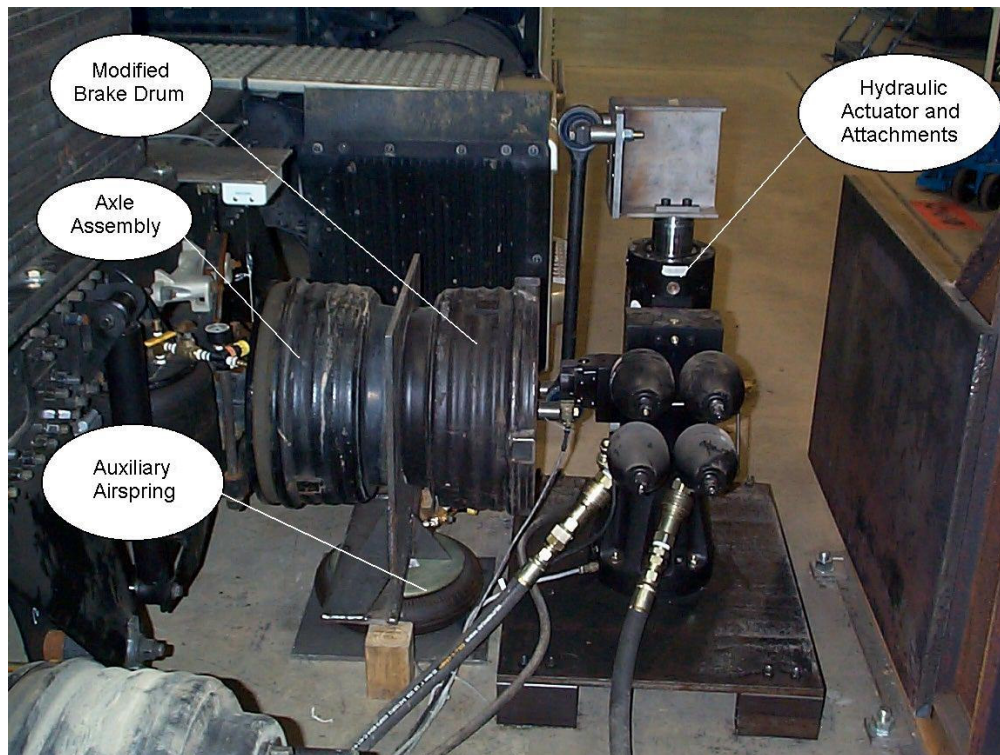


Figure 3-6. Dynamic Actuation Setup with Auxiliary Airspring

The main air supply hose from the engine-mounted air compressor was disconnected from the truck's air supply. The supply hose was originally connected to the air dryer located under the cab (Figure 3-7), but the hose was replaced with new tubing connected to an external valve and fitting (Figure 3-8). This was done so that the truck's engine would not need to be run to keep its air supply at 120 psi (827 kPa). Even with the rear suspension disconnected, the air supply is still needed for the air brakes and the cab suspension. Air from the laboratory compressor was used to pressurize the air system before testing.



Figure 3-7. Air Dryer with Inlet Bypass Hose



Figure 3-8. Inlet to Air Dryer

3.2 Dynamic Test System

Descriptions of how the vehicle was shaken and how data was collected during the tests are covered in this section.

3.2.1 Actuation of Suspension

A computer was used to control the actuation of the suspension during dynamic testing. For each test, the input – which included a chirp, bump, or pure tone signal – was created in Simulink (Version 5.3.0.10183) and then downloaded into dSPACE Control Desk (Version 1.2 P2). dSPACE provided the user interface for controlling the tests and recording the data. The dSPACE output was used as an external input to the MTS 458.20 hydraulic controller, shown in Figure 3-9. The controller regulated motion of the hydraulic actuators (MTS Model 248.03) mounted to each axle end. Each actuator could be controlled independently. This allowed to us to conduct two types of tests. During the “heave” tests, the actuators were sent identical signals. The passenger-side signal was inverted for the “roll” tests. Thus, each actuator moved in opposite directions. The physical setup for actuation of the suspension during dynamic testing, including the hydraulic actuator and attachments, was shown in Figure 3-6.



Figure 3-9. MTS 458.20 Hydraulic Controller

3.2.2 Data Acquisition

As mentioned in the previous subsection, data collection and recording of all measurements were performed with dSPACE. A dSPACE AutoBox DS 2201 data acquisition unit, converted to use 110 VAC, recorded data from all the measurement devices on a desktop computer. To be well above the Nyquist frequency, a sampling rate of 100 samples per second was chosen (the highest test frequency in any of the input signals was 16.5 Hz). Also, the built-in anti-aliasing filters of the AutoBox prevented data acquisition errors brought about by signal

aliasing. The measurements performed in dynamic testing included accelerations, displacements, and actuator load.

Accelerations were measured with PCB Model U352C65 accelerometers, such as the one shown in Figure 3-10 (a penny is shown for scale). These accelerometers were acceptable for use in the range of frequencies tested in this study (0.5 - 16.5 Hz). To power the accelerometers and increase the resolution of their output, a PCB ICP 16 channel signal conditioner was used. The accelerometers plug into the signal conditioner, which has BNC outputs that go to the AutoBox. Displacements were measured with Unimeasure VP510-10 Linear Variable Differential Transformers (LVDTs).



Figure 3-10. PCB Model U352C65 Accelerometer

3.2.3 Instrument Locations

On the test vehicles, acceleration and position were recorded at several points, including on the frame, at the back of the cab, and at the driver-side B-post. Several different instrumentation arrangements were used throughout the tests. Originally, two accelerometers were used at the B-post, five on the frame, and one at the back of the cab, as well as two LVDTs measuring frame displacement and one measuring displacement across the cab suspension. As testing progressed, more sensors were added, primarily when roll testing was introduced to the program. The final configuration had three accelerometers at the B-post, five along the frame, and four at the back of the cab. Figure 3-11 diagrams this layout, which will be expanded upon

further on in the section. Four LVDTs were used on the frame and two LVDTs were used across the cab suspension so that cab roll could be more easily measured, as diagrammed in Figure 3-12. This raised the total number of data channels to 20 (including two from the actuators themselves), which was the maximum number of channels that the AutoBox could handle.

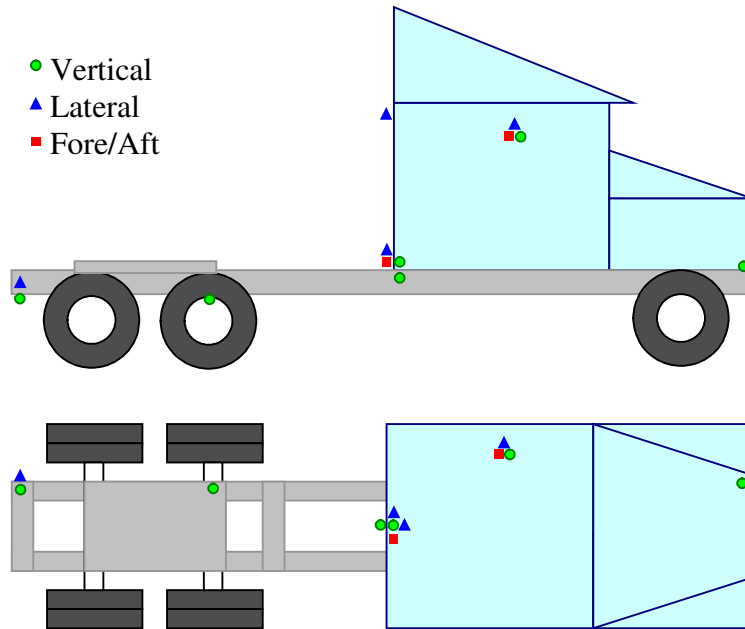


Figure 3-11. Accelerometer Layout

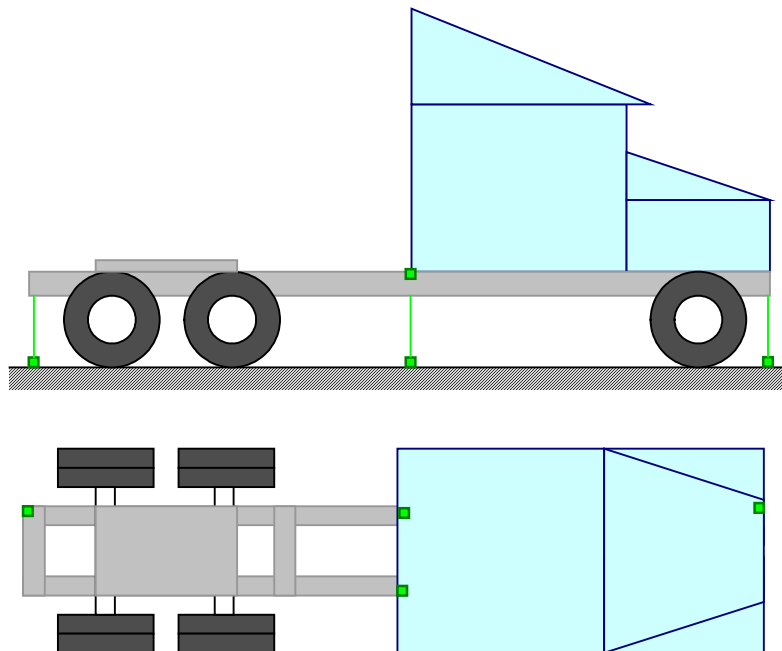


Figure 3-12. LVDT Layout

The cab suspension is shown in Figure 3-13. The two LVDTs measuring the cab suspension displacement can be seen in this view. Additionally, four accelerometers were in this area: the fore/aft and lateral accelerometers at the back of the cab (Figure 3-14a), the vertical accelerometer at the back of the cab (Figure 3-14b), and the vertical accelerometer on the frame at the cab suspension (Figure 3-15a). A second lateral accelerometer at the back of the cab was mounted higher up, at the drip rail (Figure 3-15b). Inside the cab, the three accelerometers were mounted at the B-post on the driver-side seat belt anchor (Figure 3-16). This site is commonly used in the trucking industry for evaluating ride for two reasons: (1) it is close to the driver's head (where fore-aft and lateral vibration matters the most) and (2) it is a rigid mounting location.

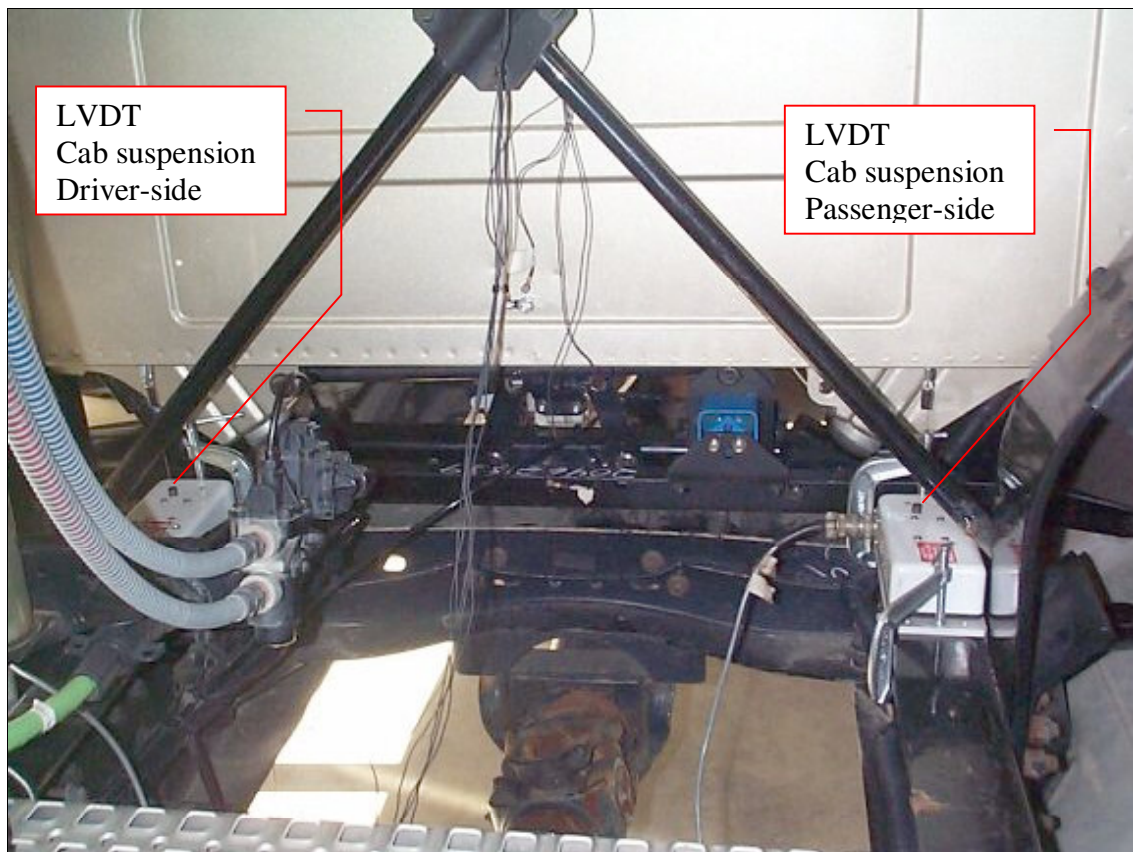


Figure 3-13. Rear Cab Suspension Sensors (LVDTs labeled)

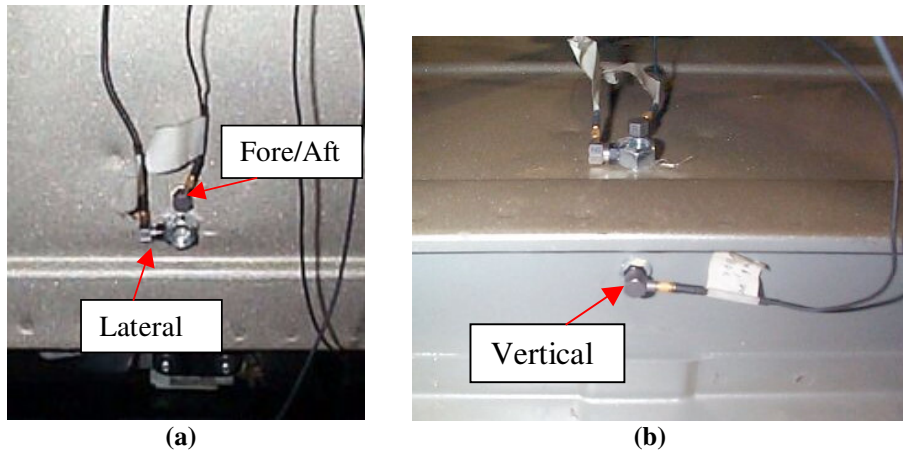


Figure 3-14. Sensors at Rear, Bottom of Cab near Cab Suspension: (a) Lateral and Fore/Aft Accelerometers; (b) Vertical Accelerometer

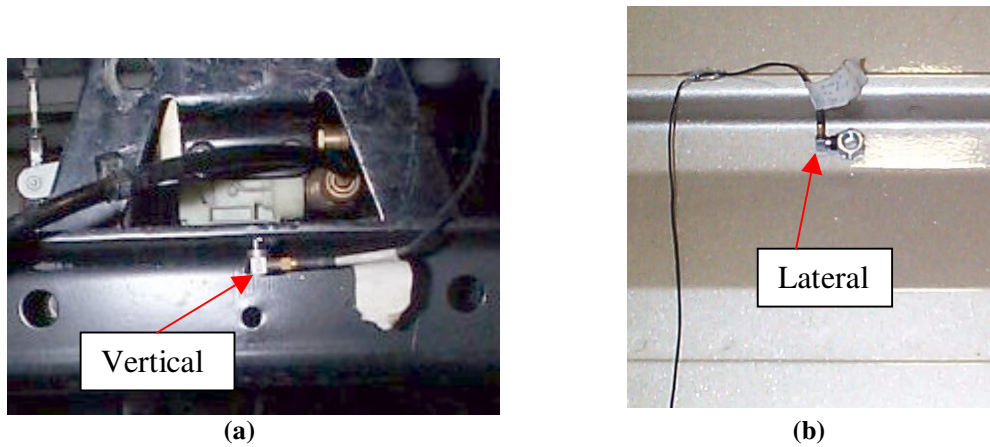


Figure 3-15. Other sensors at Back of Cab: (a) Vertical Accelerometer on Frame at Cab Suspension; (b) Lateral Accelerometer at Drip Rail

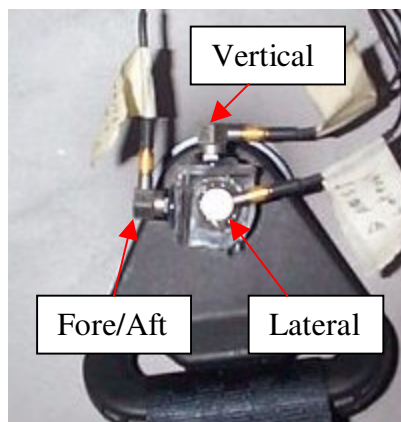


Figure 3-16. Accelerometers Mounted at B-post

More accelerometers were mounted along the frame rail: one at the front (Figure 3-17a), one at the second axle (Figure 3-17b), and two at the rear (Figure 3-18a). Initially there was another accelerometer mounted at the fifth wheel location (Figure 3-18b), but this was moved to measure B-post lateral vibration (Figure 3-16) after roll testing was added to the program. Four LVDTs measuring relative position from the ground to the frame also captured frame movement. Two of these are directly below the cab suspension, as shown in Figure 3-19. There is also one at the front (Figure 3-20a) and one at the rear (Figure 3-20b) of the driver-side frame rail.



Figure 3-17. Frame Accelerometers (a) at Front and (b) at Second Axle

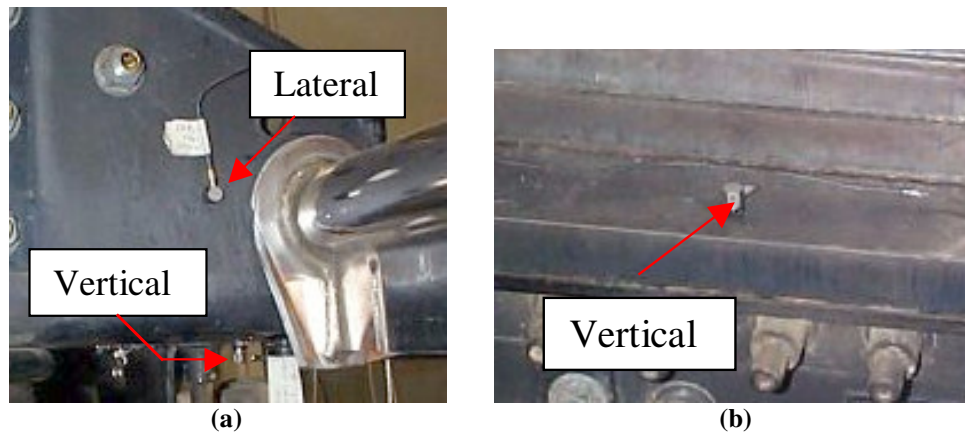


Figure 3-18. Frame Accelerometers (a) at Rear and (b) at Fifth Wheel Stack

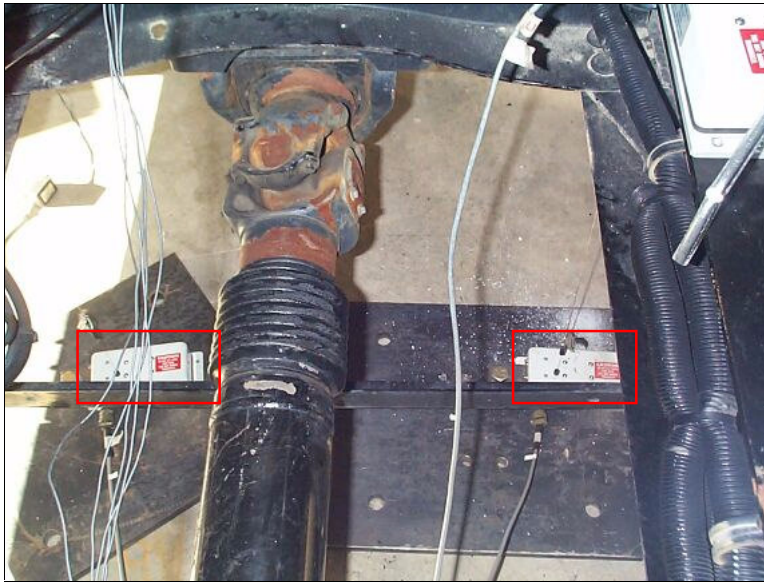


Figure 3-19. Frame LVDTs at Back of Cab



(a)



(b)

Figure 3-20. Frame LVDTs **(a)** at Front and **(b)** at Rear of Driver-Side Frame Rail

Chapter 4 Ride Number Metric

This chapter will present the ride number metric used in this research. The purpose for using this metric will be explained in the first section, followed by a summary of the results in Section 4.2. Section 4.3 will explain the calculation process. The results for each truck will be reviewed in more detail in Sections 4.4 - 4.7. Section 4.8 will compare the ride between the trucks, closing out this chapter.

4.1 Ride Metrics

Most of the results from the series of tests conducted will be shown in the Frequency response spectrums in Chapter 5. With so much data, however, it can be difficult to compare the overall performance of the trucks and suspension combinations to each other by just looking at frequency responses. Calculating a single “ride number“ for each test provides a more convenient way of comparing different truck configurations. The drawback is that, with a single number, one can't tell exactly why one suspension has a lower number. Perhaps one suspension performs better in the fore/aft direction at the cab suspension frequency. Then again, maybe it performs well in the vertical direction during the beaming mode. There is no way to tell simply from the ride number. Used in conjunction with the frequency spectrums, however, ride numbers can be very useful for a quick overview. It must be noted that ride numbers are input dependant. As such, one can only compare ride numbers resulting from the same input. With a different input signal, it is possible that the best performing suspension in these tests could change.

4.2 Summary of Results

There were several significant findings from the ride numbers. Shock M absorbers produced 9.1% lower ride numbers during the heave tests (lower numbers are better). In the roll tests, the biggest difference occurred when the suspension was switched to the prototype design, which produced ride numbers that were 20% higher on average. There was no significant difference in ride number (4.90 versus 4.91) when L4 airsprings were used in place of L5 airsprings, or vice-versa. Surprisingly, the average ride number for each truck was also very close: 4.98 for the Standard Low, 4.91 for the Thin Low, 4.90 for the Standard High, and 4.83 for the Thin High. These results are shown in Table 4-1. The calculation process will be explained next in the following section.

Table 4-1. Average ride numbers

Truck	Suspension	Heave	Roll	Total
Standard Low	Suspension F	4.44	1.82	4.68
	Suspension P	4.62	2.32	5.28
	Shock M	4.82	2.05	5.16
	Shock C	4.23	2.08	4.80
	L4 airsprings L5 airsprings	4.49 4.57	2.09 2.05	4.97 4.99
Thin Low	Suspension F	4.38	2.08	4.89
	Suspension P	4.11	2.34	4.94
	Shock M	4.56	2.26	5.18
	Shock C	3.93	2.16	4.65
	L4 airsprings L5 airsprings	4.22 4.27	2.21 2.21	4.90 4.93
Standard High	Suspension F	4.49	2.52	4.66
	Suspension P	4.68	3.05	5.13
	Shock M	4.73	2.83	5.03
	Shock C	4.44	2.74	4.76
	L4 airsprings L5 airsprings	4.57 4.60	2.77 2.81	4.87 4.92
Thin High	Suspension F	4.57	2.54	4.66
	Suspension P	4.37	3.03	5.13
	Shock M	4.57	2.83	5.03
	Shock C	4.38	2.75	4.76
	L4 airsprings L5 airsprings	4.50 4.44	2.80 2.77	4.87 4.92

4.3 Calculation Process

The ride number is calculated from the B-post accelerometers. These are representative of the accelerations that the driver would feel. To calculate the ride number, there are five steps involved. The first step is to calculate the frequency spectrum at the B-post from the time domain. After that, the ISO weights (Figure 4-1) are applied to the acceleration spectrums [7]. This is to account for the fact that the human body is more (or less) sensitive to vibrations at different frequencies. Figure 4-2 shows how this weighting affects the frequency spectrum.

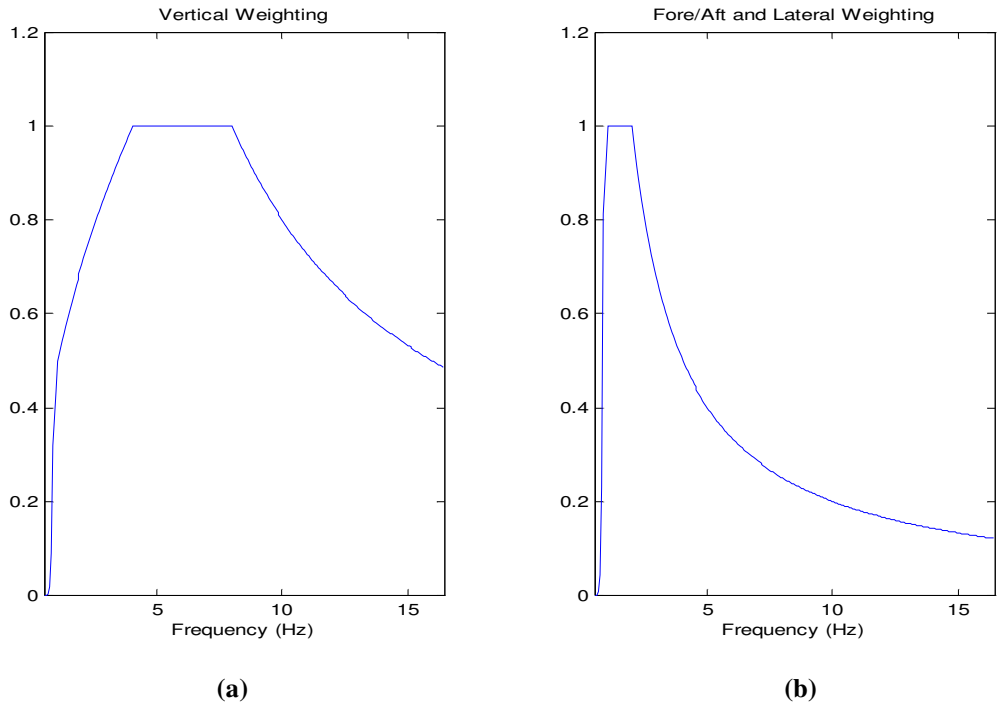


Figure 4-1. ISO weighting charts

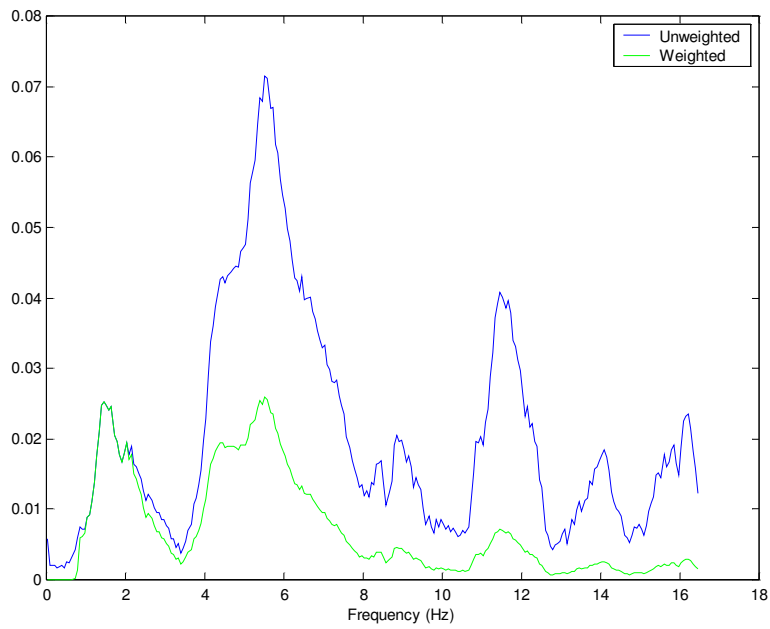


Figure 4-2. Unweighted and weighted B-post fore/aft acceleration response

The next step is to integrate the weighted frequency responses at each of the B-post accelerometers. This reduces each frequency spectrum to a single number. Because the human body is sensitive to the direction of motion as well as the frequencies, another weighting factor is applied and the B-post ride numbers are combined as shown below:

$$RideNumber = \sqrt{V_W V_N^2 + FA_W FA_N^2 + L_W L_N^2} \quad (5)$$

where, V_W is the vertical weighting factor, V_N is the vertical ride number, FA_W is the vertical weighting factor, FA_N is the vertical ride number, L_W is the vertical weighting factor, and L_N is the vertical ride number. The vertical weighting factor was 1.0; both the fore/aft and lateral weighting factors were 2.0.

When the ride number is calculated from road or track testing data, this is the last step in the process. For the lab tests, however, heave and roll inputs were applied separately while they occur simultaneously during actual vehicle operation. To account for this, a third weighting factor was applied to the data using the assumption that the truck behaves similar to a linear system. With a linear system, the total response to two or more inputs is equal to the sum of the individual responses. In other words, the predicted response to a combined heave and roll input (such as that seen during road testing) is equal to the response from the heave input plus the response to the roll input. This leaves one question: how much of the input that the axle is normally subjected to is in-phase (heave) and how much is out-of-phase (roll)? This was debated and eventually we decided that the typical road input would be about 67% heave and 33% roll. After normalizing the roll number to account for the smaller input amplitude (compared to the heave signal) used in testing, the total ride number was calculated as follows:

$$TotalRideNumber = 0.67(HeaveRideNumber) + 0.33(RollRideNumber) \quad (6)$$

Of course, other weighting factors could be selected to match driving conditions that are more biased towards either heave or roll motion. The total ride numbers were computed for each truck for all eight combinations and are shown in the following subsections. For all the ride numbers, a lower number is better. To keep the figures simple, the cab suspension combinations were labeled according to the alphanumeric code listed in Table 4-2. Using this convention, a suspension configuration consisting of Suspension P with Shock M and L4 airsprings is referred to as “PM4.”

Table 4-2. Cab suspension abbreviations for plots

Component	Symbol	Variant
Suspension Design	F	Suspension F (factory suspension)
	P	Suspension P (prototype suspension)
Shock Absorbers	C	Shock C (factory shocks)
	M	Shock M (prototype shocks)
Airsprings	4	L4 airspring (factory spring for medium sleeper)
	5	L5 airspring (factory spring for large sleeper)

4.4 Standard Low Results

Figure 4-3 shows the ride numbers from the heave tests. The M performed better in the vertical and combined tests. In the roll tests, Figure 4-4, the prototype suspension had higher accelerations, just as will be shown in the frequency spectrums in the next chapter. In Figure 4-5, the change in ride number (relative to the factory suspension configuration) is shown for each suspension. A negative number indicates a reduction in ride number and, therefore, an improvement in ride quality. The best performing suspension combination was the factory suspension (Suspension F) with Shock M. This is no surprise considering the first two plots. Also, as mentioned in the previous section (but not shown), there was little difference when the airspring is switched.

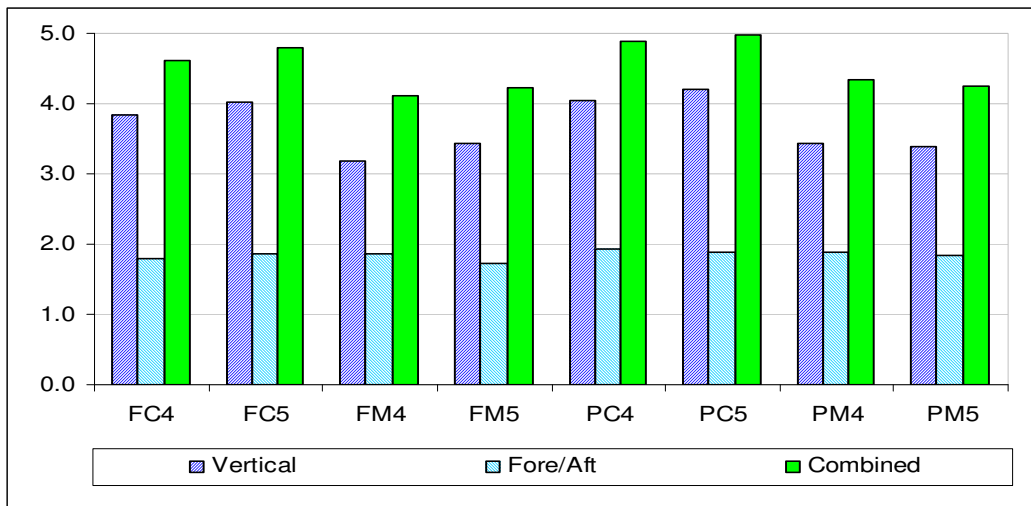


Figure 4-3. Standard Low heave ride numbers

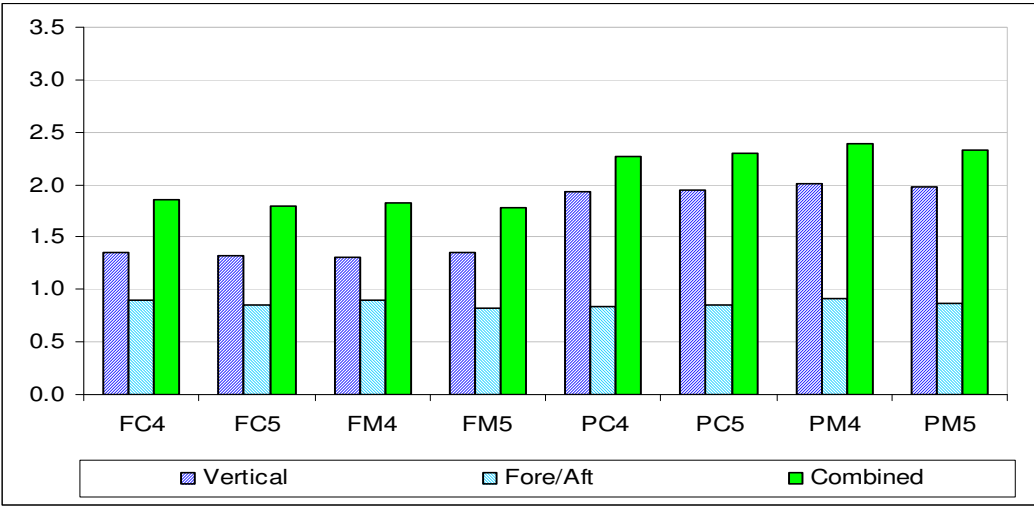


Figure 4-4. Standard Low roll ride numbers

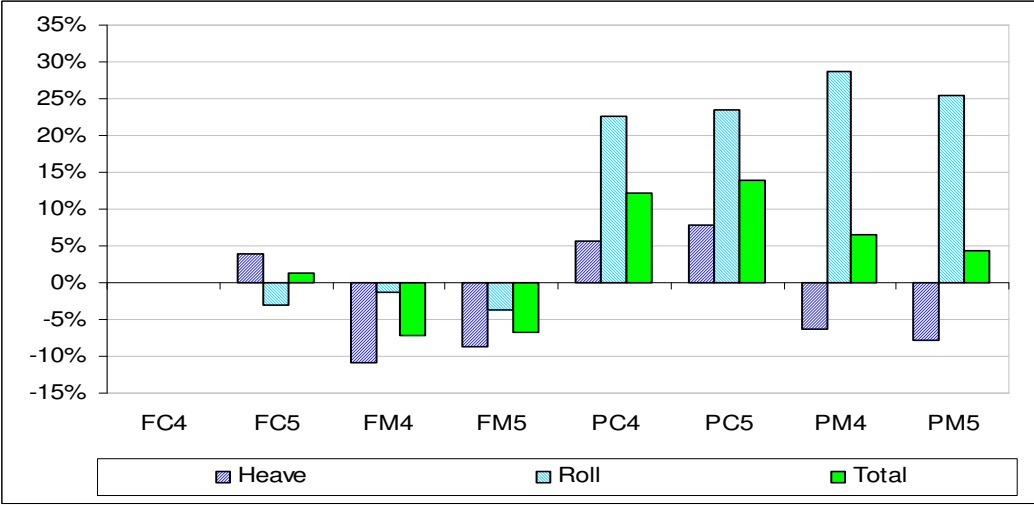


Figure 4-5. Standard Low total ride number change compared to factory configuration

4.5 Thin Low Results

The ride numbers indicate that the behavior of the Thin Low was similar to the Standard Low: better heave performance (Figure 4-6) with Shock M, better roll performance (Figure 4-7) with Suspension F, and best overall performance (Figure 4-8) with the Shock M/Suspension F combination.

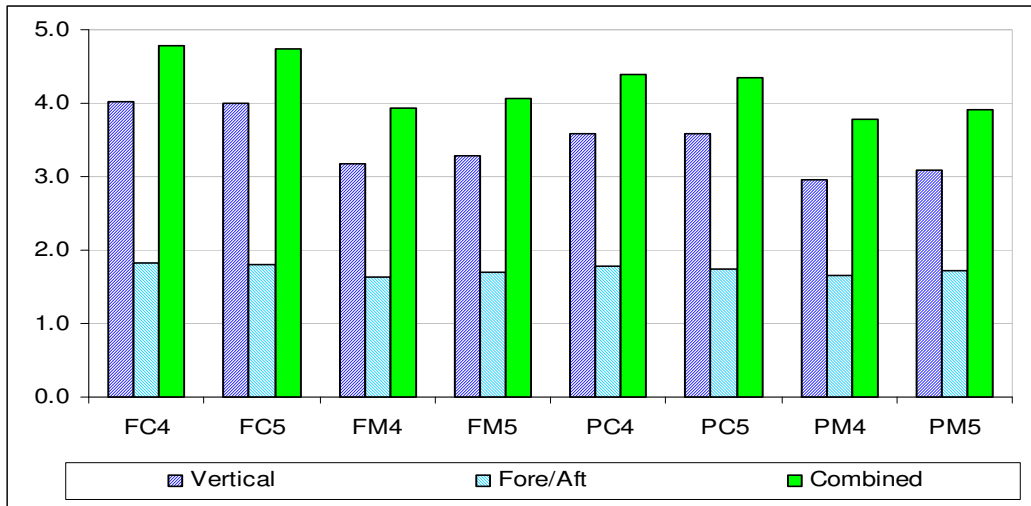


Figure 4-6. Thin Low heave ride numbers

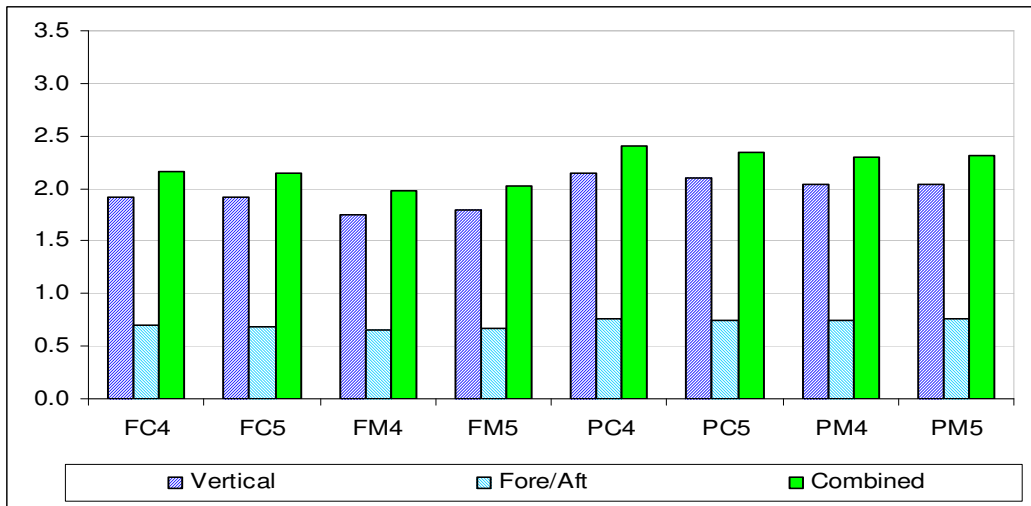


Figure 4-7. Thin Low roll ride numbers

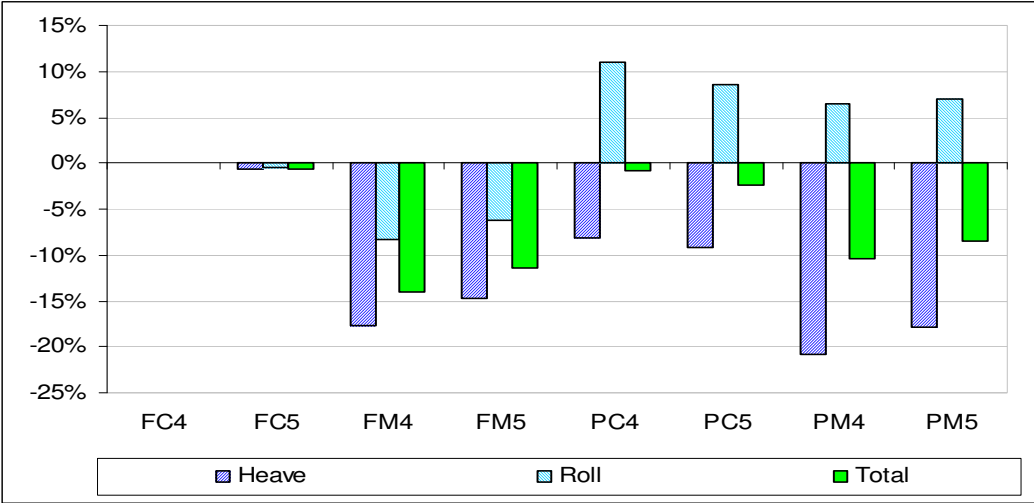


Figure 4-8. Thin Low total ride number change compared to factory configuration

4.6 Standard High Results

The Standard High also performed best with Suspension F and Shock M. The heave performance is shown in Figure 4-9, roll performance in Figure 4-10, and total performance in Figure 4-11. However, Shock C did have slightly lower fore/aft accelerations. Also note that the both 770s were equipped with lateral accelerometers at the B-posts. This accelerometer data was included in the combined performance, so the ride numbers computed for the 770s will be higher (given the same amount of vibration) than for the 660s. This is particularly evident in the roll results because of the larger lateral accelerations.

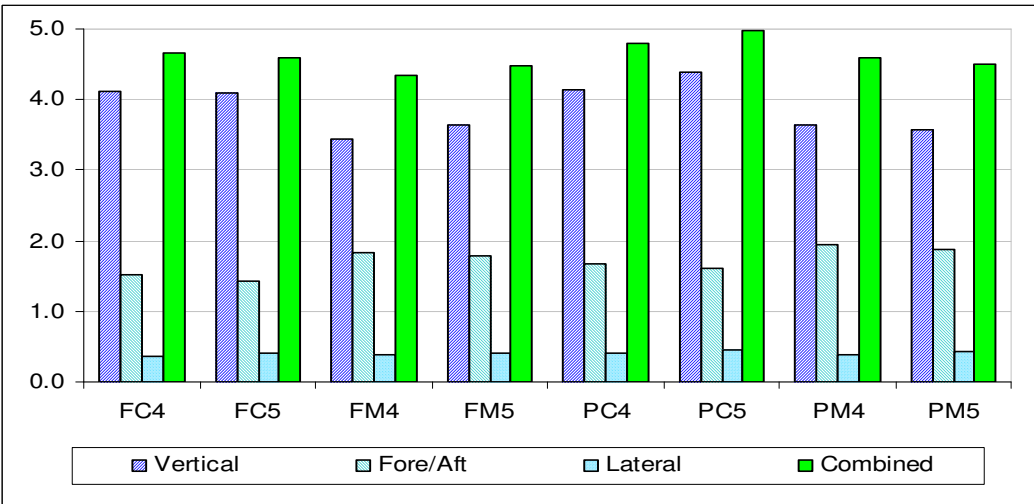


Figure 4-9. Standard High heave ride numbers

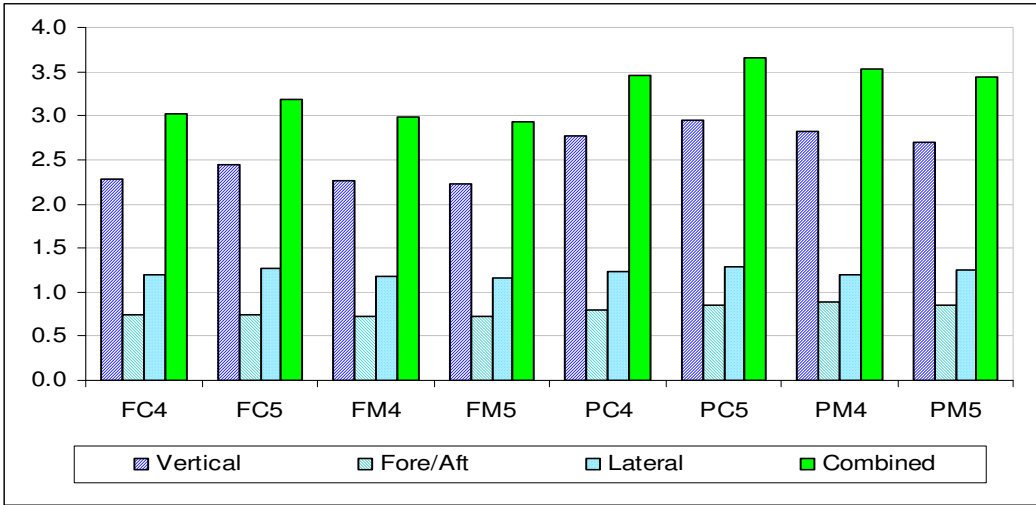


Figure 4-10. Standard High roll ride numbers

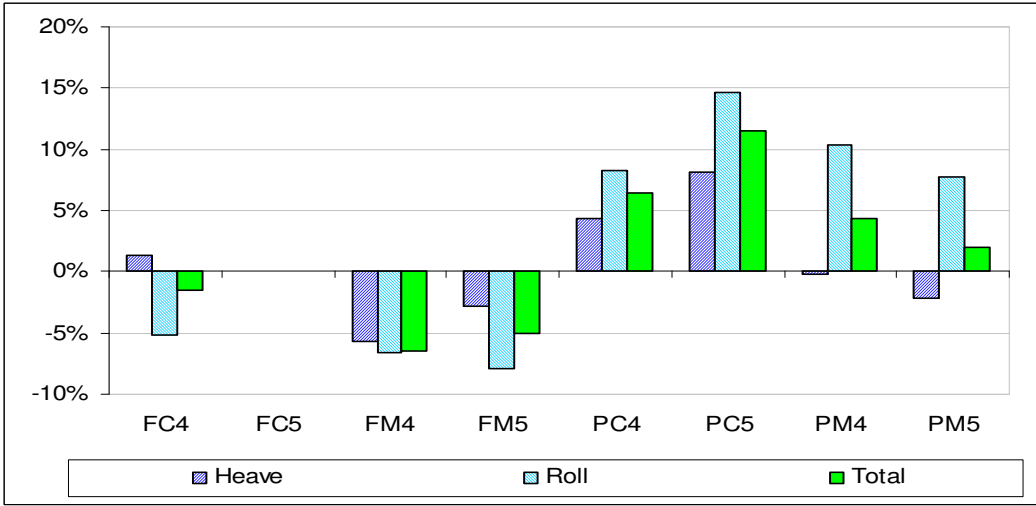


Figure 4-11. Standard High total ride number change compared to factory configuration

4.7 Thin High Results

Similar to the Standard High results, Shock M had slightly lower vertical and combined accelerations during the heave tests, as shown in Figure 4-12. In the roll tests, there was again a significant increase in vertical and total acceleration as demonstrated by the ride numbers in Figure 4-13. There was almost no change in the fore/aft and lateral ride numbers. Investigating the total ride numbers in Figure 4-14, a small surprise occurs. Unlike the other three trucks, the best performing suspension was the factory configuration – with Shock C dampers. Another difference that was not noticed – compared to other suspension combinations – is that there was

a significant change in performance when the airspring was switched. In view of this fact, it is likely that the airspring tested with the “FC5” test shown here was probably the original airspring on the truck and not the L5 airsprings used in other tests. Also, note that while Shock M did not take first place this time, the overall change in performance was less than 5% (green bars). Considering the overall picture of all eight suspension combinations, Shock M remains a better choice. As a side note, this series of tests shows that the age and variability of the airsprings are factors that could affect the suspension performance.

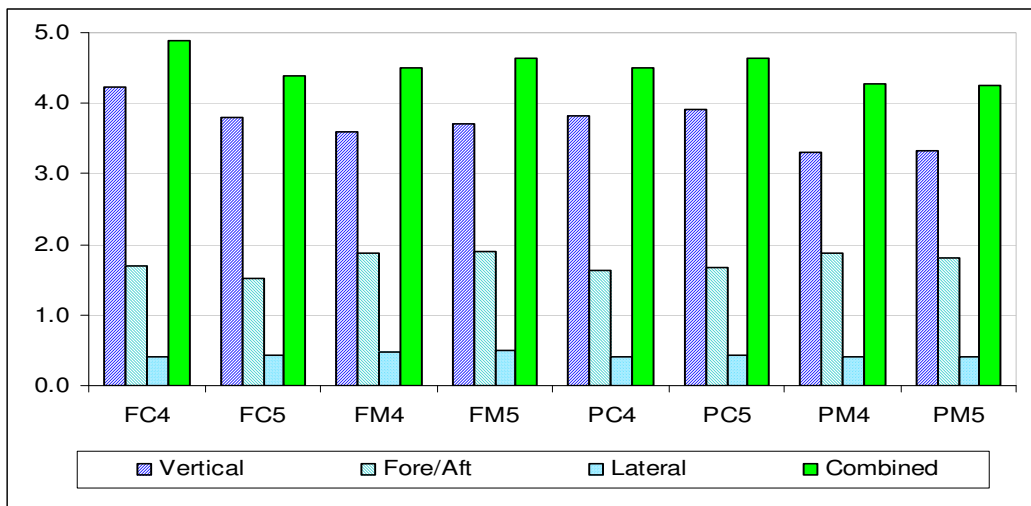


Figure 4-12. Thin High heave ride numbers

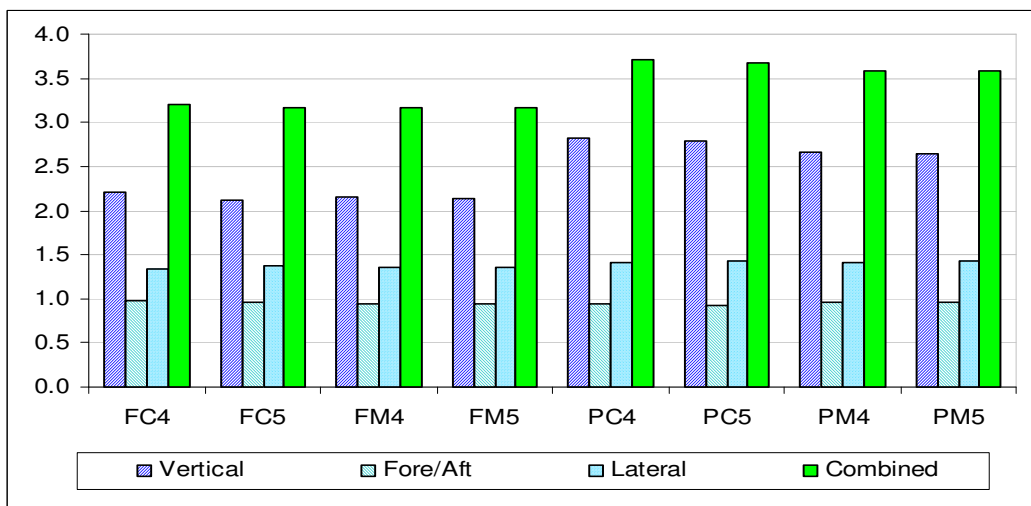


Figure 4-13. Thin High roll ride numbers

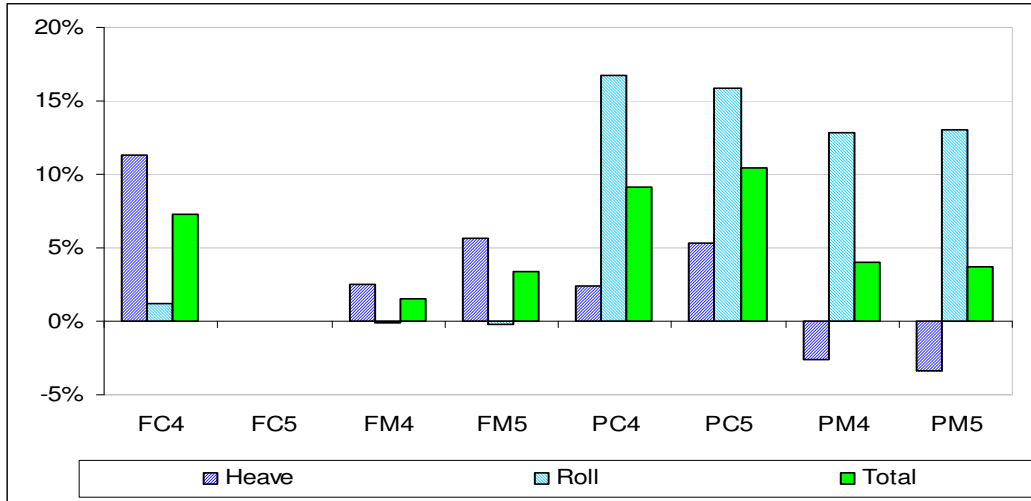


Figure 4-14. Thin High total ride number change compared to factory configuration

4.8 Comparison between Trucks

This section compares the Lightweight trucks to their Baseline counterpart. Figure 4-15 shows that the Thin Low with the factory suspension configuration had an 8% higher ride number than the Standard Low. However, when equipped with Shock M in place of Shock C, the Thin Low had a 7% lower ride number than the Standard Low. The Thin High had a 5% lower ride number than the Standard High straight from the factory, as shown in Figure 4-16. With Shock M, the ride number was 4% lower than the Standard High. When equipped with each of their best suspensions, the four trucks had total ride numbers that were very close, as depicted in Figure 4-17. Comparing each of these suspensions to the average of the four (Figure 4-18) reveals that the 660s performed better in the heave tests, but the 770s did better in the roll tests. As presented earlier, Table 4-1 lists the average ride number achieved for each suspension element.

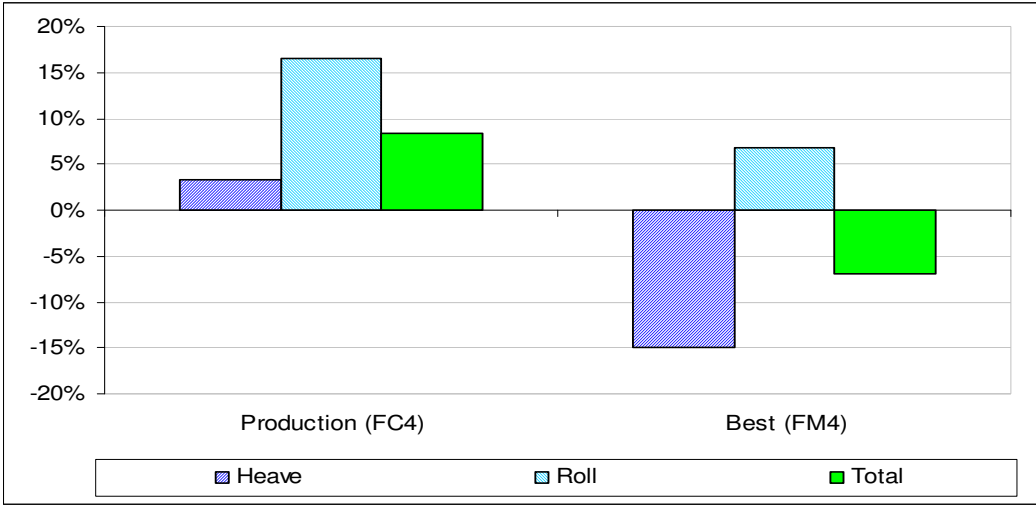


Figure 4-15. Thin Low total ride number change compared to Standard Low with factory configuration

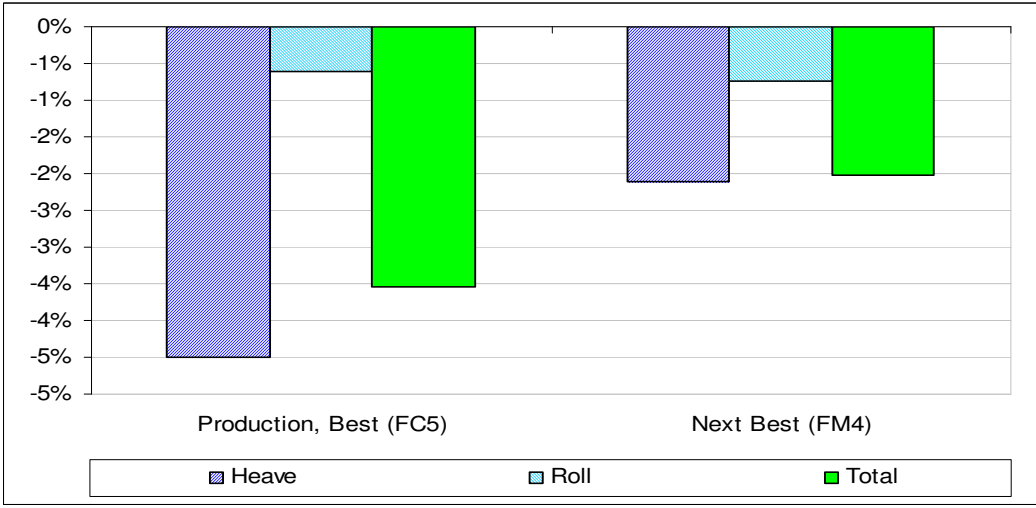


Figure 4-16. Thin High total ride number change compared to Standard High with factory configuration

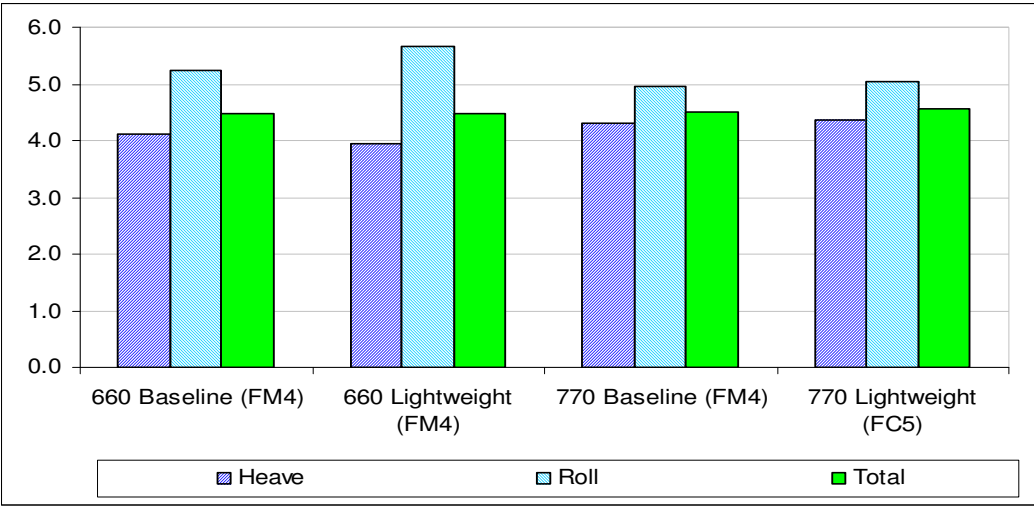


Figure 4-17. Best suspensions total ride numbers

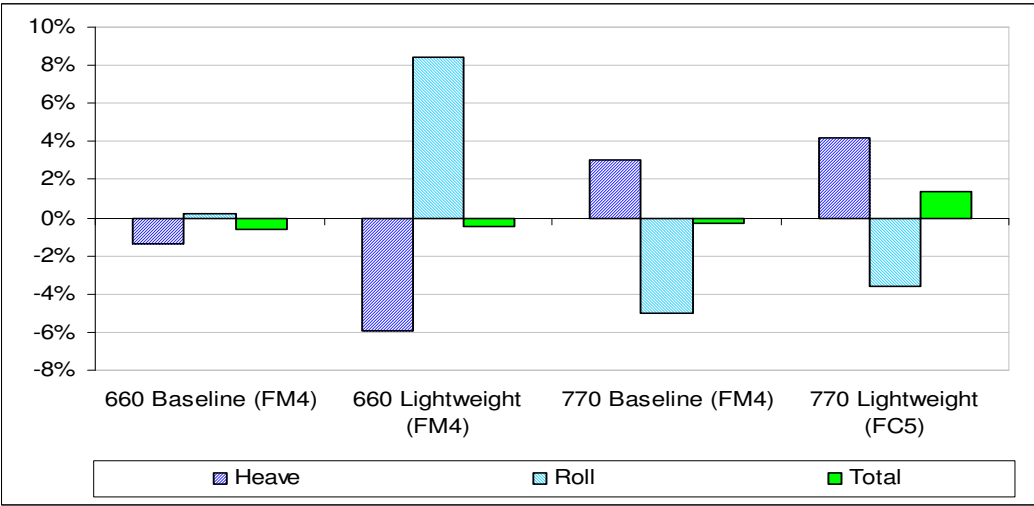


Figure 4-18. Change from mean of the best suspension for each truck

Chapter 5 Frequency Response Spectrum

This chapter will present the frequency spectrums obtained from the chirp input signal. In Section 5.1, a description of the chirp signal and its purpose will be explained. Important overall results will then be given in Section 5.2. There are five sections in this chapter: one for each truck (Sections 5.3 thru 5.6) and a final section (Section 5.7) comparing the trucks. In each section, the heave results are examined first, followed by the roll results. In addition, the “Standard Low Results” section contains a discussion of the parametric study on fuel tank level.

5.1 Chirp Input Signal

A chirp signal is a sine wave with increasing frequency. The frequency of the chirp signal used for this study increased linearly from 0.5 Hz to 16.5 Hz. A sample input wave is shown in Figure 5-1. The purpose of the chirp signal is to excite the test vehicle at all its major modes. To analyze the chirp data, the sensor outputs (in the time domain) were converted to the frequency domain. Any peak in the frequency spectrum would indicate a natural frequency of one or more of the vehicle’s components (axle suspension resonance, frame beaming, etc.).

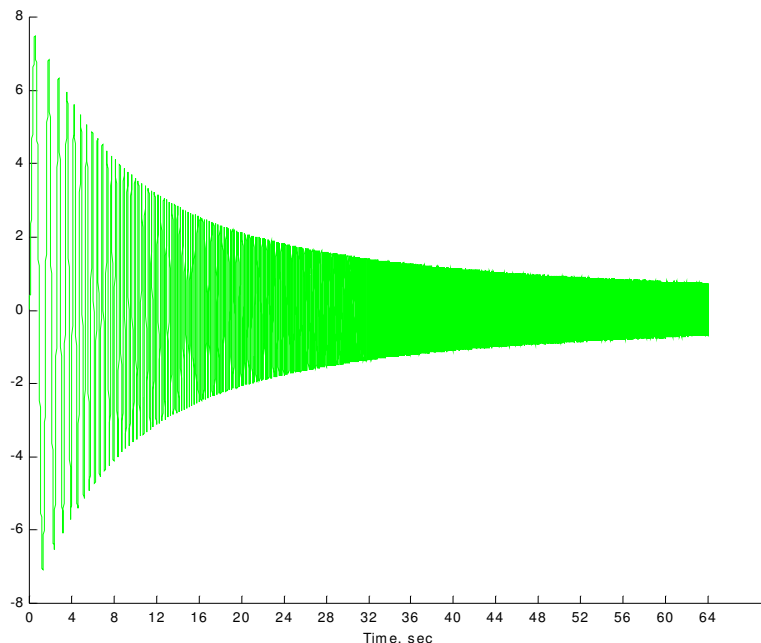


Figure 5-1. Sample chirp input signal

The frequency is attenuated with a 2 Hz low-pass filter. Because signal power increases with the square of the frequency, too much energy would have been sent to the truck without the filter, possibly damaging the test vehicle. The amplitude could instead have been set to decrease with the square of the frequency, holding the power constant; if this was done, however, the input amplitude would have been too low to properly excite the truck at the higher frequencies.

5.2 Summary of Results

The ride numbers from Chapter 4 are based on the frequency response spectrums, so the same findings noted earlier are also evident from the results shown here. During the heave tests, Shock M yielded lower B-post accelerations than original Shock C dampers; during the roll tests, the factory suspension performed better than Suspension P. The frequency response spectrums allow us to see why. For example, the results discussed later on will show that Shock C actually produce lower fore/aft B-post accelerations than Shock M, but Shock M produce better overall results due to their superior vertical acceleration performance. In addition, since the general range for beaming is known from observation, the specific beaming frequency of each truck can be determined from the frequency spectrums (Table 5-1). A higher beaming frequency is an indicator of a stiffer frame.

Table 5-1. Test vehicle summary

Test Vehicle Name	Beaming Frequency	Frame (h x t)
Standard Low	5.6 Hz	266 x 8 mm
Thin Low	5.0 Hz	266 x 7 mm
Standard High	5.8 Hz	300 x 7 mm
Thin High	6.0 Hz	300 x 6 mm

As mentioned earlier, a parametric study on how the fuel level affects vibrations was also conducted in addition to the cab suspension testing. The fuel tank study was the first batch of tests conducted. Acceleration power spectrums were used to analyze this data. For subsequent tests, the data was processed to show acceleration amplitude. As mentioned earlier, power goes up with the square of the frequency. Therefore, by plotting amplitude instead of power, the lower frequency values will be larger relative to the higher frequency amplitudes. The lower frequency values are more important to ride comfort, and plotting amplitudes allows one to better see the differences between the suspensions at these lower frequencies. The acceleration amplitude

values are display in g's (gravitational units), so that the information would be easier to relate to than using m/s². For example, a reading of 0.10 g's means that the accelerometer is feeling an additional force equal to one-tenth the normal pull of gravity. In addition, a different algorithm was used (after the fuel tank study) to produce the frequency spectrum plots from the raw time data. This new algorithm increases accuracy at the cost of decreased smoothness between frequencies.

Except for the fuel tank study, two plots are shown for each accelerometer of interest. The first shows the full frequency scale (0.5 – 16.5 Hz); the second plot contains just the frequencies 0.5 - 3.5 Hz. The cab suspension reaches resonance in this range. Because of the large accelerations at the higher frequencies, the scale often makes it difficult to see differences among the cab suspensions in this range. For the Standard Low, this second plot is just a zoomed view of the first plot; for the other trucks, the second plot was produced from a 30-second chirp signal that went from 0.5 Hz to 3.5 Hz.

5.3 Standard Low Results

This subsection shows the results on the testing on the first truck, the Standard Low truck. The parameters of this truck are listed in bold in Table 5-2. For brevity, only results from the testing with the factory L4 airsprings are shown. The results from switching airsprings were not significantly different.

Table 5-2. Important test vehicle parameters

Name	Model	Sleeper length	Wheelbase	Frame, <i>h x t</i>
Standard Low	VNL 660	61 in. (1550 mm)	215 in. (5460 mm)	266 mm x 8 mm
Thin Low	VNL 660	61 in. (1550 mm)	215 in. (5460 mm)	266 mm x 7 mm
Standard High	VNL 770	77 in. (1960 mm)	229 in. (5810 mm)	300 mm x 7 mm
Thin High	VNL 770	77 in. (1960 mm)	239 in. (6070 mm)	300 mm x 6 mm

5.3.1 Vibration Effects of Fuel Level

Fuel level affects vibration in two main ways: (1) changing the mass and (2) changing the damping. The third vibration component, stiffness, is not affected: adding liquid to the tanks does not make the truck measurably more or less rigid. These results can be seen in the plots, which are from heave tests with the factory cab suspension.

As the mass of a system increases, the resonant frequencies decrease. The mass of the truck with the plates was ~13,000 kg (29,000 lb.). Adding 190 L (50 gal) of water to both fuel

tanks added 380 kg (1018 lb.) to the mass. This is a 3% increase in mass, so only a small decrease in frequency would be observed. From the vertical accelerometer data at the cab suspension (Figures 5-2 and 5-2), a small decrease in the low frequency (< 8 Hz) peak locations can be seen each time that fuel is added. The accelerometers at the B-post show the same phenomenon as shown in Figures 5-4 and 5-5. The amplitude remains relatively unaffected at the low frequencies. Intuitively one might expect that the amplitudes would decrease as the mass increases. However, the input we are sending is a displacement signal (just as the wheels would see on-road) so the actuators automatically respond to the increased mass by increasing the driving force proportionately.

The movement of the liquid in the tanks influences the damping effects. Essentially, the liquid's center of mass is being shifted back and forth. The energy required to move this center of mass is the source of the damping. While the tank is low, as more liquid is added the mass increases and so does the damping effects. However once the tank is past one-half full, the damping decreases when liquid is added. This is because there is less room for the water to shift: the displacement of the center of mass decreases faster than the mass increase. A completely full tank (with no air) would act very similarly to a solid mass, exhibiting little or no damping. Because damping increases with velocity, there is not much difference between the plots at low frequencies. At the higher frequencies, the effects of damping are most noticeable when the tank is one-third or two-thirds full.

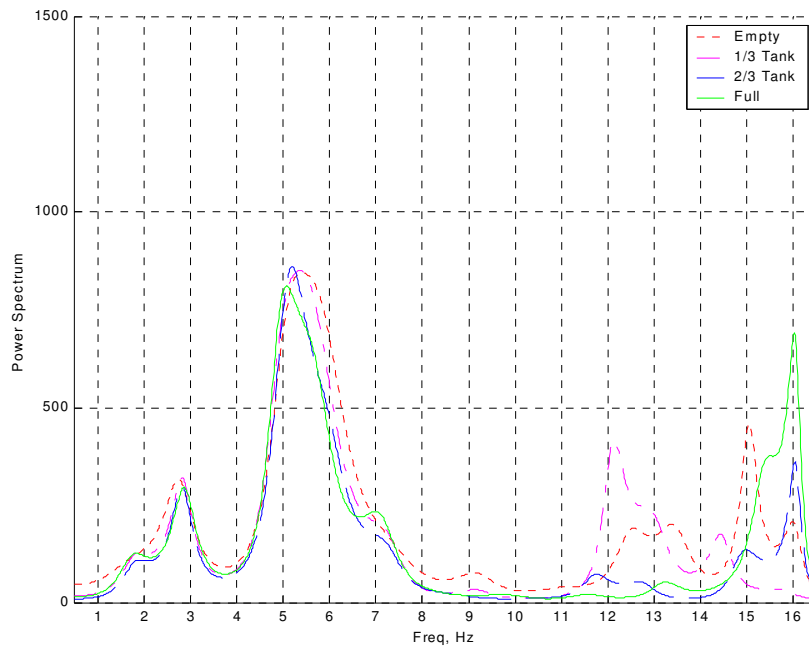


Figure 5-2. Standard Low Vertical Acceleration of Frame at Rear Cab Suspension for Various Tank Fluid Levels

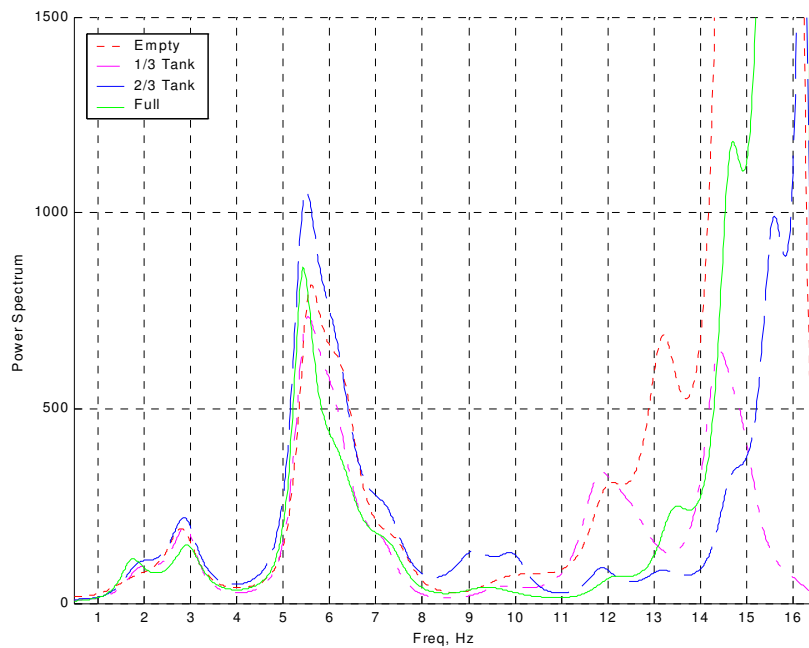


Figure 5-3. Standard Low Vertical Acceleration of Cab at Rear Cab Suspension for Various Tank Fluid Levels

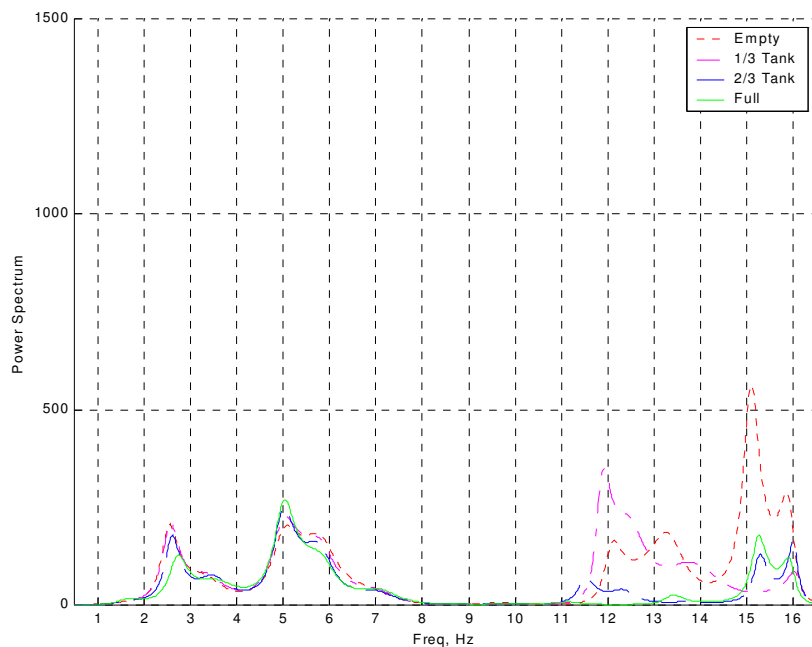


Figure 5-4. Standard Low Vertical Acceleration of B-post for Various Tank Fluid Levels

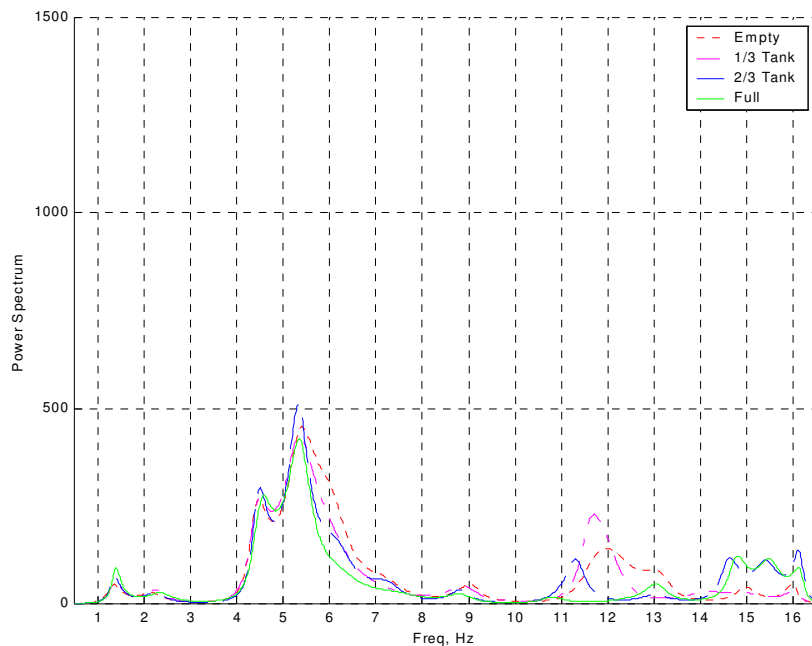


Figure 5-5. Standard Low Fore/Aft Acceleration of B-post for Various Tank Fluid Levels

5.3.2 Heave Cab Suspension Study

Figures 5-6 and 5-7 show the acceleration of the frame at the cab suspension. The beaming frequency can be seen at about 5 Hz. Examining the vertical accelerometer data at the back of the cab (Figures 5-8 and 5-9), the beaming is also quite evident. The cab natural frequency can also be seen at 2 - 3 Hz. The vertical acceleration at the B-post (Figures 5-10 and 5-11) shows two trends: at the low frequencies, Shock M (green and magenta lines) produce lower accelerations, but at higher frequencies the performance depended on the suspension and not on the shocks. The fore/aft acceleration (Figures 5-12 and 5-13) also shows a low frequency dependence on the shock, but this time Shock C performed better. Also, note that the accelerations at the cab suspension frequency were higher for vertical acceleration than for the fore/aft measurements (0.03 - 0.04 g versus 0.025 - 0.03 g).

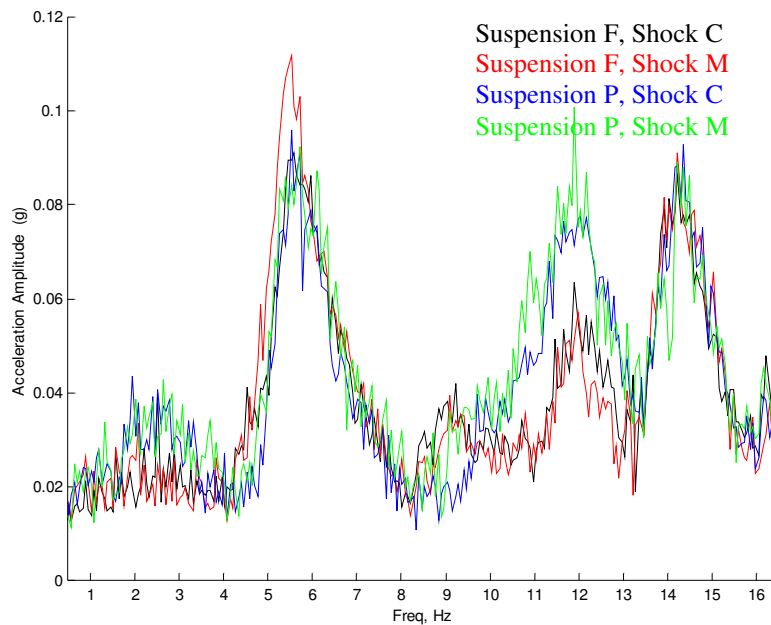


Figure 5-6. Standard Low Vertical Acceleration of Frame at Rear Cab Suspension for Different Cab Suspension

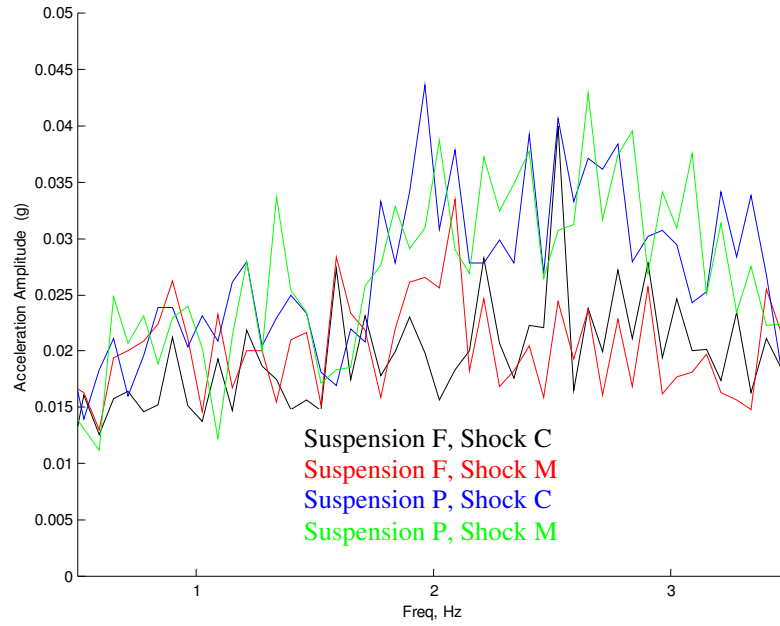


Figure 5-7. Standard Low Vertical Acceleration of Frame at Rear Cab Suspension for Different Cab Suspensions

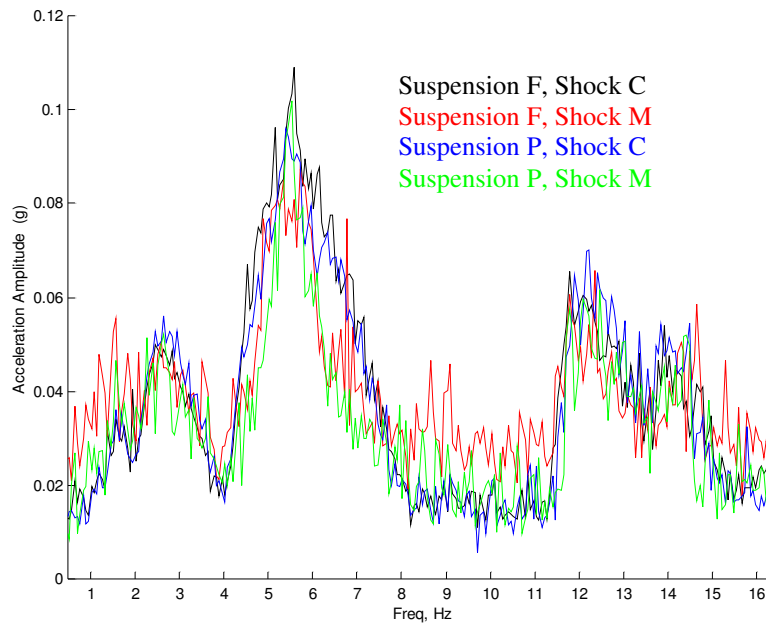


Figure 5-8. Standard Low Vertical Acceleration of Cab at Rear Cab Suspension for Different Cab Suspensions

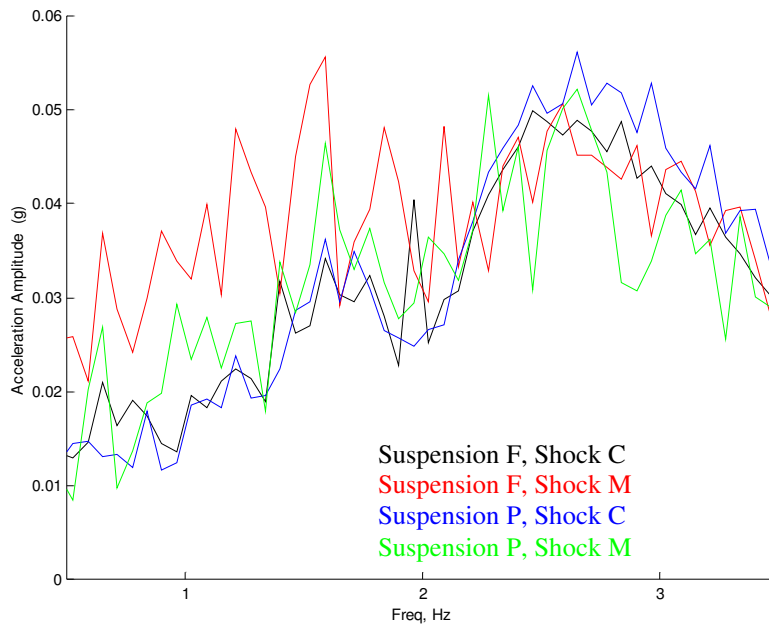


Figure 5-9. Standard Low Vertical Acceleration of Cab at Rear Cab Suspension for Different Cab Suspensions

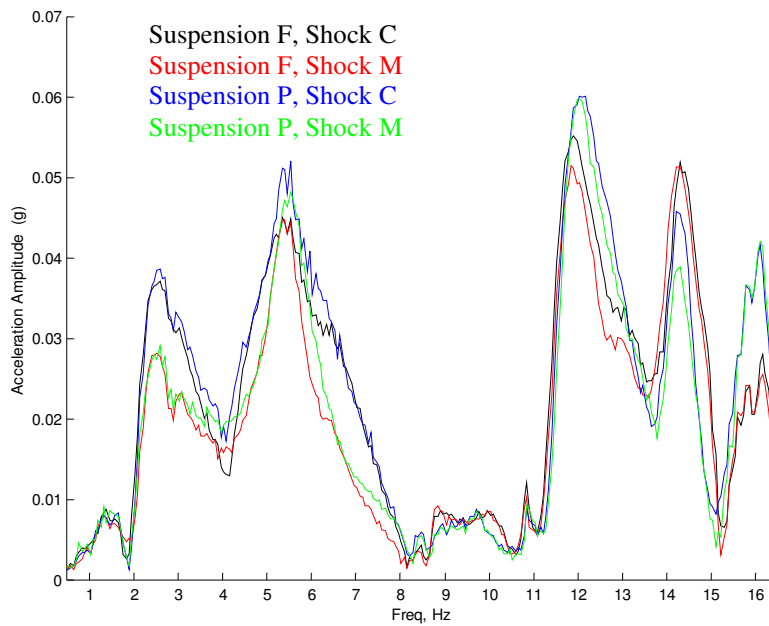


Figure 5-10. Standard Low Vertical Acceleration of B-post for Different Cab Suspensions

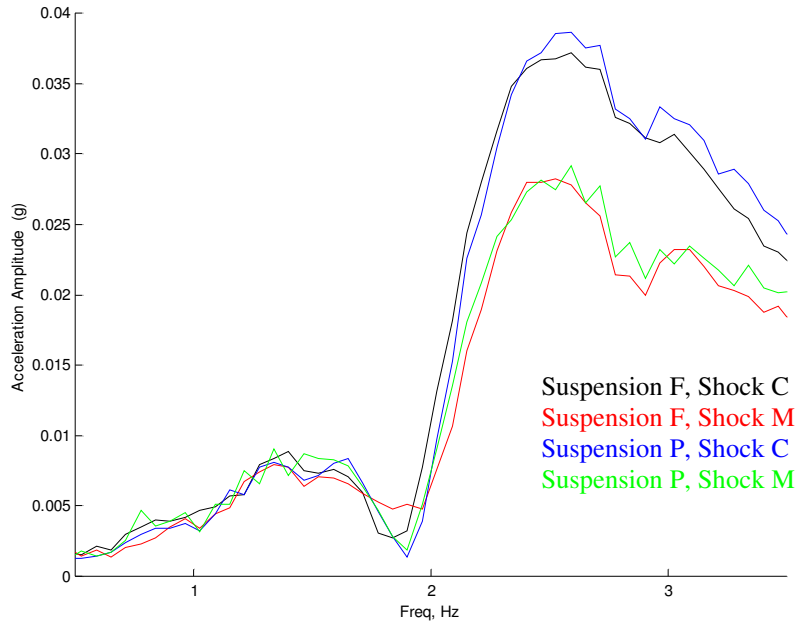


Figure 5-11. Standard Low Vertical Acceleration of B-post for Different Cab Suspensions

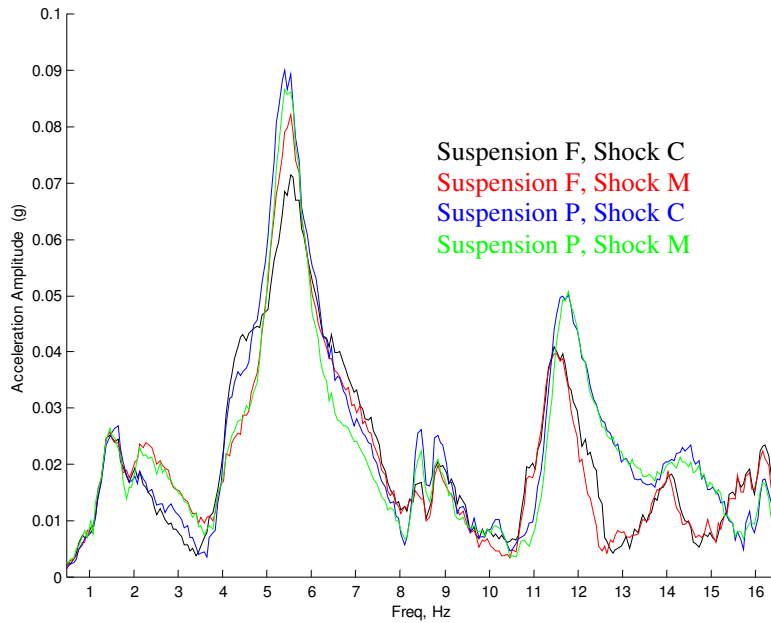


Figure 5-12. Standard Low Fore/Aft Acceleration of B-post for Different Cab Suspensions

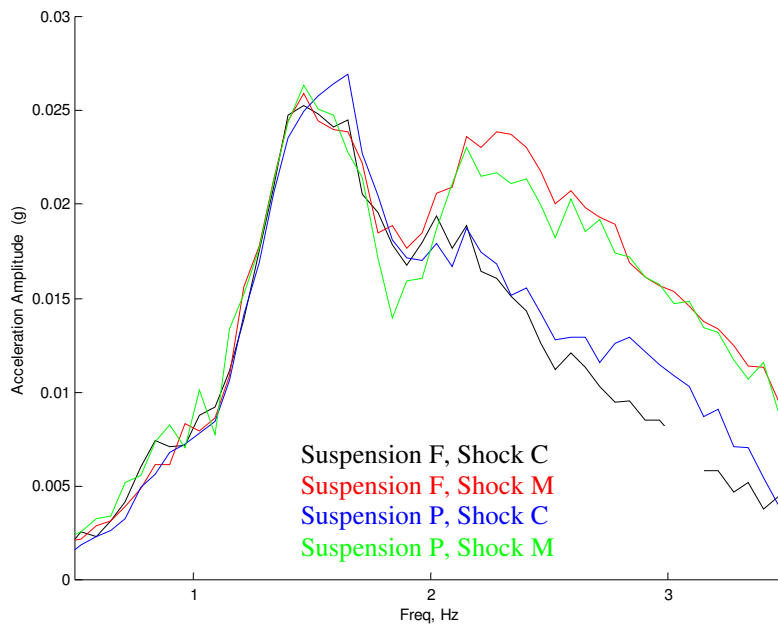


Figure 5-13. Standard Low Fore/Aft Acceleration of B-post for Different Cab Suspensions

5.3.3 Roll Cab Suspension Study

The two suspensions share the same vertical components. Therefore, it was suggested that introducing roll tests to the program would be more helpful in comparing the two cab suspensions. The roll tests use the same input as the heave tests with two exceptions: (1) the passenger signal is inverted so that the actuators are always moving in opposite directions, and (2) smaller displacements are needed to excite the truck.

The vertical shocks, which the two cab suspension designs share, control most of the heave response, so the bigger difference in response between the cab suspensions would be expected during the roll tests. This was indeed the case. The frame accelerometer indicated similar amplitudes for all the suspension combinations as shown in Figures 5-14 and 5-15. A larger portion of this vibration was getting through Suspension P (blue and green lines) as measured at the back of the cab (Figures 5-16 and 5-17). Inside the cab at the B-post vertical accelerometer, the accelerations were higher across the spectrum (Figures 5-18 and 5-19) with Suspension P. Below 10 Hz, the original cab suspension also performed better in the fore/aft direction (Figures 5-20 and 5-21). Switching vertical shocks showed little effect.

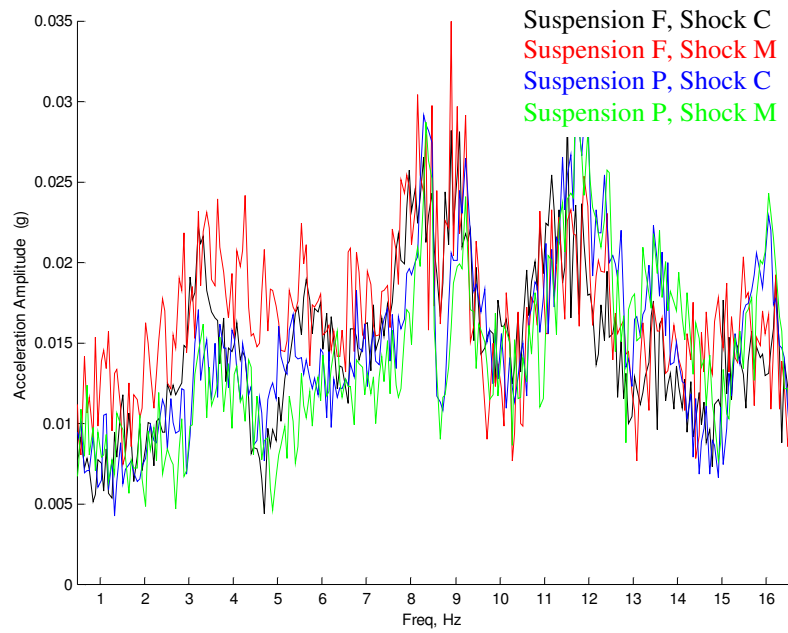


Figure 5-14. Standard Low Vertical Acceleration of Frame at Rear Cab Suspension

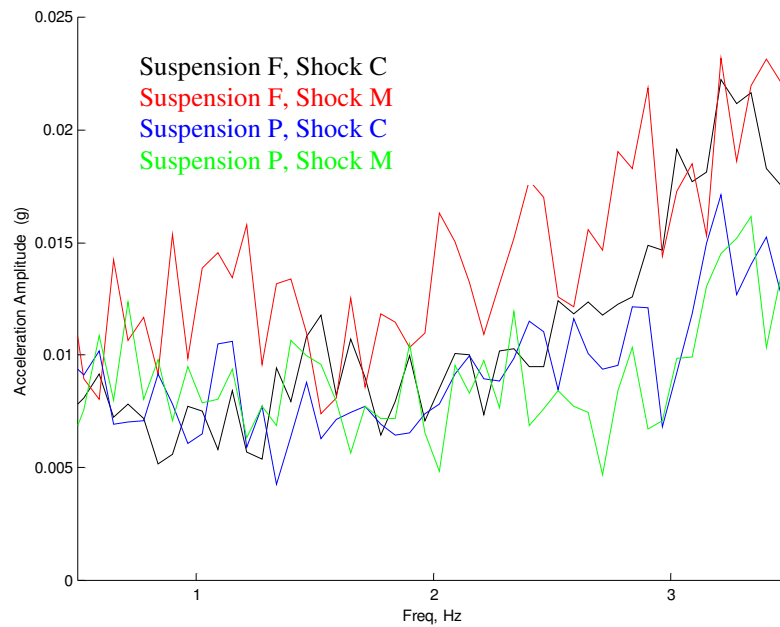


Figure 5-15. Standard Low Vertical Acceleration of Frame at Rear Cab Suspension

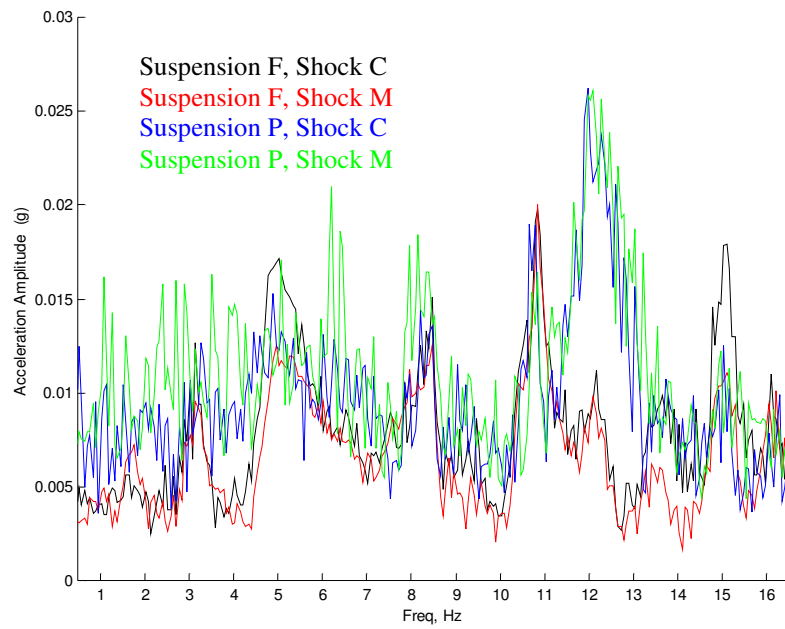


Figure 5-16. Standard Low Vertical Acceleration of Cab at Rear Cab Suspension

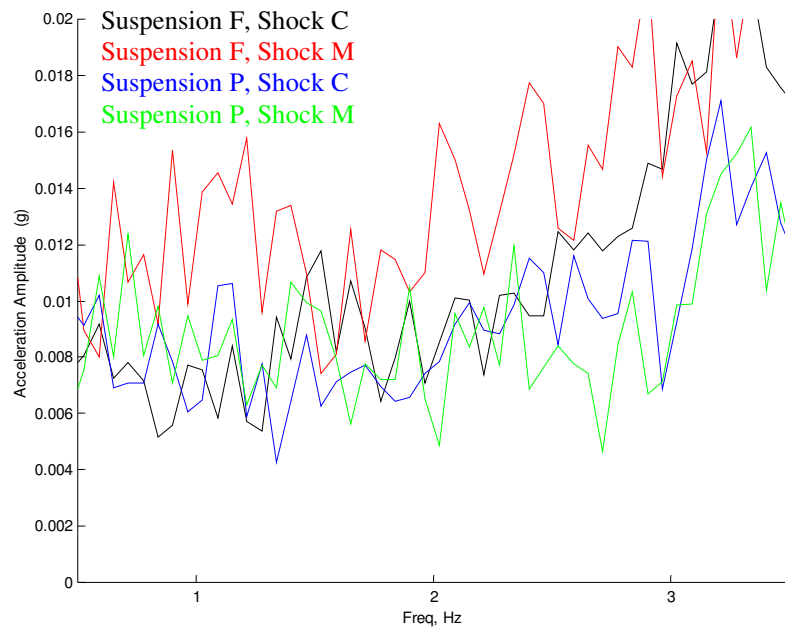


Figure 5-17. Standard Low Vertical Acceleration of Cab at Rear Cab Suspension

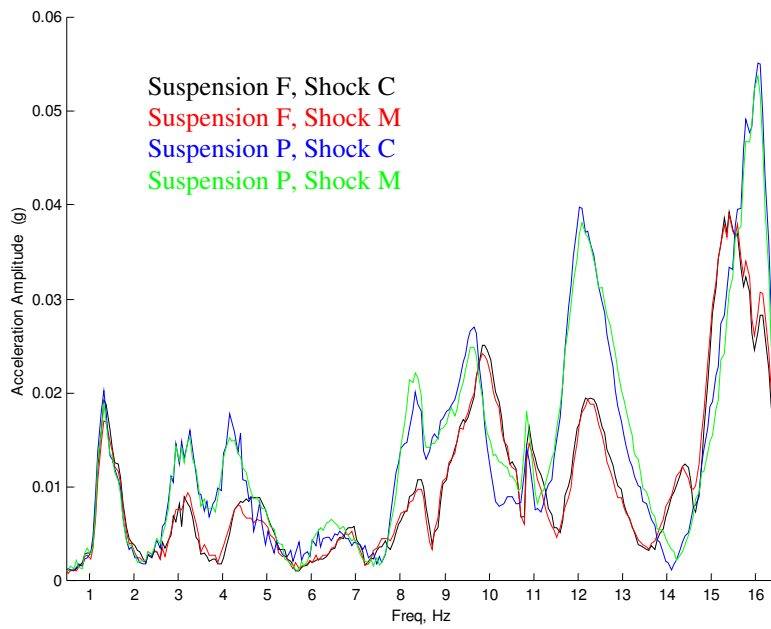


Figure 5-18. Standard Low Vertical Acceleration of B-post

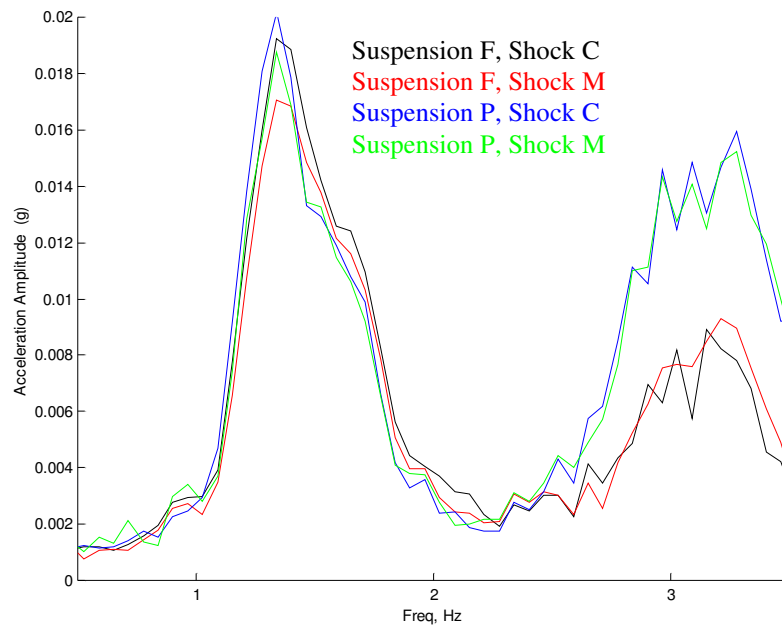


Figure 5-19. Standard Low Vertical Acceleration of B-post

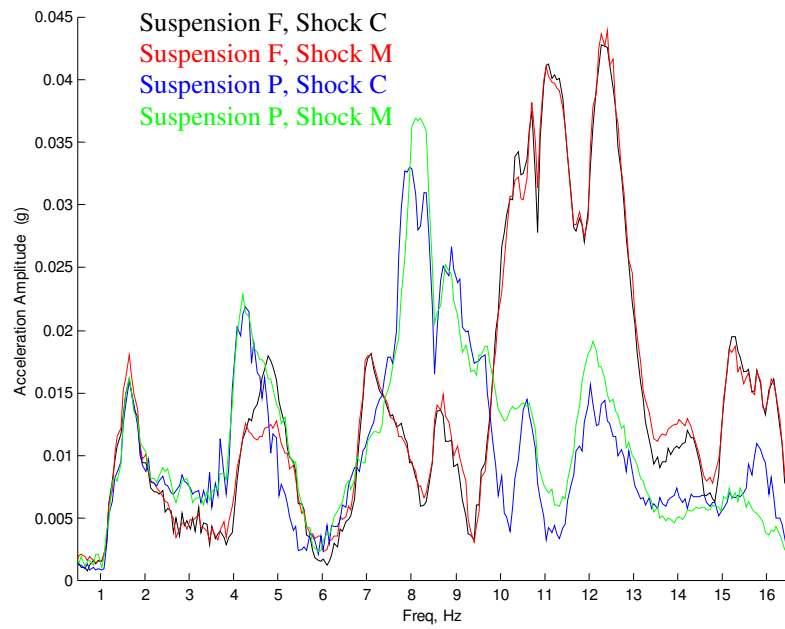


Figure 5-20. Standard Low Fore/Aft Acceleration of B-post

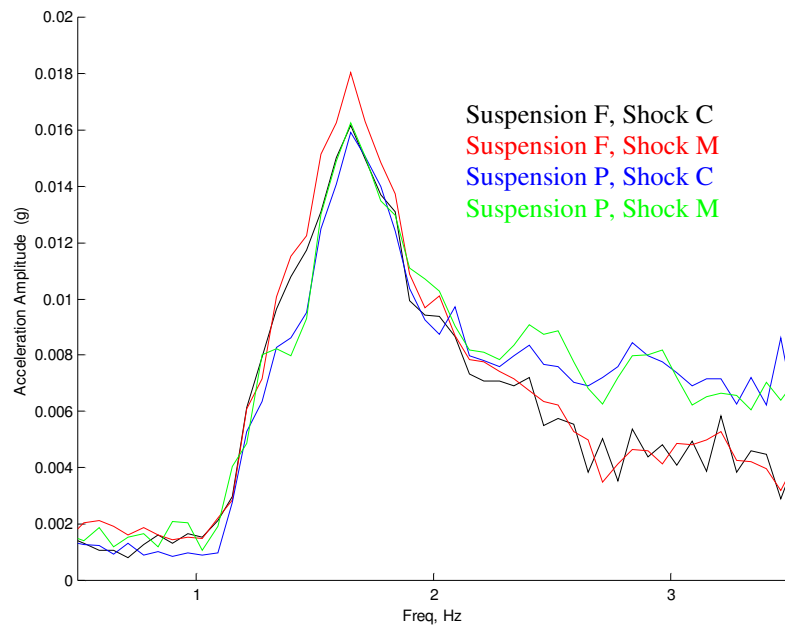


Figure 5-21. Standard Low Fore/Aft Acceleration of B-post

5.4 Thin Low Results

The results from testing the Thin Low are shown in this. The parameters of this truck are listed in bold in Table 5-3. As mentioned earlier, only the results from the L4 airsprings are shown for brevity.

Table 5-3. Important test vehicle parameters

Name	Model	Sleeper length	Wheelbase	Frame, <i>h x t</i>
Standard Low	VNL 660	61 in. (1550 mm)	215 in. (5460 mm)	266 mm x 8 mm
Thin Low	VNL 660	61 in. (1550 mm)	215 in. (5460 mm)	266 mm x 7 mm
Standard High	VNL 770	77 in. (1960 mm)	229 in. (5810 mm)	300 mm x 7 mm
Thin High	VNL 770	77 in. (1960 mm)	239 in. (6070 mm)	300 mm x 6 mm

5.4.1 Heave Cab Suspension Study

With the Thin Low, Suspension P showed slightly less acceleration at the back of the cab (Figures 5-22 and 5-23) given the same input from the frame (Figures 5-24 and 5-25). As mentioned earlier, the largest contributors to the heave (in-phase) performance of the cab suspension are the vertical shocks. This proved true here because the gas-charged Shock M gave better performance than the factory Shock C as measured by the vertical B-post accelerometer (Figures 5-26 and 5-27). Shock C resulted in lower fore-aft acceleration at the B-post (Figures 5-28 and 5-29). Driver comfort is more affected by fore-aft vibration at low frequencies, but the fore-aft vibration at the lower frequencies was about half of the vertical acceleration, indicating that reducing the vertical acceleration is a more important goal. This truck (as well as the two 770s) was equipped with a lateral accelerometer as well, primarily to measure the roll response. Fittingly, the acceleration levels (from the lateral sensor) with all the cab combinations are the same at most frequencies (Figures 5-30 and 5-31).

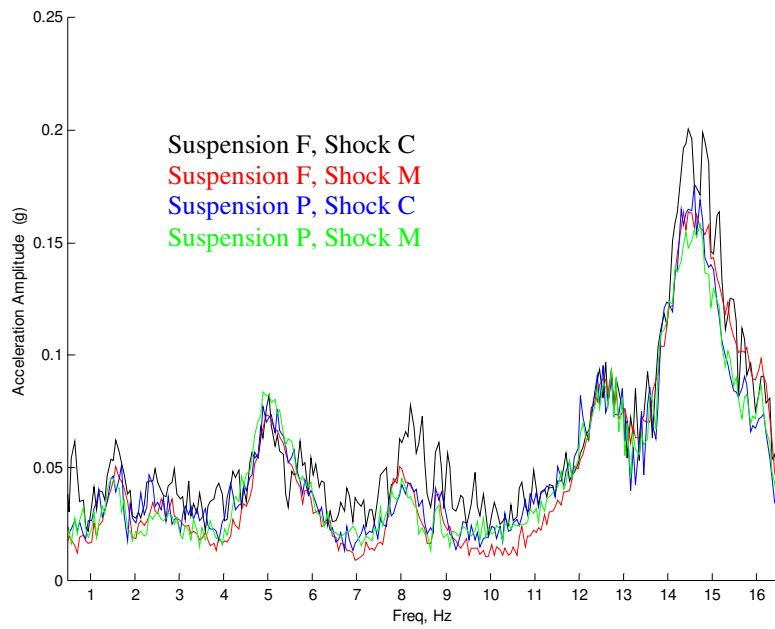


Figure 5-22. Thin Low Vertical Acceleration of Frame at Rear Cab Suspension

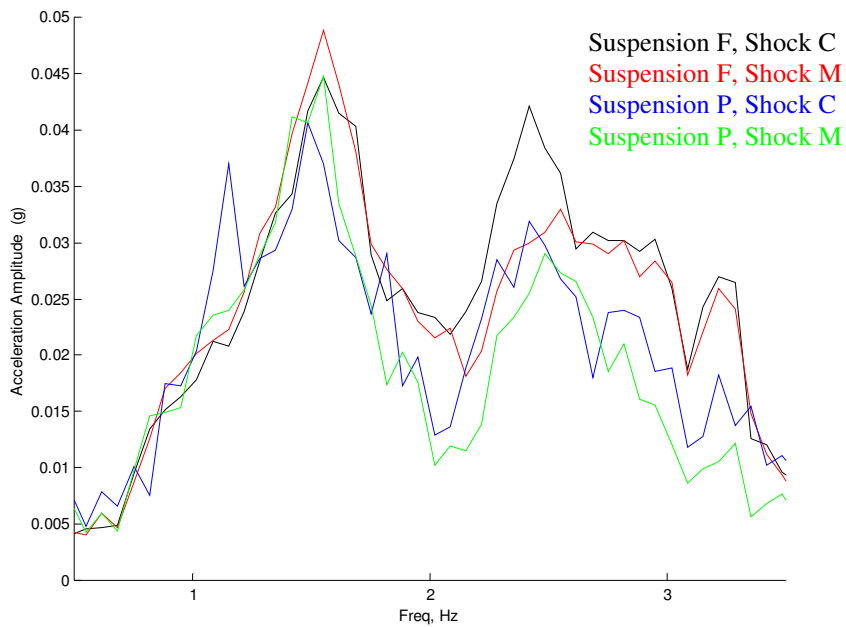


Figure 5-23. Thin Low Vertical Acceleration of Frame at Rear Cab Suspension (Low Frequencies)

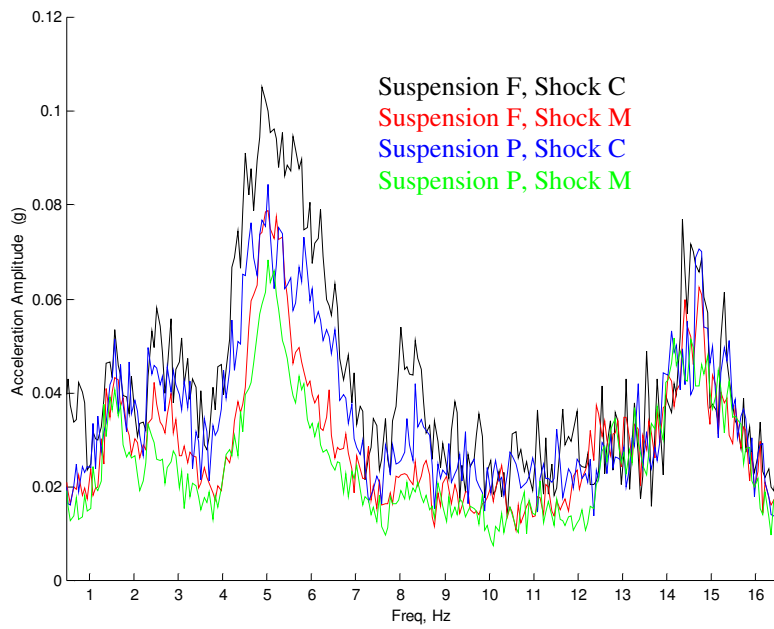


Figure 5-24. Thin Low Vertical Acceleration of Cab at Rear Cab Suspension

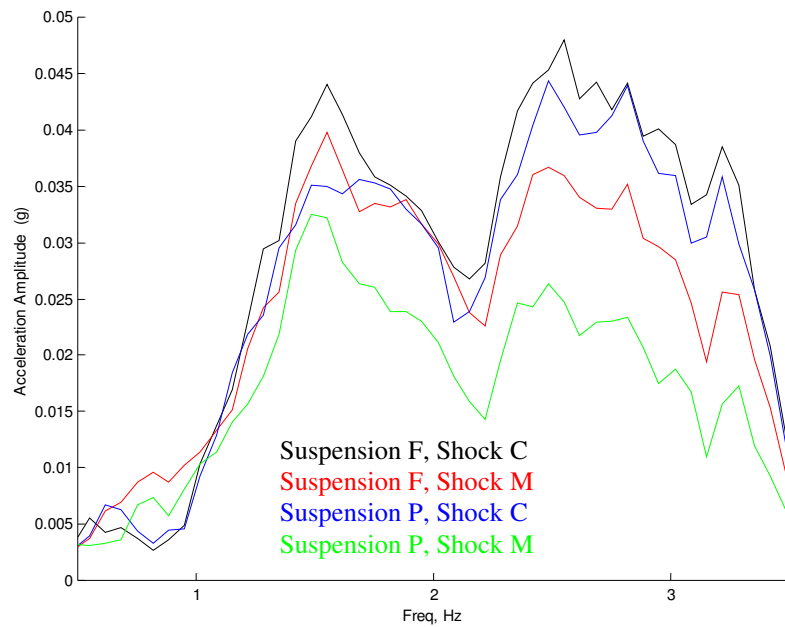


Figure 5-25. Thin Low Vertical Acceleration of Cab at Rear Cab Suspension (Low Frequencies)

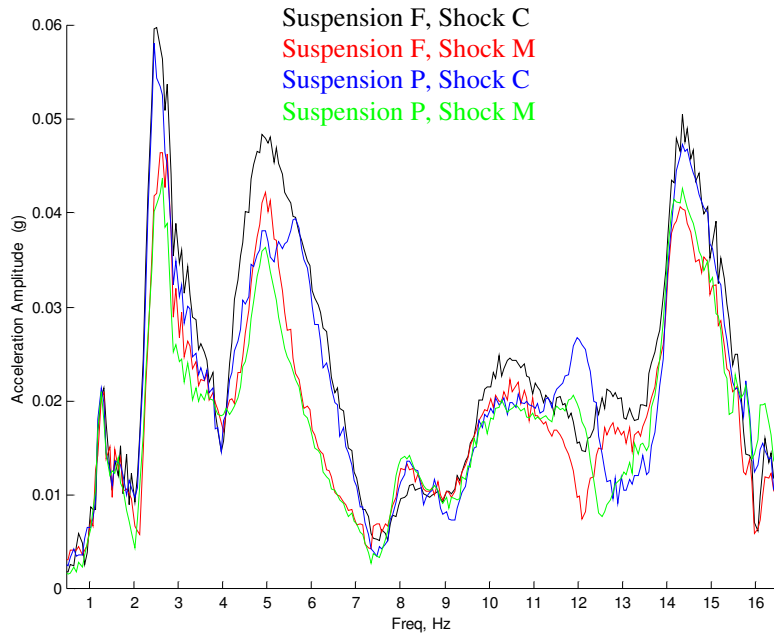


Figure 5-26. Thin Low Vertical Acceleration of B-post

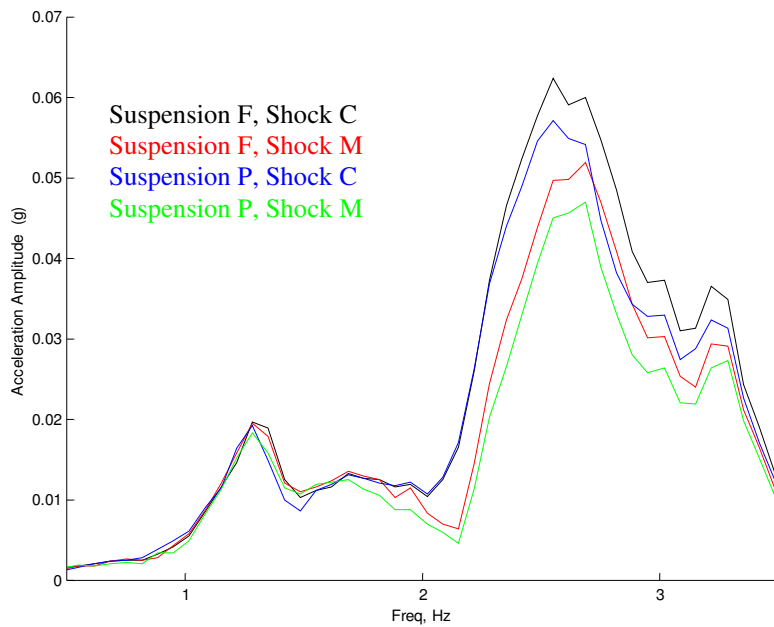


Figure 5-27. Thin Low Vertical Acceleration of B-post (Low Frequencies)

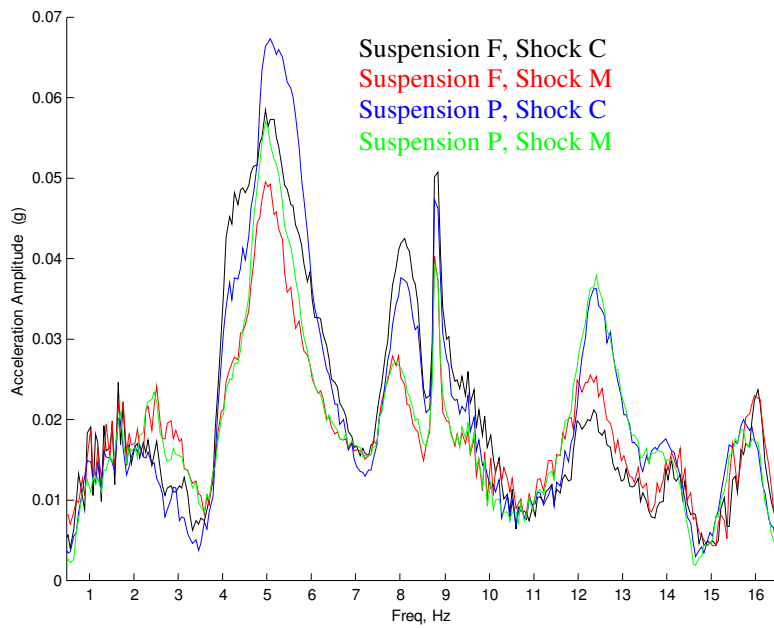


Figure 5-28. Thin Low Fore/Aft Acceleration of B-post

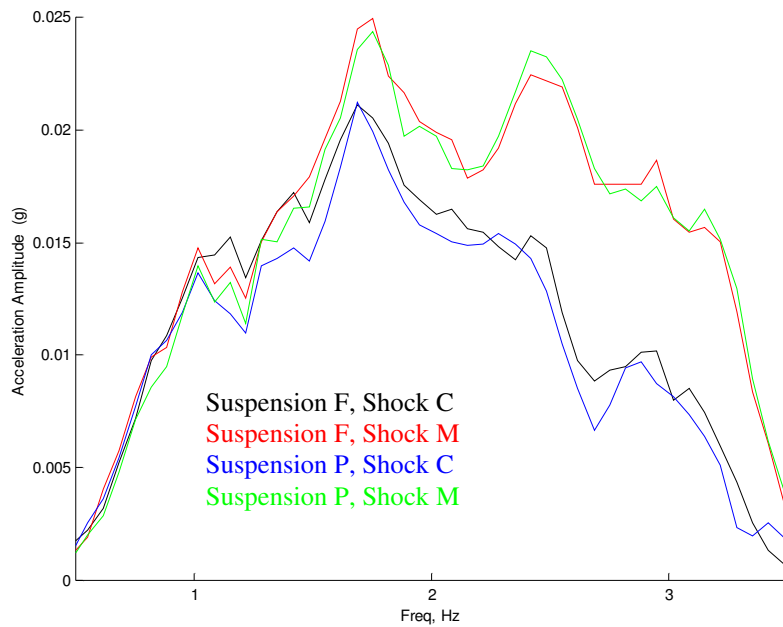


Figure 5-29. Thin Low Fore/Aft Acceleration of B-post (Low Frequencies)

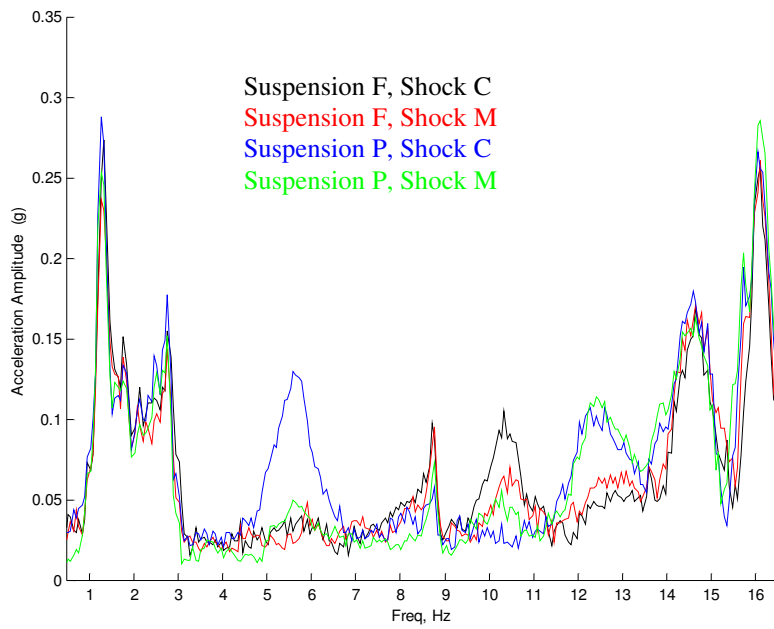


Figure 5-30. Thin Low Lateral Acceleration of B-post

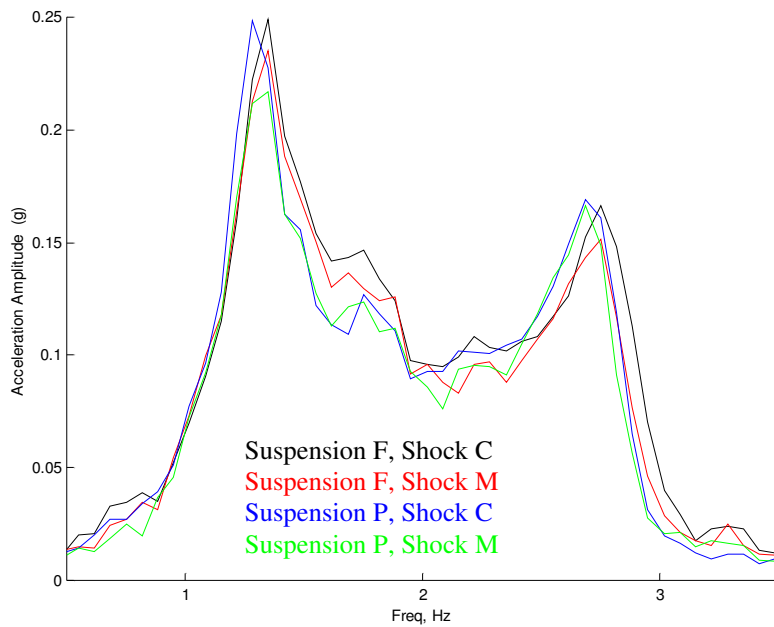


Figure 5-31. Thin Low Lateral Acceleration of B-post (Low Frequencies)

5.4.2 Roll Cab Suspension Study

As with the Standard Low, the largest difference in response between the cab suspension combinations occurred when the suspension type was switched. Figures 5-32 thru 5-35 show the accelerations at the cab suspension. Considering the B-post measurements, the prototype suspension had higher responses at the vertical (Figures 5-36 and 5-37), fore/aft (Figures 5-38 and 5-39), and lateral (Figures 5-40 and 5-41) accelerometers.

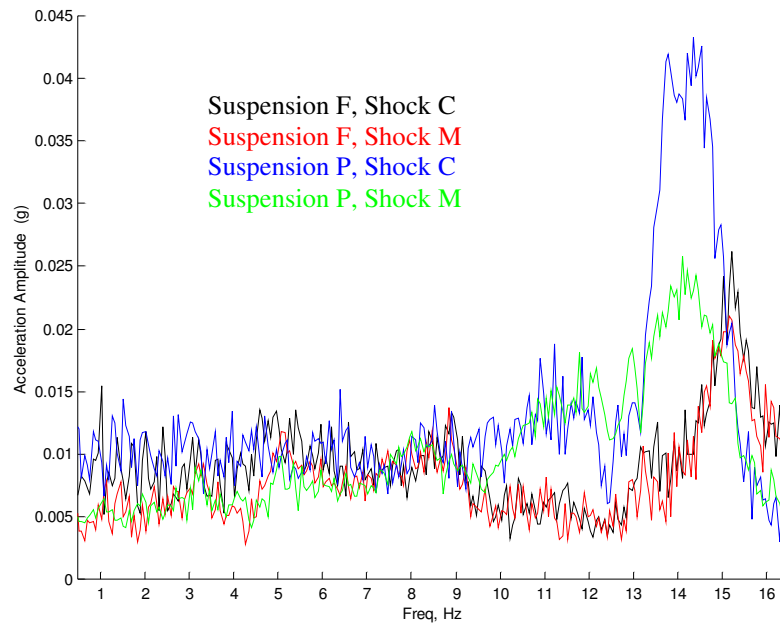


Figure 5-32. Thin Low Vertical Acceleration of Frame at Rear Cab Suspension

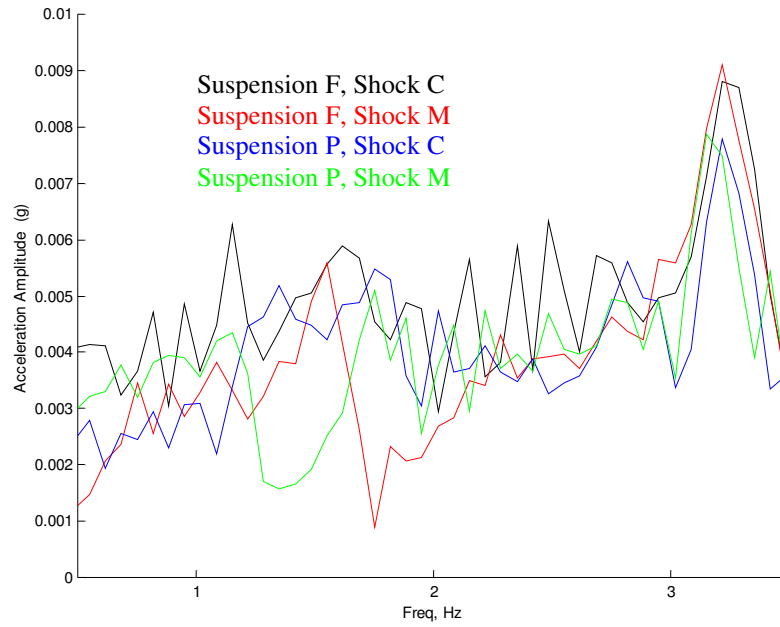


Figure 5-33. Thin Low Vertical Acceleration of Frame at Rear Cab Suspension (Low Frequency)

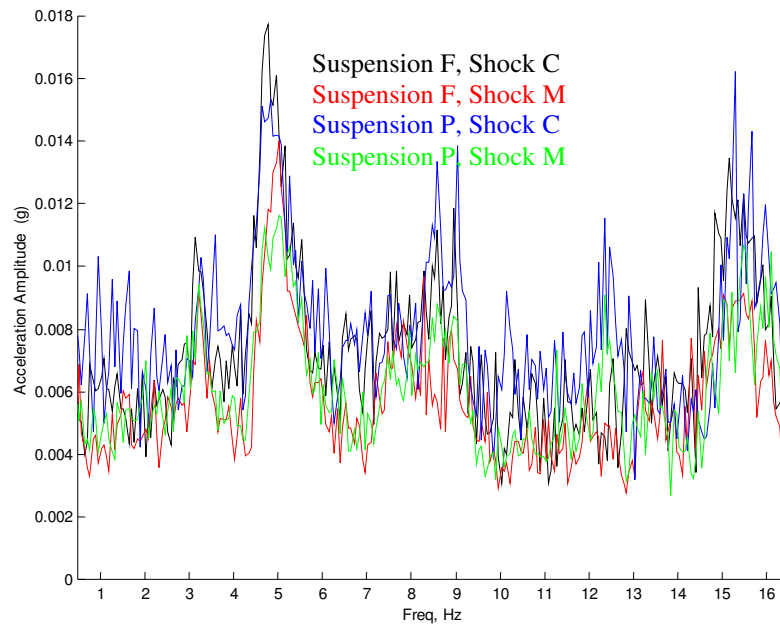


Figure 5-34. Thin Low Vertical Acceleration of Cab at Rear Cab Suspension

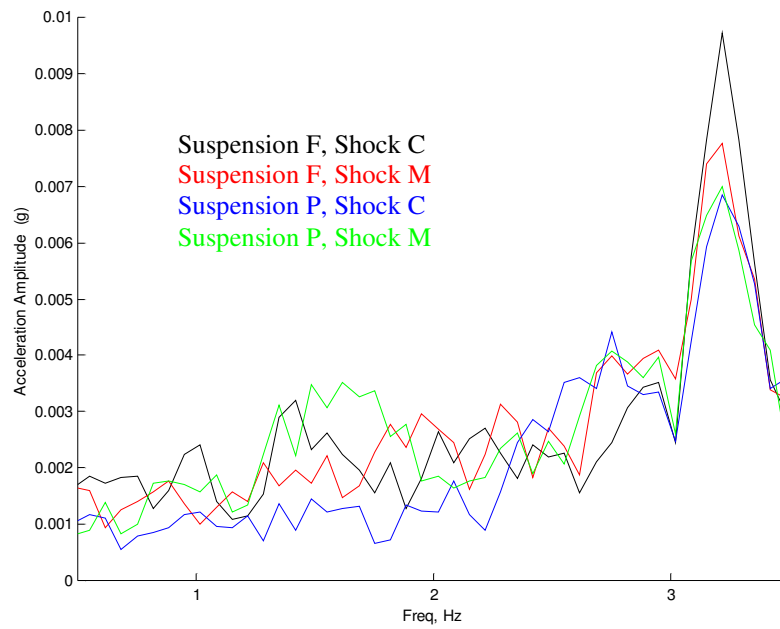


Figure 5-35. Thin Low Vertical Acceleration of Cab at Rear Cab Suspension (Low Frequency)

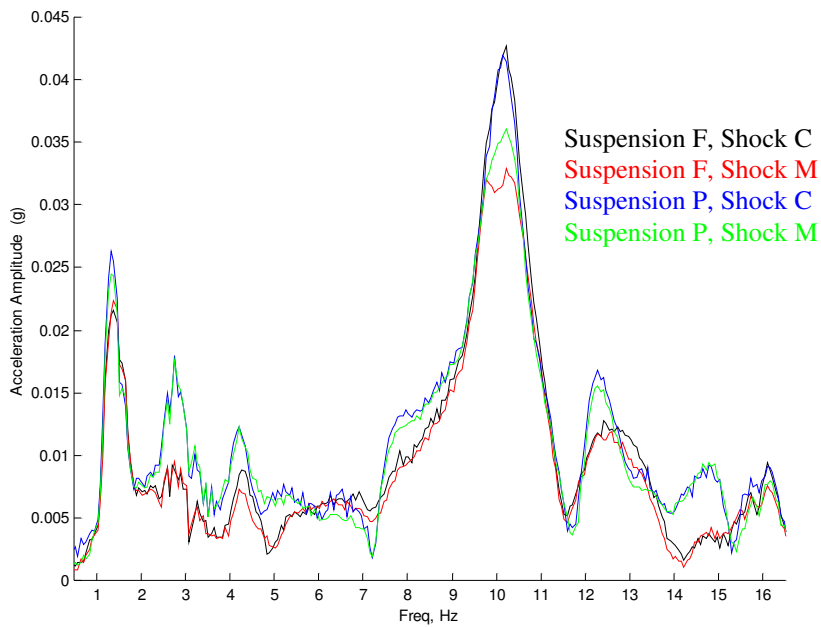


Figure 5-36. Thin Low Vertical Acceleration of B-post

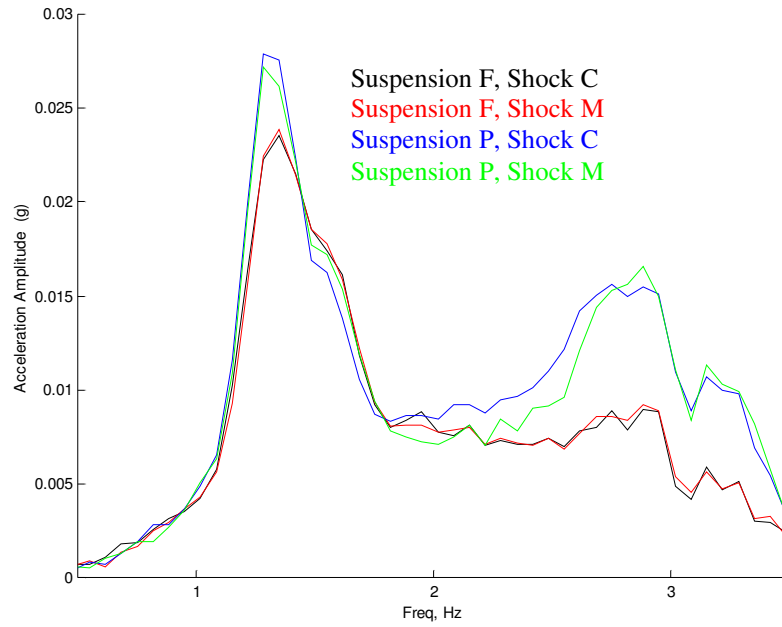


Figure 5-37. Thin Low Vertical Acceleration of B-post (Low Frequency)

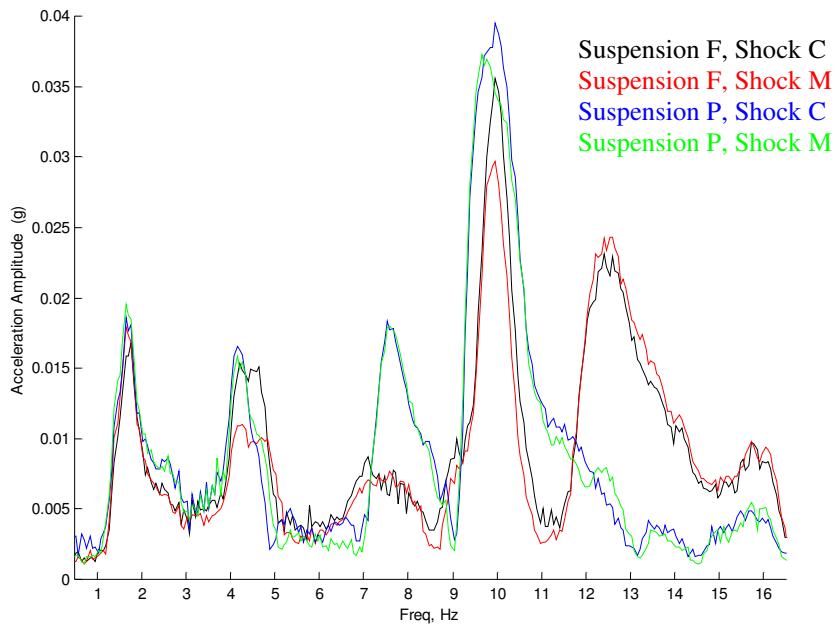


Figure 5-38. Thin Low Fore/Aft Acceleration of B-post

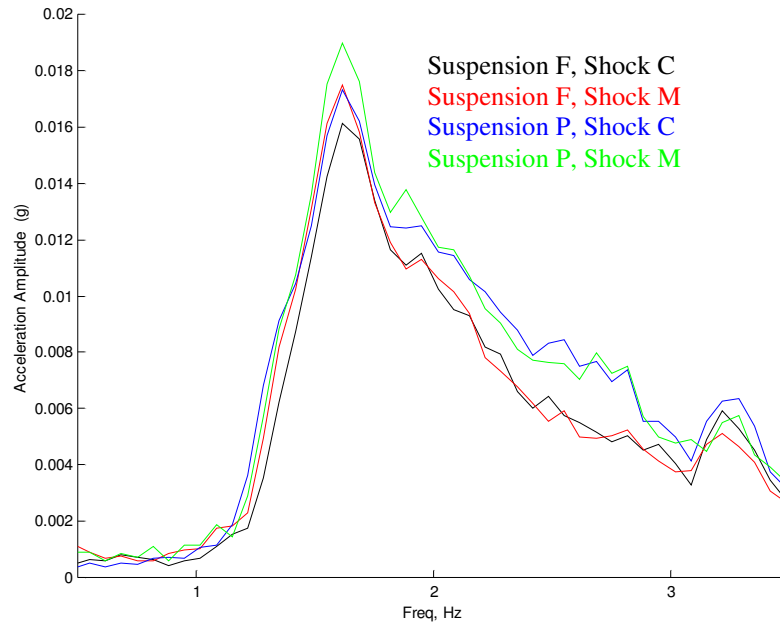


Figure 5-39. Thin Low Fore/Aft Acceleration of B-post (Low Frequency)

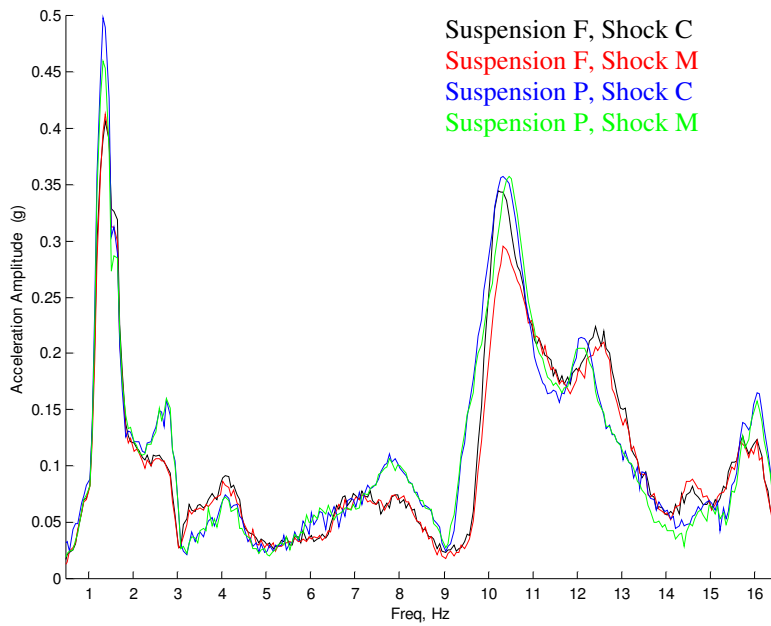


Figure 5-40. Thin Low Lateral Acceleration of B-post

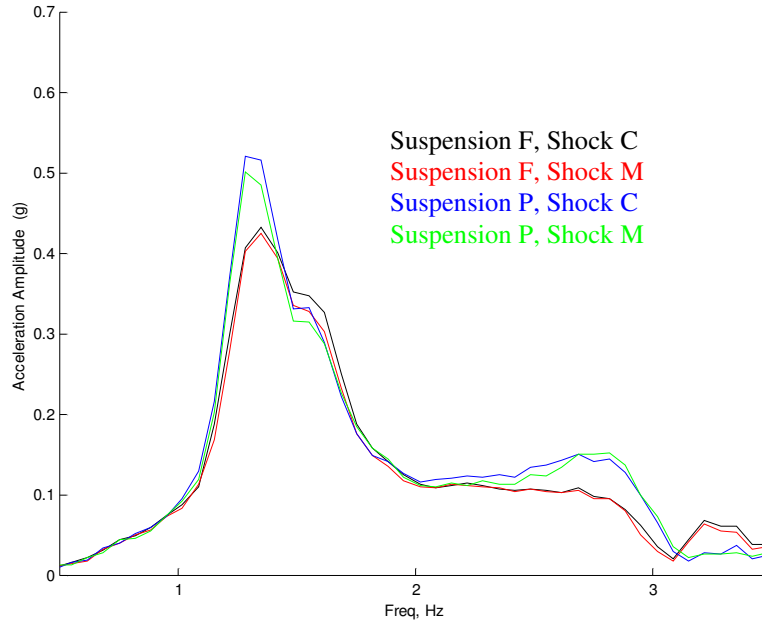


Figure 5-41. Thin Low Lateral Acceleration of B-post (Low Frequency)

5.5 Standard High Results

The Standard High results are shown in this subsection. The parameters of this truck are listed in bold in Table 5-4. With this test vehicle, no difference was noticed from switching airsprings; only the results from the factory (L5) airsprings are shown.

Table 5-4. Important test vehicle parameters

Name	Model	Sleeper length	Wheelbase	Frame, <i>h x t</i>
Standard Low	VNL 660	61 in. (1550 mm)	215 in. (5460 mm)	266 mm x 8 mm
Thin Low	VNL 660	61 in. (1550 mm)	215 in. (5460 mm)	266 mm x 7 mm
Standard High	VNL 770	77 in. (1960 mm)	229 in. (5810 mm)	300 mm x 7 mm
Thin High	VNL 770	77 in. (1960 mm)	239 in. (6070 mm)	300 mm x 6 mm

5.5.1 Heave Cab Suspension Study

The results from the Standard High truck are similar to those obtained for the 660: Shock M resulted in lower vertical accelerations at the B-post (Figures 5-46 and 5-47), but Shock C performed better in the fore/aft direction (Figures 5-48 and 5-49). The lateral accelerometer (Figures 5-50 and 5-51) shows that Suspension P performed marginally better below the beaming frequency (5 Hz), but Suspension F performed better at higher frequencies. The frame

accelerations are shown in (Figures 5-42 and 5-43) and the corresponding accelerations at the back of the cab are shown in (Figures 5-44 and 5-45).

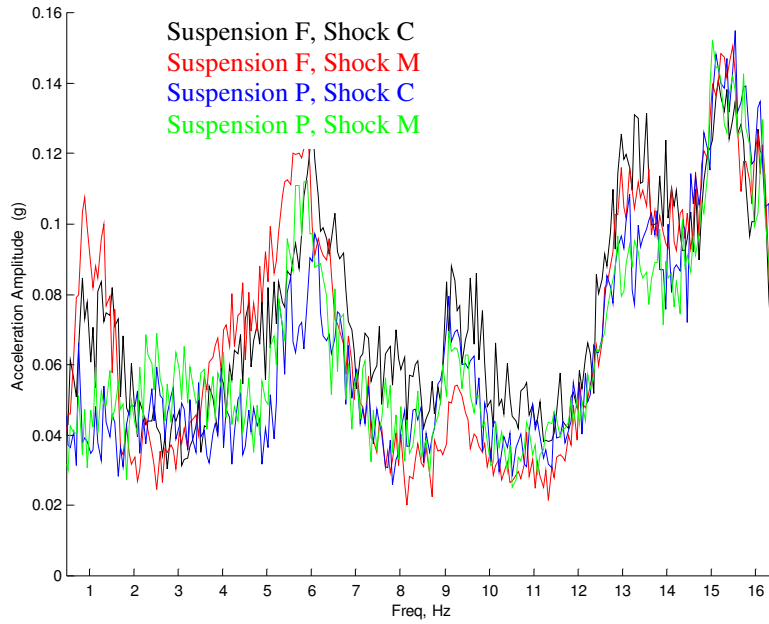


Figure 5-42. Standard High Vertical Acceleration of Frame at Rear Cab Suspension

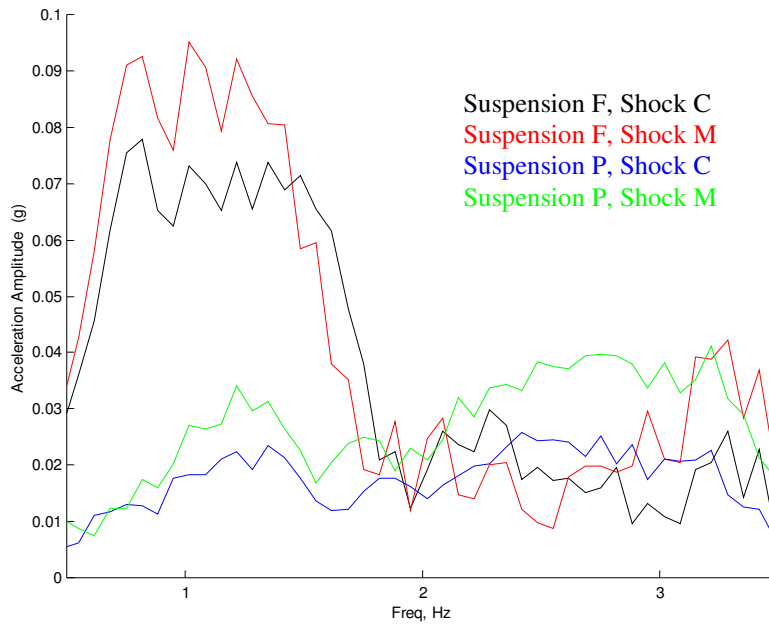


Figure 5-43. Standard High Vertical Acceleration of Frame at Rear Cab Suspension (Low Frequency)

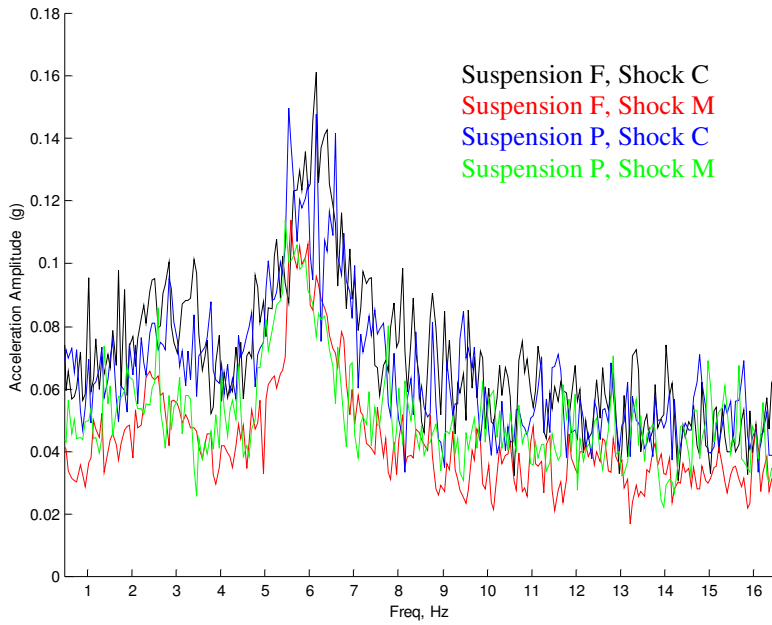


Figure 5-44. Standard High Vertical Acceleration of Cab at Rear Cab Suspension

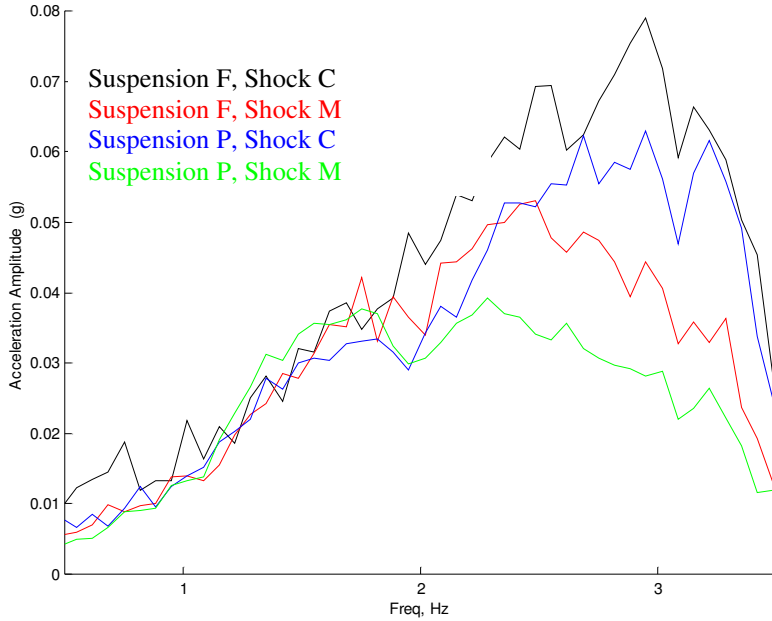


Figure 5-45. Standard High Vertical Acceleration of Cab at Rear Cab Suspension (Low Frequency)

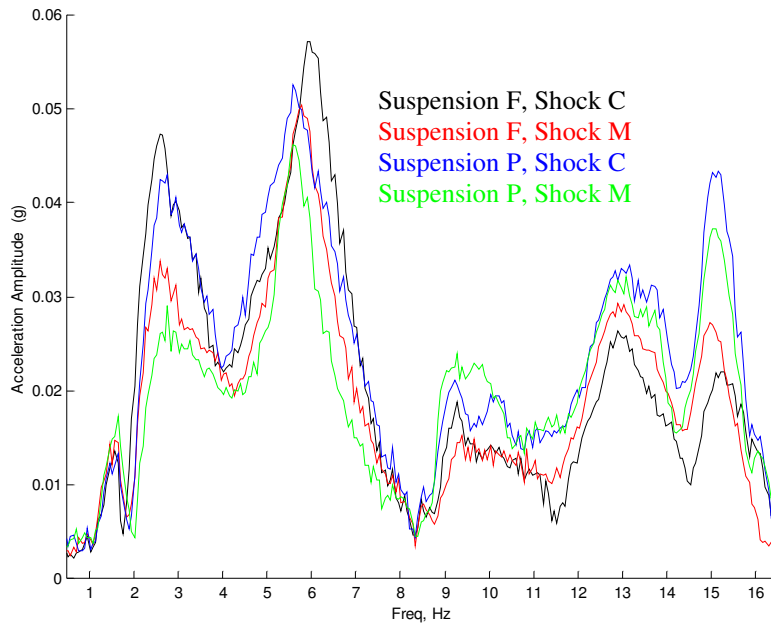


Figure 5-46. Standard High Vertical Acceleration of B-post

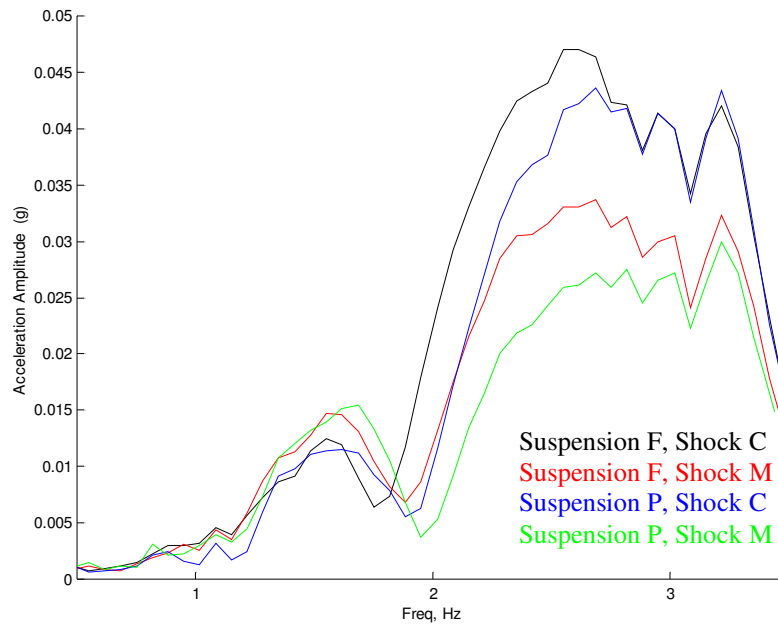


Figure 5-47. Standard High Vertical Acceleration of B-post (Low Frequency)

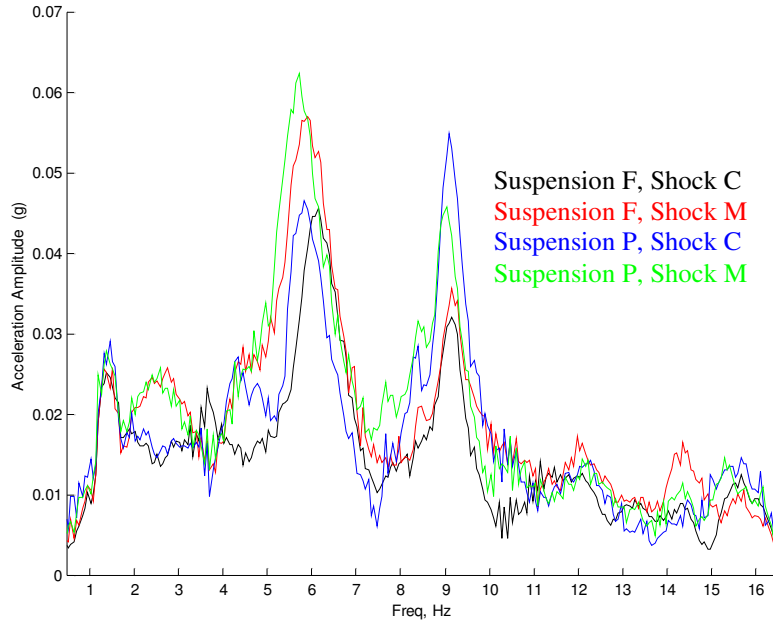


Figure 5-48. Standard High Fore/Aft Acceleration of B-post

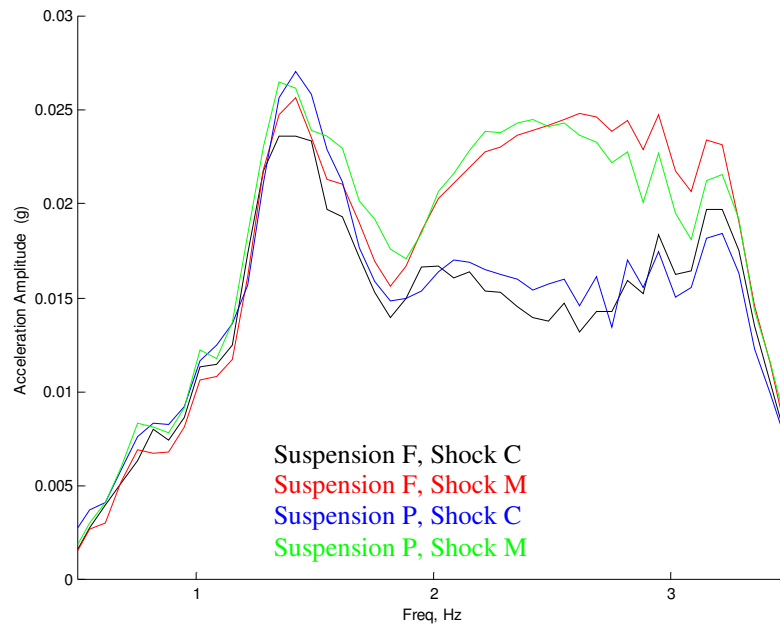


Figure 5-49. Standard High Fore/Aft Acceleration of B-post (Low Frequency)

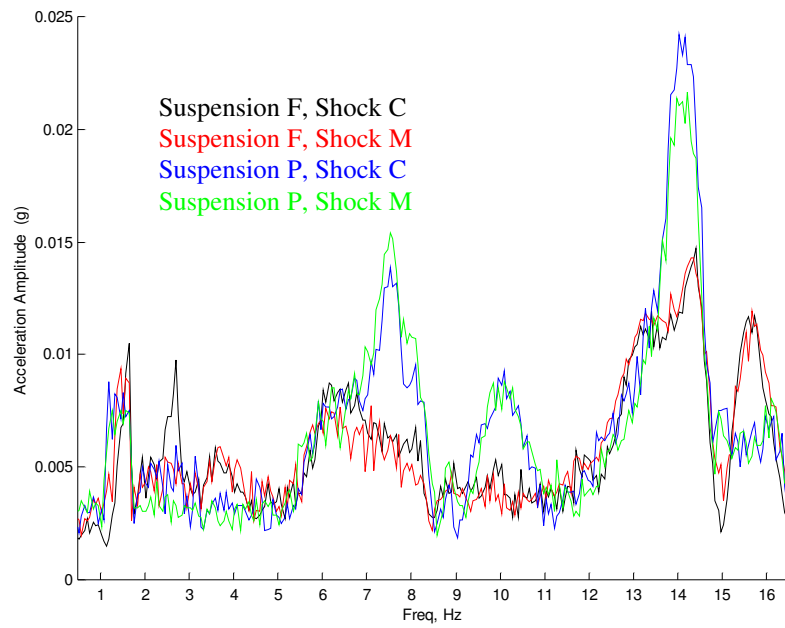


Figure 5-50. Standard High Lateral Acceleration of B-post

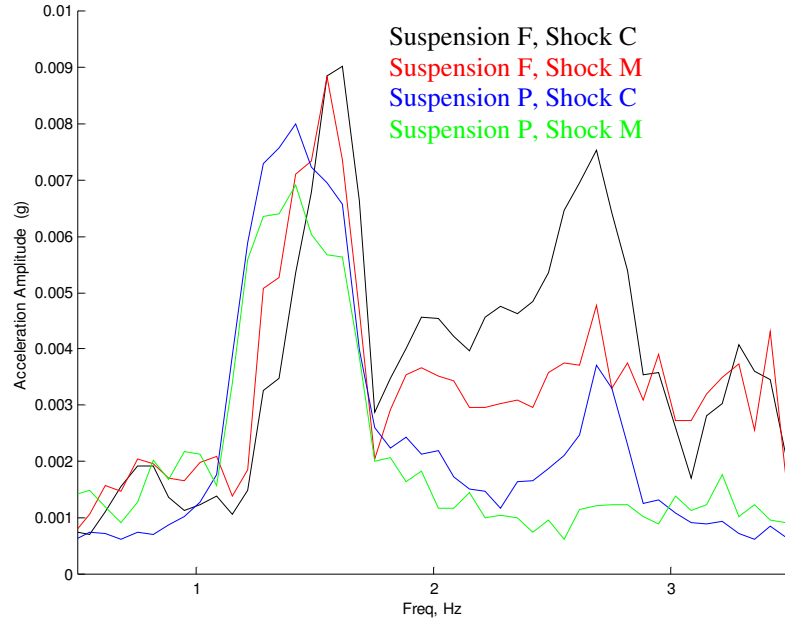


Figure 5-51. Standard High Lateral Acceleration of B-post (Low Frequency)

5.5.2 Roll Cab Suspension Study

Figures 5-52 and 5-53 show the frame acceleration at the cab suspension; Figures 5-54 and 5-55 show the cab acceleration there. Similar to the other trucks, the vertical (Figures 5-56 and 5-57), fore/aft (Figures 5-58 and 5-59), and lateral (Figures 5-60 and 5-61) accelerations at the B-post were higher for the prototype suspension at the lower frequencies.

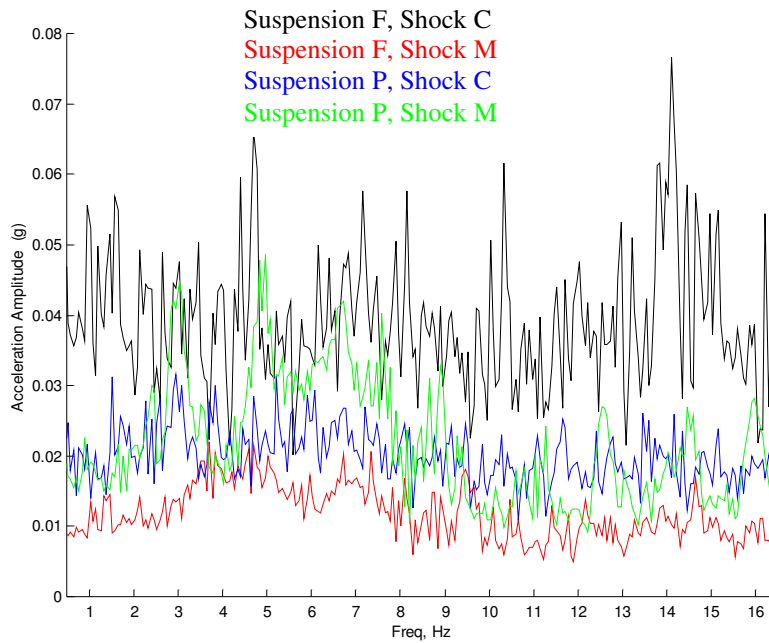


Figure 5-52. Standard High Vertical Acceleration of Frame at Rear Cab Suspension

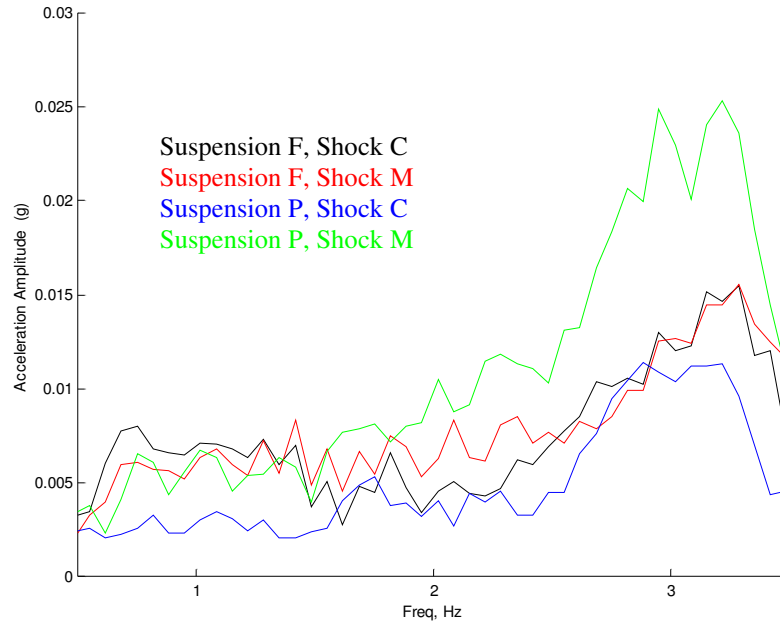


Figure 5-53. Standard High Vertical Acceleration of Frame at Rear Cab Suspension (Low Frequency)

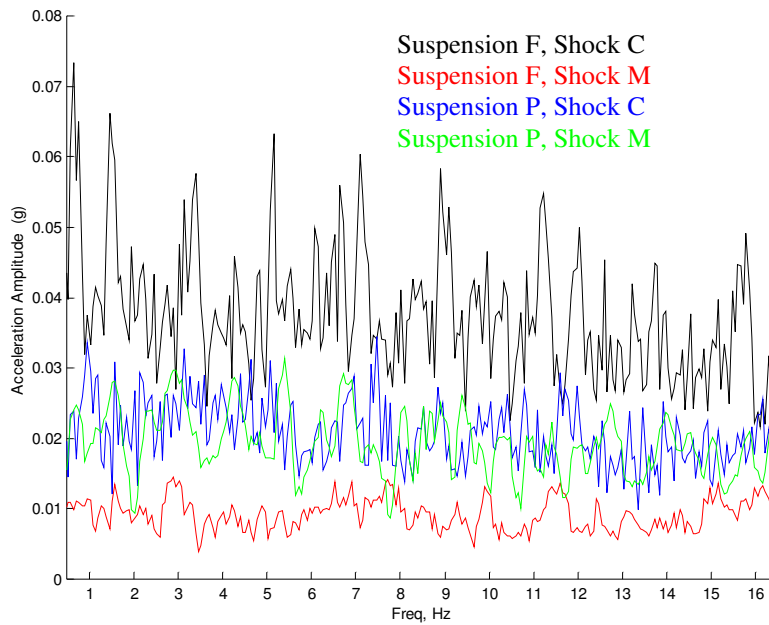


Figure 5-54. Standard High Vertical Acceleration of Cab at Rear Cab Suspension

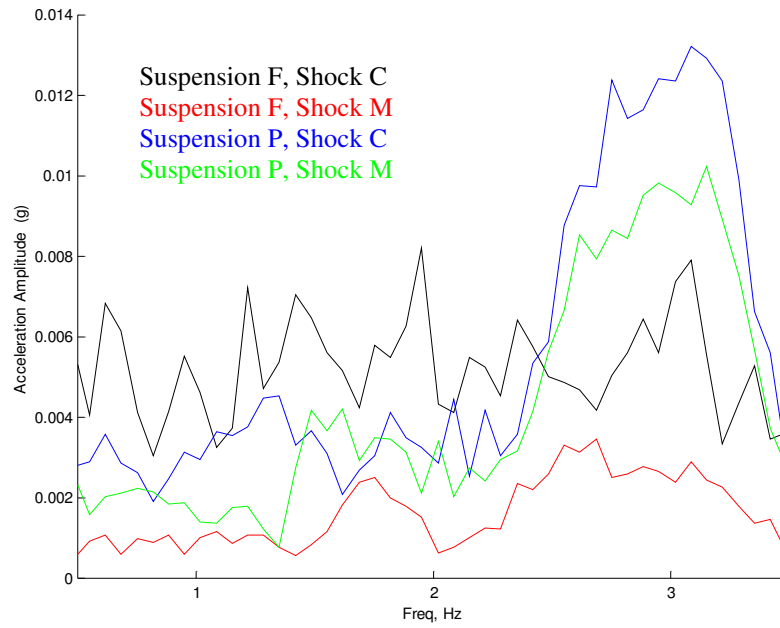


Figure 5-55. Standard High Vertical Acceleration of Cab at Rear Cab Suspension (Low Frequency)

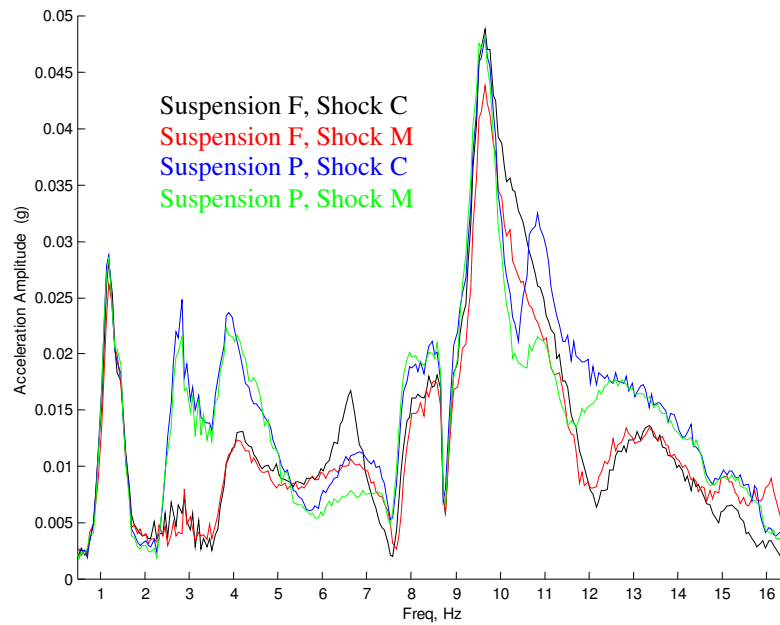


Figure 5-56. Standard High Vertical Acceleration of B-post

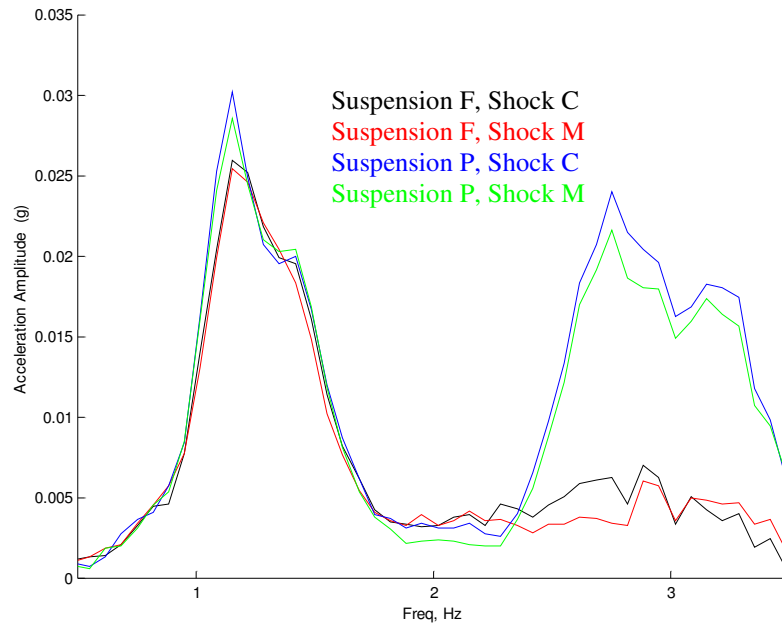


Figure 5-57. Standard High Vertical Acceleration of B-post (Low Frequency)

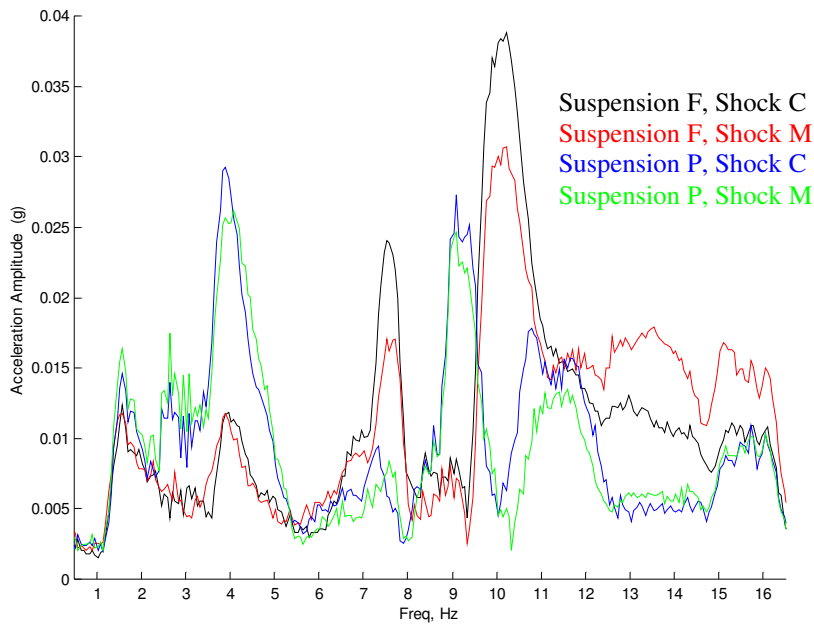


Figure 5-58. Standard High Fore/Aft Acceleration of B-post

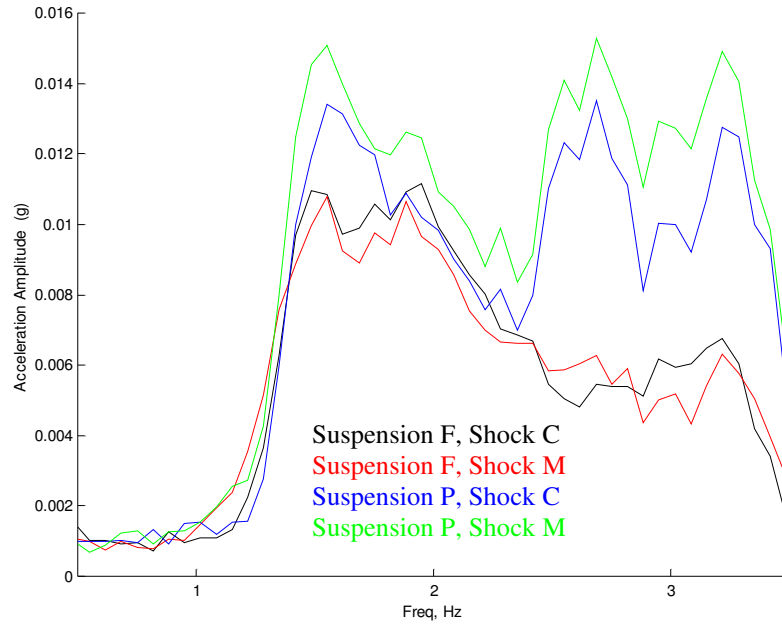


Figure 5-59. Standard High Fore/Aft Acceleration of B-post (Low Frequency)

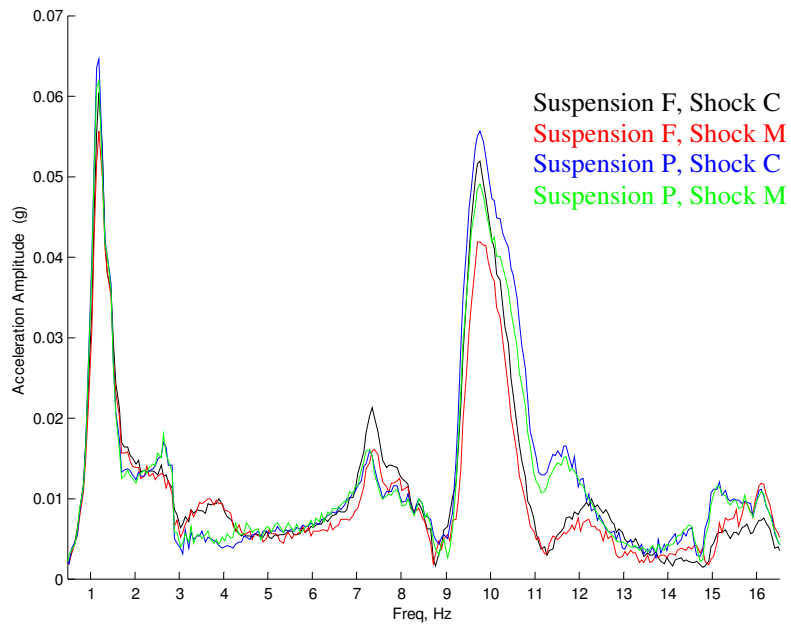


Figure 5-60. Standard High Lateral Acceleration of B-post

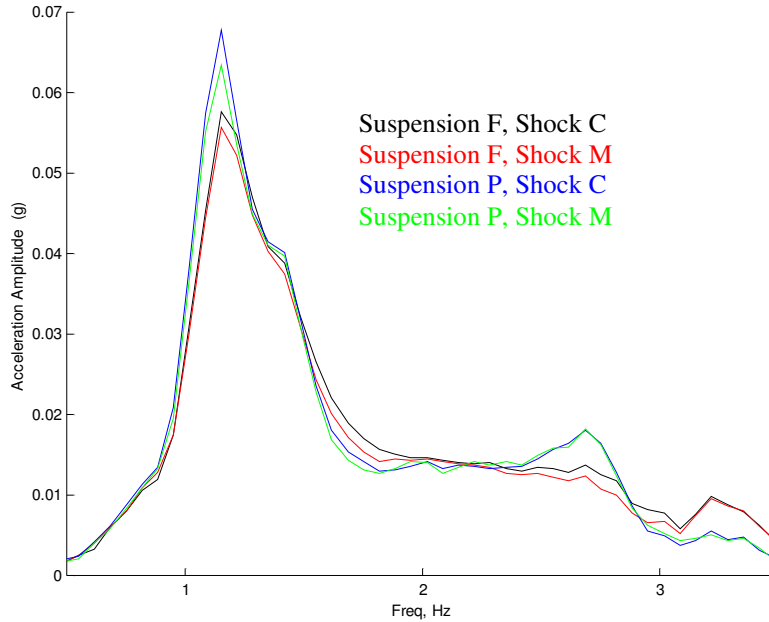


Figure 5-61. Standard High Lateral Acceleration of B-post (Low Frequency)

5.6 Thin High Results

The Standard High results are shown in this subsection. The parameters of this truck are listed in bold in Table 5-5. All the results are from testing with the L5 airsprings.

Table 5-5. Important test vehicle parameters

Name	Model	Sleeper length	Wheelbase	Frame, <i>h x t</i>
Standard Low	VNL 660	61 in. (1550 mm)	215 in. (5460 mm)	266 mm x 8 mm
Thin Low	VNL 660	61 in. (1550 mm)	215 in. (5460 mm)	266 mm x 7 mm
Standard High	VNL 770	77 in. (1960 mm)	229 in. (5810 mm)	300 mm x 7 mm
Thin High	VNL 770	77 in. (1960 mm)	239 in. (6070 mm)	300 mm x 6 mm

5.6.1 Heave Cab Suspension Study

The data from the frame accelerometer (Figures 5-62 and 5-63) came out very clean compared to the other trucks. The beaming at 6 Hz is very noticeable as well as the exhaust stack resonance at higher frequencies. The suspensions behaved in much the same manner as with the other trucks: amplifying at the cab natural frequency and attenuating the 10+ Hz vibrations from the frame as shown in Figures 5-64 and 5-65. Again, with Shock M the vertical accelerations at the B-post were lower (Figures 5-66 and 5-67) and the fore/aft accelerations were higher

(Figures 5-68 and 5-69), with not much difference in lateral acceleration as shown in Figures 5-70 and 5-71.

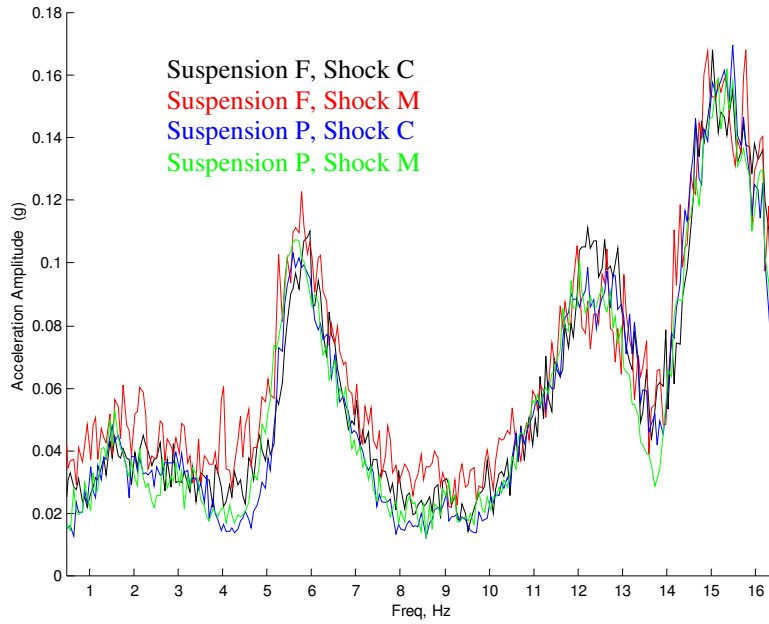


Figure 5-62. Thin High Vertical Acceleration of Frame at Rear Cab Suspension

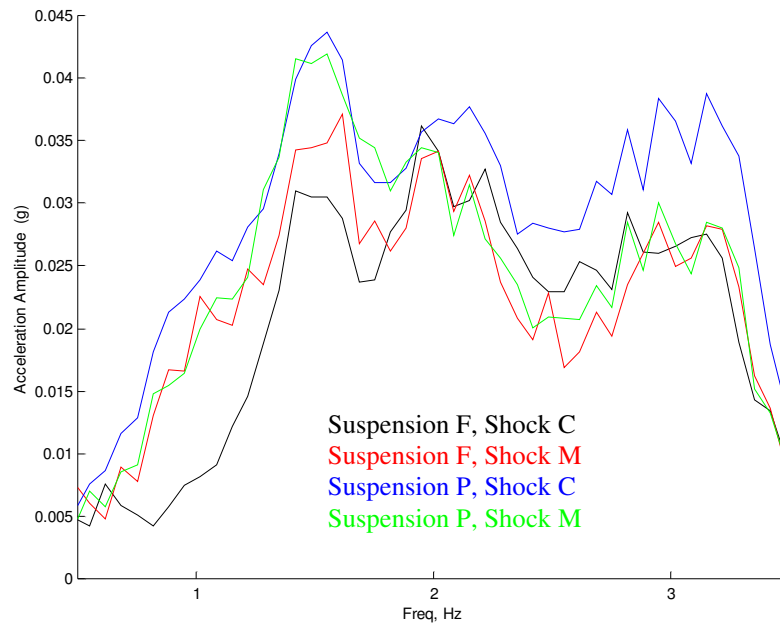


Figure 5-63. Thin High Vertical Acceleration of Frame at Rear Cab Suspension (Low Frequency)

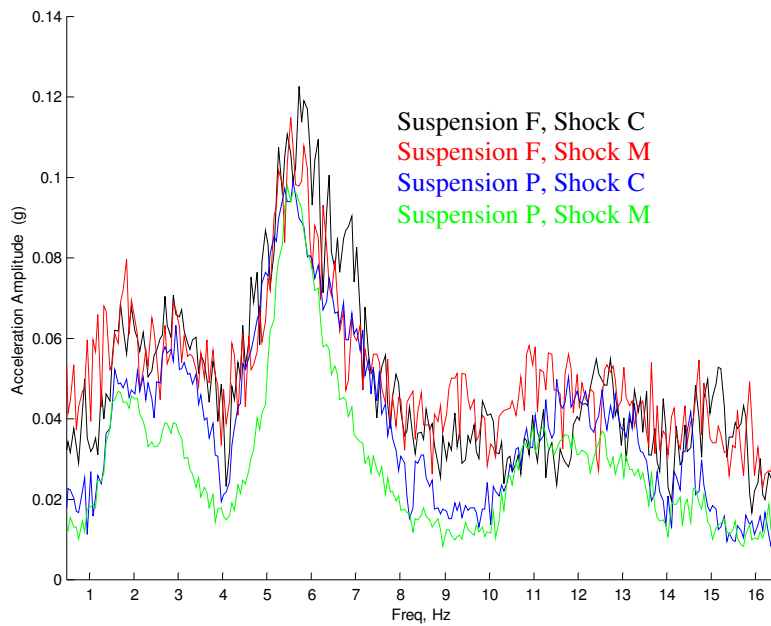


Figure 5-64. Thin High Vertical Acceleration of Cab at Rear Cab Suspension

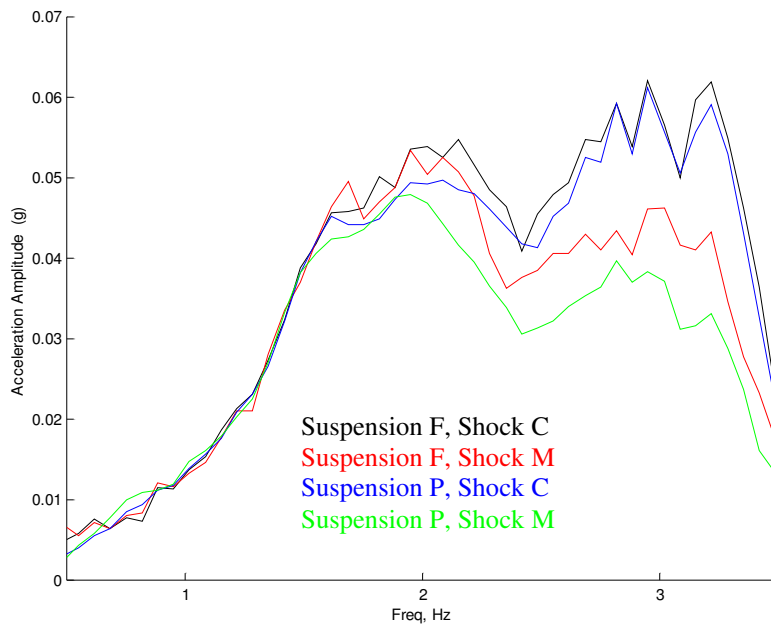


Figure 5-65. Thin High Vertical Acceleration of Cab at Rear Cab Suspension (Low Frequency)

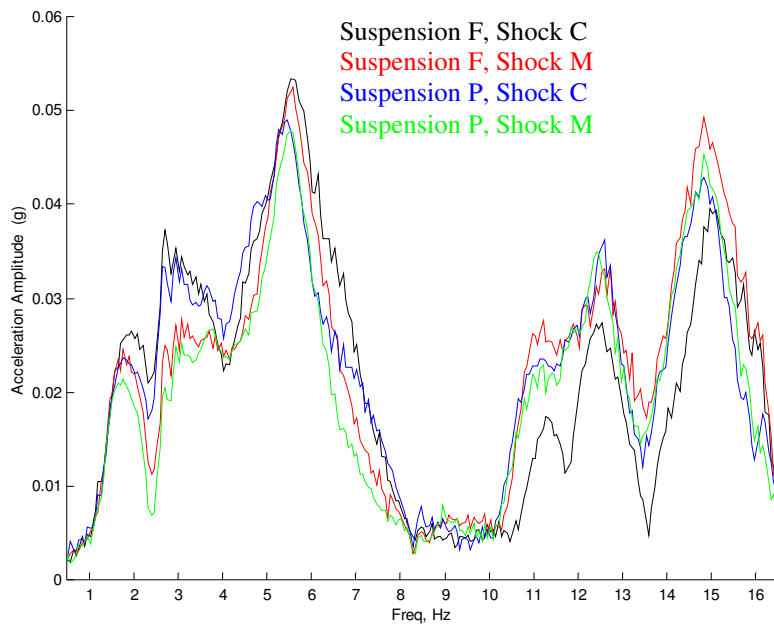


Figure 5-66. Thin High Vertical Acceleration of B-post

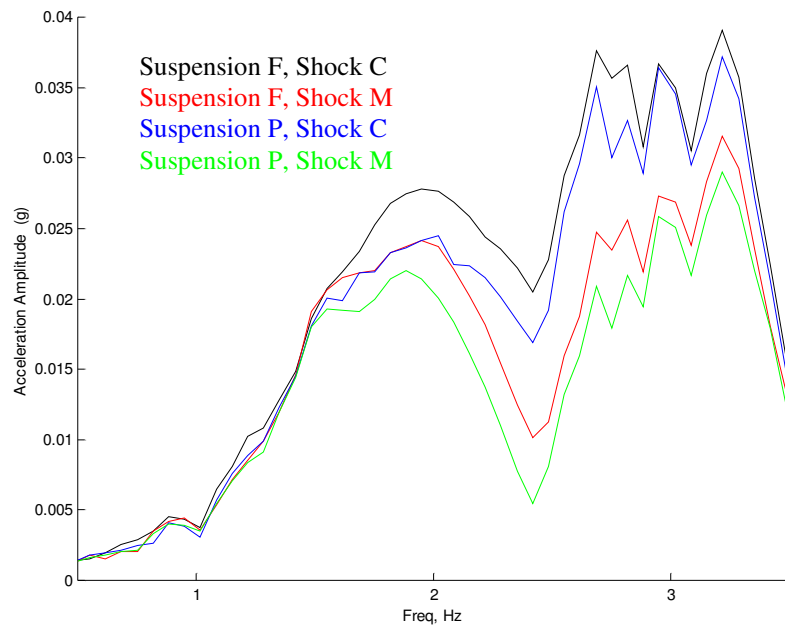


Figure 5-67. Thin High Vertical Acceleration of B-post (Low Frequency)

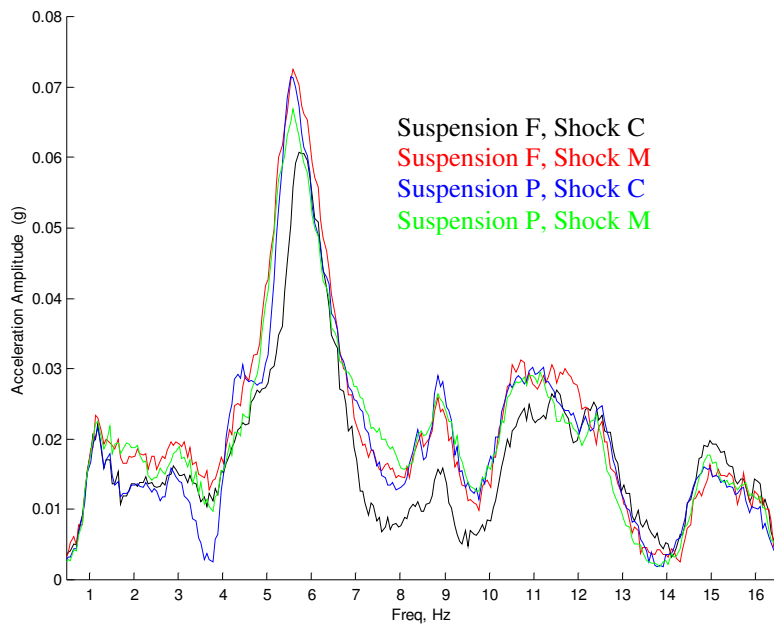


Figure 5-68. Thin High Fore/Aft Acceleration of B-post

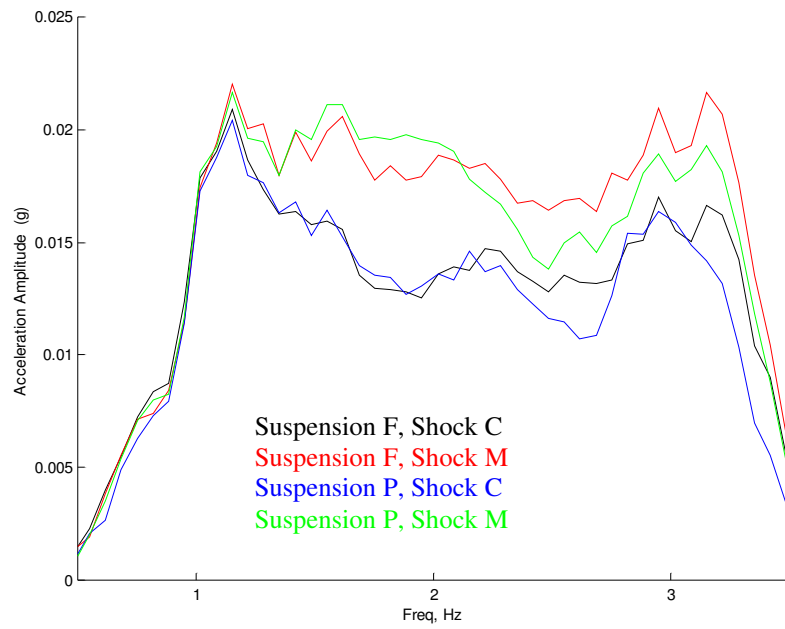


Figure 5-69. Thin High Fore/Aft Acceleration of B-post (Low Frequency)

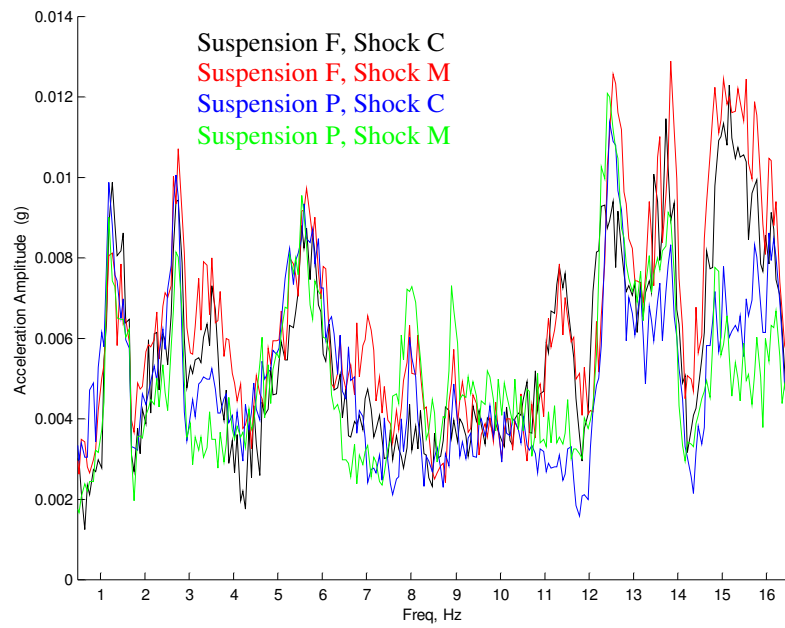


Figure 5-70. Thin High Lateral Acceleration of B-post

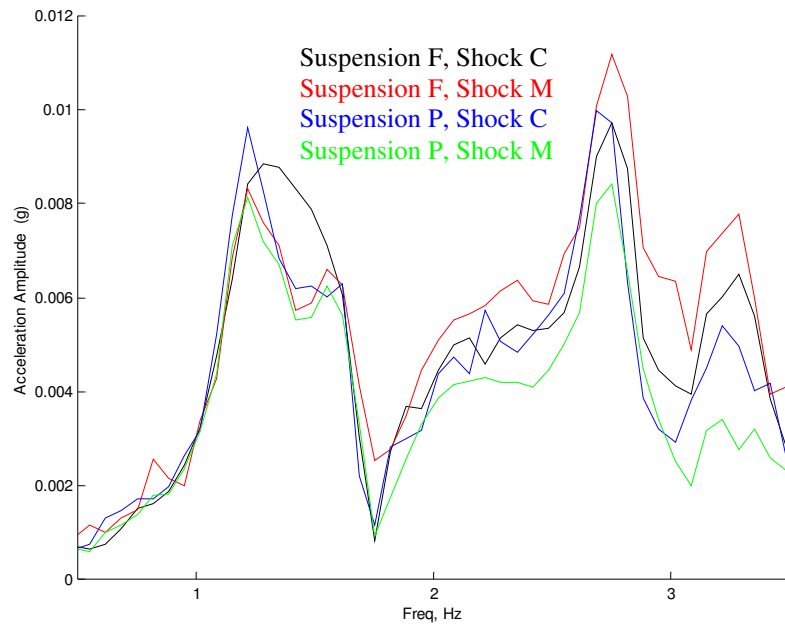


Figure 5-71. Thin High Lateral Acceleration of B-post (Low Frequency)

5.6.2 Roll Cab Suspension Study

The next four plots (Figures 5-72 thru 5-75) show the cab suspension vibrations. As indicated by the B-post accelerometers (Figures 5-76 thru 5-81), the results are in-line with the other trucks. Higher accelerations occurred with Suspension P and there was no significant difference when the shocks were switched.

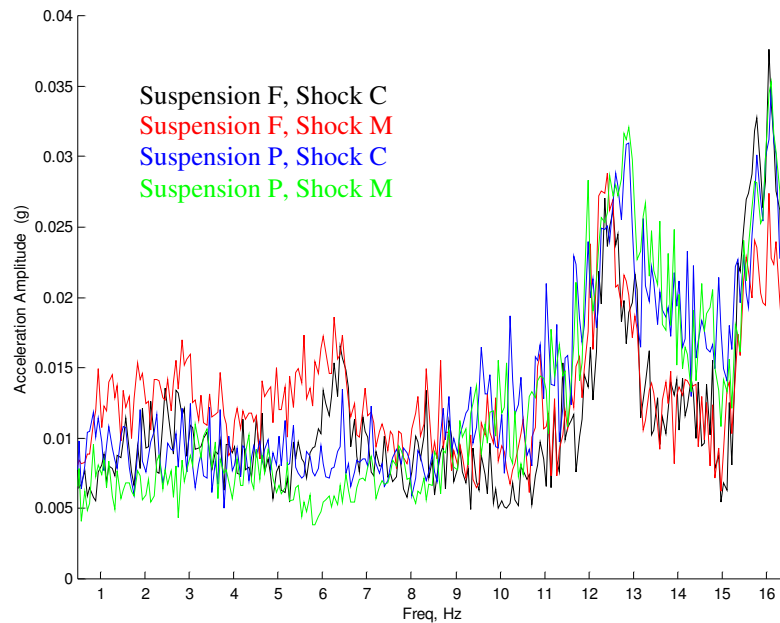


Figure 5-72. Thin High Vertical Acceleration of Frame at Rear Cab Suspension

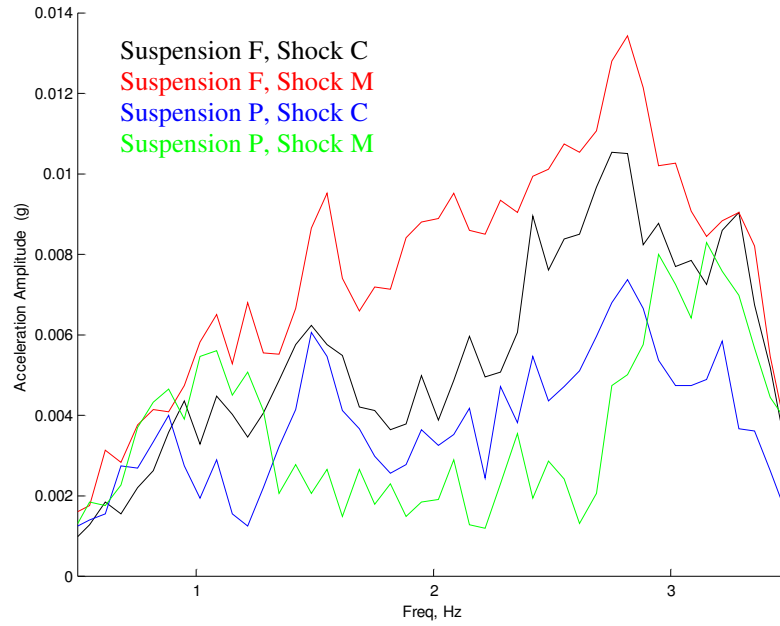


Figure 5-73. Thin High Vertical Acceleration of Frame at Rear Cab Suspension (Low Frequency)

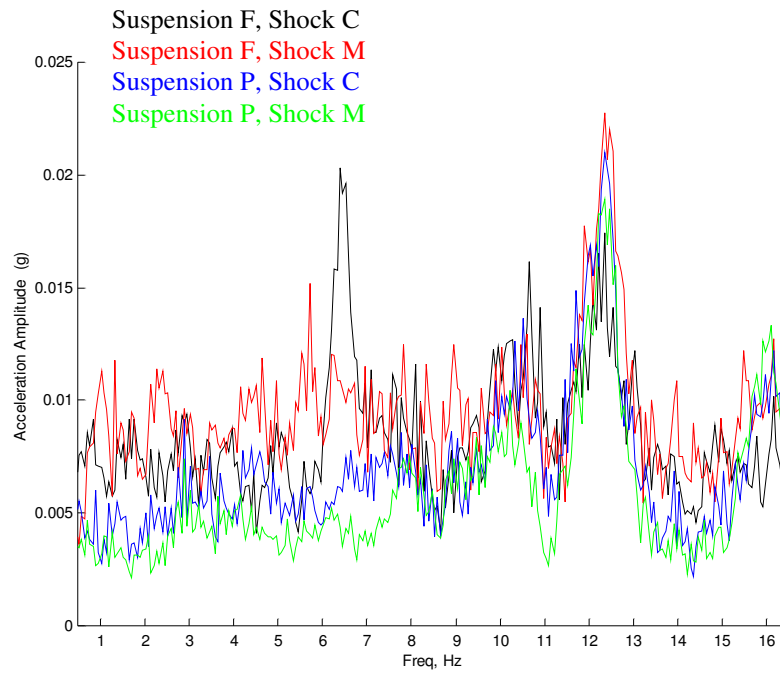


Figure 5-74. Thin High Vertical Acceleration of Cab at Rear Cab Suspension

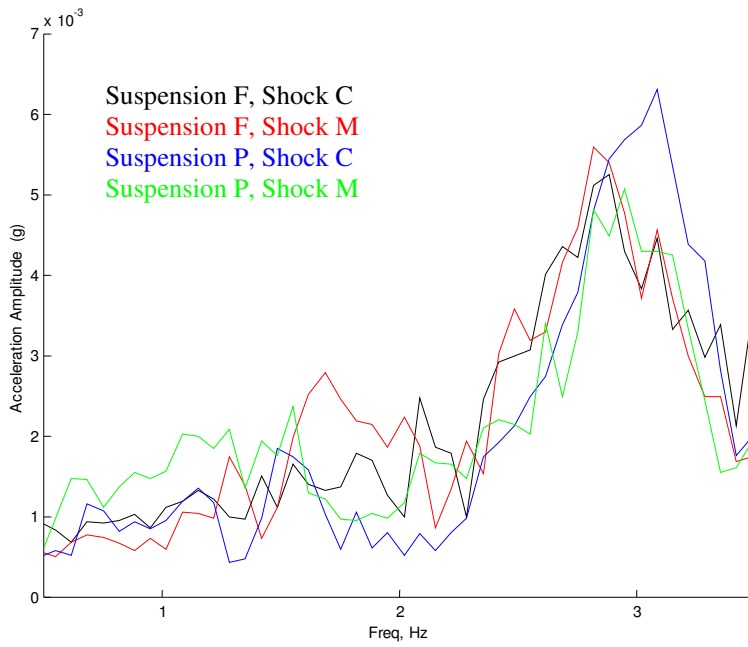


Figure 5-75. Thin High Vertical Acceleration of Cab at Rear Cab Suspension (Low Frequency)

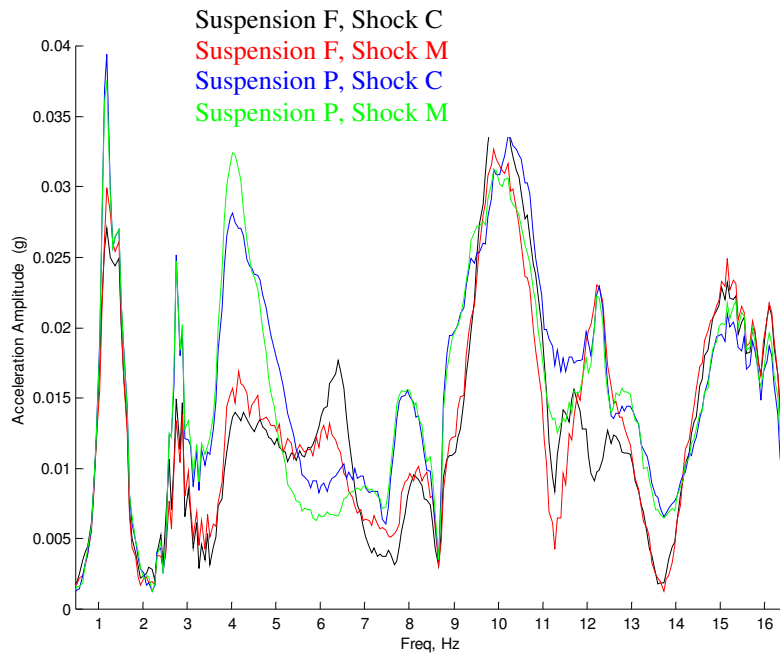


Figure 5-76. Thin High Vertical Acceleration of B-post

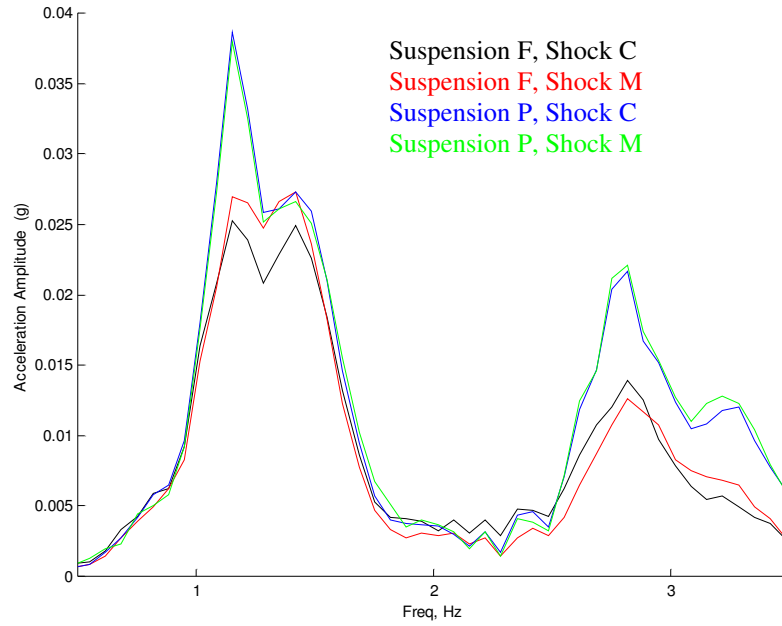


Figure 5-77. Thin High Vertical Acceleration of B-post (Low Frequency)

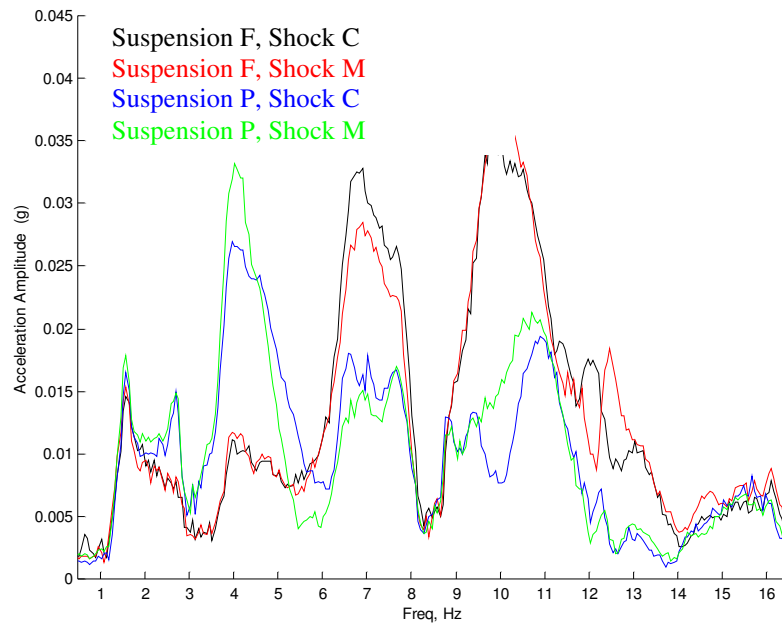


Figure 5-78. Thin High Fore/Aft Acceleration of B-post

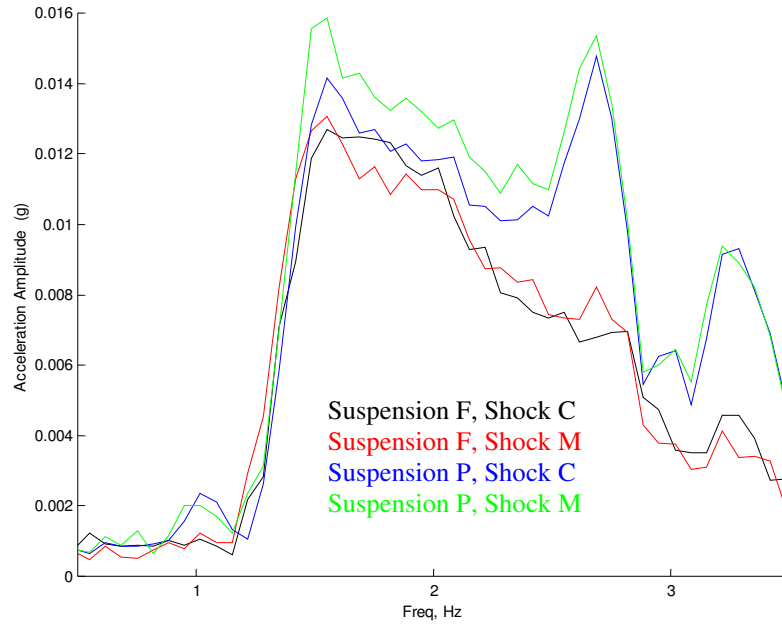


Figure 5-79. Thin High Fore/Aft Acceleration of B-post (Low Frequency)

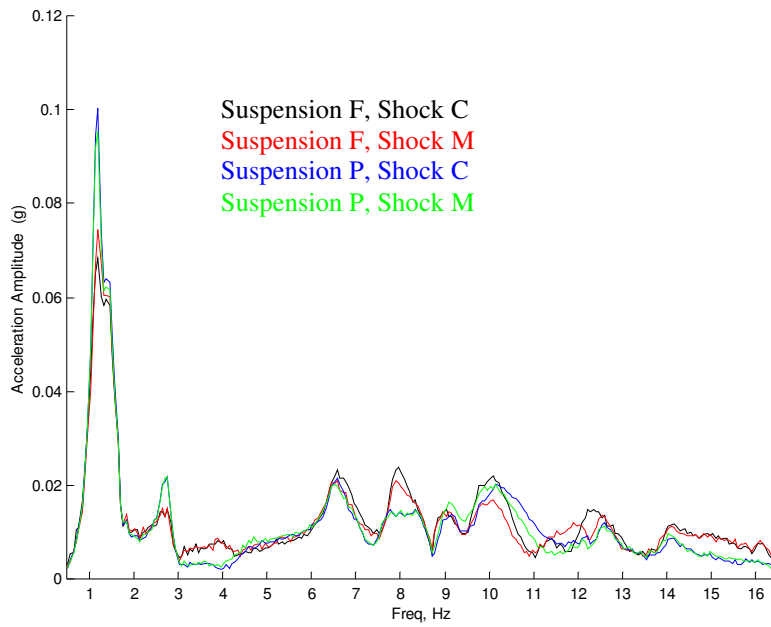


Figure 5-80. Thin High Lateral Acceleration of B-post

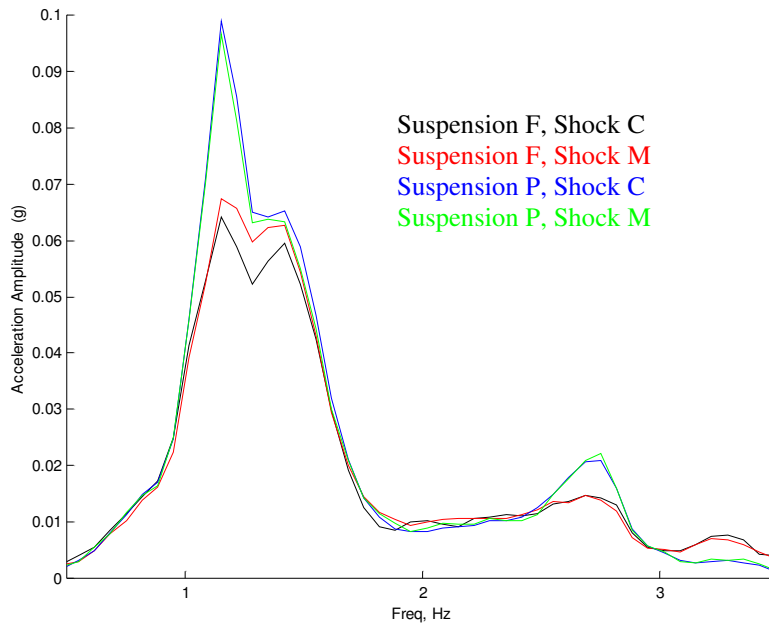


Figure 5-81. Thin High Lateral Acceleration of B-post (Low Frequency)

5.7 Comparison Between Trucks

The Standard High has the stiffest frame (based on cross-section moment of inertia) with a 300 mm x 7 mm cross-section. It also has the highest beaming frequency, 6.0 Hz. The next stiffest cross section, 300 mm x 6 mm, is on the Thin High, despite the fact that the frame is 25% thinner than the Standard Low's frame. This is because of the greater frame height. The natural frequency of the Thin High's frame is about 5.8 Hz. With a beaming frequency of about 5.6 Hz, the 266 mm x 8 mm frame of the Standard Low is close to that of the Thin High's. The Thin Low truck had the least rigid frame. Its 266 mm x 7 mm frame has a natural frequency of only 5.0 Hz.

5.7.1 Heave Comparison

The natural frequencies can be most easily seen in the vertical displacement at the back of the cab as shown in Figure 5-82. It is worth noting that the Thin High had the largest displacement of the frame at the back of the cab and at the rear (Figure 5-83). The Standard High had almost the same displacement at the rear, but a much smaller displacement at the back of the cab. If all of the frames were completely rigid, the two 770s should have had the largest

displacement at the back of the cab, due to the manner by which the trucks were shaken in the lab. Compared to the 660s, the backs of the 770s' cabs were proportionately closer to the actuators than to the front axle because of the longer cab length. In contrast, the displacement at the rear of the truck should be smaller for the 770s. The distance from the actuator to the rear was the same for all the trucks, so the trucks with the longer wheelbases would be pivoted at a smaller angle. This means that the Standard High could be experiencing a larger beaming effect than the 660s.

Working with the assumption that the two Baseline trucks have a good ride, the problem region for the Thin Low is vertical acceleration (Figures 5-84 and 5-85) at the cab natural frequency from 2 - 4 Hz. This truck's ride in the fore/aft direction is comparable to the Standard Low as shown in Figures 5-86 and 5-87. The Thin High's problem area is below 2 Hz in the vertical direction. The fore/aft ride is comparable to the Baseline trucks'.

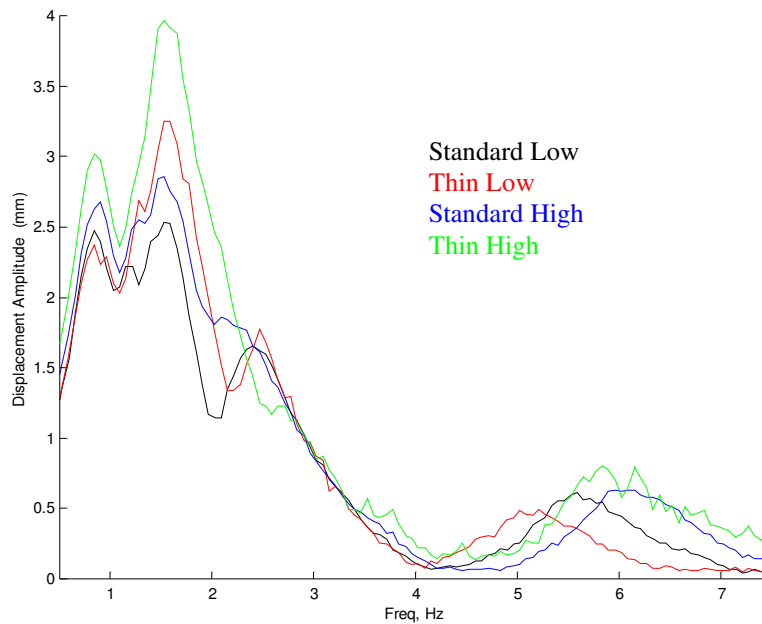


Figure 5-82. Vertical Displacement of Frame at Back of Cab

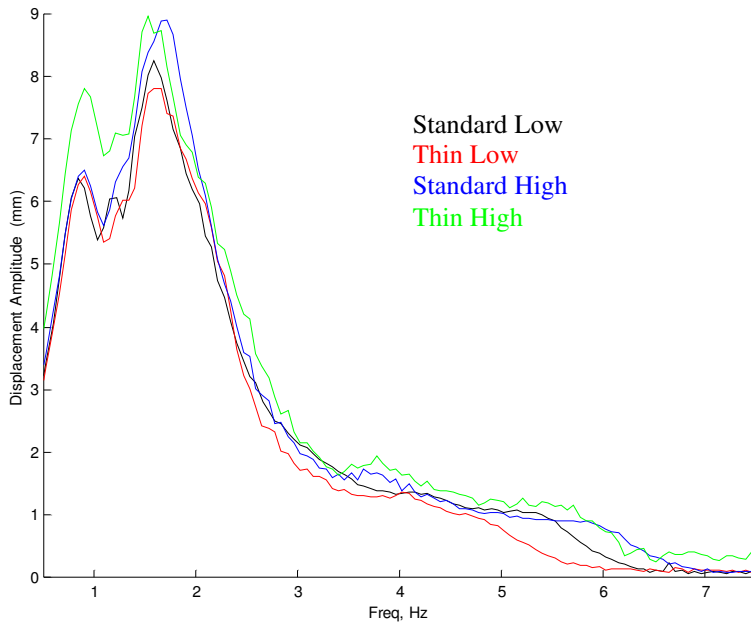


Figure 5-83. Vertical Displacement of Rear of Frame

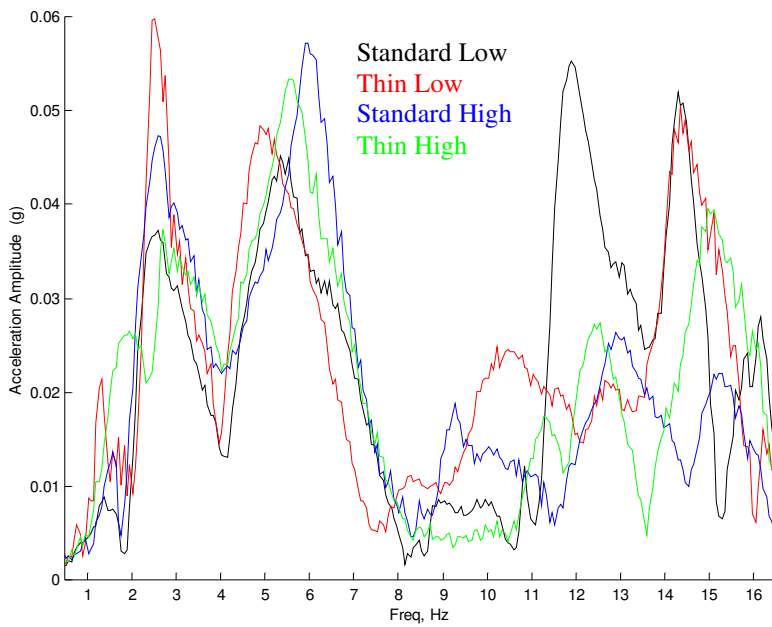


Figure 5-84. Vertical Acceleration of B-post

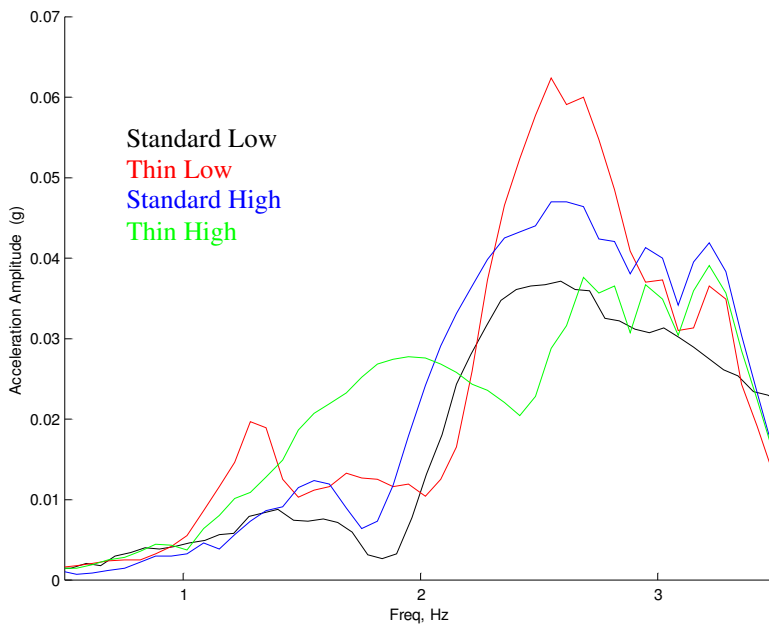


Figure 5-85. Vertical Acceleration of B-post (Low Frequency)

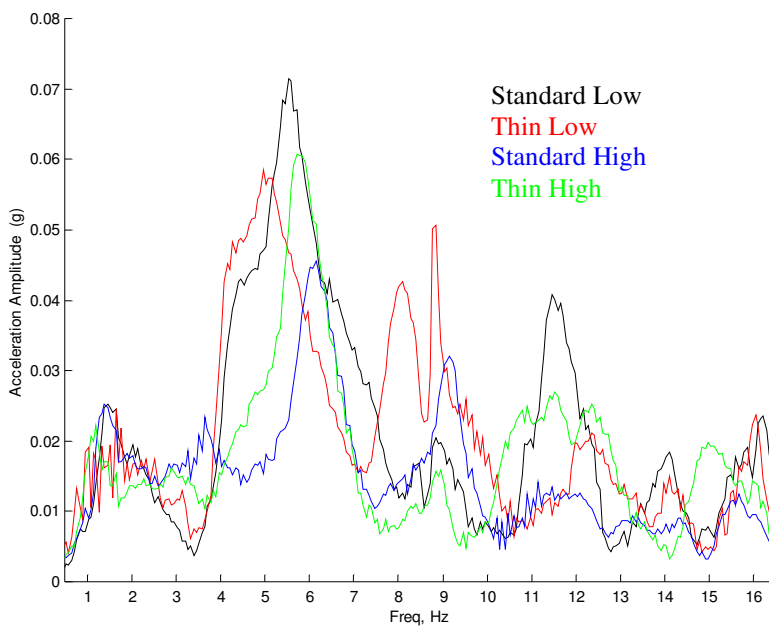


Figure 5-86. Fore/Aft Acceleration of B-post

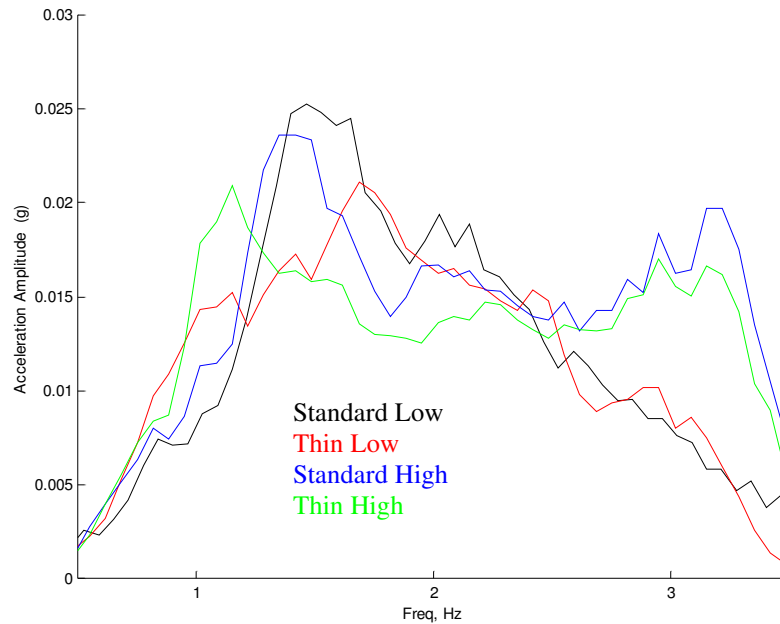


Figure 5-87. Fore/Aft Acceleration of B-post (Low Frequency)

5.7.2 Roll Comparison

The input amplitudes at the axle were increased for the 770s to create more motion at the higher frequencies (4 mm max for the 660s, 5 mm max for the 770s). As a result, magnitudes cannot be directly compared. Figures 5-88 and 5-89 show the frame vibrations at the back of the cab. The frame displacements of the Thin High were noticeably higher than that of the Standard High at the lower frequencies. At the B-post, the Thin High had noticeably higher vibrations at the cab suspension resonance in the vertical direction compared to the Standard High (Figures 5-90 and 5-91). The ride was acceptable in the fore/aft direction as shown in Figures 5-92 and 5-93.

The Thin Low also had higher frame movements than its corresponding Baseline truck as measured at the back of the cab (Figure 5-88), but lower amplitudes were measured at the back of the frame (Figure 5-89). From 2 - 4 Hz, the Thin Low had higher vertical acceleration than the Standard Low (Figures 5-90 and 5-91), but the fore/aft B-post acceleration was similar to the Standard Low (Figures 5-92 and 5-93).

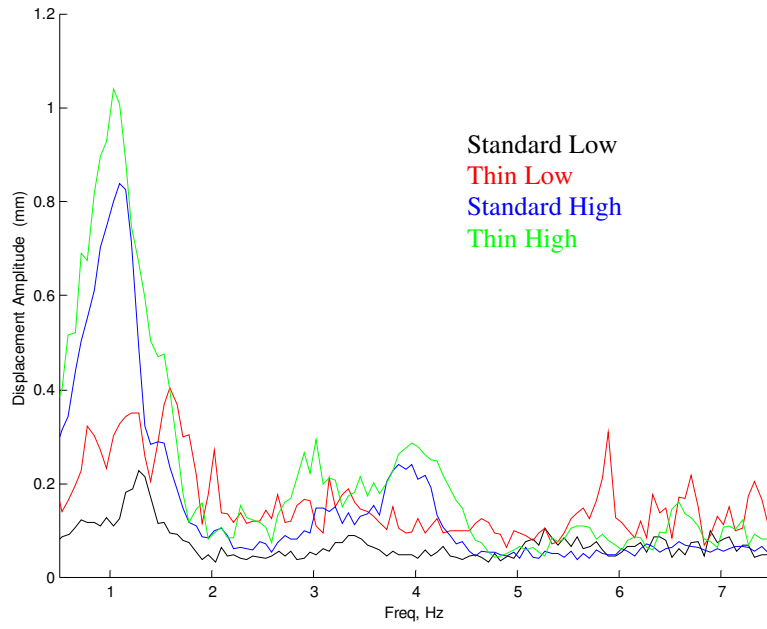


Figure 5-88. Vertical Displacement of Frame at Back of Cab

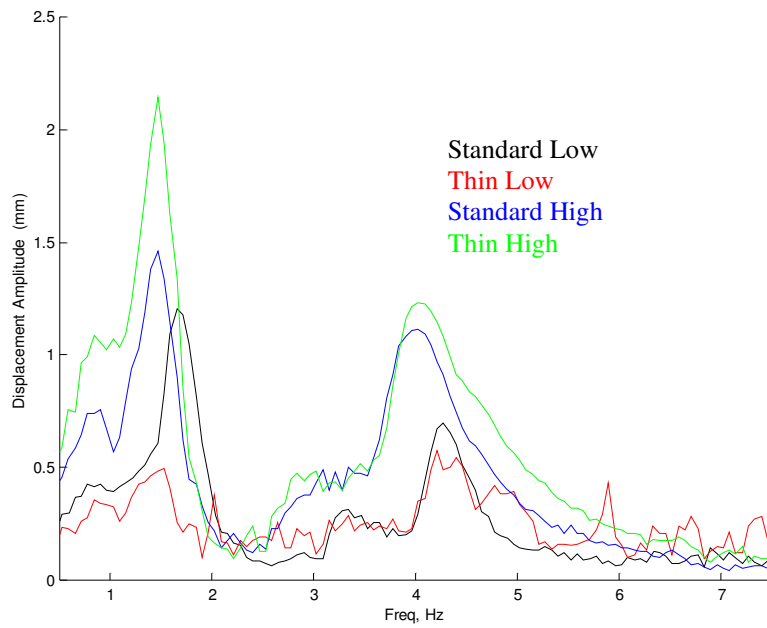


Figure 5-89. Vertical Displacement of Rear of Frame

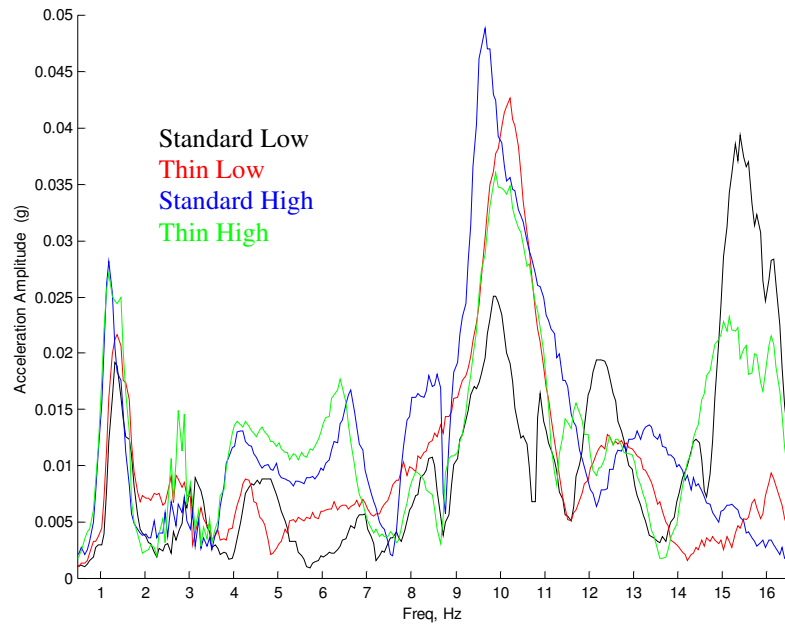


Figure 5-90. Vertical Acceleration of B-post

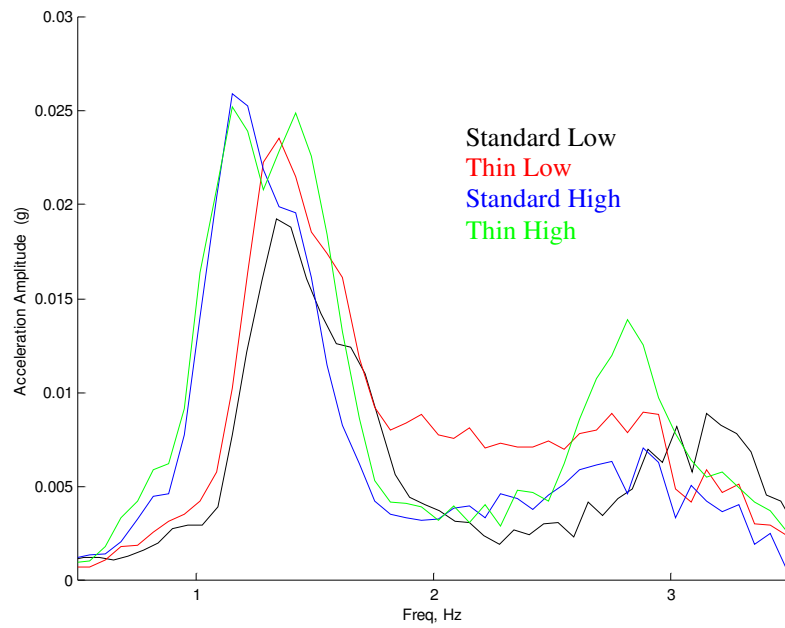


Figure 5-91. Vertical Acceleration of B-post (Low Frequency)

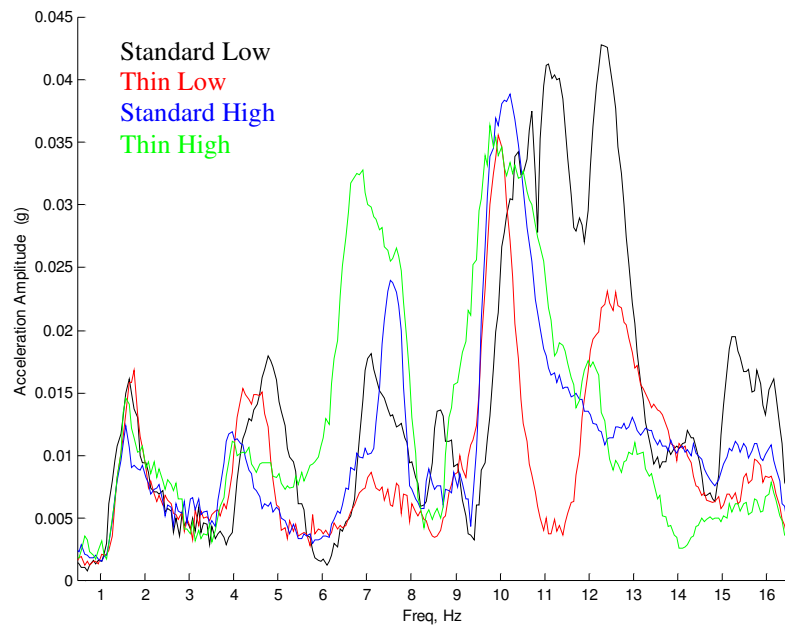


Figure 5-92. Fore/Aft Acceleration of B-post

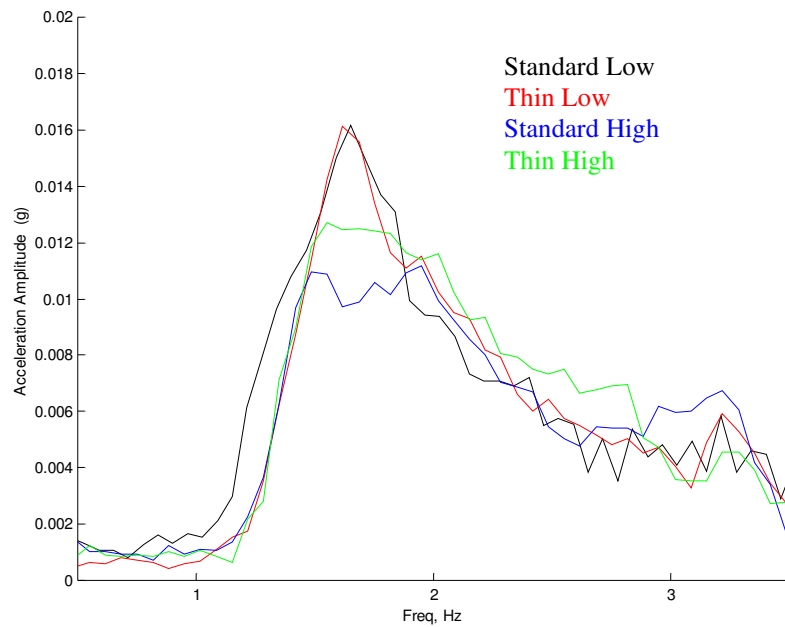


Figure 5-93. Fore/Aft Acceleration of B-post (Low Frequency)

Chapter 6 Vibration Transmissibility

This chapter discusses vibration transmissibilities and transfer functions. Section 6.1 explains what transfer functions and transmissibilities are and how they are used. Section 6.2 explains how the transmissibility plots were developed. The next five subsections contain the results: one for each of the four trucks and a final one comparing the trucks. Each of these five subsections is again subdivided into heave and roll results.

6.1 Transfer Functions and Transmissibilities

A transfer function gives the relationship between an input variable and an output variable. It can be a continuous mathematical function, or it can be calculated discretely, as is often the case when dealing with digital data. If the dimensions of the two variables are the same – comparing data from two accelerometers, for example – then the transfer function is called the transmissibility. Transmissibilities are intuitive tools that ease visualizing what is occurring, especially when motion is concerned. For example, if the acceleration transmissibility between two points is equal to 2 at a certain frequency, then that means that the location of the output sensor is moving twice as much as the location of the input sensor at that frequency.

Transmissibility plots look similar to the chirp frequency plots. The main difference is that – for a linear system – the transmissibility plots are independent of the input signals. If the amplitude of the input signal is doubled, the frequency response plot will double as well. The transmissibility plot, however, would not change because both the input and the output will double so the ratio between them will stay the same. Of course, *no* real system is *completely* linear, so the output may not exactly double with twice the input.

Another advantage of transmissibility is that one can eliminate resonances caused by parts of the truck that are not of interest. For example, when comparing the cab suspensions, the effects of the axle resonance are quite evident. By examining the transmissibility between the frame at the rear cab suspension (RCS) and at the cab at the RCS, the effect of the axle suspension can be eliminated (in a linear system). Creating this transmissibility simulates the effect of having the frame at the RCS vibrate at a constant amplitude at all frequencies. Consequently, one can see when the cab suspension is attenuating (decreasing) or amplifying the accelerations received from the frame.

In most of the plots, transmissibilities are used between two accelerometers. In some cases, however, transfer functions between accelerometers and LVDTs (which measure displacement) were used instead to better capture some of the test vehicle's dynamics.

6.2 Calculation Process

The first step in creating the transmissibilities is to calculate the root mean squared (RMS) value of the instrument of choice. The RMS is calculated as its name implies: it is the (square) root of the sum of the squares of each data point. This relationship is shown below:

$$RMS = \sqrt{\sum_{i=1}^N x_i^2 / N} \quad (7)$$

where x_i is a single data point and N is the number of data points. The RMS of a value is a common method of representing the power of a periodic signal. To create a transmissibility plot, the RMS value must be calculated at each frequency (44-54 pure tones total) for both the input and the output. This process must be repeated for each channel (22), for each truck (four), for every suspension combo (eight) and for both test types (roll and heave).

The pure tone signals were used to find transmissibilities. This is a single-frequency, constant-amplitude sinusoidal wave. Incidentally, it is possible to create transmissibility plots from the chirp frequency plots. However, these plots would not be quite as accurate for what we want. For example, even when the axle is shaken at 5 Hz, the instruments will pick up energy at other frequencies because of non-linearities in the system. Thus, shaking the truck at 5 Hz will affect the magnitudes across the spectrum. The objective of the transmissibility plots is to just show the vibration levels transferred when the truck is shaken at a certain frequency.

6.3 Standard Low Results

This section discusses the results of the pure tone tests of the first test truck (listed in bold in Table 6-1).

Table 6-1. Important test vehicle parameters

Name	Model	Sleeper length	Wheelbase	Frame, $h \times t$
Standard Low	VNL 660	61 in. (1550 mm)	215 in. (5460 mm)	266 mm x 8 mm
Thin Low	VNL 660	61 in. (1550 mm)	215 in. (5460 mm)	266 mm x 7 mm
Standard High	VNL 770	77 in. (1960 mm)	229 in. (5810 mm)	300 mm x 7 mm
Thin High	VNL 770	77 in. (1960 mm)	239 in. (6070 mm)	300 mm x 6 mm

6.3.1 Heave Cab Suspension Study

Figure 6-1 shows the input displacement of the actuators. Note that the displacement was stepped down between 3.3 and 4.2 Hz. This was necessary because the higher amplitude put in too much energy into the truck at high frequencies. Because of the non-linear nature of the truck's vibration dynamics, this also means that the transmissibilities at the higher frequencies are slightly lower than they would be if the input amplitude had not been decreased.

To evaluate the rear cab suspension, the most useful transmissibility to consider is between the vertical accelerometer on the frame at the RCS and the one right above on the cab, shown in Figure 6-2. This figure shows that at most frequencies, Suspension P is performing better, as indicated by the lower transmissibility levels. The grouping at 1 - 1.5 Hz is due to the front- and rear-axle natural frequencies while frame beaming is responsible for the peaks near 5 Hz. As for the peaks from 2 - 3.5 Hz, that is where the cab suspension's natural frequency occurs. This can be seen more clearly in the transmissibility (Figure 6-3) between the same frame accelerometer and the vertical accelerometer at the B-post. Surprisingly, the fore/aft B-post (Figure 6-4) versus the frame plot indicates attenuation at the cab's natural frequency. Part of the reason is due to the kinematics. If one assumes that the cab pivots about its front suspension during heave excitation (which was observed during testing), then the B-post fore/aft accelerometer has a much shorter radius arm than the accelerometer at the back of the cab.

The next three plots give a clearer picture of where the axle natural frequencies are. Figure 6-5 (frame accelerometer above axle versus actuator input) clearly shows the rear axle suspension natural frequency at about 1.7 Hz. By comparing the accelerometer at the front of the frame to the accelerometer located above the excited axle, Figure 6-6 shows the front suspension natural frequency at about 1 Hz (the cab natural frequency is at 2 - 3 Hz and beaming occurs at about 5 Hz). For more evidence on the location of the beaming frequency, we can compare the accelerometer above the second axle to the accelerometer at the end of the frame (Figure 6-7) and to the accelerometer located on the frame at the back of the cab (Figure 6-8).

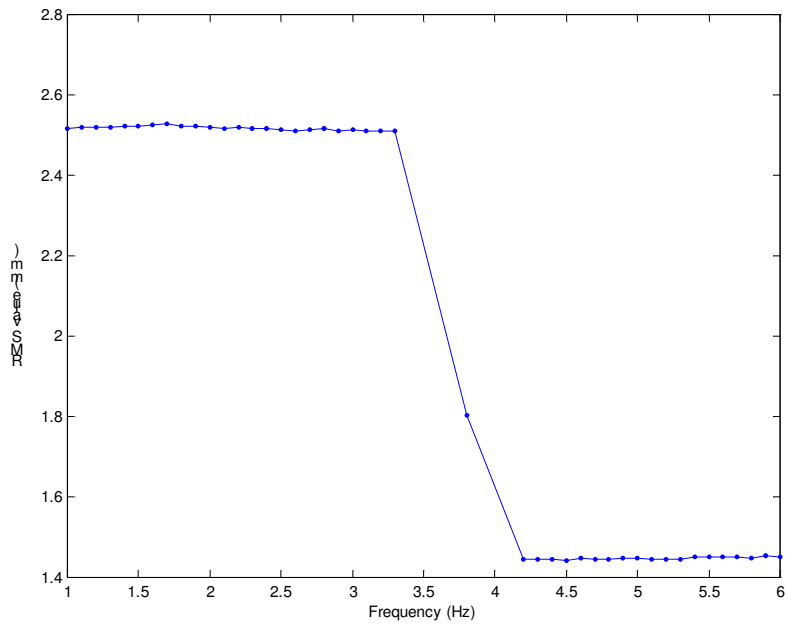


Figure 6-1. Actuator Displacement, Driver

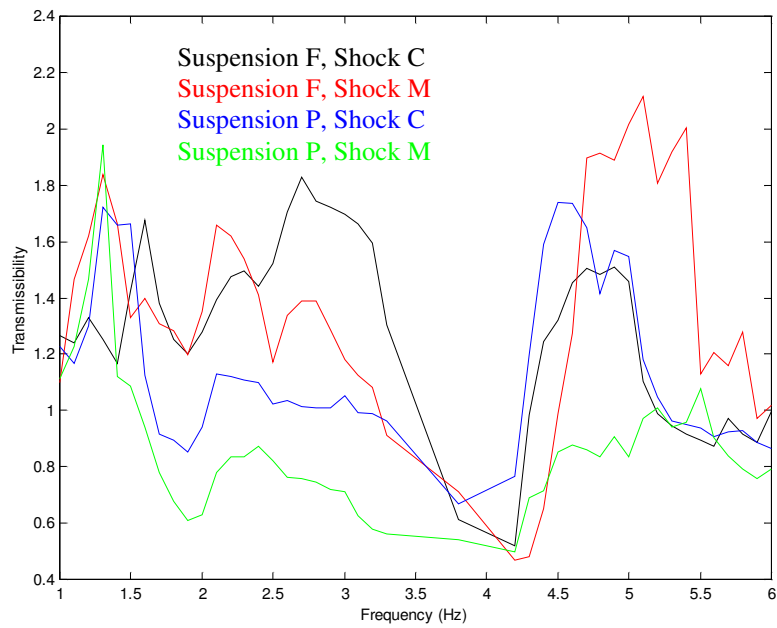


Figure 6-2. Vertical Acceleration of Cab, RCS, Center, vs. Vertical Acceleration of Frame, RCS, Center

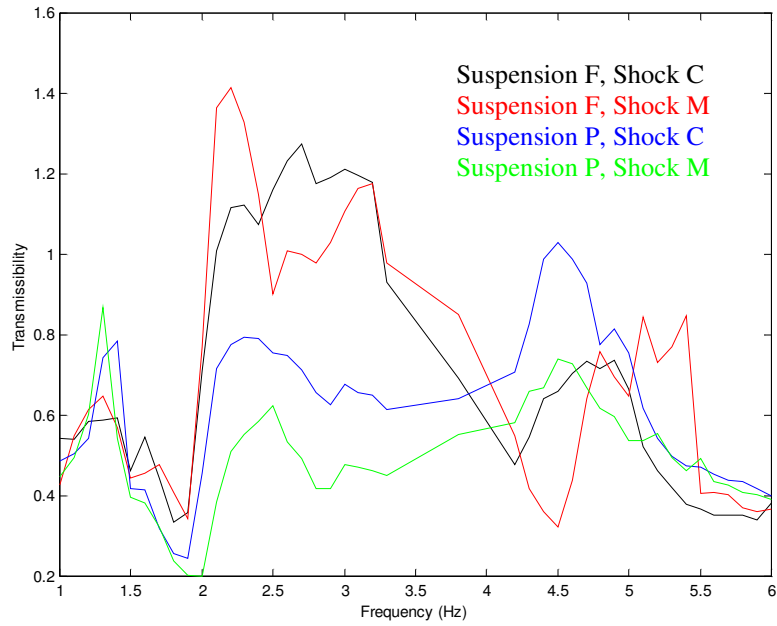


Figure 6-3. Vertical Acceleration of B-post, Driver, vs. Vertical Acceleration of Frame, RCS, Center

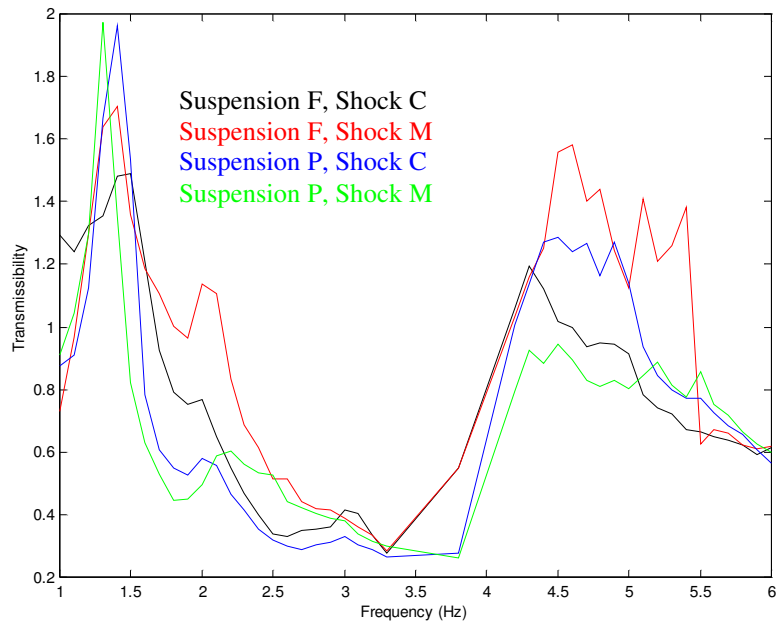


Figure 6-4. Fore/Aft Acceleration of B-post, Driver, vs. Vertical Acceleration of Frame, RCS, Center

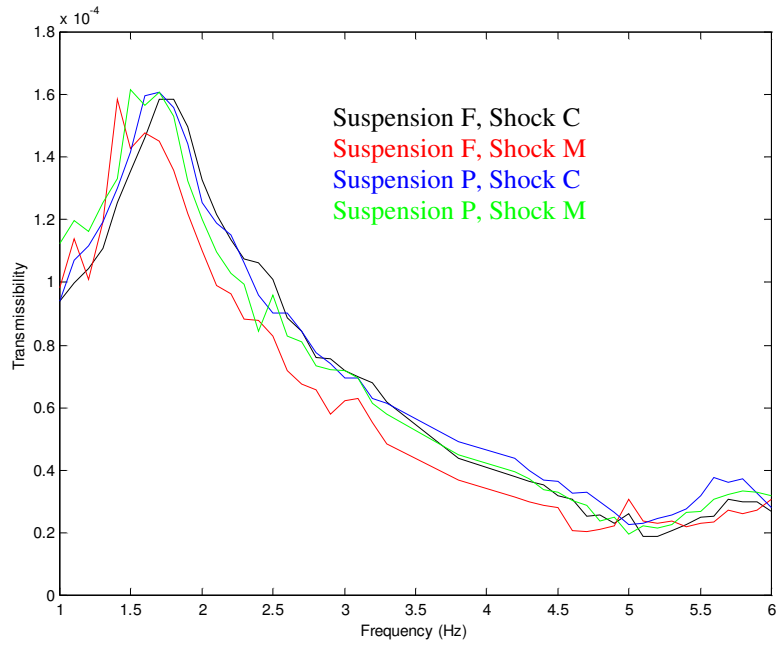


Figure 6-5. Vertical Acceleration of Frame, Second Axle, Driver, vs. Actuator Displacement, Driver

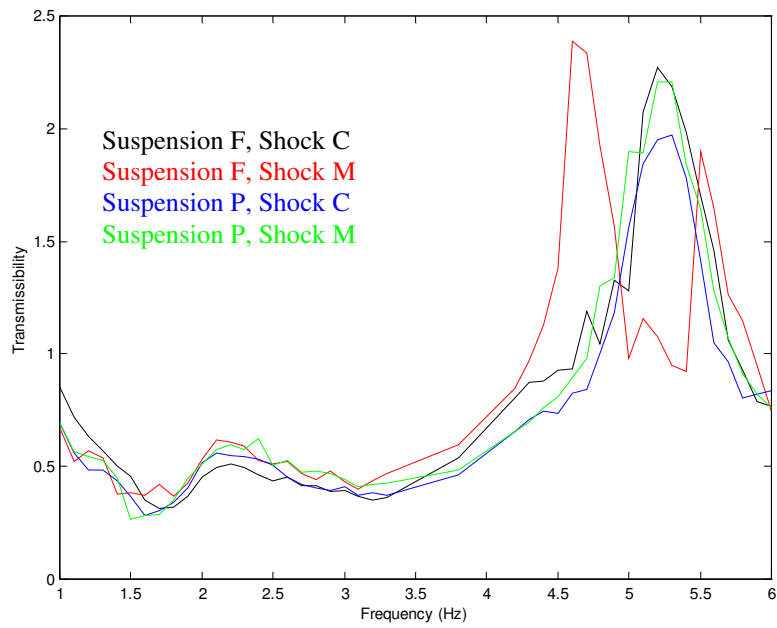


Figure 6-6. Vertical Acceleration of Frame, Front, Driver, vs. Vertical Acceleration of Frame, Second Axle, Driver

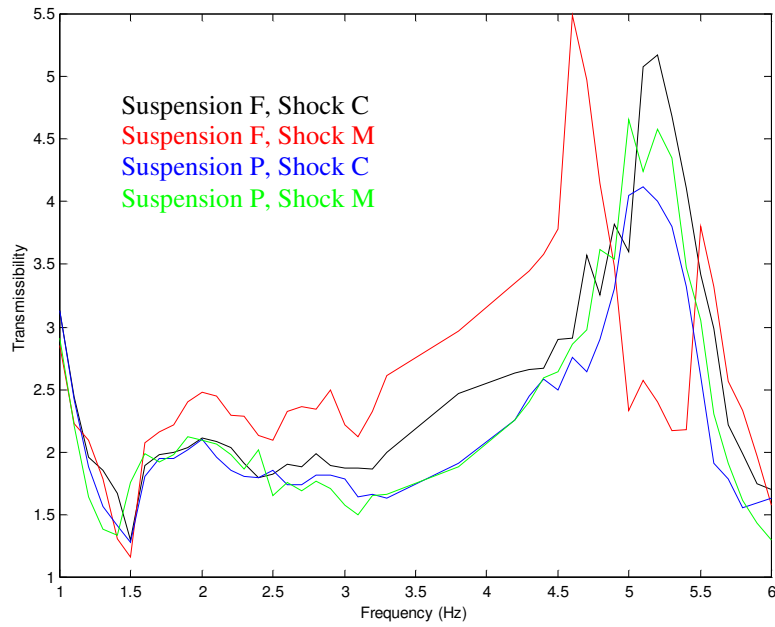


Figure 6-7. Vertical Acceleration of Frame, Rear, Driver, vs. Vertical Acceleration of Frame, Second Axle, Driver

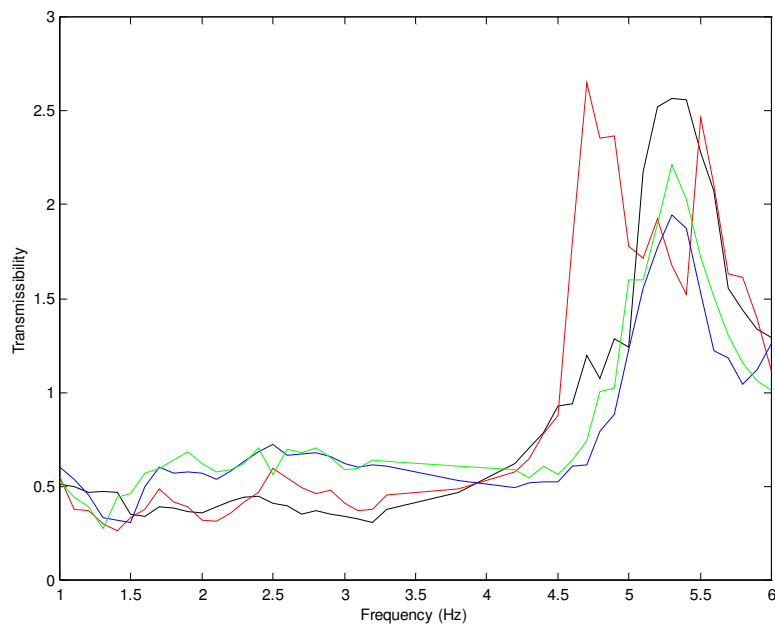


Figure 6-8. Vertical Acceleration of Frame, RCS, Driver, vs. Vertical Acceleration of Frame, Second Axle, Driver

6.3.2 Roll Cab Suspension Study

The actuator displacement for the roll tests is shown in Figure 6-9. This time the input is dropped at 2 Hz, and again at 3 Hz. The accelerometer located on the frame below the rear cab suspension (RCS) is in a good spot for heave testing, but it does not pick up roll very well because it is close to the roll axis of the truck frame. Therefore, the displacement across the cab suspension versus the displacement of the frame at this location was examined to observe the suspension's roll natural frequency (Figure 6-10). The roll frequency of the cab is very low, about 1.3 - 1.4 Hz. This is confirmed by examining the B-post transmissibility as before, in Figure 6-11. Additionally, this figure shows that the transmissibilities between Suspension F and Suspension P are not all that different.

An interesting phenomenon can be observed by looking at the transmissibility between the lateral accelerometer at the base of the cab and the one near the drip rail, about 5 feet up the back of the cab (Figure 6-12). Below about 1.5 Hz, the transmissibility is relatively high, indicating that the cab roll center is close to the lower accelerometer. This is what one would expect (for the cab to roll around a point close to the suspension). Once the frequency reaches about 3 Hz, however, the transmissibility drops, indicating that the roll center is moving closer to the drip-rail mounted accelerometer. Just as if someone pulled out the rug from under your feet, the lower part of the cab moves faster than the top because it can't respond quickly enough to the input at the higher frequencies (another indication of a low natural frequency).

The axle roll natural frequencies are found the same way as the heave frequencies. Comparing the vertical acceleration above the excited axle with the input displacement (Figure 6-13) indicates that the roll natural frequency of the drive axle is at about 1.6 Hz. The front axle roll natural frequency is at about 2.5 - 3 Hz, as indicated by the front accelerometer versus the accelerometer above the drive axle, shown in Figure 6-14.

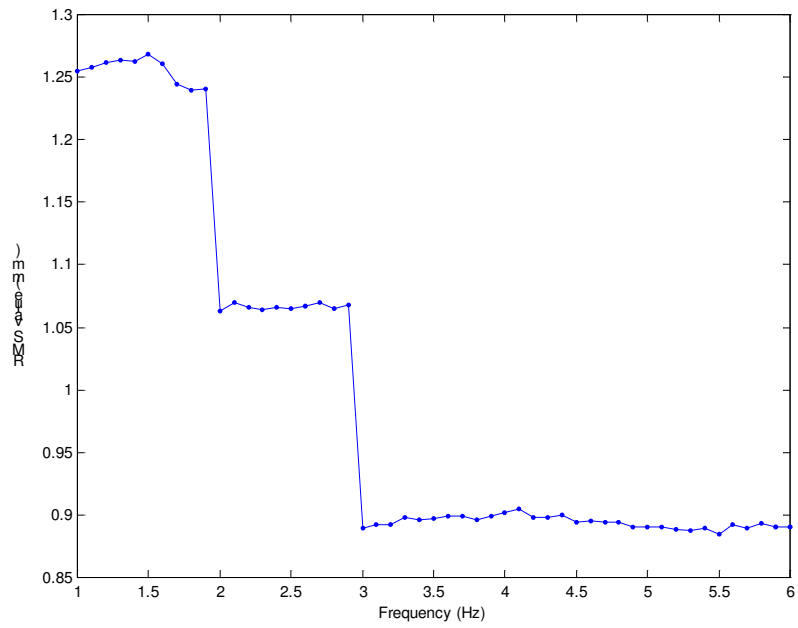


Figure 6-9. Actuator Displacement, Driver

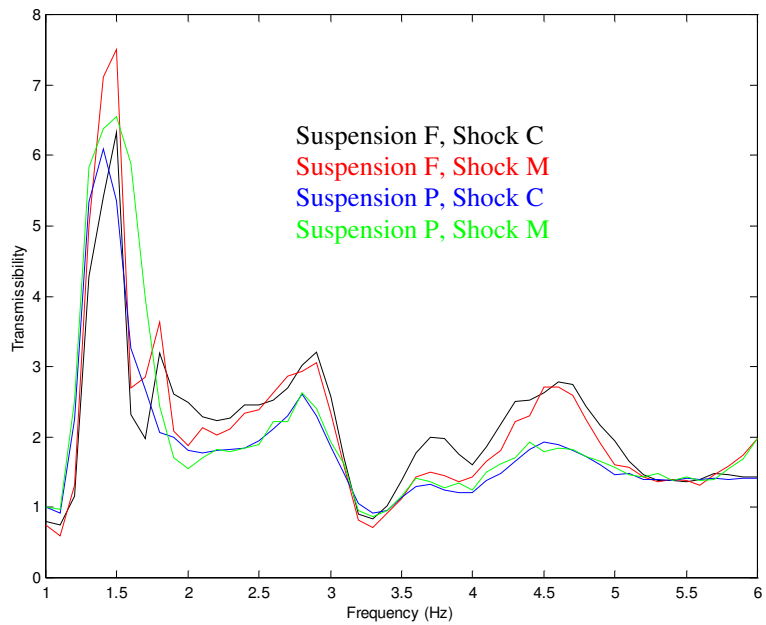


Figure 6-10. Vertical Displacement across RCS, Driver, vs. Vertical Displacement of Frame, Back of Cab, Driver

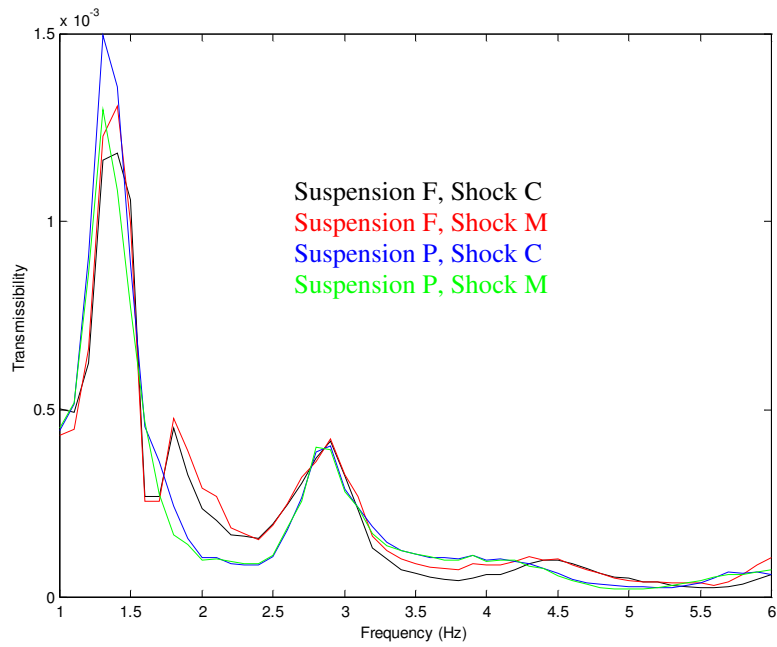


Figure 6-11. Vertical Acceleration of B-post, Driver, vs. Vertical Displacement of Frame, Back of Cab, Driver

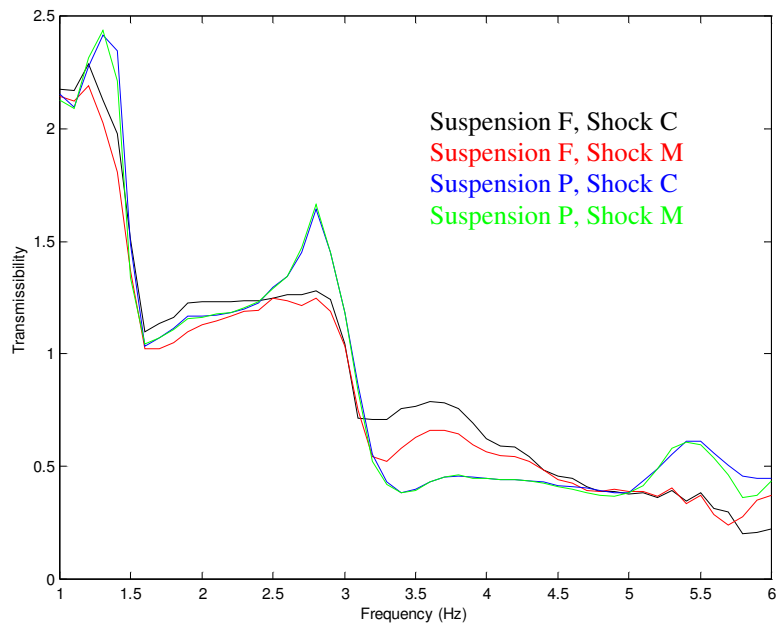


Figure 6-12. Lateral Acceleration of Cab, Drip Rail, Center, vs. Lateral Acceleration of Cab, RCS, Center

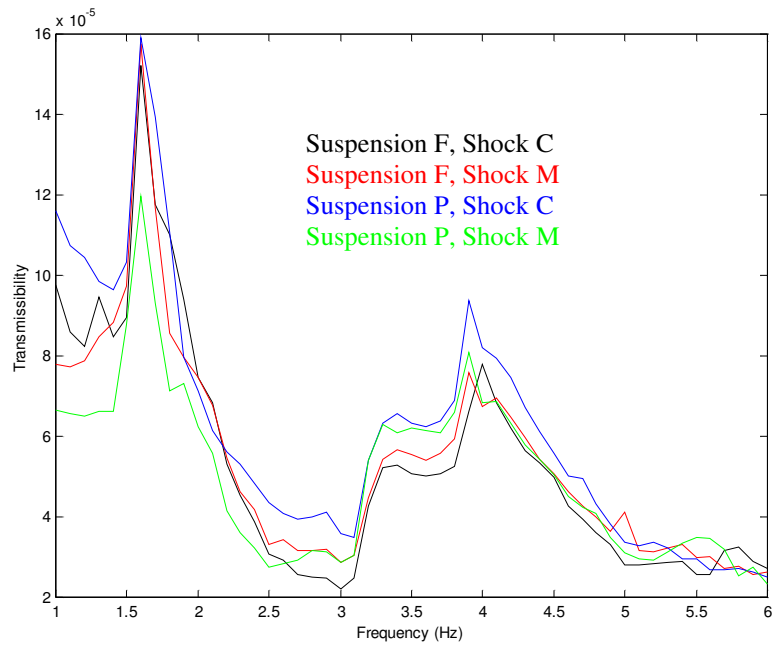


Figure 6-13. Vertical Acceleration of Frame, Second Axle, Driver, vs. Actuator Displacement, Driver

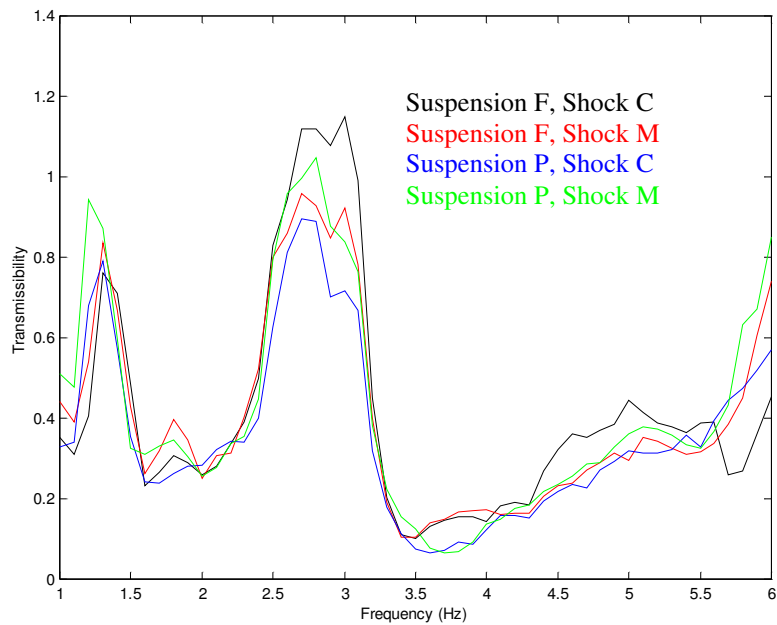


Figure 6-14. Vertical Acceleration of Frame, Front, Driver, vs. Vertical Acceleration of Frame, Second Axle, Driver

6.4 Thin Low Results

This section discusses the results of the pure tone tests of the second test truck, listed in bold in Table 6-2 below.

Table 6-2. Important test vehicle parameters

Name	Model	Sleeper length	Wheelbase	Frame, <i>h x t</i>
Standard Low	VNL 660	61 in. (1550 mm)	215 in. (5460 mm)	266 mm x 8 mm
Thin Low	VNL 660	61 in. (1550 mm)	215 in. (5460 mm)	266 mm x 7 mm
Standard High	VNL 770	77 in. (1960 mm)	229 in. (5810 mm)	300 mm x 7 mm
Thin High	VNL 770	77 in. (1960 mm)	239 in. (6070 mm)	300 mm x 6 mm

6.4.1 Heave Cab Suspension Study

The same displacements were used for every truck, so the actuator input is not repeated here. The first transmissibility examined is between the two accelerometers at the cab suspension (Figure 6-15). Although the transmissibility at 2.5 Hz (near the natural frequency) is low, it is still double the transmissibility at 2 Hz. The large inputs created by the axle resonance at low frequencies and the beaming at 5 Hz skew the transmissibility results. In Figures 6-16 and 6-17, that show the B-post transmissibilities, we again see that beaming dominates the plot but the cab natural frequency is more evident. Also, note that while Shock M transmits more of the frame input to the cab at the beaming frequency, less of this energy makes it to the B-post position.

Beaming can also be seen at the front of the truck (Figure 6-18), particularly with Shock M, but is not as noticeable at the rear of the truck (Figure 6-19). At the frame accelerometer located at the cab suspension (Figure 6-20), the beaming frequency is very apparent at 4.5 - 6.0 Hz.

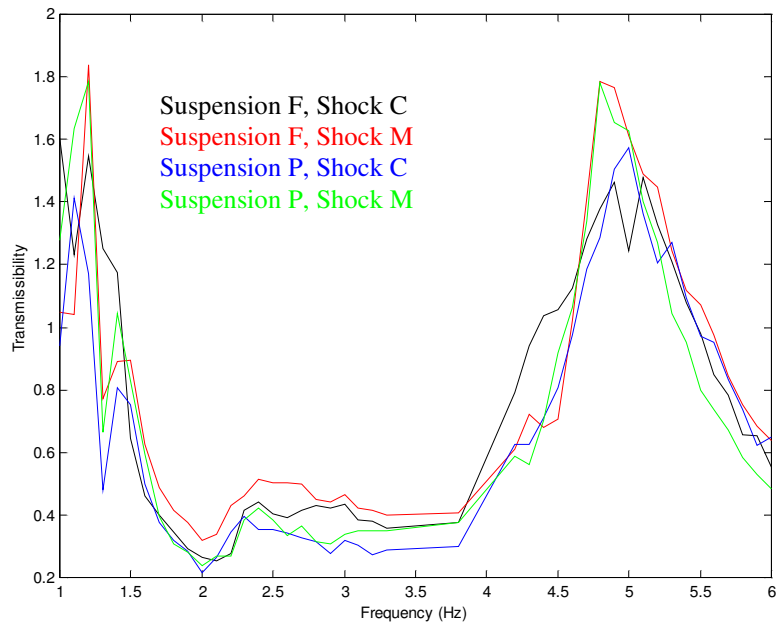


Figure 6-15. Vertical Acceleration of Cab, RCS, Center, vs. Vertical Acceleration of Frame, RCS, Center

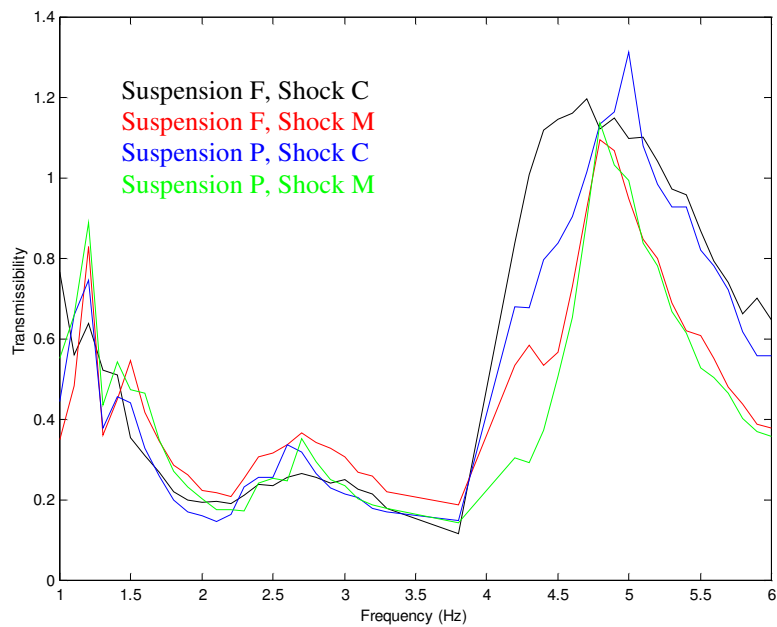


Figure 6-16. Vertical Acceleration of B-post, Driver, vs. Vertical Acceleration of Frame, RCS, Center

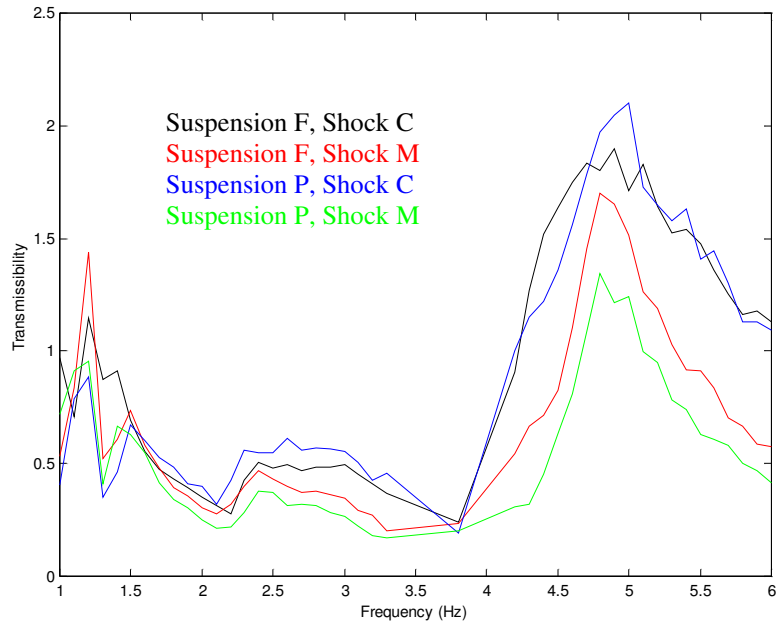


Figure 6-17. Fore/Aft Acceleration of B-post, Driver, vs. Vertical Acceleration of Frame, RCS, Center

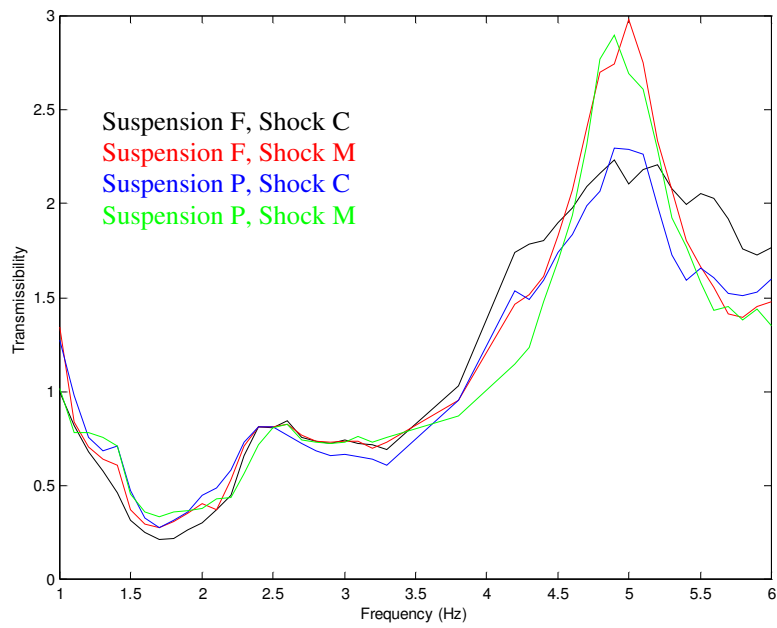


Figure 6-18. Vertical Acceleration of Frame, Front, Driver, vs. Vertical Acceleration of Frame, Second Axle, Driver

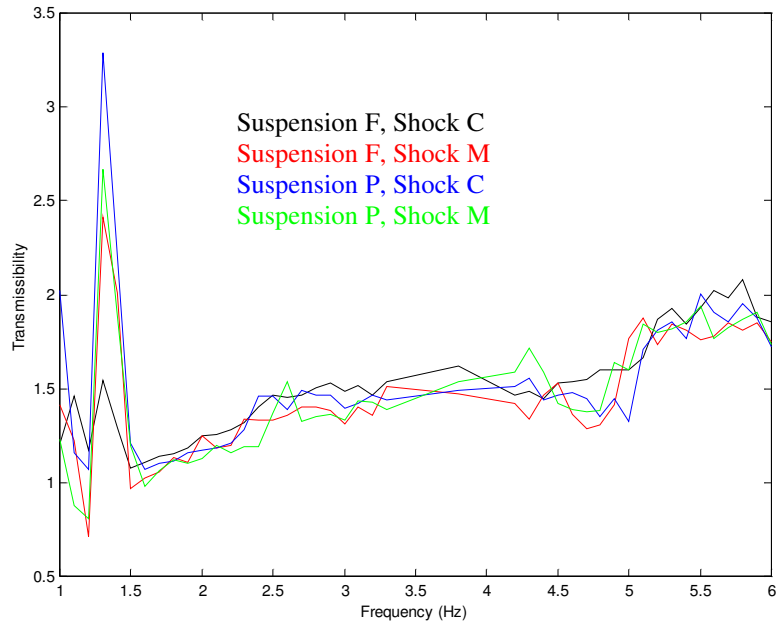


Figure 6-19. Vertical Acceleration of Frame, Rear, Driver, vs. Vertical Acceleration of Frame, Second Axle, Driver

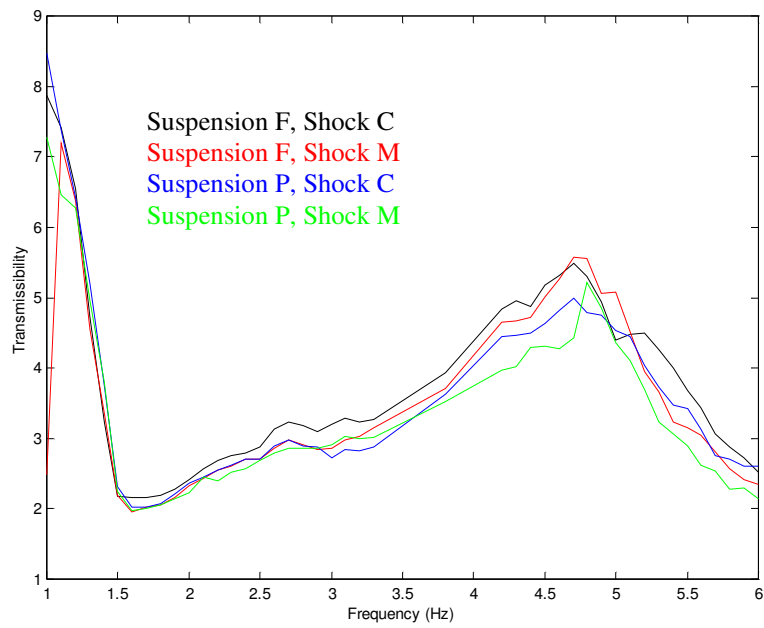


Figure 6-20. Vertical Acceleration of Frame, RCS, Driver, vs. Vertical Acceleration of Frame, Second Axle, Driver

6.4.2 Roll Cab Suspension Study

With this 660, a significant difference in the cab suspension transmissibility occurs between the two cab suspensions (Figure 6-21). Suspension P has about double the transmissibility at its roll resonance of 1.4 Hz. This resonance can also be seen in the cab by the lateral and vertical accelerometers (Figure 6-22 and 6-23). As demonstrated by Figure 6-24, the same change in cab roll center is indicated in this 660 as well.

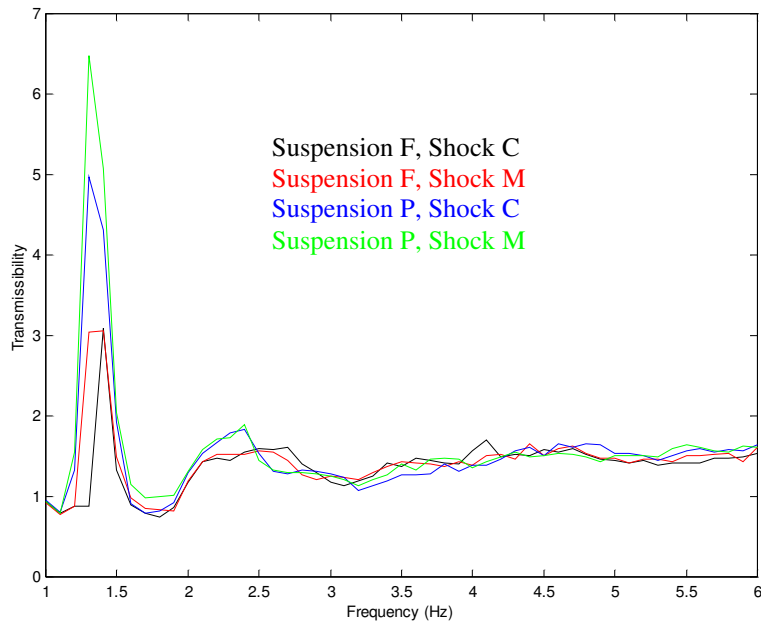


Figure 6-21. Vertical Displacement across RCS, Driver, vs. Vertical Displacement of Frame, Back of Cab, Driver

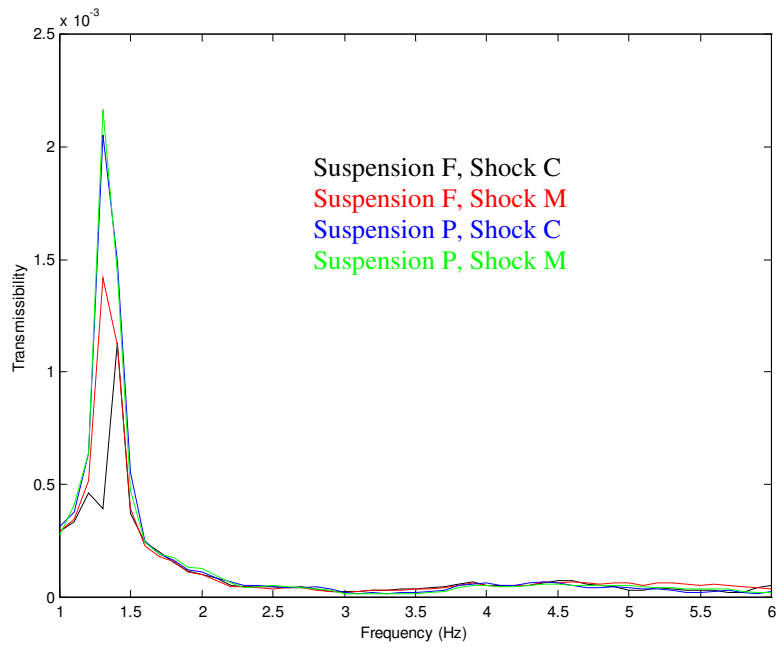


Figure 6-22. Lateral Acceleration of B-post, Driver, vs. Vertical Displacement of Frame, Back of Cab, Driver

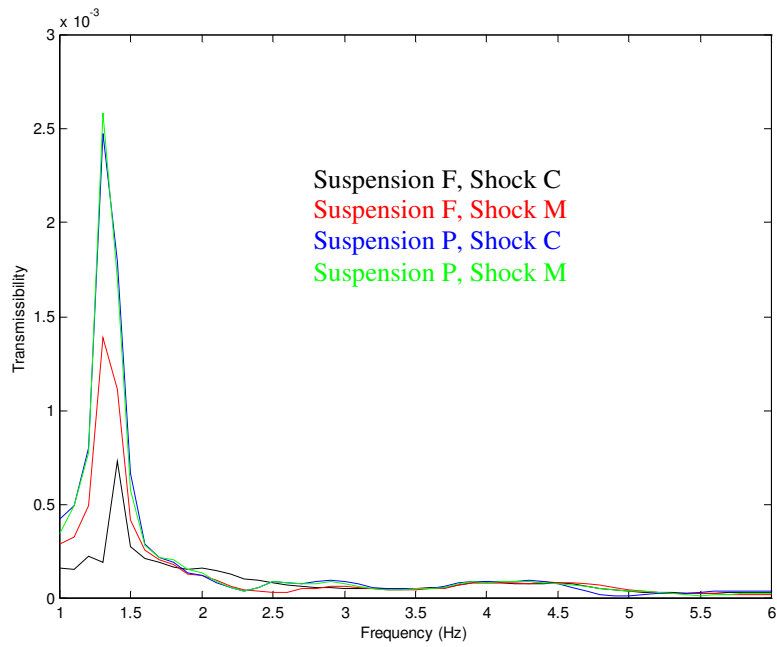


Figure 6-23. Vertical Acceleration of B-post, Driver, vs. Vertical Displacement of Frame, Back of Cab, Driver

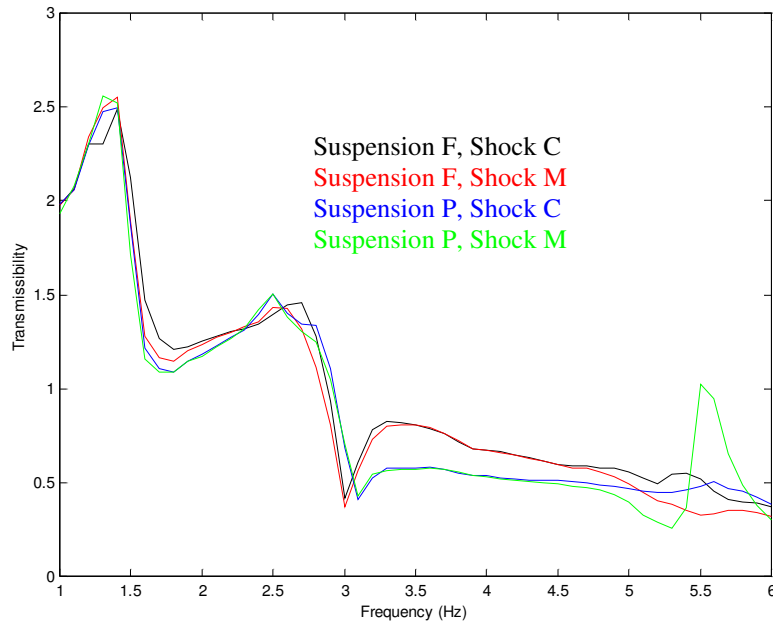


Figure 6-24. Lateral Acceleration of Cab, Drip Rail, Center, vs. Lateral Acceleration of Cab, RCS, Center

6.5 Standard High Results

The results of the pure tone tests of the third test truck (listed in bold in Table 6-3 below) are shown in this section.

Table 6-3. Important test vehicle parameters

Name	Model	Sleeper length	Wheelbase	Frame, $h \times t$
Standard Low	VNL 660	61 in. (1550 mm)	215 in. (5460 mm)	266 mm x 8 mm
Thin Low	VNL 660	61 in. (1550 mm)	215 in. (5460 mm)	266 mm x 7 mm
Standard High	VNL 770	77 in. (1960 mm)	229 in. (5810 mm)	300 mm x 7 mm
Thin High	VNL 770	77 in. (1960 mm)	239 in. (6070 mm)	300 mm x 6 mm

6.5.1 Heave Cab Suspension Study

The transmissibilities of the cab suspension (Figure 6-25) and between the frame and B-posts (Figure 6-26 and 6-27) are not as smooth as would be expected, but they still give us important information. The transmissibility at the cab suspensions' natural frequencies (2 - 3.5 Hz) is much lower for Suspension P. At the axle natural frequency and during beaming, however, Suspension F isolates the cab better. Considering the transmissibility from the frame accelerometer at the axle to the other three frame accelerometers on the truck (Figure 6-29 thru

6-31) we see the reverse: Suspension P has a higher transmissibility at the cab frequency and a lower transmissibility elsewhere. This indicates that the frame is absorbing more of the input energy during cab resonance when equipped with Suspension P, but the cab is taking in more of the energy during other frequencies.

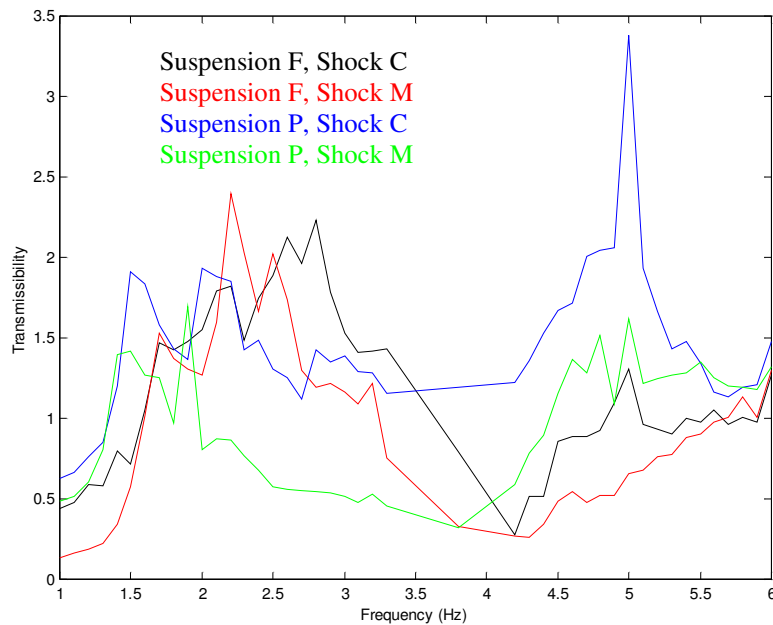


Figure 6-25. Vertical Acceleration of Cab, RCS, Center, vs. Vertical Acceleration of Frame, RCS, Center

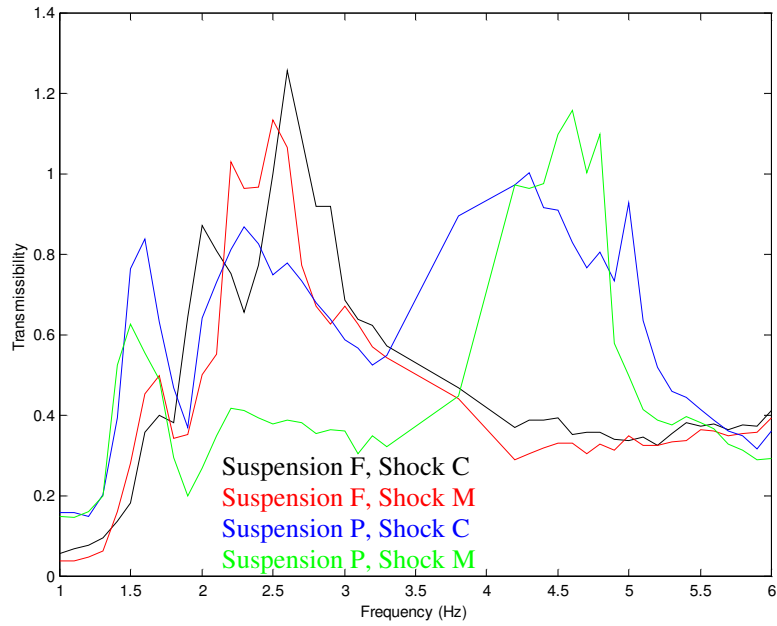


Figure 6-26. Vertical Acceleration of B-post, Driver, vs. Vertical Acceleration of Frame, RCS, Center

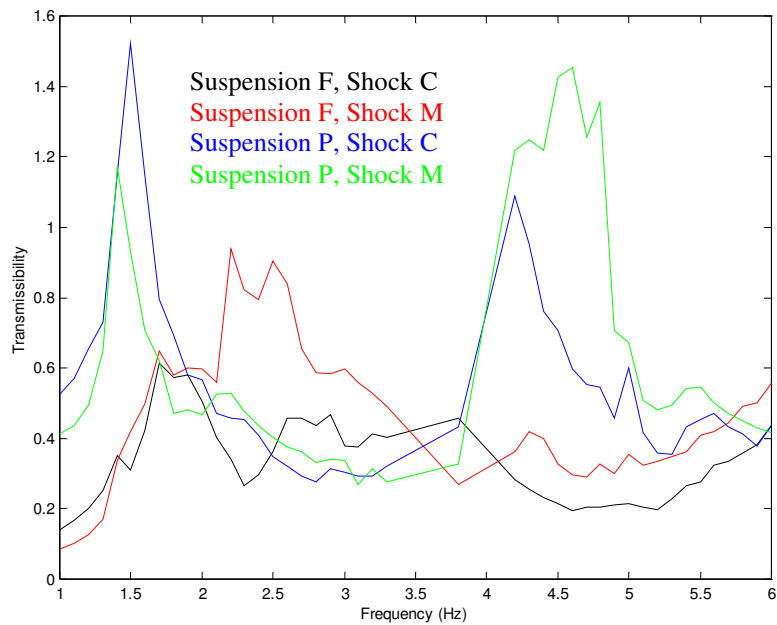


Figure 6-27. Fore/Aft Acceleration of B-post, Driver, vs. Vertical Acceleration of Frame, RCS, Center

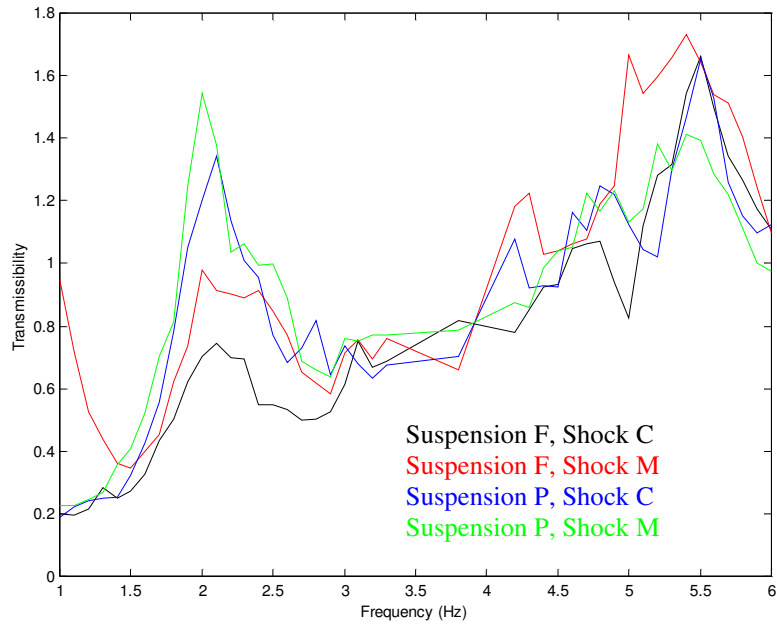


Figure 6-28. Vertical Acceleration of Frame, Front, Driver, vs. Vertical Acceleration of Frame, Second Axle, Driver

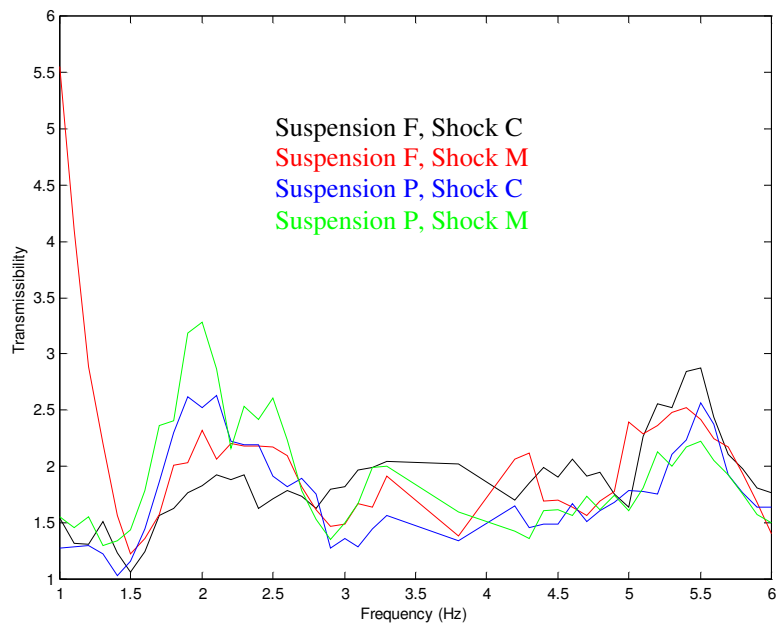


Figure 6-29. Vertical Acceleration of Frame, Rear, Driver, vs. Vertical Acceleration of Frame, Second Axle, Driver

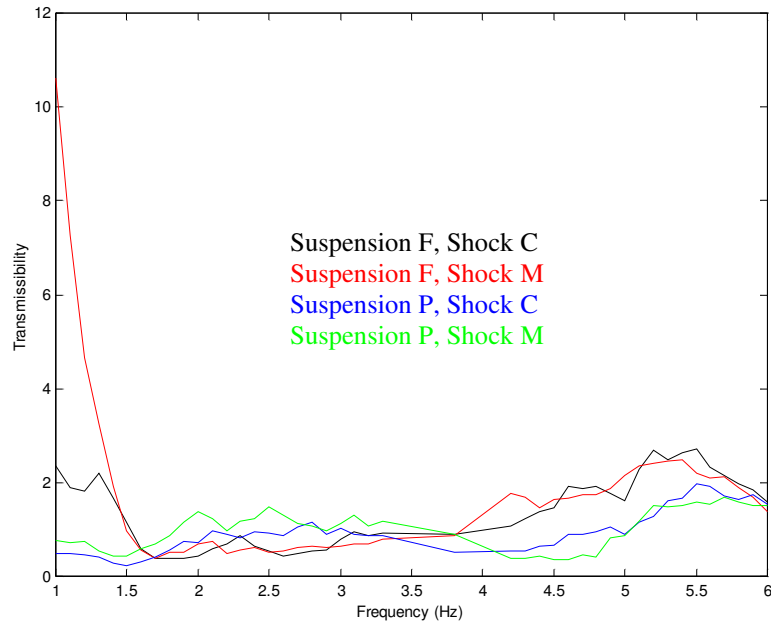


Figure 6-30. Vertical Acceleration of Frame, RCS, Driver, vs. Vertical Acceleration of Frame, Second Axle, Driver

6.5.2 Roll Cab Suspension Study

At the cab suspension, the transmissibility across the cab favors Suspension P (Figure 6-31). However, Suspension P performs better at the front axle roll frequency (2.5 - 4 Hz). Figure 6-32 and 6-33, which have the B-post results, also indicate that Suspension F is performing better at the low frequencies. Figure 6-34 (lateral sensor comparison) shows the roll center movement that was present in the 660 trucks.

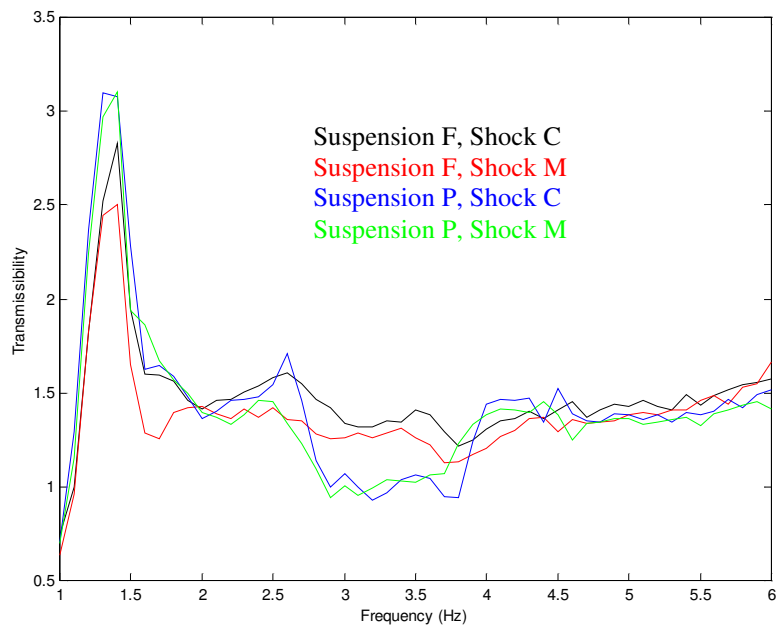


Figure 6-31. Vertical Displacement across RCS, Driver, vs. Vertical Displacement of Frame, Back of Cab, Driver

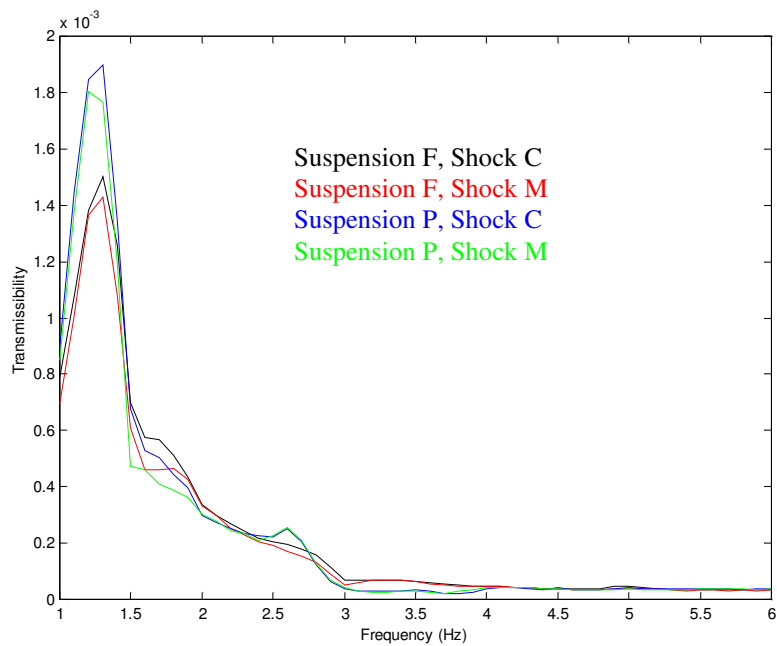


Figure 6-32. Lateral Acceleration of B-post, Driver, vs. Vertical Displacement of Frame, Back of Cab, Driver

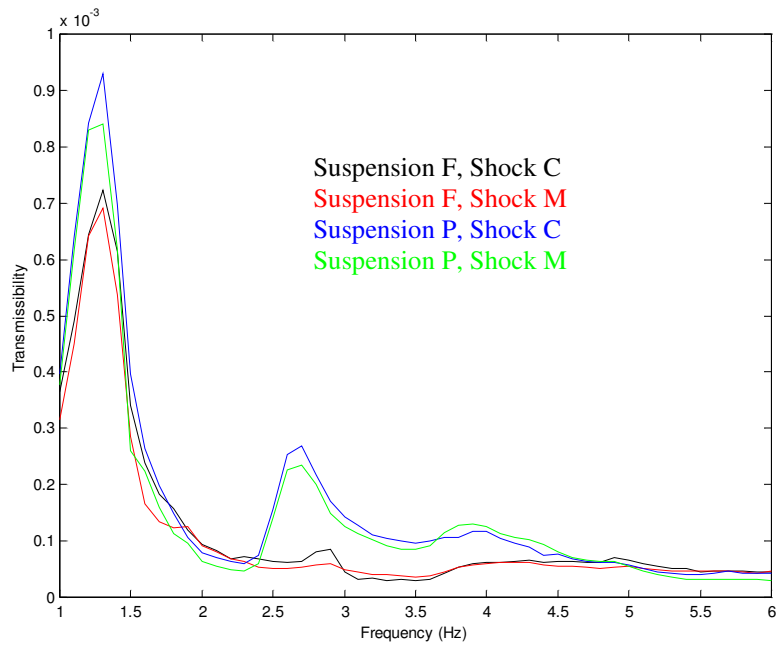


Figure 6-33. Vertical Acceleration of B-post, Driver, vs. Vertical Displacement of Frame, Back of Cab, Driver

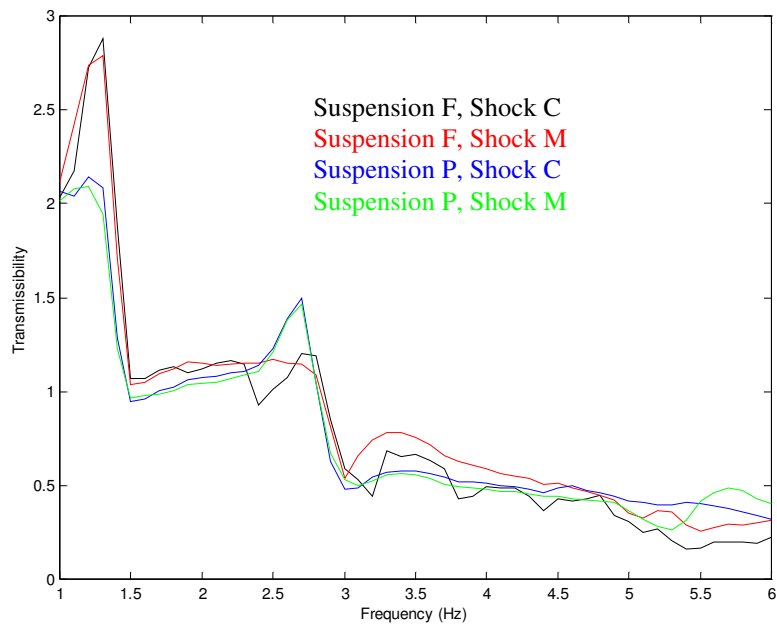


Figure 6-34. Lateral Acceleration of Cab, Drip Rail, Center, vs. Lateral Acceleration of Cab, RCS, Center

6.6 Thin High Results

The fourth and final truck (listed in bold in Table 6-4 below) has its pure tone results shown in this section.

Table 6-4. Important test vehicle parameters

Name	Model	Sleeper length	Wheelbase	Frame, $h \times t$
Standard Low	VNL 660	61 in. (1550 mm)	215 in. (5460 mm)	266 mm x 8 mm
Thin Low	VNL 660	61 in. (1550 mm)	215 in. (5460 mm)	266 mm x 7 mm
Standard High	VNL 770	77 in. (1960 mm)	229 in. (5810 mm)	300 mm x 7 mm
Thin High	VNL 770	77 in. (1960 mm)	239 in. (6070 mm)	300 mm x 6 mm

6.6.1 Heave Cab Suspension Study

Compared to Shock C, Shock M reduces the transmissibility of the cab suspension (Figure 6-35) for the Thin High. At the B-post, the vertical (Figure 6-36) and fore/aft (Figure 6-37) accelerometer transmissibilities also support this conclusion when the truck has Suspension P, but shows Shock C coming out ahead when the truck has Suspension F. Beaming is noticeable in this truck, as indicated by the frame accelerometer transmissibilities (Figure 6-38 thru 6-40).

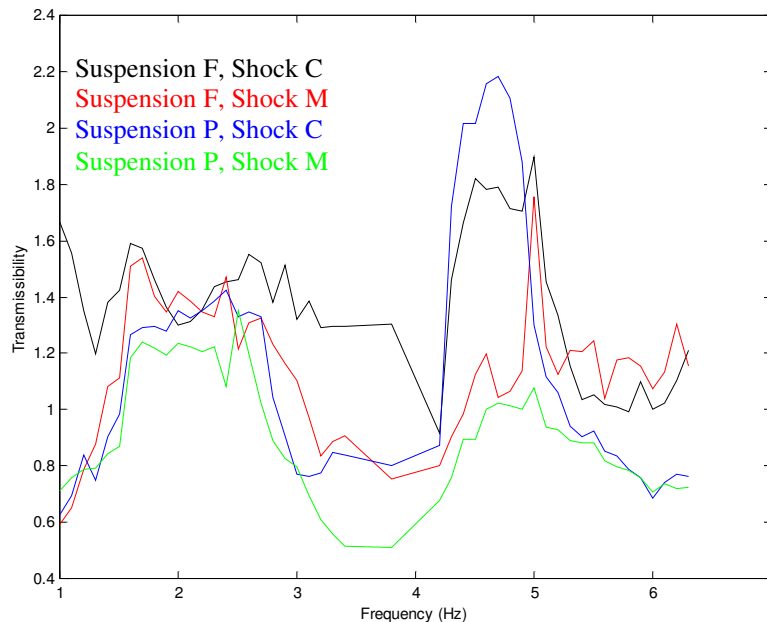


Figure 6-35. Vertical Acceleration of Cab, RCS, Center, vs. Vertical Acceleration of Frame, RCS, Center

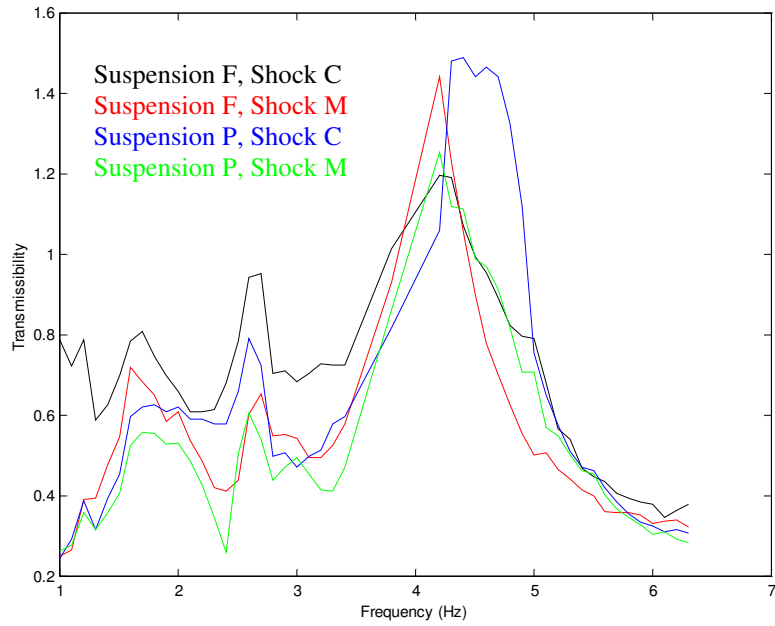


Figure 6-36. Vertical Acceleration of B-post, Driver, vs. Vertical Acceleration of Frame, RCS, Center

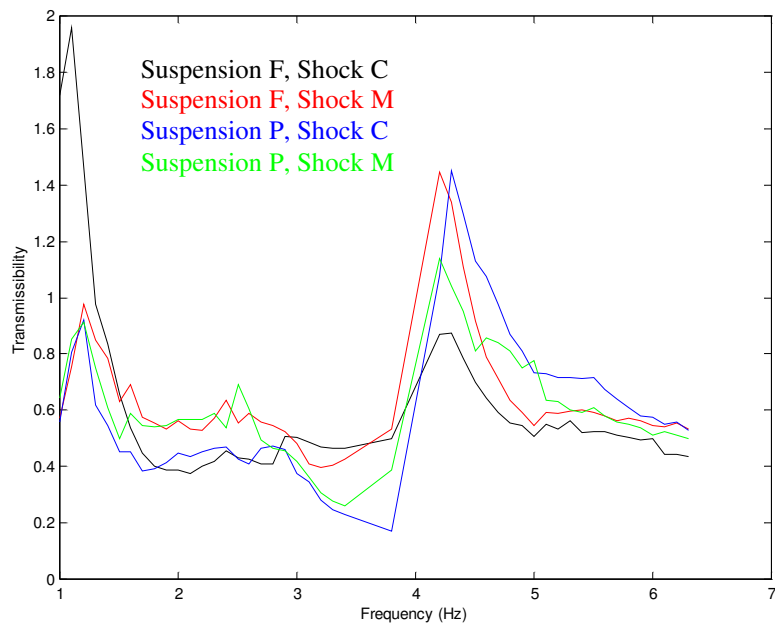


Figure 6-37. Fore/Aft Acceleration of B-post, Driver, vs. Vertical Acceleration of Frame, RCS, Center

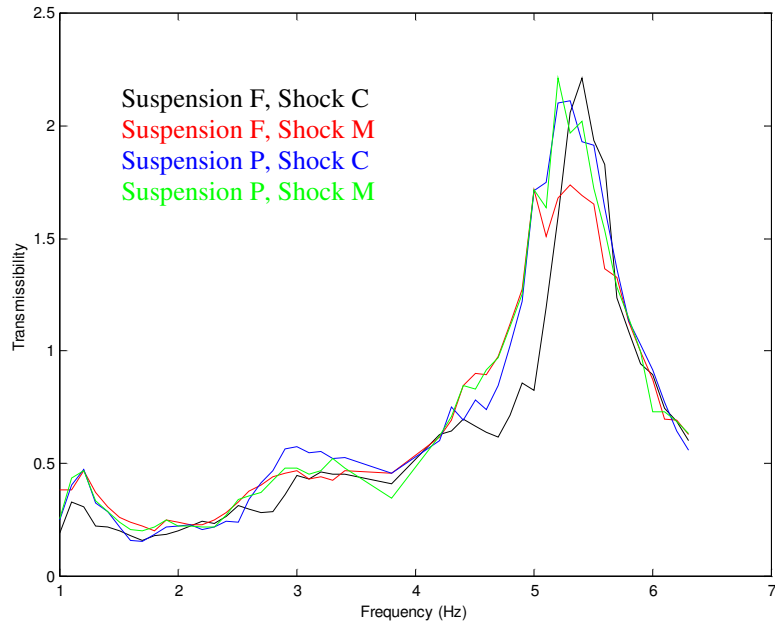


Figure 6-38. Vertical Acceleration of Frame, Front, Driver, vs. Vertical Acceleration of Frame, Second Axle, Driver

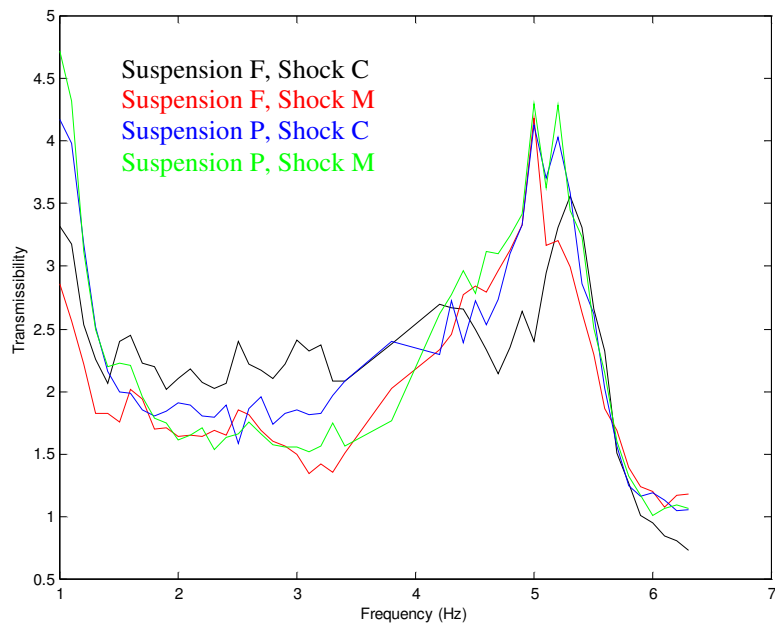


Figure 6-39. Vertical Acceleration of Frame, Rear, Driver, vs. Vertical Acceleration of Frame, Second Axle, Driver

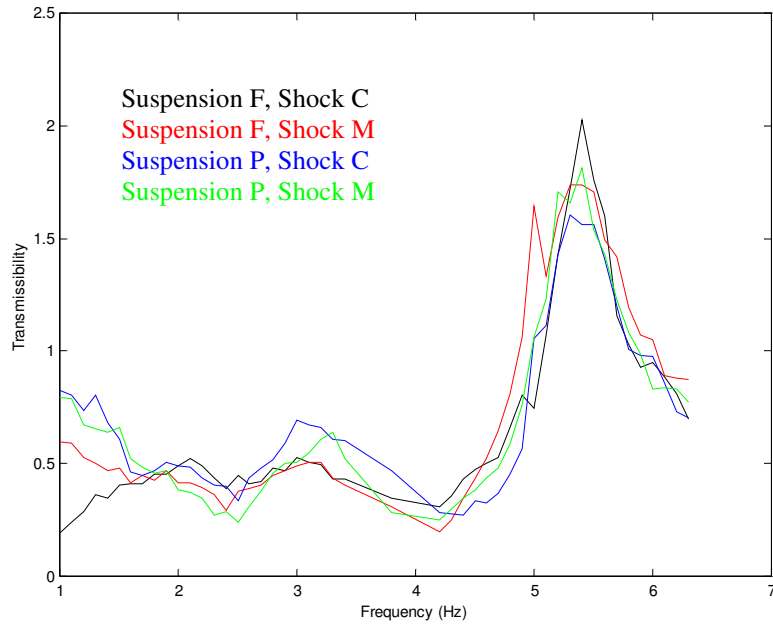


Figure 6-40. Vertical Acceleration of Frame, RCS, Driver, vs. Vertical Acceleration of Frame, Second Axle, Driver

6.6.2 Roll Cab Suspension Study

Just as with the Thin Low, at the cab roll natural frequency Suspension F has about half the transmissibility of Suspension P (Figure 6-41). Inside the cab at the B-post, the story is the same (Figure 6-42 and 6-43). The Thin High shows almost the exact same change in roll center (Figure 6-44) that was demonstrated in the other trucks.

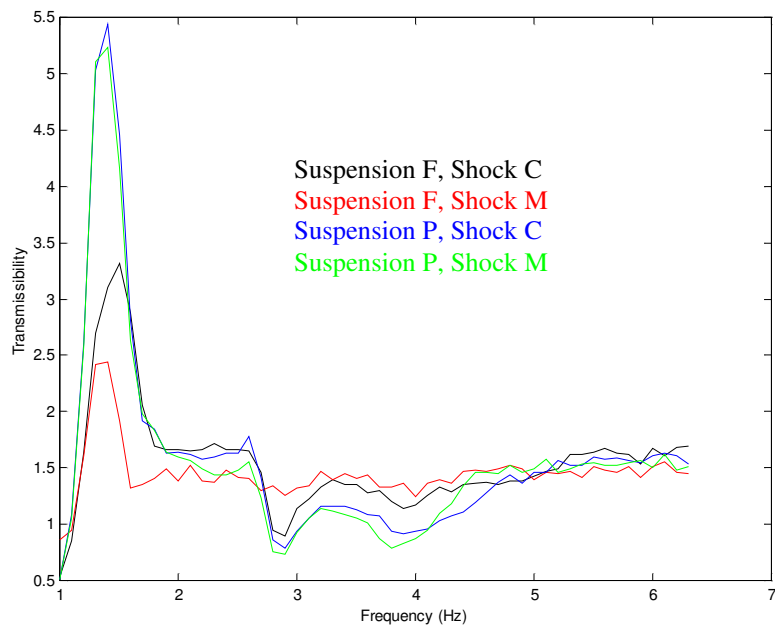


Figure 6-41. Vertical Displacement across RCS, Driver, vs. Vertical Displacement of Frame, Back of Cab, Driver

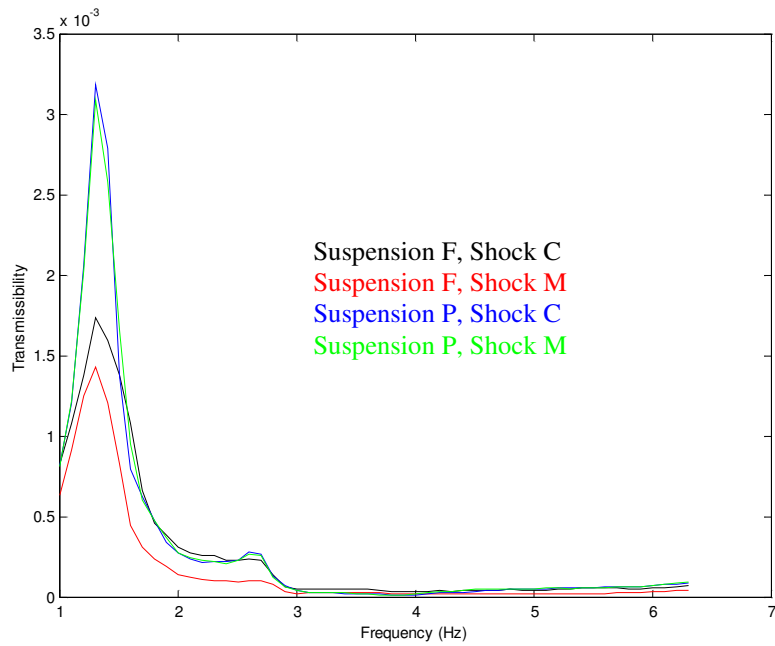


Figure 6-42. Lateral Acceleration of B-post, Driver, vs. Vertical Displacement of Frame, Back of Cab, Driver

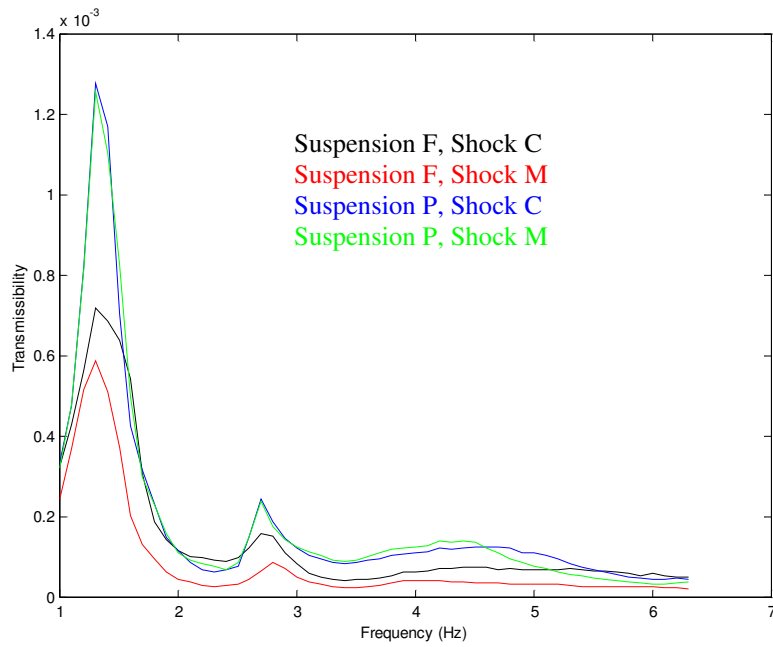


Figure 6-43. Vertical Acceleration of B-post, Driver, vs. Vertical Displacement of Frame, Back of Cab, Driver

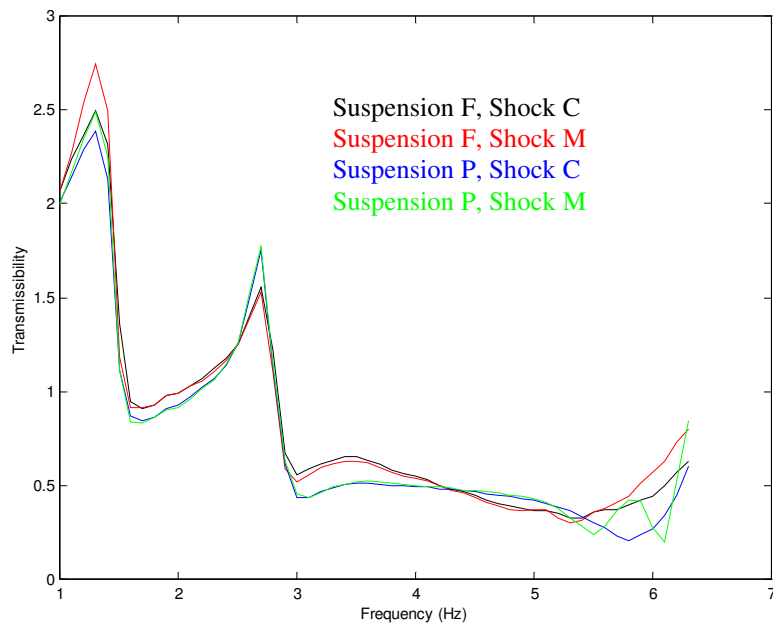


Figure 6-44. Lateral Acceleration of Cab, Drip Rail, Center, vs. Lateral Acceleration of Cab, RCS, Center

6.7 Comparison Between Trucks

This section compares the results from all four trucks with the factory suspension. The truck parameters are again listed for convenience in Table 2.1 below.

Table 6-5. Important test vehicle parameters

Name	Model	Sleeper length	Wheelbase	Frame, <i>h x t</i>
Standard Low	VNL 660	61 in. (1550 mm)	215 in. (5460 mm)	266 mm x 8 mm
Thin Low	VNL 660	61 in. (1550 mm)	215 in. (5460 mm)	266 mm x 7 mm
Standard High	VNL 770	77 in. (1960 mm)	229 in. (5810 mm)	300 mm x 7 mm
Thin High	VNL 770	77 in. (1960 mm)	239 in. (6070 mm)	300 mm x 6 mm

6.7.1 Heave Comparison

The Thin Low suspension is less affected by the cab suspension resonance (Figure 6-45) than the other trucks. This can also be seen when the transmissibility to the vertical acceleration at the B-post is examined (Figure 6-46). At the fore/aft accelerometer, shown in Figure 6-47, the transmissibility level is the same as for the other trucks at the cab suspension frequency but much higher at the beaming frequency. The two 660s, especially the Lightweight, amplify the road input (through the axle suspension) much more than the 770s (Figure 6-48). The Thin Low transmits the vibrations from the rear axle area of the frame uniformly across the frequency range, as shown in Figure 6-49. The other trucks have higher transmissibilities at the beaming frequency, and lower transmissibilities at the cab suspension resonance.

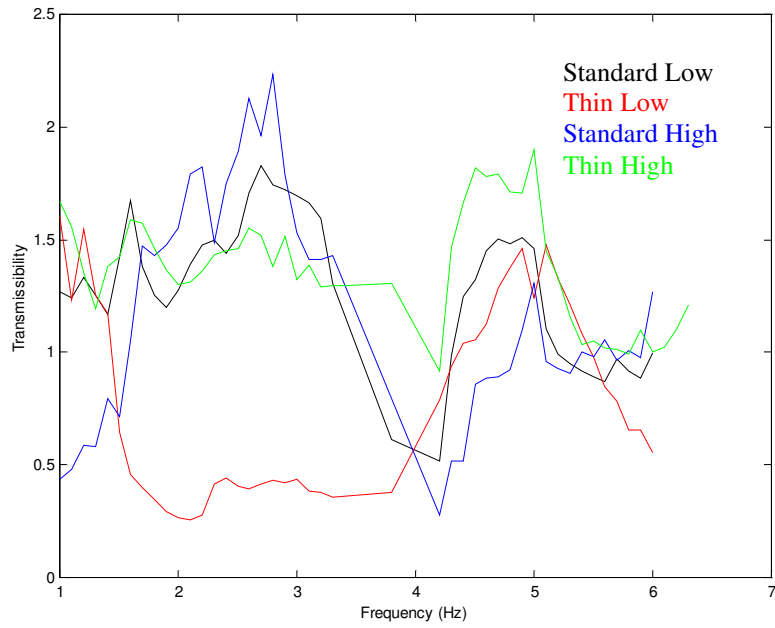


Figure 6-45. Vertical Acceleration of Cab, RCS, Center, vs. Vertical Acceleration of Frame, RCS, Center

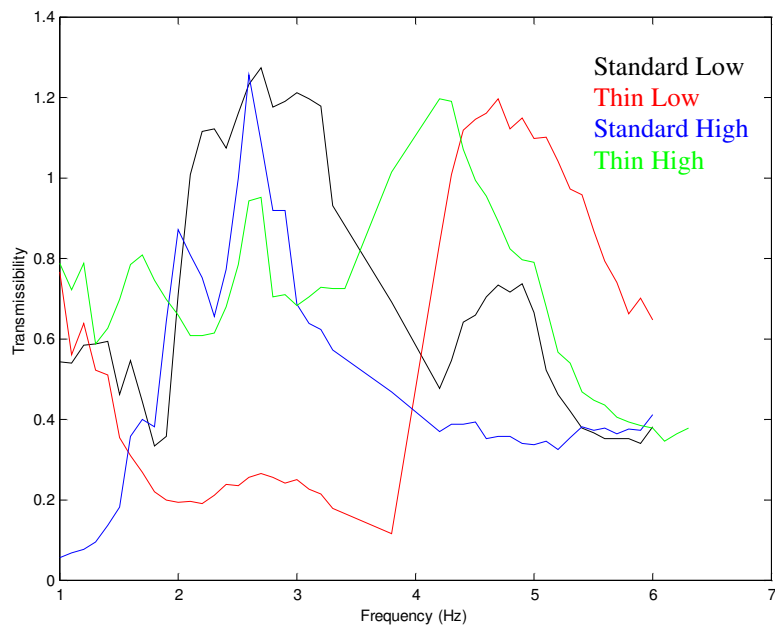


Figure 6-46. Vertical Acceleration of B-post, Driver, vs. Vertical Acceleration of Frame, RCS, Center

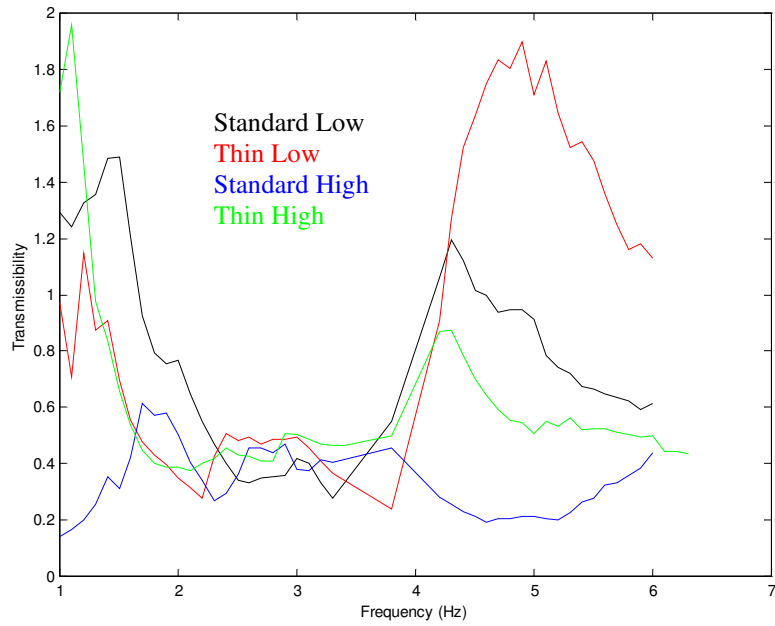


Figure 6-47. Fore/Aft Acceleration of B-post, Driver, vs. Vertical Acceleration of Frame, RCS, Center

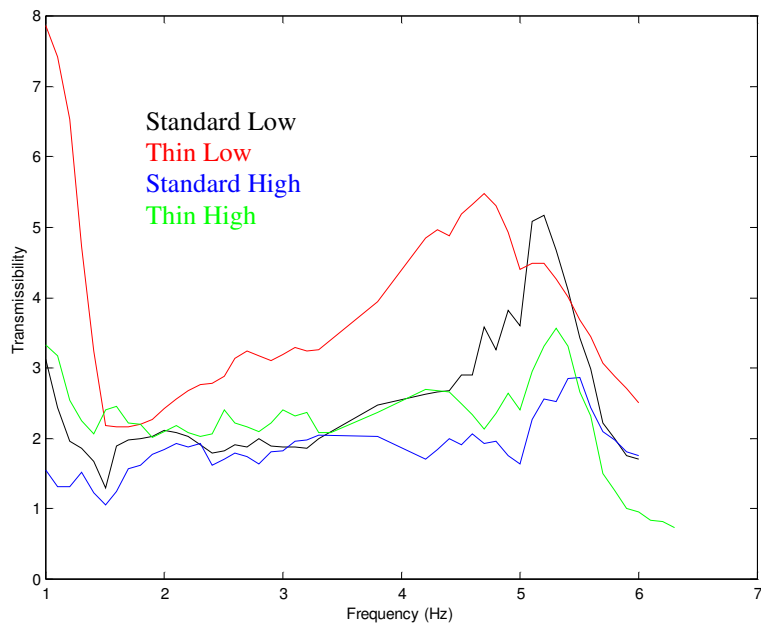


Figure 6-48. Vertical Acceleration of Frame, Rear, Driver, vs. Vertical Acceleration of Frame, Second Axle, Driver

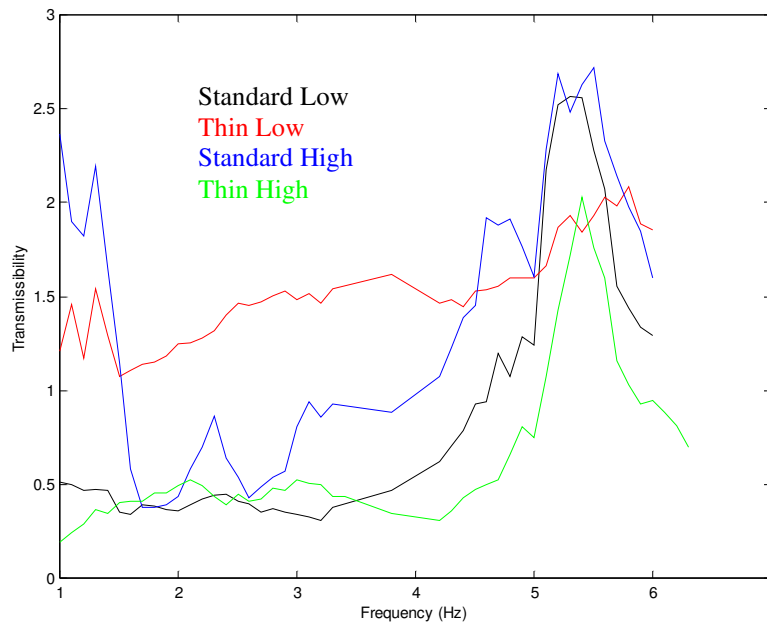


Figure 6-49. Vertical Acceleration of Frame, RCS, Driver, vs. Vertical Acceleration of Frame, Second Axle, Driver

6.7.2 Roll Cab Suspension Study

This time it was the Standard Low that transmitted the most acceleration across the suspension (Figure 6-50). Figure 6-51 also shows that the Standard Low transmits the most vibration from the frame to the cab. As measured by the lateral accelerometer at the B-post (Figure 6-52), the Thin Low actually had a lower transmissibility. The Standard Low is not shown on this plot because the lateral accelerometer at the B-post was not added until later.

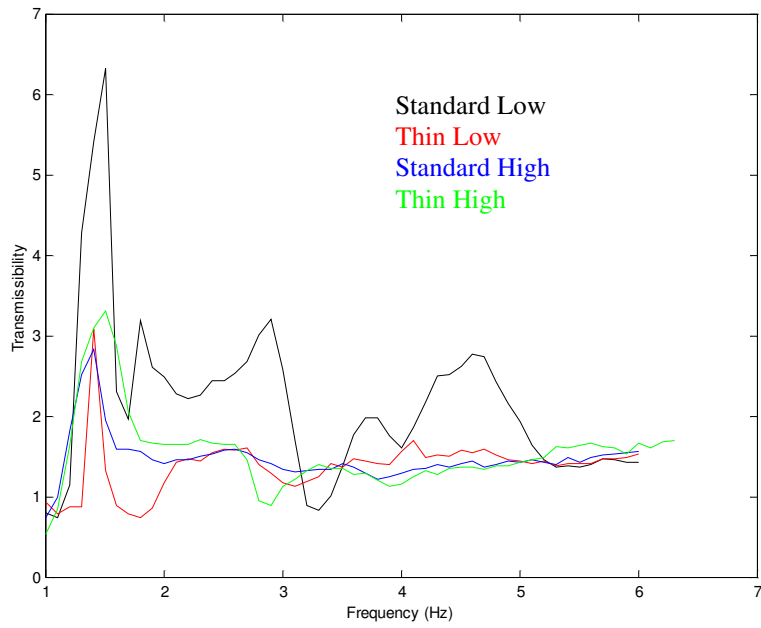


Figure 6-50. Vertical Displacement across RCS, Driver, vs. Vertical Displacement of Frame, Back of Cab, Driver

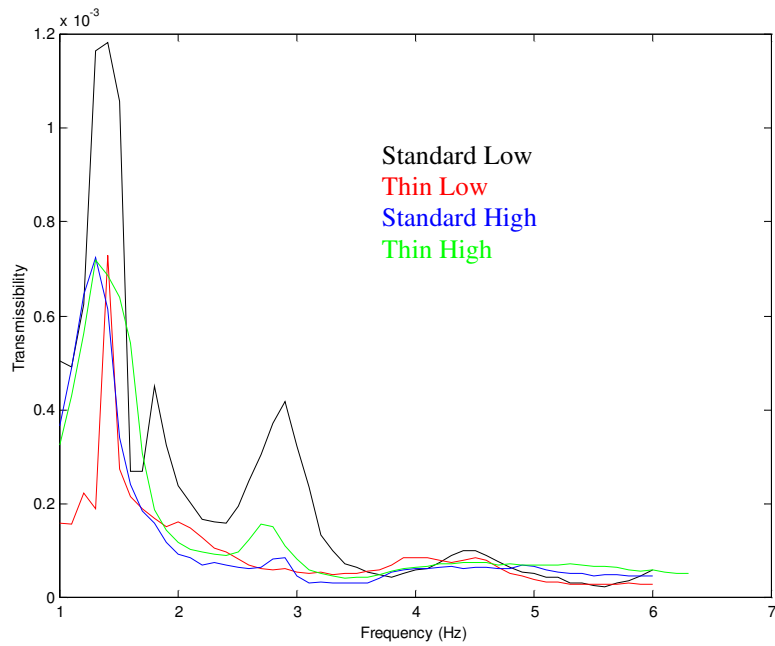


Figure 6-51. Vertical Acceleration of B-post, Driver, vs. Vertical Displacement of Frame, Back of Cab, Driver

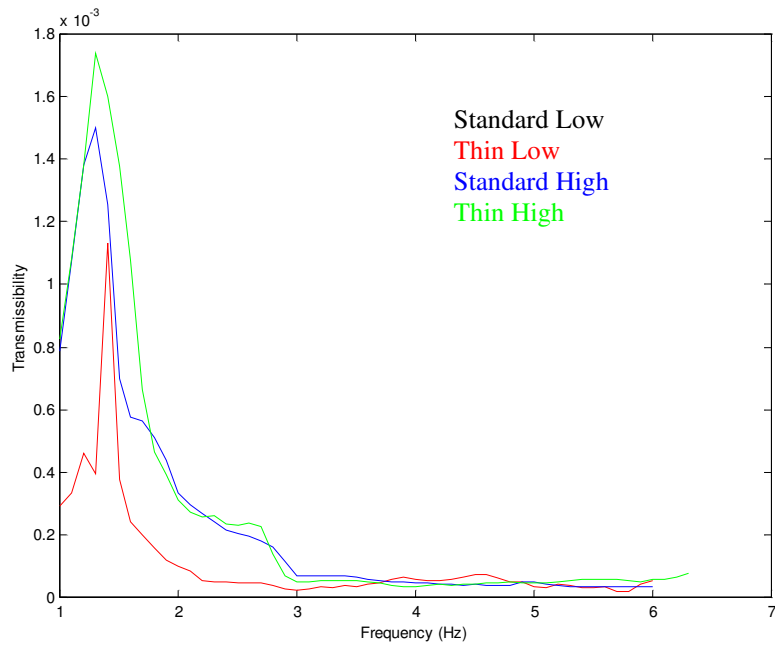


Figure 6-52. Lateral Acceleration of B-post, Driver, vs. Vertical Displacement of Frame, Back of Cab, Driver

Chapter 7 Bump Response

This chapter discusses the response of the truck to a hard bump. The input bump signal and the reasons for using it are described in Section 7.1. Section 7.2 summarizes the results. The calculation process explained next (Section 7.3), followed by the results from each truck(Sections 7.4 thru 7.7).

7.1 Bump Input

The bump signal is a step input. The truck was given a small displacement (0.2 inches) upward, allowed to settle, and then lowered to its initial position for the heave tests. A sample signal is shown in Figure 7-1. The bump response can gives us two pieces of information about the test vehicle. The decay rate in amplitude – the damping – can be seen in the time domain. A higher damping ratio will cause a faster decay of the transients, but it reduces the amount of isolation at higher frequencies. In addition to the decay rate, the system’s ability to isolate the frame and cab from road impacts is indicated to some extent by the maximum peak-to-peak amplitude of the time response.

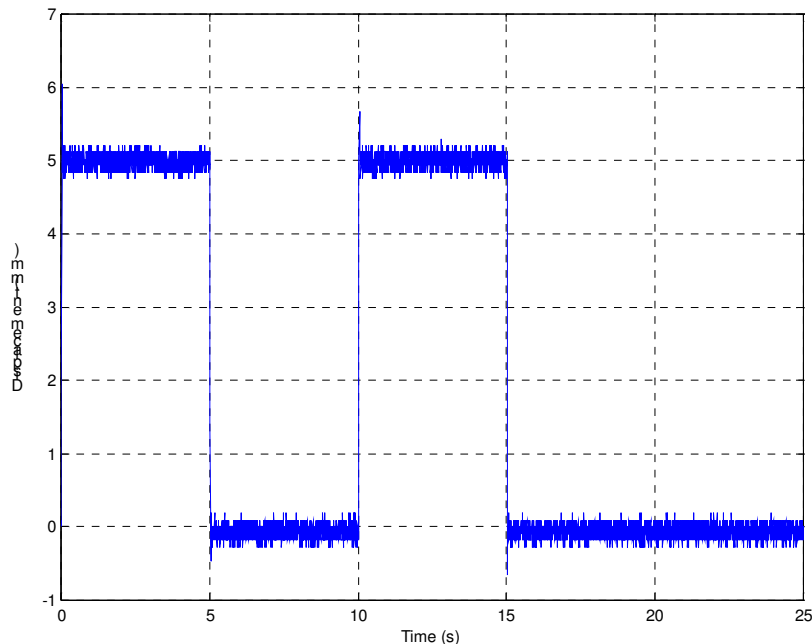


Figure 7-1. Sample bump input displacement at the actuator

7.2 Summary of Results

The bump tests yielded promising results for the prototype suspension. On average during the heave tests, Suspension P produced 17.2% lower peak-to-peak acceleration at the B-post in the fore/aft direction as compared with the factory suspension. In the vertical direction, the acceleration reduction was 5.8%. Measuring at the back of the cab, the peak-to-peak vertical acceleration obtained with Suspension P was less than 75% of the acceleration obtained with Suspension F. The average damping ratio calculated from the vertical accelerometer at the back of the cab (with the procedure described later in Section 7.3) was 0.144 for the factory suspension and 0.161 for the prototype suspension.

Shock M showed an 11.7% improvement over the factory shocks as measured by the B-post vertical accelerometer, but the peak-to-peak fore/aft acceleration was only slightly better (0.2%) than that achieved with Shock C. At the back of the cab, Shock C had only a 2.9% higher vertical acceleration. Surprisingly, the average damping ratio only changed from 0.151 to 0.154 when Shock M was used in place of Shock C absorbers.

The lateral accelerometers were used to evaluate the roll response of the truck. At the B-post, the peak-to-peak acceleration was 9.0% lower for Suspension P than for Suspension F. As expected, the average roll damping ratio (calculated from the lateral accelerometer at the drip rail) was much lower for Suspension P: 0.082 versus 0.105. Switching shocks yielded better results as well. When Shock M was used in place of Shock C, the peak-to-peak lateral B-post acceleration was 5.3% lower on average. The roll damping ratio changed from 0.095 (Shock C) to 0.091 (Shock M).

7.3 Calculation Process

The log decrement method was used to calculate the damping ratio. This method finds the damping ratio by comparing the amplitude of two displacement peaks. In a single-degree-of-freedom system, the vibration amplitude will decay exponentially and each peak will be smaller than the one before. With a complex system with multiple degrees of freedom, the mass will vibrate at a combination of frequencies in response to an impact. This means that the third peak could be higher than the second peak, although the amplitude will still eventually decrease. Because of this, two damping ratios were calculated: one between the first and second peaks and

one between the first and third peaks. The actual damping ratio lies between these two values; therefore, the two values were averaged them to obtain a single number.

Displacement data must be used to get the damping ratio. The resolution of the LVDTs was too large to get accurate damping from the small displacements, so data from the accelerometers was used (Figure 7-2). This data was filtered to remove the high frequency noise and the very low frequency ($< 1\text{Hz}$) content that fell below the accelerometers' operating range. The data was then digitally integrated twice to get displacement. The red X's on the displacement plot are the three peak values used to find the damping ratio.

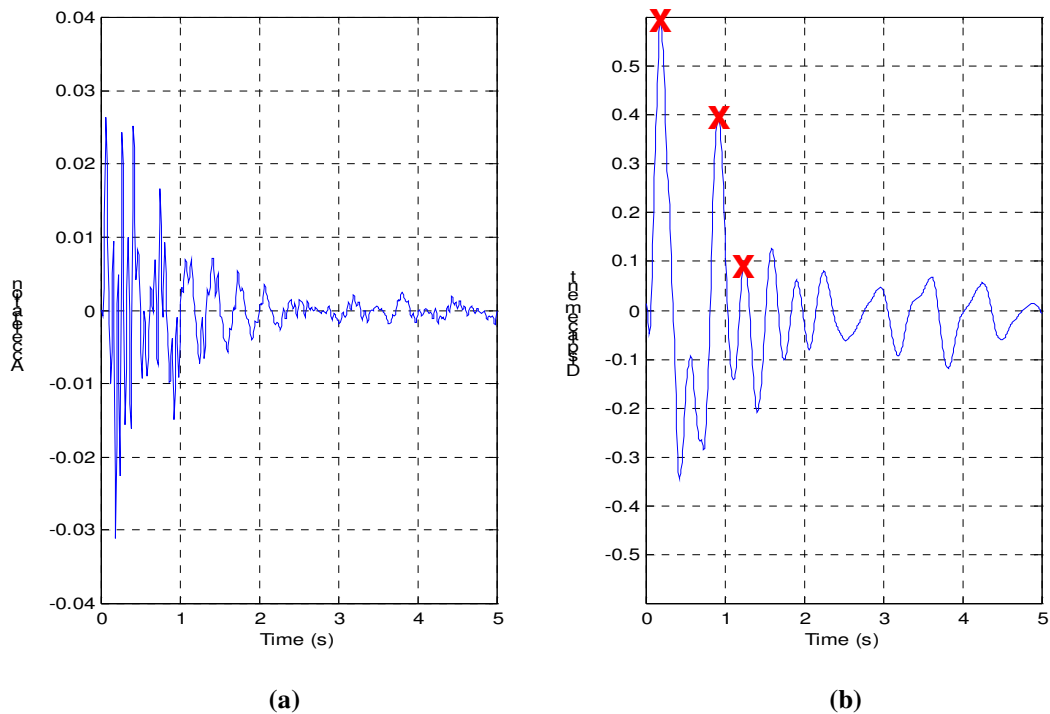


Figure 7-2. Sample data from accelerometers: (a) acceleration and (b) displacement

The process to get the peak values was much easier. The acceleration peak values were just the average of the maximum values obtained with each bump (there were two bumps per signal). The minimum value was also obtained so that a peak-to-peak number could be calculated. Using the same method, the displacement peak-to-peak was determined from the displacement data.

7.4 Standard Low Results

The best-placed sensors for measuring the damping in the heave mode were the vertical and fore/aft accelerometers on the B-post and the vertical accelerometer at the back of the cab. Figure 4-3 shows the peak-to-peak acceleration resulting from the bump input (note: the same labeling convention, shown in Table 7-1, is used here as was used earlier in “Ride Number Metric”). The scale is the same for all the trucks for ease of comparison. Although the accelerations at the rear of the cab were different, there was not a significant difference at the B-post. The peak-to-peak displacement is shown in the Figure 4-4. Shock C does seem to have slightly higher displacement peaks. The damping ratio (Figure 4-5) of the PM4 combination is relatively high, but nothing else really stands out.

Table 7-1. Cab suspension abbreviations for plot

Component	Symbol	Variant
Suspension Design	F	Suspension F (factory suspension)
	P	Suspension P (prototype suspension)
Shock Absorbers	C	Shock C (factory shocks)
	M	Shock M (prototype shocks)
Airsprings	4	L4 airspring (factory spring for medium sleeper)
	5	L5 airspring (factory spring for large sleeper)

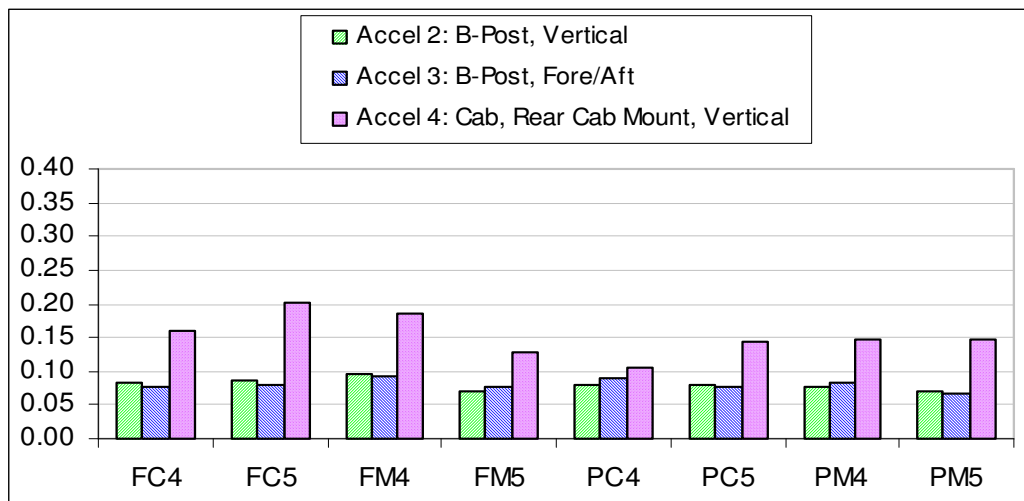


Figure 7-3. Standard Low peak-to-peak accelerations (heave)

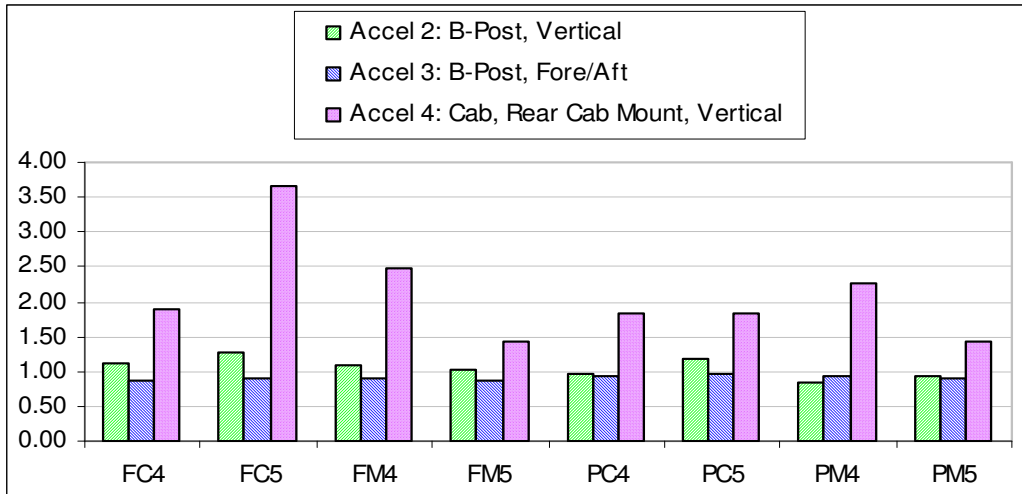


Figure 7-4. Standard Low peak-to-peak displacements (heave)

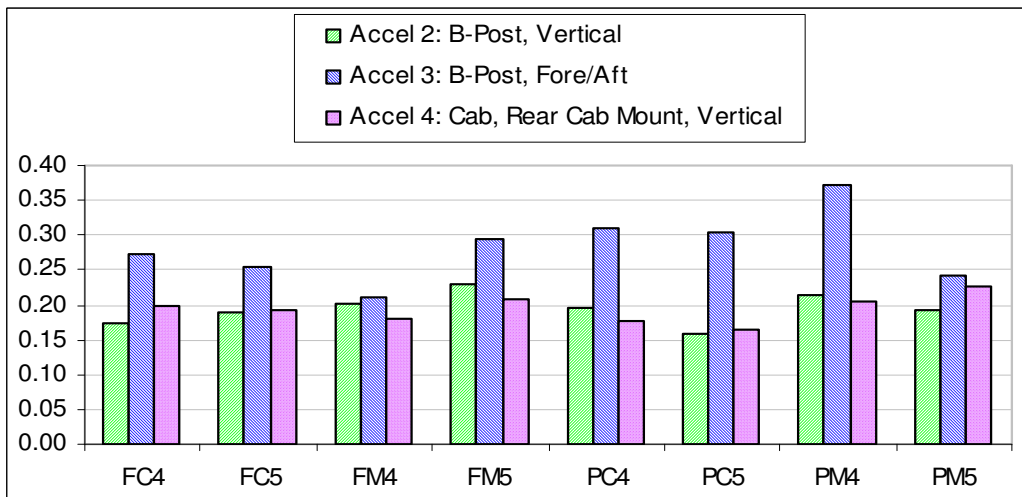


Figure 7-5. Standard Low damping ratios (heave)

An average was computed for each of the six suspension parameters. For example, of the eight cab suspension combinations, four of them use Suspension P. These four results were averaged together. This was repeated for the other five components and the results were regrouped into Table 7-2. The peak-to-peak acceleration is contained in the third column, the peak-to-peak displacement in the fourth column, and the damping ratio in the last column. The average of the two suspensions is also the average of all eight suspension combinations. The same holds true for the shocks and springs. This makes it easier to figure out which set of suspension components (i.e., suspension type, shocks, or springs) has the most effect on each of the three bump measurements; one just has to look for the components that have the largest

difference. For example, look at the peak-to-peak acceleration of the first sensor. The difference between Suspension F and Suspension P is 0.057 g; between Shock M and Shock C, 0.043 g; and, between L4 and L5 springs, 0.076 g. This tells us that the airsprings had the most significant effect on the vertical peak-to-peak acceleration at the B-post for the Thin Low. Similarly, one can tell from the table that the airsprings had very little damping effect on the vertical acceleration at the B-post.

Table 7-2. Standard Low parametric evaluation (heave)

Sensor	Parameter	Acc p-p	Disp p-p	Zeta
Accel 2: B-post, Vertical	Suspension F	0.0835	1.1260	0.1982
	Suspension P	0.0778	0.9828	0.1900
	Shock M	0.0785	0.9691	0.2088
	Shock C	0.0828	1.1397	0.1794
	L4 airsprings	0.0845	1.0087	0.1957
	L5 airsprings	0.0769	1.1000	0.1925
Accel 3: B-post, Fore/Aft	Suspension F	0.0821	0.8828	0.2581
	Suspension P	0.0785	0.9270	0.3068
	Shock M	0.0797	0.9001	0.2794
	Shock C	0.0809	0.9097	0.2855
	L4 airsprings	0.0857	0.8968	0.2915
	L5 airsprings	0.0749	0.9130	0.2734
Accel 4: Cab, Rear Cab Mount, Vertical	Suspension F	0.1682	2.3592	0.1952
	Suspension P	0.1366	1.8416	0.1931
	Shock M	0.1514	1.9055	0.2052
	Shock C	0.1534	2.2953	0.1831
	L4 airsprings	0.1499	2.1156	0.1900
	L5 airsprings	0.1550	2.0851	0.1983

The out-of-phase bump (roll input) was analyzed in a similar fashion to that used with the heave input. First, appropriate sensors were chosen to give the best indication of roll. In this case, the lateral accelerometer at the drip rail along the back of the cab and the lateral accelerometer on the driver-side B-post (when available) were analyzed. Figure 7-6 shows that Suspension P resulted in lower peak-to-peak accelerations of the cab. Although the trend is not as strong, the same is true for the displacement, as shown in Figure 7-7. The damping ratios, depicted in Figure 7-8, were also lower for Suspension P, which was expected because Suspension P has no horizontal dampers. The same conclusions can be obtained from the roll summary table, Table 7-3.

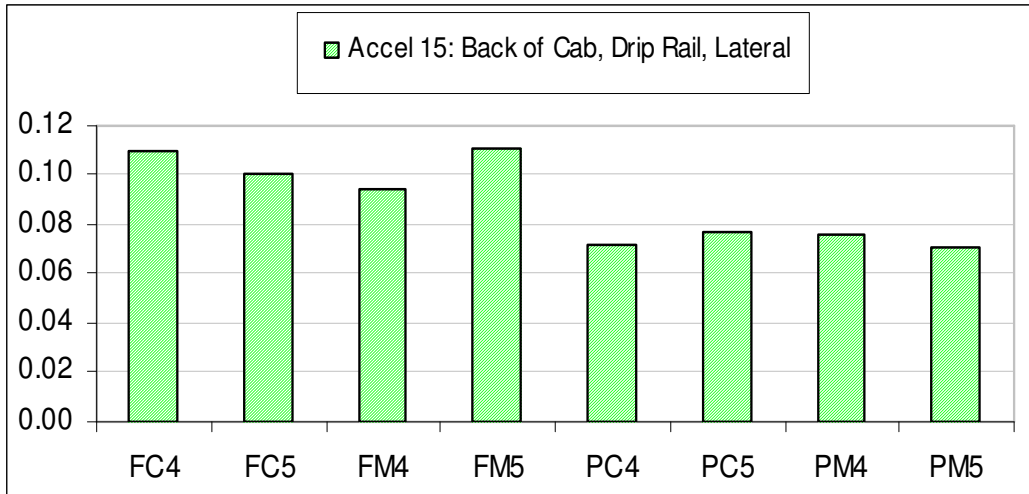


Figure 7-6. Standard Low peak-to-peak accelerations (roll)

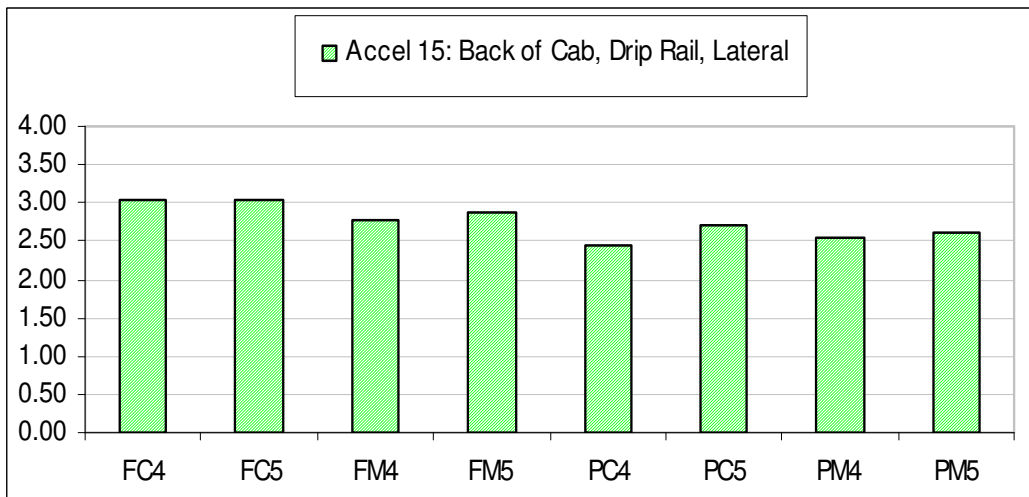


Figure 7-7. Standard Low peak-to-peak displacements (roll)

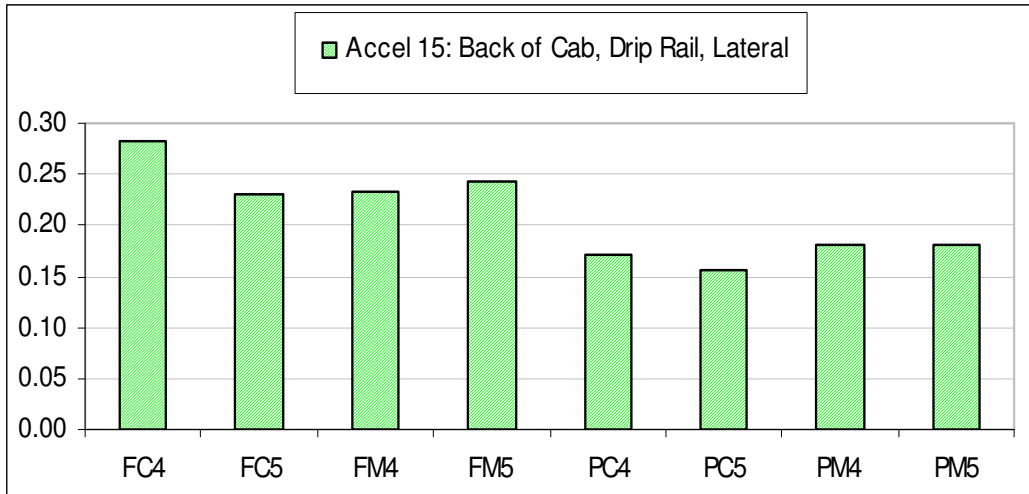


Figure 7-8. Standard Low damping ratios (roll)

Table 7-3. Standard Low parametric evaluation (roll)

Sensor	Parameter	Acc p-p	Disp p-p	Zeta
Accel 15: Back of Cab, Drip Rail, Lateral	Suspension F	0.1037	2.9243	0.2473
	Suspension P	0.0738	2.5760	0.1725
	Shock M	0.0881	2.6933	0.2097
	Shock C	0.0895	2.8071	0.2101
	L4 airsprings	0.0878	2.7020	0.2170
	L5 airsprings	0.0898	2.7983	0.2028

7.5 Thin Low Results

During heave motion, Suspension P showed significantly lower accelerations on the Thin Low (Figure 7-9). Figure 7-10 shows that the displacements were about even. The damping ratio was a little higher for Suspension P at the back of the cab (Figure 7-11), even taking into account that the spike at the PC5 suspension is probably an outlier. Looking at Table 7-4, Suspension F had almost double the vertical acceleration of Suspension P. Shock M had the lowest peak-to-peak displacement at the rear cab accelerometer, although Shock C produced much lower accelerations there. This acceleration advantage was not carried through to the cab, in view of Shock M's lower B-post accelerations and displacements.

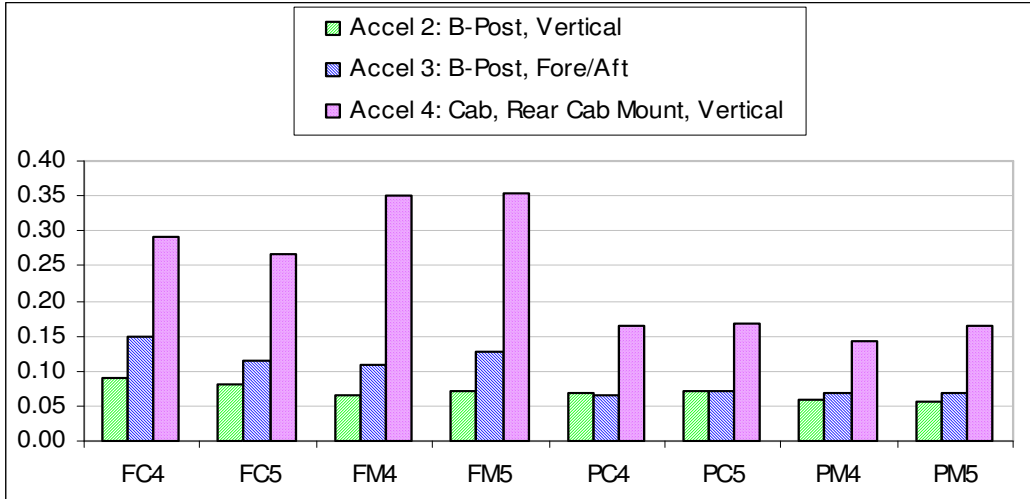


Figure 7-9. Thin Low peak-to-peak accelerations (heave)

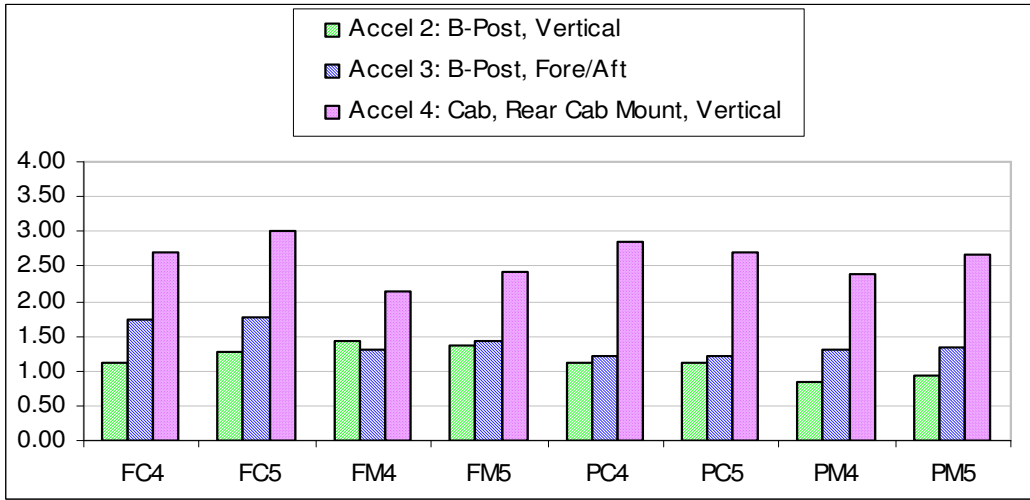


Figure 7-10. Thin Low peak-to-peak displacements (heave)

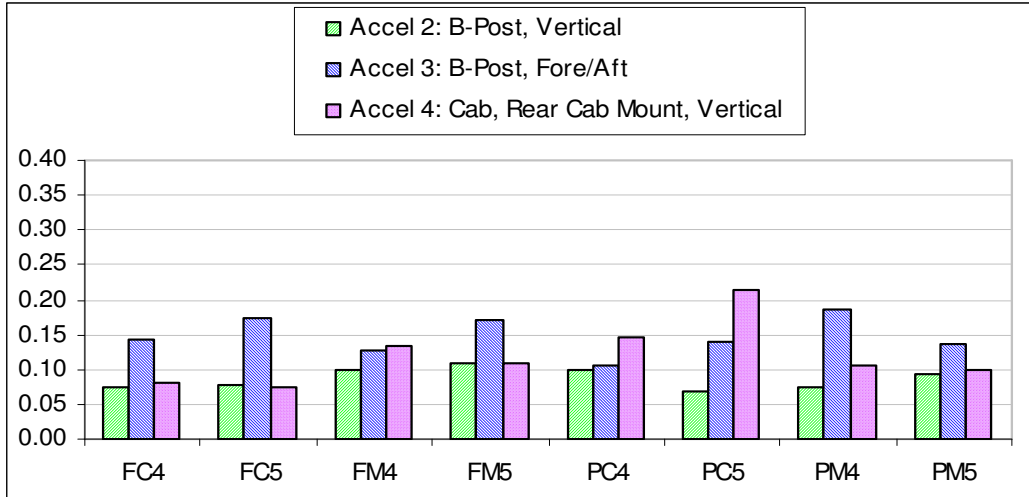


Figure 7-11. Thin Low damping ratios (heave)

Table 7-4. Thin Low parametric evaluation (heave)

Sensor	Parameter	Acc p-p	Disp p-p	Zeta
Accel 2: B-post, Vertical	Suspension F	0.0772	1.2949	0.0901
	Suspension P	0.0634	1.0009	0.0832
	Shock M	0.0629	1.1440	0.0934
	Shock C	0.0776	1.1518	0.0799
	L4 airsprings	0.0712	1.1271	0.0863
L5 airsprings	0.0693	1.1687	0.0870	
Accel 3: B-post, Fore/Aft	Suspension F	0.1243	1.5545	0.1535
	Suspension P	0.0682	1.2645	0.1416
	Shock M	0.0923	1.3389	0.1545
	Shock C	0.1003	1.4802	0.1406
	L4 airsprings	0.0979	1.3827	0.1401
L5 airsprings	0.0946	1.4364	0.1550	
Accel 4: Cab, Rear Cab Mount, Vertical	Suspension F	0.3149	2.5645	0.0994
	Suspension P	0.1597	2.6607	0.1408
	Shock M	0.2519	2.4080	0.1119
	Shock C	0.2227	2.8172	0.1283
	L4 airsprings	0.2369	2.5206	0.1160
L5 airsprings	0.2377	2.7046	0.1242	

By all indications, the Thin Low had much lower responses to the roll bump than the Standard Low. Figure 7-12 shows that the acceleration peak-to-peak value was relatively low for all the cab suspension combinations. The displacements were also even, as shown in Figure 7-19. No real difference was contained in the damping (Figure 7-14). Table 7-5 shows that none of the particular suspension components changed the truck's roll impact response much.

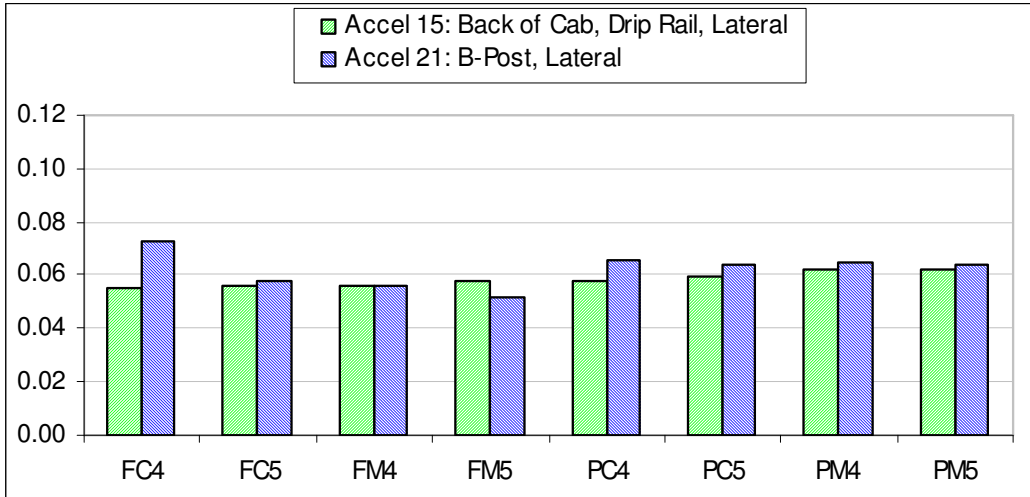


Figure 7-12. Thin Low peak-to-peak accelerations (roll)

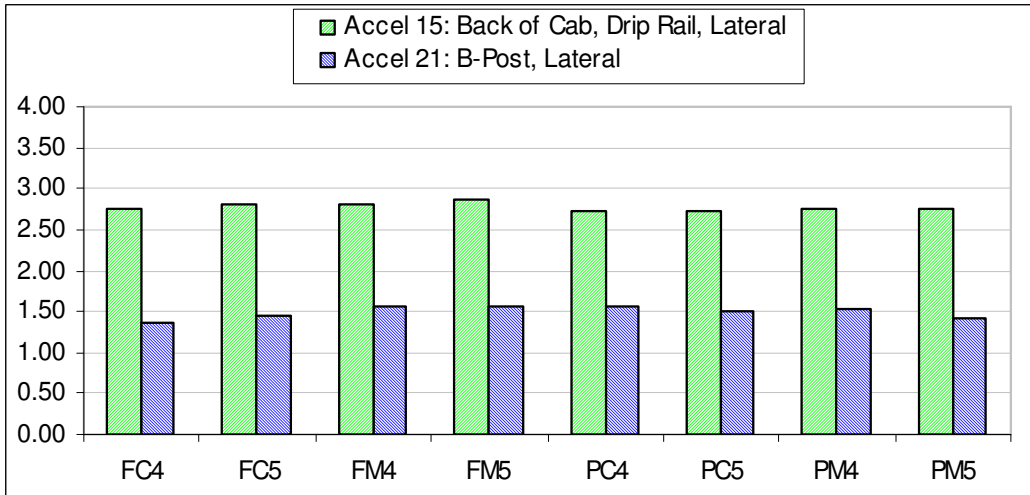


Figure 7-13. Thin Low peak-to-peak displacements (roll)

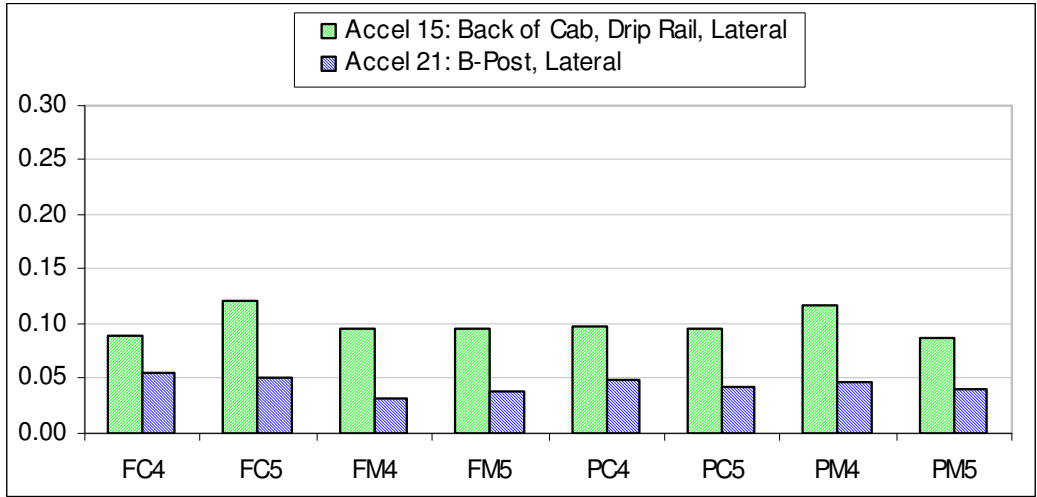


Figure 7-14. Thin Low damping ratios (roll)

Table 7-5. Thin Low parametric evaluation (roll)

Sensor	Parameter	Acc p-p	Disp p-p	Zeta
Accel 21: B-post, Lateral	Suspension F	0.0596	1.4835	0.0442
	Suspension P	0.0646	1.4992	0.0447
	Shock M	0.0592	1.5102	0.0392
	Shock C	0.0650	1.4725	0.0496
	L4 airsprings	0.0649	1.5057	0.0456
L5 airsprings	0.0593	1.4770	0.0433	
Accel 15: Back of Cab, Drip Rail, Lateral	Suspension F	0.0562	2.8121	0.1008
	Suspension P	0.0605	2.7397	0.0996
	Shock M	0.0594	2.7995	0.0992
	Shock C	0.0574	2.7523	0.1011
	L4 airsprings	0.0577	2.7647	0.1001
L5 airsprings	0.0590	2.7871	0.1003	

7.6 Standard High Results

The Standard High also had relatively low peak accelerations (Figure 7-15) and displacements (Figure 7-16). The suspensions with the L4 springs seem to have slightly lower values however. The suspension plot (Figure 7-17) visually indicates uniform damping, and the parameter evaluation table (Table 7-6) does not indicate a significant difference in the damping ratio at the back of the cab among the components. The difference in displacement at the back of the cab and vertically at the B-post can be seen in the table.

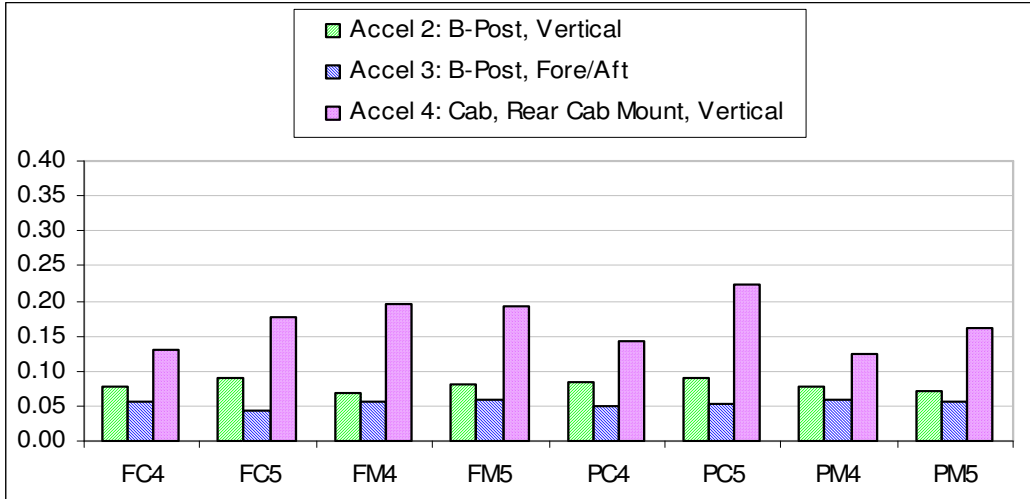


Figure 7-15. Standard High peak-to-peak accelerations (heave)

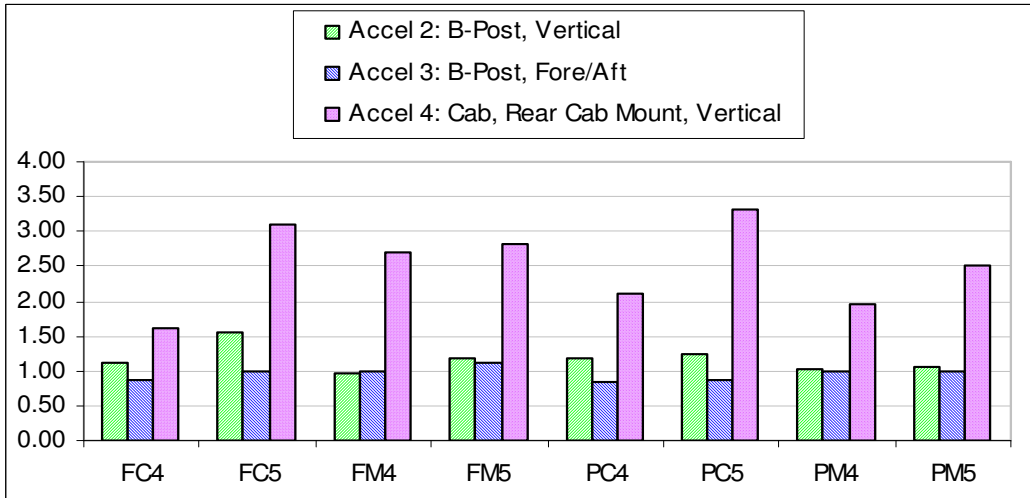


Figure 7-16. Standard High peak-to-peak displacements (heave)

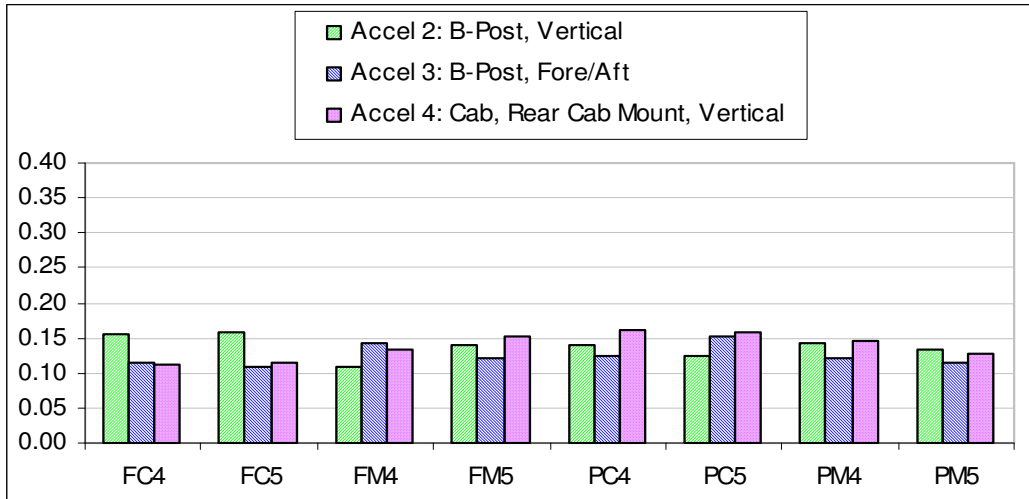


Figure 7-17. Standard High damping ratios (heave)

Table 7-6. Standard High parametric evaluation (heave)

Sensor	Parameter	Acc p-p	Disp p-p	Zeta
Accel 2: B-post, Vertical	Suspension F	0.0791	1.2028	0.1403
	Suspension P	0.0813	1.1194	0.1350
	Shock M	0.0750	1.0579	0.1313
	Shock C	0.0854	1.2643	0.1440
	L4 airsprings	0.0768	1.0657	0.1362
Accel 3: B-post, Fore/Aft	Suspension F	0.0539	0.9969	0.1221
	Suspension P	0.0552	0.9265	0.1280
	Shock M	0.0575	1.0267	0.1252
	Shock C	0.0516	0.8967	0.1248
	L4 airsprings	0.0556	0.9227	0.1260
Accel 4: Cab, Rear Cab Mount, Vertical	Suspension F	0.1748	2.5608	0.1281
	Suspension P	0.1630	2.4673	0.1488
	Shock M	0.1692	2.4931	0.1402
	Shock C	0.1687	2.5350	0.1367
	L4 airsprings	0.1489	2.0919	0.1385
	L5 airsprings	0.1889	2.9362	0.1384

Comparable to the performance seen by the heave input, neither the peak accelerations nor the peak displacements indicate a significant difference between the suspensions for roll (Figure 7-18 and Figure 7-19). Figure 7-17 shows that there was a difference in damping between the suspensions. Suspension F had lower damping at the B-post lateral sensor, but

higher damping at the back of the cab (Table 7-7). Shock M also had a lower measured damping coefficient (at the cab suspension).

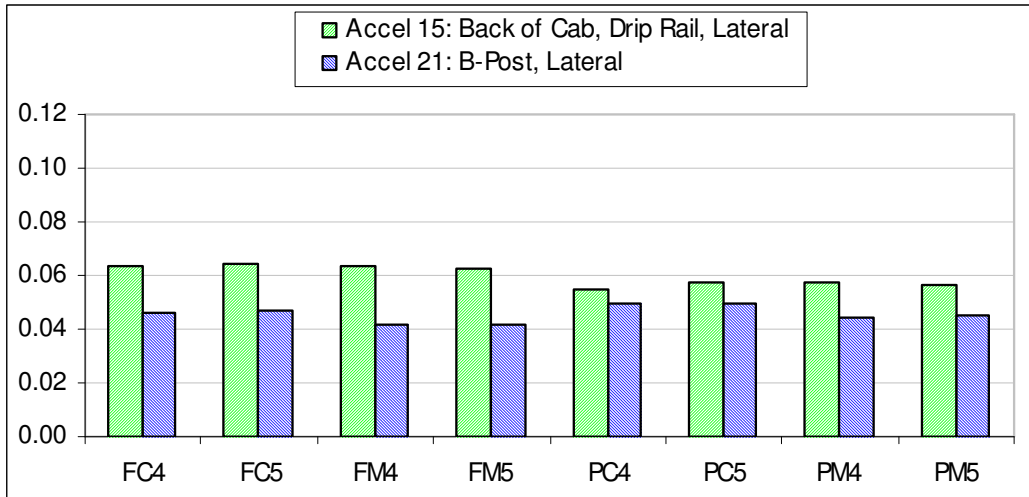


Figure 7-18. Standard High peak-to-peak accelerations (roll)

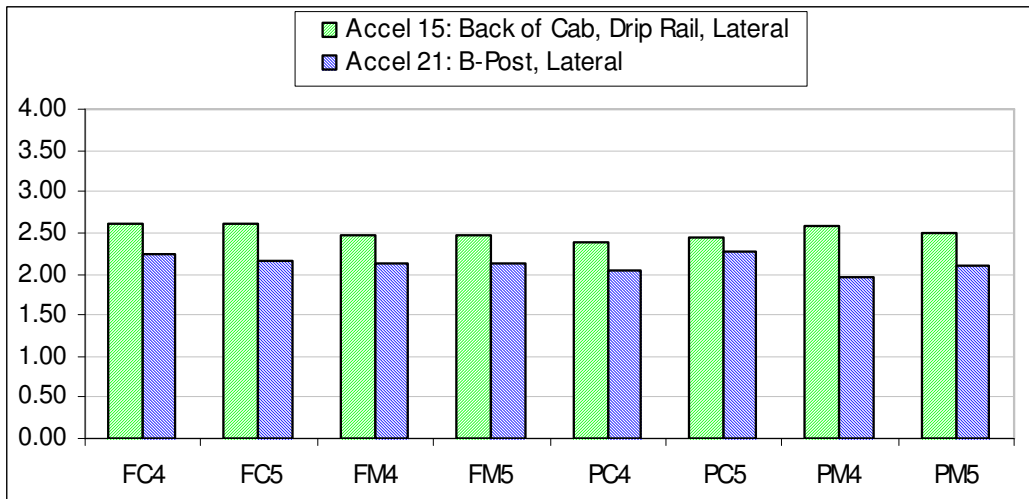


Figure 7-19. Standard High peak-to-peak displacements (roll)

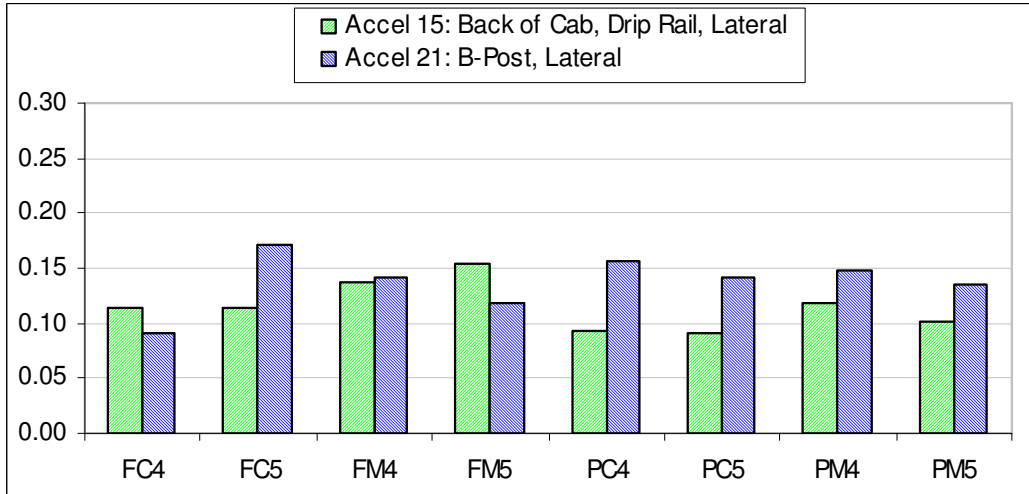


Figure 7-20. Standard High damping ratios (roll)

Table 7-7. Standard High parametric evaluation (roll)

Sensor	Parameter	Acc p-p	Disp p-p	Zeta
Accel 21: B-post, Lateral	Suspension F	0.0441	2.1686	0.1301
	Suspension P	0.0469	2.0904	0.1451
	Shock M	0.0433	2.0794	0.1354
	Shock C	0.0478	2.1795	0.1398
	L4 airsprings	0.0453	2.0941	0.1337
	L5 airsprings	0.0457	2.1648	0.1415
Accel 15: Back of Cab, Drip Rail, Lateral	Suspension F	0.0635	2.5344	0.1301
	Suspension P	0.0564	2.4662	0.1012
	Shock M	0.0599	2.5007	0.1279
	Shock C	0.0600	2.4998	0.1034
	L4 airsprings	0.0598	2.5010	0.1160
	L5 airsprings	0.0601	2.4996	0.1153

7.7 Thin High Results

For the Thin High, the acceleration peaks were lower at the acceleration of the cab near the cab suspension for Suspension P, except when equipped with both Shock C dampers and L4 airsprings (Figure 7-21). The displacements indicate the same thing in Figure 7-22. From the results of these tests, higher damping is indicated for the Thin High (Figure 7-23) than for the Standard High. Shock M produce lower values for all three measurements as measured by the B-post vertical accelerometer (Table 7-8). This same accelerometer indicates that the heave damping was much higher for Suspension F.

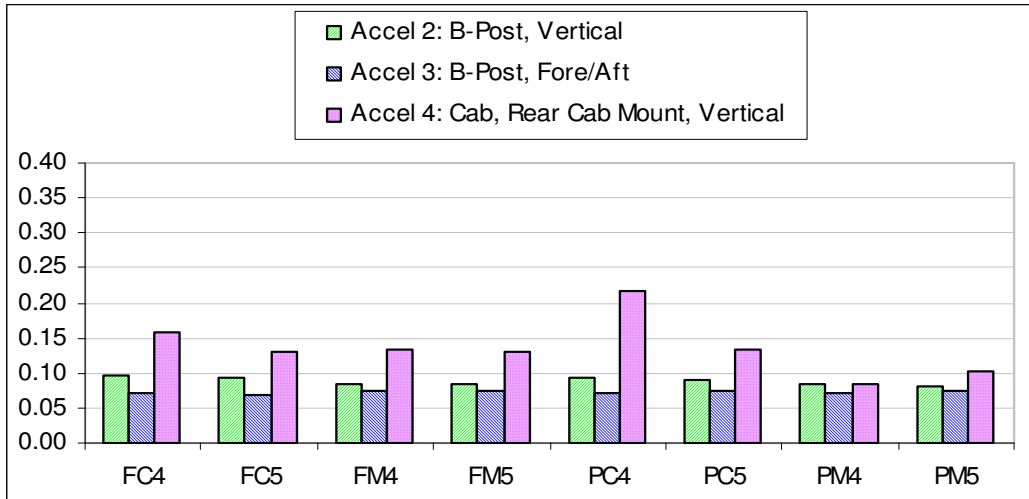


Figure 7-21. Thin High peak-to-peak accelerations (heave)

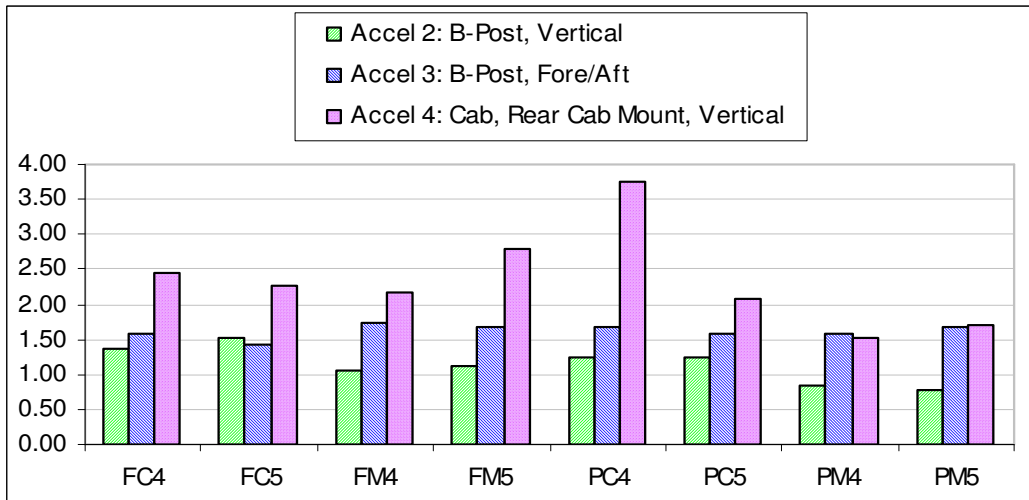


Figure 7-22. Thin High peak-to-peak displacements (heave)

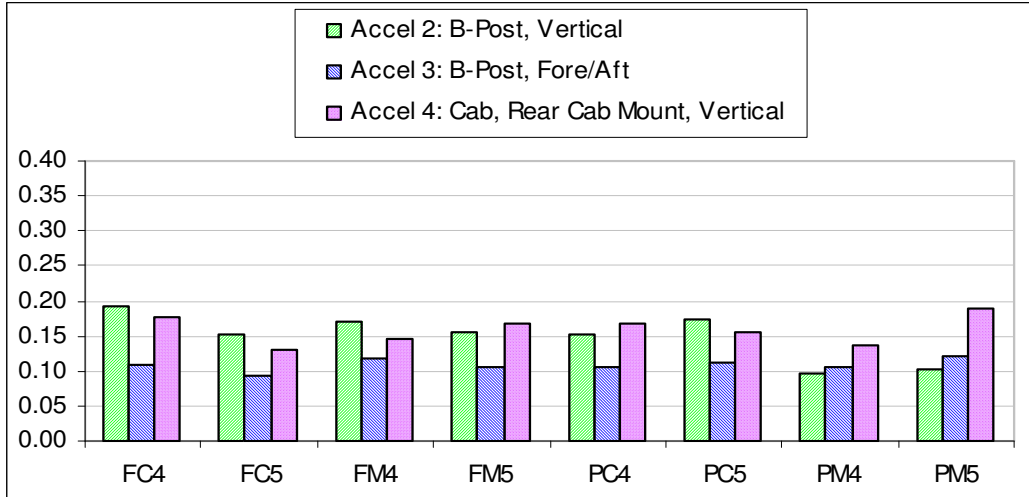


Figure 7-23. Thin High damping ratios (heave)

Table 7-8. Thin High parametric evaluation (heave)

Sensor	Parameter	Acc p-p	Disp p-p	Zeta
Accel 2: B-post, Vertical	Suspension F	0.0882	1.2573	0.1673
	Suspension P	0.0865	1.0296	0.1305
	Shock M	0.0823	0.9448	0.1303
	Shock C	0.0924	1.3421	0.1676
	L4 airsprings	0.0881	1.1267	0.1529
Accel 3: B-post, Fore/Aft	Suspension F	0.0716	1.6070	0.1066
	Suspension P	0.0728	1.6261	0.1111
	Shock M	0.0736	1.6655	0.1131
	Shock C	0.0709	1.5676	0.1046
	L5 airsprings	0.0718	1.5893	0.1081
Accel 4: Cab, Rear Cab Mount, Vertical	Suspension F	0.1380	2.4166	0.1541
	Suspension P	0.1333	2.2623	0.1619
	Shock M	0.1119	2.0444	0.1591
	Shock C	0.1595	2.6344	0.1570
	L4 airsprings	0.1472	2.4691	0.1565
L5 airsprings	0.1241	2.2098	0.1595	

The acceleration peak-to-peak values for the roll test are shown in Figure 7-24. No suspension combination seems to stand out. The displacements were also nearly the same for different suspensions, as shown in Figure 7-25. Compared to the other three test vehicles, however, the displacements of the Thin High were notably higher. Conversely, the roll damping

values (Figure 7-26) were much lower than the other trucks; this could have been a result of the larger displacements. In addition, Suspension P displayed the lower roll damping ratios expected by its design. In fact, at the B-post the damping ratio was about half of the damping ratio of Suspension F as seen in Table 7-9.

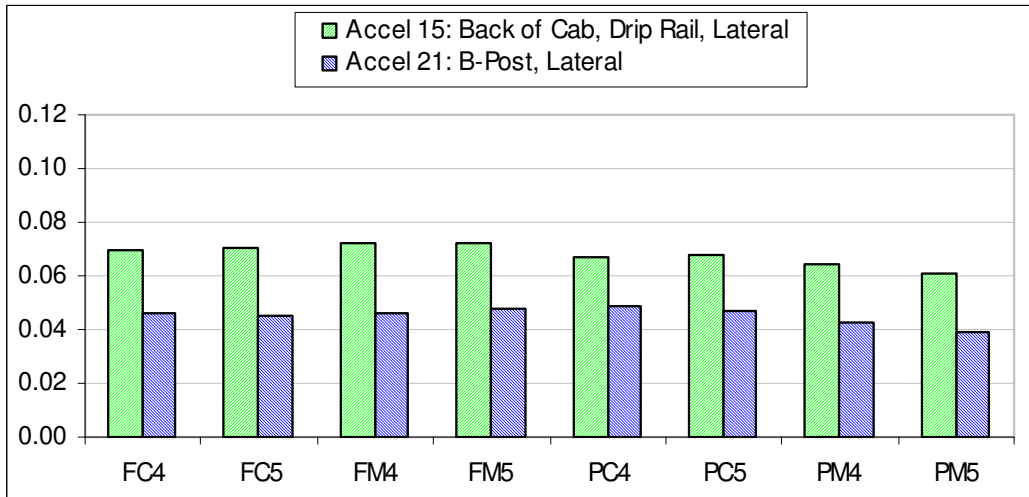


Figure 7-24. Thin High peak-to-peak accelerations (roll)

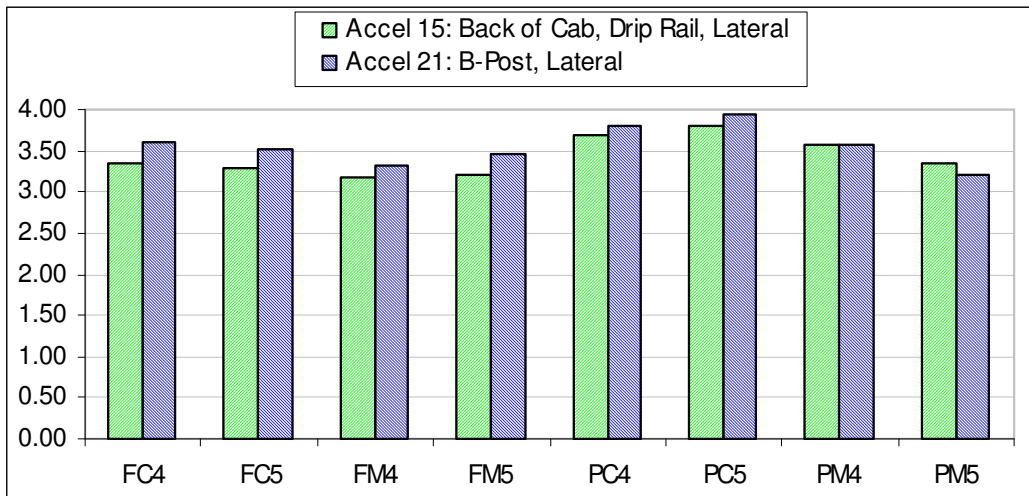


Figure 7-25. Thin High peak-to-peak displacements (roll)

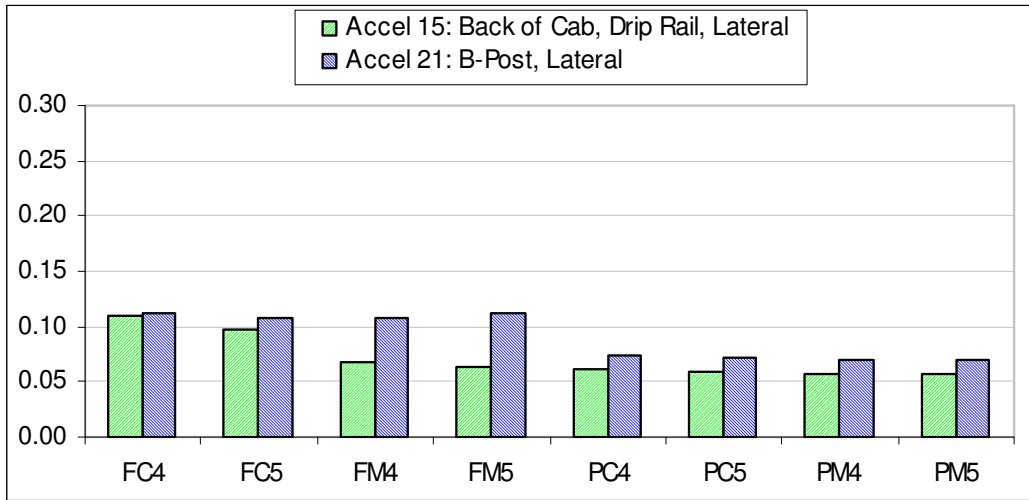


Figure 7-26. Thin High damping ratios (roll)

Table 7-9. Thin High parametric evaluation (roll)

Sensor	Parameter	Acc p-p	Disp p-p	Zeta
Accel 21: B-post, Lateral	Suspension F	0.0462	3.4741	0.1100
	Suspension P	0.0456	3.7485	0.0540
	Shock M	0.0451	3.5059	0.0724
	Shock C	0.0467	3.7168	0.0916
	L4 airsprings	0.0460	3.5745	0.0909
Accel 15: Back of Cab, Drip Rail, Lateral	L5 airsprings	0.0458	3.6481	0.0731
	Suspension F	0.0709	3.2490	0.0844
	Suspension P	0.0663	3.6349	0.0442
	Shock M	0.0685	3.3556	0.0468
	Shock C	0.0687	3.5284	0.0818
	L4 airsprings	0.0683	3.4445	0.0735
	L5 airsprings	0.0689	3.4394	0.0552

Chapter 8 Conclusion and Recommendations

Our tests confirmed that the Thin Low, at certain frequencies, had higher vibration amplitudes at the B-post than the Standard Low. The low-frequency vertical motion – as opposed to the fore/aft or lateral motion – is the main problem with the ride, because the vertical amplitudes were much greater at these frequencies. When Shock M was used with the Thin Low truck in place of the factory Shock C vertical shocks, the ride was much improved (as measured by the B-post vertical accelerometer) and was comparable to the Standard Low. In fact, this study found the same kind of improvement in the ride of all of the trucks tested when Shock M was used in place of Shock C. A slight increase in the fore/aft acceleration occurred with Shock M, but the benefits outweighed the costs in ride control. The Thin High had a comparable ride to the Standard High even without modifying the cab suspension. The Thin High still had a stiffer frame than the Standard Low, judging from the frames' natural frequencies.

There were several trends noted from studying the cab suspensions. No significant difference was found when switching between the L4 and L5 airsprings on any of the tests. Although, switching the vertical shock absorbers did have a significant effect on the B-post measurements as mentioned earlier. Concerning Suspension P, there were several findings. The most noticeable trend occurred during the roll chirp tests, when an increase in motion was observed (compared to Suspension F). Lowering the cab suspension's roll natural frequency could improve the roll frequency response. The heave frequency response of the new suspension was on par with the current suspension. In addition, with Suspension P cab suspension, the peak-to-peak measurements resulting from the bump input were slightly lower, on average.

Subjective testing is still needed for the Lightweight trucks as well as for Suspension P. Subjective testing would accomplish three goals. First, it would correlate the vibration levels of the B-post with actual driver comfort. Does Shock M really produce a better ride? Only the driver knows. Because the effects of the seat suspension are not included in this study the correlation between B-post vibration and driver comfort is even more important to confirm. Second, the road input at the axles on the road will be different than in the lab, so different frequencies may become important. The final benefit to road testing is this: even if the ride quality is degraded, it still may be acceptable to the driver. We know that heavy trucks ride worse than cars, but this does not mean that companies will stop buying trucks.

References

1. Gillespie, Thomas D., 1985, "Heavy Truck Ride," Society of Automotive Engineers, Inc., pp. 42, 14, 38, and 23.
2. Inman, D.J., 2001, "Engineering Vibration", Prentice-Hall, Inc, Upper Saddle River, NJ, pp. 461-465.
3. Smith, A. R., 1965, "Frame Beaming, Fifth Wheel Location – Special Body Mounting and Loading Problems," Tandem Truck Ride and Vibration Problems SAE Special Publications, v 260 Jan, SAE, Warrendale, PA, USA, pp. 815-821.
4. Ibrahim, I.M., Crolla, D A., Barton, D C, 1996, "Effect Of Frame Flexibility on the Ride Vibration Of Trucks," *Computers & Structures*, v 58 n 4 Feb, pp. 709-713.
5. Nosworthy, T.H., 1985, "The Correlation of Objective Ride Measures to Subjective Jury Evaluations of Class 8 COE Vehicles," Truck and Bus Meeting and Exposition, SAE paper # 850985, Dec.
6. Sakuma, N., Kadono, I., Dohi, M., Nakai, H., 1986, "Heavy Duty Truck Ride-Comfort Analysis by Computer Simulation," *International Journal of Vehicle Design*, v 7 n 5-6 Sep, pp. 279-290.
7. SAE J1013, Aug 1992, "Measurement of Whole Body Vibration of the Seated Operator of Off-Highway Work Machines," Society of Automotive Engineers.
8. Nakano, K., Suda, Y., Nakadai, S., Tsunashima, H., Washizu, T., 1999, "Self-powered Active Control Applied to a Truck Cab Suspension," *Jsaе Review*, v 20 n 4, pp. 511-516.
9. Tong, R.T., Amirouche, F., Palkovics, L., 2000, "Ride Control - A Two State Suspension Design for Cabs and Seats," *Vehicle System Dynamics*, v 33 n SUPPL., pp. 578-589.
10. Conaway, R., McKenzie, T.A., May 1992, "Vibration Dampening Suspension Device for the Cab of a Truck Vehicle," United States Patent 5109939.
11. Bodin, J., Barnhardt, S.L., Nilsson, N.B., Andersson, M.H., Sep 1996, "Heavy Duty Motor Vehicle Cab Suspension," United States Patent 5553911, Assignee: Volvo GM Heavy Truck Corporation, Greensboro, NC.
12. Londt, E.E., Robinson, D.S., Mar 1991, "Passive Mechanical Damping System for a Truck," United States Patent 4998592, Assignee: Navistar International Transportation Corporation, Chicago, IL.
13. McHorse, J.V., Atchley, J.T., June 2000, "Vehicle Cab Suspension System," United States Patent 6073714, Assignee: Freightliner Corporation, Portland, OR.

Vita

Paul Stephen Patricio was born in Nairobi, Kenya, less than 2° south of the equator. He is really a great guy. He grew up in the Northern Virginia, and was lucky enough to attend one of the top engineering schools at in-state rates. After graduating with a BSME from Virginia Tech in 1998, he went to work for Volvo Trucks North America in nearby Dublin, VA. Paul wanted a job where he could do more design work and decided that the best way to accomplish that was to obtain a Masters. With his life-long interest in cars, the Advanced Vehicle Dynamics Lab became a perfect home for him (literally, sometimes). Two years later, Paul got his degree and moved on to bigger and better things.